IMMUNOREGULATORY EFFECTS OF VITAMIN D_3 ON MAST CELLS DURING IMMUNOGLOBULIN E-DEPENDENT IMMUNE RESPONSES

A thesis submitted in partial fulfilment of the PhD degree

in

School of Molecular & Biomedical Science
Faculty of Sciences
The University of Adelaide

by

Chunping (Anastasia) Yu

April 2014

Table of contents

IMMUNOREGULATORY EFFECTS OF VITAMIN D_3 ON MAST CELLS DURING IMMUNOGLOBULIN E-DEPENDENT IMMUNE RESPONSES 1
Table of contents 2
Declaration 8
Abbreviations 10
Acknowledgments 14
Thesis summary 15
CHAPTER 1 17
LITERATURE REVIEW 17
1.1. Mast Cells (MCs) 18
1.2. Basic Biology of MCs 18
1.2.1. MC Ontogeny and Tissue Distribution 18
1.2.2. Homing of MCPs 19
1.2.3. Trafficking of Mature MCs 20
1.2.4. MC Heterogeneity 22
1.2.5 MC Development and Maturation 23
1.2.6. MC Activation 24
1.2.7. MC-derived Mediators 25
1.2.8. FcεRI Signalling in MCs 26
1.3. Biological Functions of MCs in IgE-dependent Allergic Reactions 28
1.3.1. IgE-dependent Allergic Reactions and MCs 28
1.3.2. Functions of MCs during Early-phase Allergic Reactions 29
1.3.3. Functions of MCs during Late-phase Allergic Reactions 30
1.3.4. Functions of MCs during Chronic Allergic Reactions 31
1.3.5. Treatment Strategies for Allergic Reactions and MCs 33
1.4. Other Biological Functions of MCs 34
1.4.1. Roles of MCs in Homeostasis 34
1.4.2. Roles of MCs in Parasitic Infections 35
1.4.3. Roles of MCs in Bacterial and Viral Infections 36
1.4.4. Roles of MCs in Cancers 37
1.4.5. Roles of MCs in Chronic Obstructive Pulmonary Diseases (COPD) 38

1.4.6. Negative Immunoregulatory Roles of MCs 39
1.5. Experimental Tools for MC Research 41
1.5.1. In Vitro Tools 41
1.5.2. In Vivo Tools 43
1.6. $VitD_3$ (Cholecalciferol) 46
1.7. Biosynthesis and Metabolism of $VitD_3$ 47
1.8. Biological Activities of $VitD_3$: UVB Protection and Immunoregulation 48
1.8.1. The Genomic Pathway (Figure 1.5a) 48
1.8.2. The Non-genomic Pathway (Figure 1.5b) 51
1.9. $VitD_3$ and MCs 52
1.9.1. $VitD_3$-mediated Immunoregulation of MCs 52
1.9.2. Potential Mechanisms for $VitD_3$-mediated Immunoregulation of MCs 53
1.10. Rationales for this Study 54
1.11. Hypothesis 55
1.12. Project Aims 56
1.13. Expected Outcomes and Significance 60
CHAPTER 2 62
MATERIALS & GENERAL METHODS 62
2.1. Commercial Reagents 63
2.1.1. Common Tissue Culture Reagents 63
2.1.2. Vitamin D_3 Analogues 64
2.1.3. Cytokines and Recombinant Proteins 64
2.1.4. Hybridomas 64
2.1.5. Antibodies for Tissue Culture 64
2.1.6. Reagents for SPE-7 Purification 65
2.1.7. β-Hexosaminidase Release Assay Reagents 65
2.1.8. ELISA/EIA Kits and Reagents 65
2.1.9. Flow Cytometry Reagents 66
2.1.10. Histochemistry & Immunohistochemistry Reagents 66
2.1.11. SDS-PAGE & Western Blotting Reagents 67
2.1.12. Primers (all used at 5 μg/mL): Geneworks 68
2.1.13. Molecular Biology Reagents 68

2.1.14. In Vivo Experiment Reagents 69
2.2. Solutions and Buffers 69
2.2.1. Tissue Culture Media and Solutions 69
2.2.2. Buffers and Solutions for SPE-7 Purification 73
2.2.3. Buffers and Solutions for β-Hexosaminidase Release Assay 75
2.2.4. ELISA Buffers and Solutions 76
2.2.5. Flow Cytometry Buffers and Solutions 77
2.2.6. Histology/Immunohistology Solutions 77
2.2.7. Buffers and Solutions for SDS-PAGE & Western Blotting 79
2.2.8. Molecular Biology Buffers and Solutions 82
2.2.9. Buffers and Solutions for In Vivo Experiments 83
2.3. Purification of Mouse α-DNP IgE (SPE-7 clone) 84
2.3.1. Conjugation of DNP and BSA 84
2.3.2. Coupling of DNP-BSA to HiTrap NHS-activated HP column 85
2.3.3. De-activation of Excess Active Groups 86
2.3.4. Purification of SPE-7 from Hybridoma Culture Supernatant 86
2.4. Mice 87
2.5. General Methods 88
2.5.1. Culturing of mBMCMCs 88
2.5.2. Culturing of hCBMCs 88
2.5.3. Culturing of WEHI-3 hybridoma 89
2.5.4. Culturing of SPE-7 hybridoma 89
2.5.2. Flow Cytometry 90
2.5.2.1. Surface Ag Labelling 90
2.5.2.2. Intracellular Ag Labelling 90
2.5.3. In Vitro Procedures 91
2.5.3.1. β-hexosaminidase Release Assay 91
2.5.3.2. Histamine Release Assay 92
2.5.3.3. IgE + sAg Stimulation of mBMCMCs 93
2.5.3.4. IgE-mediated stimulation of hCBMCs 94
2.5.3.5. Cytokine Measurement by ELISA 94
2.5.3.6. VitD_3 Treatment (without stimulation) 95

2.5.3.7. Measurement of 1α,25(OH)$_2$D$_3$ 95
2.5.4. Molecular Biology 96
2.5.4.1. Genotyping of WT and *VDR*$^{-/-}$ Mice 96
2.5.4.2. RNA Extraction 97
2.5.4.3. Complementary DNA (cDNA) Synthesis 98
2.5.4.4. qRT-PCR 98
2.5.5. SDS-PAGE and Western Blot Analysis 99
2.5.5.1. Preparation of Total Cell Lysates 99
2.5.5.2. SDS-PAGE 100
2.5.5.3. Protein Transfer and Western Blot Analysis 100
2.5.6. In Vivo and Related Procedures 101
2.5.6.1. Engraftment of mBMCMCs 101
2.5.6.2. PCA with Topical Application of 1α,25(OH)$_2$D$_3$ or 25OHD$_3$ 101
2.5.6.3. Ear Tissue Histology and Numeration of Tissue MCs 102
2.5.6.4. Ear Tissue Lysate Preparation and Analysis 102
2.5.6.5. Total RNA Extraction from Ear Tissues 103
2.5.6.6. Serum Preparation and Analysis 103
2.5.7. Histochemistry and Immunohistochemistry 103
2.5.7.1. Cytospin Slide Preparation 103
2.5.7.2. May-Grűnwald Giemsa Staining 104
2.5.7.3. Kimura Staining of hCBMCs 104
2.5.7.4. Toluidine Blue Staining 104
2.5.7.5. Immunohistochemistry 104
2.5.8. Centrifugation 105
2.5.9. Statistical Analyses 105
CHAPTER 3 107
1α,25(OH)$_2$D$_3$ POTENTIATES THE NEGATIVE IMMUNOREGULATORY PROPERTIES OF MAST CELLS DURING IgE+sAg-MEDIATED ACTIVATION *IN VITRO* 107
3.1. Introduction 108
3.2. Results 110
3.2.1. WT and VDR$^{-/-}$ mBMCMCs exhibit similar phenotypical and functional characteristics 110

3.2.2. 1α,25(OH)$_2$D$_3$ does not affect the efficiency of IgE preload, the expression of surface molecules, and survival of mBMCMCs 111

3.2.3. 1α,25(OH)$_2$D$_3$ reduces IgE + sAg-mediated mBMCMC degranulation in a VDR-dependent manner 112

3.2.4. 1α,25(OH)$_2$D$_3$ VDR-dependently down-regulates the de-novo synthesis and secretion of pro-inflammatory cytokines but up-regulates that of the anti-inflammatory IL-10, from IgE + sAg-activated mBMCMCs 114

3.2.5. Curcumin reduces IgE + sAg-mediated cytokine production by mBMCMCs in a VDR- and non-genomic VitD$_3$ pathway-dependent manner 115

3.3. Discussion 116

CHAPTER 4 123

MAST CELLS CAN CONVERT 25OHD$_3$ TO 1α,25(OH)$_2$D$_3$ AND THUS ENABLE 25OHD$_3$ TO IMMUNOSUPPRESS IgE + sAg-ACTIVATED MAST CELLS *IN VITRO* 123

4.1. Introduction 124

4.2. Results 126

4.2.1. Mouse BMCMCs constitutively express CYP27B1 in their cytosol 126

4.2.2. 25OHD$_3$ up-regulates CYP27B1 expression in mBMCMCs in a VDR-dependent manner 126

4.2.3. 25OHD$_3$ dose-dependently induces endogenous synthesis of 1α,25(OH)$_2$D$_3$ by mBMCMCs 127

4.2.4. 25OHD$_3$ treatment reduces IgE + sAg-mediated degranulation and pro-inflammatory cytokine production of mBMCMCs in a dose- and VDR-dependent manner 128

4.3. Discussion 129

CHAPTER 5 134

TOPICALLY APPLIED 1α,25(OH)$_2$D$_3$ AND 25OHD$_3$ CAN REDUCE THE CUTANEOUS PATHOLOGY ASSOCIATED WITH IgE-MEDIATED PASSIVE CUTANEOUS ANAPHYLAXIS IN A MAST CELL VITAMIN D RECEPTOR-DEPENDENT MANNER *IN VIVO* 134

5.1. Introduction 135

5.2. Results 138

5.2.1. Topical 1α,25(OH)2D3 application alone does not affect ear thickness of WT mice 138

5.2.2. Topical 1α,25(OH)$_2$D$_3$ application at the site of inflammation can suppress PCA-associated ear swelling 138

5.2.3. Topical 1α,25(OH)$_2$D$_3$ application reduced the extent of MC degranulation and the expression of various MC-derived mediators associated with PCA in vivo 139

5.2.4. VDR expression is required for the suppressive effect of 1α,25$(OH)_2D_3$ on PCA-associated cutaneous pathology 141
5.2.5. The PCA-suppressing effect of topical 1α,25$(OH)_2D_3$ treatment requires specifically VDR expression by cutaneous MCs 142
5.2.6. Topical 25OHD_3 can suppress PCA-associated ear swelling via similar mechanisms to 1α,25$(OH)_2D_3$ 145
5.2.7. The suppressive effect of topical 25OHD_3 on PCA-associated cutaneous pathology also requires MC expression of VDR 147
5.3. Discussion 148
CHAPTER 6 155
FROM THE MOUSE TO THE HUMAN – TRANSLATIONAL ASPECTS 155
6.1. Introduction 156
6.2. Results 158
6.2.1. 1α,25$(OH)_2D_3$ reduces IgE + α-IgE-mediated TNFα but not IL-10 production by hCBMCs 158
6.3.2. Human CBMCs constitutively express CYP27B1, which can be up-regulated by 25OHD_3 treatment 159
6.3.3. Human CBMCs produce endogenous 1α,25$(OH)_2D_3$ following 25OHD_3 treatment in a dose-dependent manner 159
6.3. Discussion 160
CHAPTER 7 164
CONCLUDING REMARKS & FUTURE DIRECTIONS 164
References 171

Declaration

This work contains no material which has been accepted for the award of any other degree or diploma in any university or other tertiary institution to me (Chunping Yu) and, to the best of my knowledge and belief, contains no material previously published or written by another person, except where due reference has been made in the text. I give consent to this copy of my thesis, when deposited in the University Library, being made available for loan and photocopying according to the provisions of the Copyright Act 1968. I also give permission for the digital version of my thesis to be made available on the web, via the digital research repository of the University of Adelaide, the Library catalogue, the Australasian Digital Theses Program and also through web search engines, unless permission has been granted by the University to restrict access for any unforseen reasons. Finally, I acknowledge that the copyright of the published works listed below resides with the copyright holder(s) of those works.

List of publications

- Yu, C., Fedoric, B., Anderson, P.H., Lopez, A.F., and Grimbaldeston, M.A., 2011, Vitamin D_3 signalling to mast cells: a new regulatory axis. *The International Journal of Biochemistry & Cell Biology*, Vol. 43, p 41 – 46.
- Biggs, L., Yu, C., Fedoric, B., Lopez, A.F., Galli, S.J., and Grimbaldeston, M.A., 2010, Evidence that vitamin D_3 promotes mast cell-dependent reduction of chronic UVB-induced skin pathology in mice. *J Exp Med*, Vol. 207, p 455- 463.

- Yip, K., Kolesnikoff, N., Yu, C., Hauschild, N., Taing, H., Biggs, L., Goltzman, D., Gegory, P., Anderson, P., Samuel, M., Galli, S., Lopez, A., and Grimbaldeston, M., 2014, Mechanisms of vitamin D_3 metabolite repression of IgE-dependent mast cell activation. *Journal of Allergy and Clinical Immunology*, published online.

…….. ……...

Chunping Yu Dr. Michele Grimbaldeston

Abbreviations

$1\alpha,25(OH)_2D_3$: 1α,25-dihydroxyvitamin D_3

$25OHD_3$: 25-hydroxyvitamin D_3

6C: 6-*s*-*cis*

6T: 6-*s*-*trans*

Ab: antibody

ACD: anticoagulant citrate dextrose

Ag: antigen

APS: ammonium persulphate

ASM: airway smooth muscle

A1AT: α_1-antitrypsin

BM: bone marrow

BSA: bovine serum albumin

BTK: Bruton's tyrosine kinase

cAMP: cyclic AMP

CCL: CC-chemokine ligand

CHS: contact hypersensitivity

COPD: chronic obstructive pulmonary disease

CTMC: connective tissue mast cell

CYP24A1: 25-hydroxyvitamin D_3-24-hydroxylase

CYP27B1: 25-hydroxyvitamin D-1α-hydroxylase enzyme

DAG: Diacylglycerol

DBP: $VitD_3$-binding protein

DC: dendritic cell

DMEM: Dulbecco's modified eagle medium

DMSO: dimethyl sulphoxide

DNP: dinitrophenyl

DT: diphtheria toxin

ECL: enhanced chemiluminescence

EIA: enzyme immunoassay

ELISA: enzyme-linked immunosorbent assay

EMTU: epithelial-mesenchymal trophic unit

ERK: extracellular signal regulated kinase

FCS: fetal bovine serum

FcεRI: high affinity IgE receptor

FDNB: 1-fluoro-2,4,-dinitrobenzene

GAB: growth-factor-receptor-bound protein

GMP: granulocyte/macrophage progenitor

hCBMC: human cord-blood-derived MCs

HDC: histidine decarboxylase

HIV: human immunodeficiency virus

HMEM: Hank's MEM

HRP: horse radish peroxidase

HS: horse serum

HSA: human serum albumin

HSC: haematopoietic stem cell

IFN: interferon

Ig: immunoglobulin

IL: interleukin

IMDM: Iscove's modified Dulbecco's medium

$InsP_3$: inositol-1,4,5,-triphosphate

ITAM: immunoreceptor tyrosine-based activation motif

LN: lymph node

LT: leukotriene

MAPK: mitogen-activated protein kinase

mBMCMC: mouse bone marrow-derived cultured mast cell

MC: mast cell

MCP: mast cell progenitor

MC_T: tryptase positive mast cell

MC_{TC}: tryptase and chymase positive mast cell

MEK: MAPK kinase

miR: microRNA

MKP: mitogen-activated protein kinase phosphatase

MMC: mucosal mast cell

MMCP: mouse mast cell protease

MMP: matrix metalloproteinase

NEAA: non-essential amino acid

NF-κB: nuclear factor-κB

PBS: phosphate buffered saline

PCA: passive cutaneous anaphylaxis

PCR: polymerase change reaction

Pen/Strep: Penicillin/Streptomycin

PG: prostaglandin

PI3K: phosphatidylinositol-3-OH kinase

PKB (AKT): protein kinase B

PKC: protein kinase C

PL: phospholipase

PLA_2: phospholipase A_2

PLC_γ: phospholipase C_γ

PMA: phorbol-12 myristate-13 acetate

PtdIns(3,4,5)P_3: phosphatidylinositol-3,4,5,-trisphosphate

PTH: parathyroid hormone

qRT-PCR: quantitative real-time PCR

RIA: radioimmunoassay

RT: room temperature

RT-PCR: real-time PCR

RXR: retinoid X receptor

sAg: specific antigen

SCF: stem cell factor

SDS-PAGE: sodium dodecyl sulfate - polyacrylamide gel electrophoresis

TCR: T cell receptor

TGF: transforming growth factor

Th: T helper

TLR: toll-like receptor

TNF: tumor necrosis factor

T_{reg}: T regulatory cell

TSLP: thymic stromal lymphopoietin

UV: ultraviolet

VDR: vitamin D receptor

VDRE: vitamin D response element

VDR_{mem}: plasma membrane-associated vitamin D receptor

VitD: vitamin D

WT: wild-type

Acknowledgments

First and foremost, I would like to thank my supervisors, Dr. Michele Grimbaldeston, Prof. Shaun McColl, and Prof. Angel Lopez, for their constant guidance and support throughout my PhD study, especially Michele for offering me such a stimulating and challenging project and for demonstrating to me personally what scientific research is really about. A big thank also goes to Shaun, for securing me a scholarship that allows me to begin my PhD study in the first place and for helping with reviewing my thesis towards the end.

I also want to thank everyone in the lab, Dr. Boris Federic, Lisa Biggs, Zhen Liu, Houng Taing and Renee Gilbey, as well as Jyotsna, Kiwi and Samantha in our neighbour lab. It was your friendship and unconditional encouragement that kept me sane and able to continuously moving forward. A special thank you must go to Boris, who has generously offered help with quite a few large-scale animal experiments. For everyone else in the Centre for Cancer Biology, I would like to express my appreciation for making me feel like a part of a big family.

Finally, I want to dedicate this thesis to my husband, Yang Lu, and all my family overseas, as without your deep understanding and unconditional love and support, I would not be able to stay focused and complete my experiments in a three-year time frame.

Thesis summary

Mast cells (MCs) can exert anti-inflammatory effects via production of interleukin (IL)-10 in a number of Immunoglobulin (Ig)E-independent immune responses. Recently, we reported that 1α,25-dihydroxyvitamin D_3 (1α,25$(OH)_2D_3$), the biologically active form of vitamin D_3 ($VitD_3$), can induce IL-10 production from mouse bone marrow-derived cultured MCs (mBMCMCs). For the current project, we further investigated if the well-recognised pro-inflammatory properties of MCs in IgE-dependent immune settings can be reduced upon 1α,25$(OH)_2D_3$ administration and, if so, which mechanisms are likely to be responsible. In the presence of 1α,25$(OH)_2D_3$, IgE + specific antigen (sAg)-stimulated mBMCMCs exhibited reduced degranulation, as well as decreased production of the pro-inflammatory cytokines, TNFα and IL-6, in a vitamin D receptor (VDR)-dependent manner. Concomitantly, 1α,25$(OH)_2D_3$ significantly up-regulated the production of IL-10. In addition, we demonstrated for the first time the expression of CYP27B1, the enzyme that generates 1α,25$(OH)_2D_3$ from its inactive precursor 25-hydroxyvitamin D_3 ($25OHD_3$) in both mBMCMCs and human cord-blood-derived MCs (hCBMCs). This enables mBMCMCs to produce endogenous 1α,25$(OH)_2D_3$ and thus granting $25OHD_3$ similar VDR-dependent immunosuppressive effects to 1α,25$(OH)_2D_3$ on activated MCs either directly or indirectly.

By employing a mouse IgE-mediated MC-dependent passive cutaneous anaphylaxis (PCA) model as well as four mouse groups with different cutaneous MC profiles in the ears, including wild-type (WT) C57BL/6 mice, MC-deficient C57BL/6-*Kit*$^{W\text{-}sh/W\text{-}sh}$ mice and C57BL/6-*Kit*$^{W\text{-}sh/W\text{-}sh}$ mice engrafted with either WT or VDR-deficient (*VDR*$^{-/-}$)

mBMCMCs, we found that topical application of either $1\alpha,25(OH)_2D_3$ or $25OHD_3$ significantly curtailed the magnitude of PCA-associated ear swelling, potentially by reducing the extent of MC degranulation and/or the secretion of various MC-derived cytokines. Notably, these PCA-suppressive effects required the presence of dermal MCs and their expression of VDR.

Taken together, data presented in this thesis provide evidence that $1\alpha,25(OH)_2D_3$ and $25OHD_3$, the latter likely via its conversion to the active metabolite by MCs, can suppress IgE + sAg-mediated MC activation in a VDR-dependent manner both *in vitro* and *in vivo*. This suggests the therapeutic potential for various $VitD_3$ analogues to treat MC-dependent IgE-associated allergic disorders.

CHAPTER 1

LITERATURE REVIEW

1.1. Mast Cells (MCs)

First discovered as granular cells by Dr von Recklinghausen in 1863 and named "mastzellen" (i.e. well-fed cells) by Dr Paul Ehrlich in 1878, MCs can be identified as FcεRI (the high affinity immunoglobulin [Ig]E receptor) and c-kit (CD117; receptor for stem cell factor [SCF]) double positive cells with numerous metachromatic granules in their cytoplasm that stain with aniline dyes such as toluidine blue. [1, 2] Since their initial discovery over a century ago, MCs have gained increasing attention, due largely to their wide distribution throughout the body, their high plasticity in phenotypical and functional properties, and their substantial involvement in a large array of physiological and pathophysiological processes including, in particular, IgE-dependent allergic reactions. [3, 4] The recent findings that MCs are capable of playing anti-inflammatory as well as pro-inflammatory roles during a number of innate and acquired immune responses have sparked further interest in seeking strategies which can drive the functionality of MCs towards the anti-inflammatory end of the spectrum. [5-8] The ultimate aim of the current project is to investigate alternatives in IgE-mediated MC activation by anti-inflammatory exogenous stimuli with a particular emphasis on biologically active Vitamin D_3 ($VitD_3$).

1.2. Basic Biology of MCs

1.2.1. MC Ontogeny and Tissue Distribution

Human MCs originate from $CD34^+$ pluripotent haematopoietic stem cells (HSCs) in the bone marrow (BM), which differentiate to form $CD34^+CD117^+CD13^+$ MC progenitors (MCPs). [3] MCPs then enter the circulation and migrate to tissues where they take up

residence and undergo maturation in the presence of cytokines such as IL-6 and SCF. In mice, the situation is more complicated as mouse HSCs give rise to granulocyte/macrophage progenitors (GMPs) in the BM, and MCPs can develop either from GMPs or from HSCs directly. Moreover, a group of GMP-derived common basophil/MC progenitors are found in mouse spleen and have been shown to also give rise to MCPs. [4, 9] According to Chen *et al*. [10], a population of $Lin^{-}c\text{-}kit^{+}Sca\text{-}1^{-}Ly6c^{-}FcεRI^{-}CD27^{-}β7^{+}T1/ST2^{+}$ cells exist in adult mouse BM, which gave rise only to MCs in culture and could reconstitute the MC compartment when transferred into MC-deficient mice. Similar to human MCPs, mouse MCPs then circulate through blood and do not mature until they reach the anatomical location in which they will ultimately reside. Unlike their human counterparts, however, mouse MCPs require IL-3 and/or SCF for maturation and differentiation. Typically, mature MCs are found throughout vascularised tissues, often in close proximity to blood and lymphatic vessels and/or at surfaces that are exposed to the environment, such as the skin, airway and gastrointestinal tract. [4, 11] Although currently unknown for humans, in mice at least, committed MCPs (besides mature MCs) are also abundant in the small intestine [12, 13] and at sites of chronic inflammation; which, in the latter case, is due largely to inflammation-induced up-regulation of MC-attracting chemokines. [14].

1.2.2. Homing of MCPs

The wide anatomical distribution of mature MCs implies the migration of MCPs to a large variety of tissues occurs after leaving the BM. Although the precise mechanism(s) for such tissue-specific homing process remains to be fully understood, it has been suggested that there is a sequential expression of surface molecules, such as adhesion

molecules and chemokine receptors, on MCPs. Only the progenitors expressing an appropriate set of these molecules are able to enter the corresponding tissue and/or interact with cells within that tissue. Thus the tissue-specificity in these scenarios is conferred by the specific receptor-ligand interaction between MCPs and resident cells of a particular tissue. [15] The constitutive recruitment of MCPs to the small intestine in mice, for instance, is directed by tissue-derived CXCR2 ligands (i.e. chemokines) as both human and mouse MCPs express the corresponding chemokine receptor, CXCR2. [13, 16] Interaction between CXCR2 and their ligands subsequently facilitates the adhesion between α4β7 integrin (expressed on MCPs) and vascular cell adhesion molecule-1 and/or mucosal addressin cell adhesion molecule-1 (both are counter-ligands for α4β7 integrin expressed on intestinal endothelial cells), thus further promoting the homing and retainment of MCPs in the tissue. [12] The recruitment of MCPs to asthmatic lungs, on the other hand, relies on the inducible changes in the chemotaxis-adhesion pathways upon the onset of the allergic reaction, as normal lungs are not common residence for either MCPs or mature MCs. [13, 14] In this case, although the nature of the chemoattractants responsible remains to be identified, the adhesive interaction between vascular cell adhesion molecule-1 (up-regulated on endothelial cells due to inflammation) and α4β7 and α4β1 integrins (both expressed on MCPs) has been demonstrated to be crucial. [14]

1.2.3. Trafficking of Mature MCs

Mature MC populations are not generally found in peripheral blood of healthy individuals. They can, however, be readily observed under *c-kit* gain-of-function mutation disease settings, such as mastocytosis. [3] In addition, the discovery of a large variety of MC chemotactic factors, including chemokines (e.g. monocytes chemoattractant protein-1 and

CC-chemokine ligand [CCL]5/RANTES), anaphylatoxins (e.g. C3a and C5a), angiogenic factors (e.g. platelet-derived growth factor and vascular endothelial growth factor) and a number of cytokines (e.g. IL-3 and transforming growth factor [TGF]-β), urges the reconsideration of the possibility that mature MCs do exist in peripheral blood under physiological and/or pathological conditions. [17] Furthermore, interaction between SCF and its receptor c-kit has been shown to alter the functional state of integrins on the surface of tissue MCs. This, together with the evidence that chemokine receptor expression on these cells also vary, suggests that mature MCs may detach from their original residence via changes in adhesion molecule expression and migrate towards particular chemotactic factor(s) at other sites. [18]

Supporting evidence for this notion has been observed *in vivo*. Early work done by Wang *et al*. [17] showed MC migration from the skin to the draining lymph nodes (LNs) and subsequently to the spleen during the sensitization phase of dinitrofluorobenzene-induced contact hypersensitivity (CHS) in mice. A more recent study by Byrne *et al*. [19] also demonstrated CXCR4/CXCL12-mediated migration of mature MCs from the skin to the B cell-rich areas of draining LNs upon ultraviolet (UV) irradiation. During liver regeneration in rats after partial hepatectomy, MC migration into the liver was shown to be crucial for the restoration of hepatic MC population. [20] Furthermore, human MCs expressing CCR1 and CCR4 are able to migrate towards the chemokine CCL5/RANTES, both *in vitro* and *in vivo*. [21, 22] Recent findings that the pro-inflammatory cytokines tumor necrosis factor (TNF)α and IL-6 can induce chemotaxis and chemokinesis of tissue MCs, respectively, provide a plausible explanation for the accumulation of MCs at sites of inflammation. [23]

1.2.4. MC Heterogeneity

To date, two major subsets of MCs have been described in rodents: mucosal MCs (MMCs) and connective tissue MCs (CTMCs); which show differences in many aspects such as tissue distribution, granule contents, histochemical staining properties, and response to certain stimuli or inhibitors. [4, 24] For example, MMCs predominate in the lung, intestinal and other mucosae, and preferentially express chymases including mouse MC protease (MMCP)-1 and -2; whereas CTMCs predominate in connective tissues and serosal cavities (e.g. peritoneal cavity), and express chymases MMCP-4, and -5 (also MMCP-9 in the case of uterine MCs), tryptases MMCP-6, and -7, and carboxypeptidase A. [25] Human MCs also exhibit heterogeneity and are classified, based on their serine protease contents, as tryptase positive MCs (MC_T) and tryptase and chymase double positive MCs (MC_{TC}), with the latter also containing carboxypeptidase A). [26-28] Although the tissue distribution of human MC subsets is not as distinctive as their mouse counterparts, MC_T and MC_{TC} do share some characteristics with MMCs and CTMCs, respectively. Because MC heterogeneity in different tissues is largely influenced by the microenvironment presented, it is likely to be more diverse and dynamic than merely two or three polarized phenotypes. The plasticity of MCs is conferred by their ability to express certain profiles of proteases according to the particular microenvironmental conditions they encounter in the tissue that they reside. [4] For example, when mBMCMCs and cultured peritoneal MCs from (WB/ReJ×C57BL/6)F_1 (WBB6F_1) WT mice (both expressing MMCP-1, -2, -4, -5, and -6) were transplanted into the stomach wall of MC-deficient WBB6F_1-*Kit*$^{W/Wv}$ mice, they appeared in both the mucosa, where they had down-regulated MMCP-1, -4, -5 and -6, and muscularis propria, where they had

down-regulated MMCP-1 and -2. On the other hand, when fully differentiated peritoneal MCs from WT mice (expressing MMCP-2, -4, -5 and -6) were transplanted, they also adopted to the stomach mucosa by down-regulating MMCP-4, -5 and -6 when injected at a considerably low number to allow local proliferation.

1.2.5 MC Development and Maturation

As mentioned previously, circulating MCPs do not undergo maturation until they have reached their destined anatomical location. It seems natural, therefore, that MC development and maturation should be driven by growth factors and cytokines present in the local microenvironment. [24, 29] SCF, produced primarily by fibroblasts, is probably the most critical MC growth factor. Interaction between SCF and its receptor c-kit, provides vital signals for the development of murine MCs as both the *W* and *Sl* mice, which have mutations in the chromosomal loci coding for c-kit and SCF, respectively, have profound deficiency in tissue MCs. [30, 31] Sawai *et al.* [32] reported that SCF can also promote the development of human MCs, as demonstrated by its proliferative effect during MC culturing from human umbilical cord-blood.

In addition to SCF, a number of cytokines are also proven important for MC development and/or maturation in mice and/or humans. T cell-derived cytokine IL-3 alone, for instance, is required to generate mBMCMCs. These mBMCMC have been used extensively in research of MC biology, although they resemble more closely MMCs or immature MCs, with respect to size, granularity and functional properties. [33] To obtain more CTMC-like cells *in vitro*, other cytokine(s) such as SCF, or IL-4, or both together, are also required. [34-36] It is worth mentioning that IL-10, a well-known anti-inflammatory cytokine is

another enhancer for MC growth, as whilst it alone does not induce MC colony formation, it demonstrates synergistic action with IL-3, SCF, or IL-4 in the proliferation of mBMCMC. [36] Culturing human MCs *in vitro*, on the other hand, requires SCF and IL-6. In the presence of both cytokines, MCs can be generated from human cord blood-derived mononuclear cells as well as $CD34^+$ cells. [36, 37]

1.2.6. MC Activation

There are many mechanisms by which MCs can be activated but perhaps the most well recognised is IgE-dependent activation. Most, if not all, MCs in the body are sensitised with IgE molecules of different specificities bound via their high-affinity FcεRI receptors. Cross-linking of these IgE molecules by their corresponding Ag leads to aggregation of FcεRI receptors and ultimately MC activation. Upon such IgE + sAg-mediated activation, MCs generally undergo an immediate and highly regulated granule-emptying process called degranulation. Depending on the strength of the stimuli, MCs can either release all their granule contents at once through compound and/or multi-vesicular exocytosis, or gradually empty their granules via piecemeal exocytosis. [38] More importantly, MCs are capable of participating in multiple cycles of activation for mediator release, although the regeneration of a fully reconstituted granular compartment can take up to 72 h. [39]

In addition to IgE receptor cross-linking, MCs express a wide array of receptors and can be activated by a variety of other stimuli, including growth factors (e.g. SCF) [40], cytokines (e.g. IL-1, IL-3 and IL-33) [41], chemokines (e.g. macrophage inflammatory protein-1α) [42], anaphylatoxins (e.g. C3a and C5a) [43], neuropeptides (e.g. substance P and calcitonin gene-related peptide) [44, 45], Ig free light-chains [46], and pathogen-derived

Ags (i.e. signalling through toll-like receptor (TLR)s, TLR-2, -3, -4, -7 and -9) [47-50]. Unlike IgE + sAg-mediated activation, activation of MC by non-IgE-related stimuli does not always lead to degranulation. Even when it does, the degranulation is usually piecemeal in nature, leading to a differential and selective, rather than a "wholesale", release of MC-derived mediators (Section 1.2.7). [51] For example, IL-1 and granulocyte/macrophage colony stimulating factor induce the release, only in the picomolar range, of histamine; whereas calcitonin gene-related peptide triggers piecemeal secretion of MMCP-1 from mBMCMCs. [45, 52] Furthermore, monomeric IgE, in the absence of sAg, can also stimulate mBMCMCs. In this case, however, it does not induce degranulation or leukotriene synthesis by the cells but rather a more potent production of proinflammatory cytokines, such as TNFα, IL-6, IL-4 and IL-13,. [53]

1.2.7. MC-derived Mediators

MC-derived mediators (summarized in **Table 1.1**) fall into three main categories: pre-formed mediators, lipid-derived mediators, and cytokines, chemokines and growth factors. Most of these mediators are both pleiotropic and redundant, meaning that each mediator has more than one function, whilst more than one mediator may exhibit the same biological effect. [3, 54, 55]

Pre-formed mediators are synthesized and stored in the cytoplasmic granules. They are generally released within seconds to minutes of MC activation, especially of the IgE-dependent type (Section 1.2.6). Depending on the microenvironment for maturation of any particular MC, its detailed profile of pre-formed mediators may vary. Nevertheless, three broad classes of molecules are always present, including histamine, neutral

Table 1.1. Mast cell-derived immunological mediators and their functions [24, 54, 55, 57]*

MC-derived Mediators		Functions
Pre-formed Mediators	Histamine	Vasodilation; Muscle contraction
	Proteoglycans (e.g. heparin)	Protease packaging and stabilization; Angiogenesis
	Neutral proteases	Matrix degradation; Leukocyte recruitment
Lipid-derived Mediators	Prostaglandins (e.g. PGD_2)	Neutrophil recruitment; Vasodilation; Edema
	Leukotrienes (e.g. LTB_4)	Leukocyte recruitment; Bronchoconstriction
	PAF	Bronchoconstriction
Cytokines, Chemokines, and Growth Factors	TNF**	Leukocyte recruitment; Angiogenesis; Fibroblast activation
	IL-1	Leukocyte recruitment; Angiogenesis
	IL-2	Lymphocyte activation
	IL-3	Leukocyte growth factor
	IL-4	Immunomodulatory (Th2)
	IL-6	Activation of leukocyte and fibroblasts
	IL-8	Neutrophil recruitment
	IL-10	Immunomodulatory (Th2; anti-inflammatory)
	IL-13	Immunomodulatory (Th2); B cell activation
	IL-15**	T cell recruitment and activation
	IL-18	Lymphocyte activation; Angiogenesis
	IFN-γ	Activation of macrophages; Immunomodulatory (Th1)
	TGF-β	Immunomodulatory (anti-inflammatory); Angiogenesis
	VEGF & FGF_2	Angiogenesis
	Chemokines (e.g. CCL2, 3, 4, 5, 11, 20 and CXCL1, 2, 8, 9, 10, 11)	Leukocyte recruitment
	Growth factors (e.g. SCF, GM-CSF, GnRH-1, b-FGF, NGF)	Development, differentiation, maturation and proliferation of various types of cells including MCs

PAF, platelet-activating factor; IL, interleukin; IFN, interferon; TGF, transforming growth factor; VEGF, vascular endothelial growth factor; FGF, fibroblast growth factor; SCF, stem cell factor; GM-CSF, Granulocyte-macrophage colony stimulating factor; GnRH, gonadotropin-releasing hormone; NGF, nerve growth factor.

* The functions listed are immunology-related, with particular regards to during allergic reactions.

** TNF and IL-15 can also be pre-formed and stored in MC granules (see text for more details).

proteases, and proteoglycans, where the former two are generally embedded in a matrix consisted of the latter inside MC granules. [56] Certain mouse MC populations also contain pre-formed TNFα, which serves as an immediate source of this cytokine during IgE-mediated immune responses. [57] In general, the generation of lipid-derived mediators begins within minutes to hours of MC activation, through the cleavage of arachidonic acid from membrane phospholipids. [24] Examples of this category of mediators are prostaglandins (PGs) such as PGD_2 and PGE_2, leukotrienes (LTs) such as LTB_4 and LTC_4, and platelet-activating factor. Within hours of activation, MCs start the *de novo* synthesis of a wide range of cytokines, chemokines and growth factors (**Table 1.1**). [54] Again, depending on the individual development and activation circumstances, the quality as well as quantity of these mediators generated and secreted may differ from MC to MC. It is noteworthy that very few cytokines such as TNFα and IL-15 can be both pre-formed and newly synthesized at later stages of an immune response [57, 58], possibly due to their rapid effects upon release, including vasodilation and/or leukocyte recruitment. [59, 60]

1.2.8. FcεRI Signalling in MCs

FcεRI on MCs is expressed as a heterotetrameric receptor composed of an IgE-binding α-subunit, a signal-amplifying membrane-tetraspanning β-subunit and two identical disulfide-linked γ-subunits, each containing an immunoreceptor tyrosine-based activation motif (ITAM) that is important for conveying activating signals to MCs. [61, 62] Cross-linking of FcεRI-bound IgE molecules with their sAg leads to aggregation of two or more FcεRI receptors and subsequent activation of the receptor-associated protein tyrosine kinases LYN and FYN. LYN, in turn, either phosphorylates the ITAMs in FcεRI and thus recruits and activates another protein tyrosine kinase SYK, or initiates the RAS-mitogen-

activated protein kinase (MAPK) signalling cascade. [62-64] The RAS-MAPK pathway, consisted of RAS, RAF, MAPK kinase (MEK) and MAPKs (e.g. extracellular signal regulated kinase [ERK]1/2, JNK and p38), activates a variety of transcription factors as well as phospholipase A_2 (PLA_2, which participates in arachidonic acid metabolism), thereby regulating the synthesis of protein and lipid-derived mediators, respectively. [65-67] By triggering the phospholipase C_γ (PLC_γ) pathway, SYK subsequently generates diacylglycerol (DAG) and activates protein kinase C (PKC), the latter of which is a regulator for RAS-MAPK pathway as well as MC degranulation and gene transcription. In addition to DAG, PLC_γ activation also generates inositol-1,4,5,-trisphosphate ($InsP_3$), leading to regulation of intracellular calcium (Ca^{2+}) responses and, again, MC degranulation and gene transcription. [68, 69] FYN, on the other hand, phosphorylates the adaptor protein growth-factor-receptor-bound protein (GAB)2, which in turn activates the phosphatidylinositol-3-OH kinase (PI(3)K) pathway. The product of this pathway, phosphatidylinositol-3,4,5,-trisphosphate (PtdIns(3,4,5)P_3), is an important lipid mediator that regulates the activity of various enzymes, such as Bruton's tyrosine kinase (BTK) and protein kinase B (PKB/AKT). Whilst BTK is capable of activating PLC_γ and its downstream events, AKT up-regulates gene transcription either directly or indirectly via activation of nuclear factor (NF)-κB. [70-73] Furthermore, although not shown in **Figure 1.1**, several adapter proteins, in particular the linker for T cell activation and non-T-cell activation linker, also play crucial roles in IgE-dependent MC activation as they (upon phosphorylation by LYN/SYK) help assembling other signalling components in the vicinity of the engaged FcεRI molecules. [74-76]

Figure 1.1. Simplified scheme of FcεRI signalling events in MCs.

Cross-linking of FcεRI-bound IgE with sAg induces aggregation of two or more FcεRI molecules and activates the receptor-associated protein tyrosine kinases LYN, SYN and FYN. By subsequent activation of other key signalling components, such as the RAS-MAPK pathway, PLC_{γ}, PI(3)K, and PKC, degranulation, phospholipid metabolism and/or gene transcription could be resulted, leading to the secretion of a wide array of immunological mediators. See text for more details. Figure is adapted from Galli *et al*. [64]

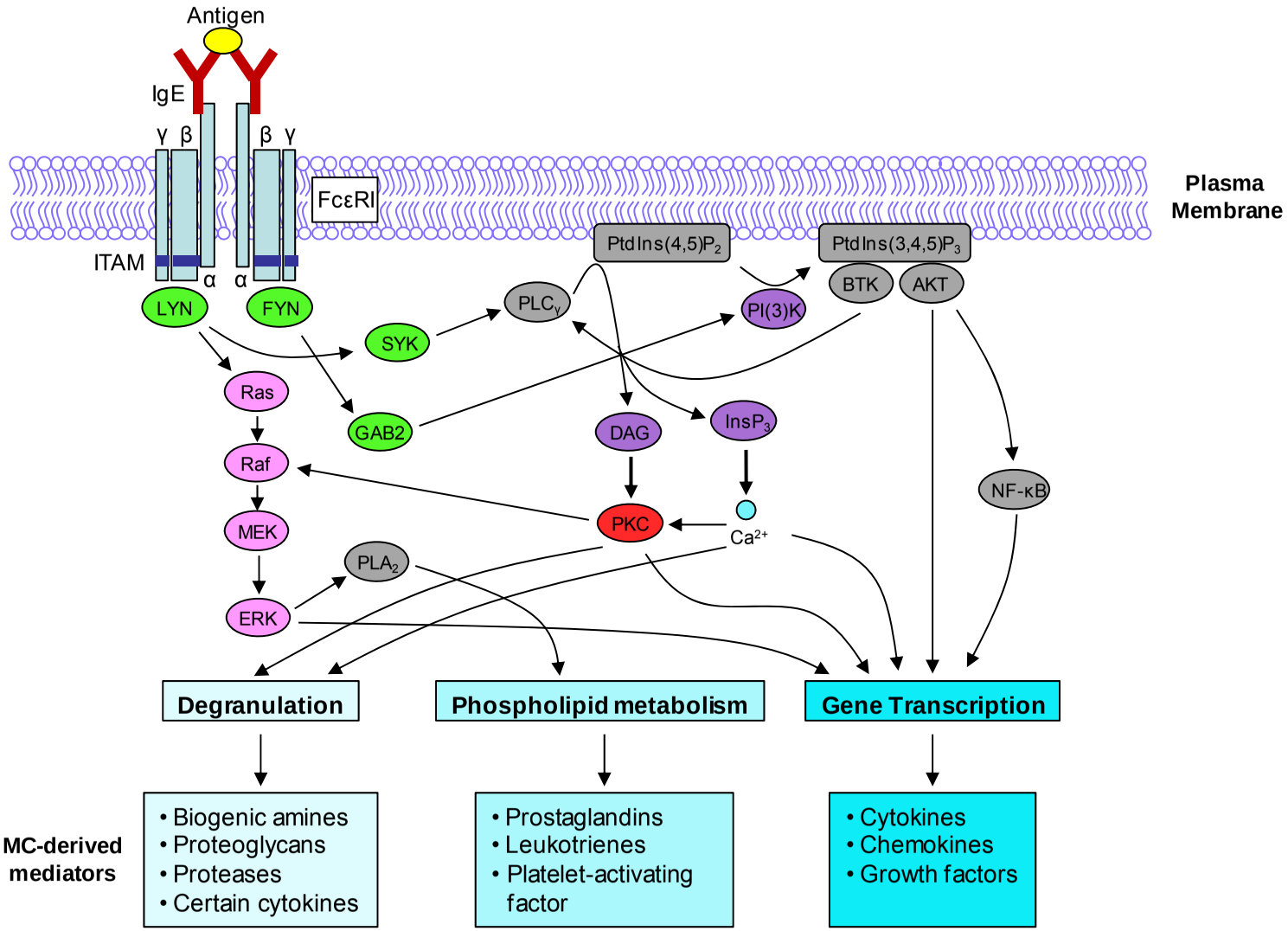
Antigen
IgE
γ β
β γ
FcεRI
ITAM
α
α
LYN
FYN
SYK
PLCγ
PtdIns(4,5)P2
PtdIns(3,4,5)P3
PI(3)K
BTK
AKT
Plasma Membrane
Ras
GAB2
DAG
InsP3
Raf
MEK
ERK
PKC
Ca2+
PLA2
NF-κB
Degranulation
Phospholipid metabolism
Gene Transcription
MC-derived mediators
• Biogenic amines
• Proteoglycans
• Proteases
• Certain cytokines
• Prostaglandins
• Leukotrienes
• Platelet-activating factor
• Cytokines
• Chemokines
• Growth factors

1.3. Biological Functions of MCs in IgE-dependent Allergic Reactions

1.3.1. IgE-dependent Allergic Reactions and MCs

According to the recent national health survey [77], over 25% of Australian population (approximately 5 million people) suffer from IgE-dependent allergic responses. Among children (under the age of 15) and young adults (aged between 15 and 24) in particular, asthma (12%) and hayfever/allergic rhinitis (19%) represent the most prevalent conditions, respectively. What is more alarming, there seems to be stronger overall growth in the number of allergy-affected older Australians in recent years and, if the trend continues, there will be a 70% increase in the number of allergy suffers (to approximately 8 million) by 2050. [78] In addition to reduced quality of life for individuals with allergy, the financial cost of allergies in 2007 alone reached AUS$7.8 billion, with lost productivity and health system expenditure being the major contributing factors, and thus inflicted a substantial burden on the Australian economy. [78] Furthermore, similar increases in the occurrence of allergy are being observed worldwide, especially in western countries, with the marked increase of allergies in children and young adults being the major concern. [79] As a consequence, extensive amounts of research have been carried out to investigate the causes and mechanisms of allergic disorders.

The term “allergy”, first described by Clemens von Pirquet in 1906, refers to an abnormal immune response directed against non-infectious environmental substances named allergens. [64, 80] Although allergy can either involve or not involve allergen-specific IgE molecules, this thesis will focus on IgE-dependent allergic responses, some examples of which are anaphylaxis, hayfever, atopic dermatitis (eczema), allergic asthma, and some

food allergies. [64, 81] Most, if not all, of these reactions are triggered by Ags that induce IgE production and subsequent "sensitisation" of host MCs. Common sources of allergens include pollens, house-dust-mite faecal particles, animal dander, certain foods (e.g. peanuts, fish, milk and eggs), latex and insect venoms. [64] The induction of IgE production by these allergens reflect their ability to elicit a T helper (Th)2 response and increase the levels of IL-4 and IL-13, thus promoting immunoglobulin class switching (i.e. towards IgE) recombination in B cells. [82-84] Furthermore, MCs express CD40L on their surface and can therefore stimulate B cells through CD40. [85] This, together with the ability of already sensitised MCs to produce IL-4 and IL-13, raises the possibility that MCs can further drive IgE production, sensitisation of additional cells, and epitope spreading. Thus well before the onset of any allergic responses, MCs have set the stage for a detrimental outcome. [64, 86]

In general, IgE-dependent allergic reactions can be classified into three temporal phases: early-phase reactions, late-phase reactions and chronic reactions. [64] The key features of, as well as the roles of MCs during, each of these phases will be described in details in the following sections.

1.3.2. Functions of MCs during Early-phase Allergic Reactions

Early-phase allergic reactions (**Figure 1.2**), also referred to as Type I immediate hypersensitivity reactions, occur within minutes of allergen exposure and are mainly caused by MC-derived pre-formed mediators (Section 1.2.7) at the affected site. [81] For example, rapidly released histamine, PGDs and LTs are responsible for the commonly seen vasodilation, increased vascular permeability and bronchoconstriction during early-

Figure 1.2. Early-phase allergic reactions (in the airway)

The binding of a particular allergen to its cognate FcεRI-bound IgE molecules leads to receptor aggregation, MC activation, and the secretion of all three classes of MC-derived mediators. The rapidly released mediators, such as histamine and TNFα, result in bronchoconstriction, vasodilation, increase vascular permeability and increased mucus production from goblet cells. MCs also promote an influx of other inflammatory leukocytes, by up-regulating adhesion molecules on vascular endothelial cells (e.g. via TNFα) as well as secreting chemotactic mediators (e.g. PGD_2 and LTB_4) and chemokines (e.g. IL-8 and CCL2), and thus contributing to the transition from early- to late-phase reaction. See text for more details. Figure is adapted from Galli *et al*. [64]

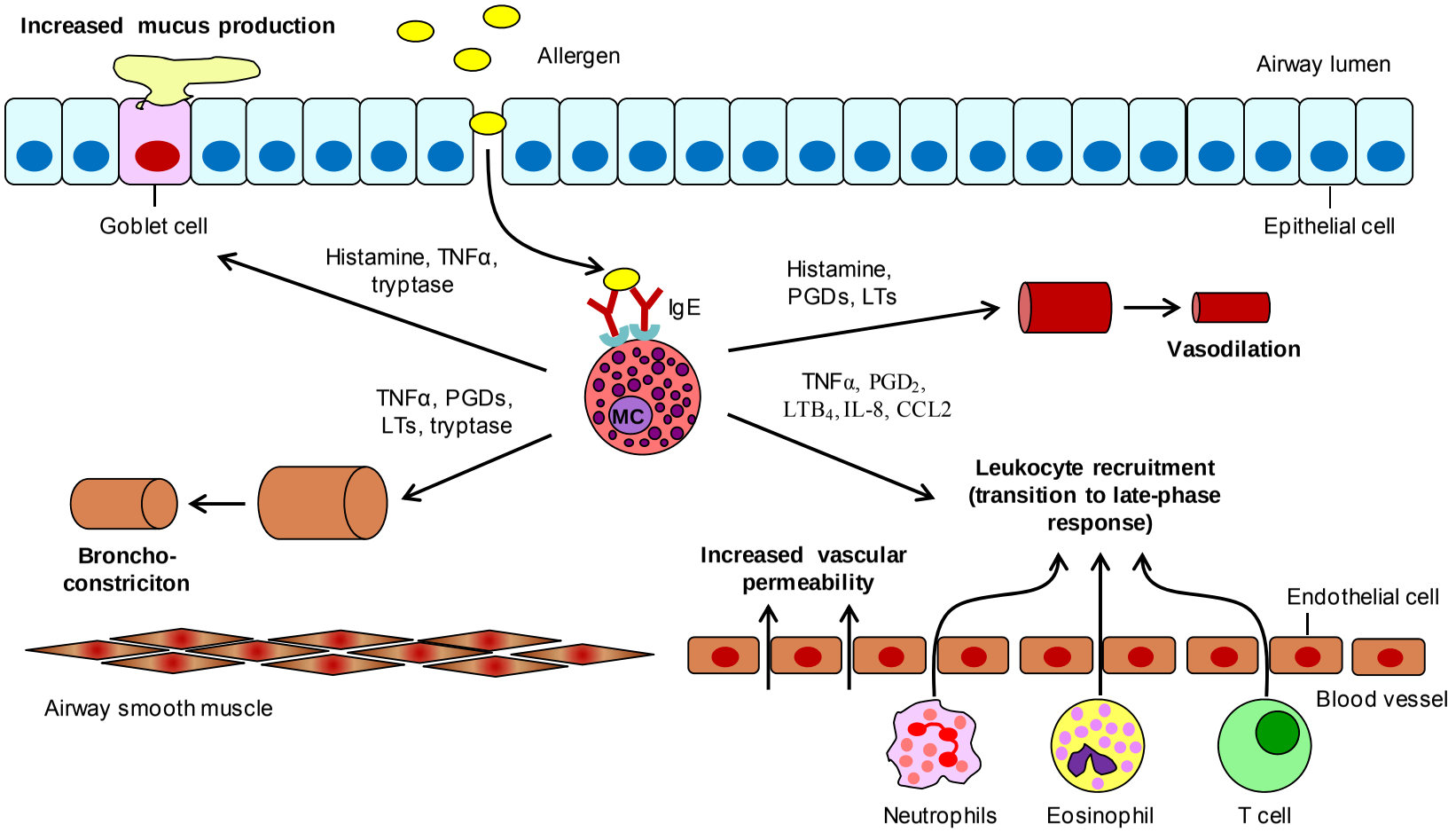
Increased mucus production
Allergen
Airway lumen
Goblet cell
Epithelial cell
Histamine, TNFα, tryptase
IgE
Histamine, PGDs, LTs
Vasodilation
TNFα, PGDs, LTs, tryptase
MC
TNFα, PGD2, LTB4, IL-8, CCL2
Broncho-constriciton
Leukocyte recruitment (transition to late-phase response)
Increased vascular permeability
Endothelial cell
Blood vessel
Airway smooth muscle
Neutrophils
Eosinophil
T cell

phase airway inflammation. [87, 88] Several mediators, such as histamine, TNFα and tryptase, can also lead to increased mucus production by goblet cells. Moreover, MCs can initiate the recruitment and/or activation of other leukocytes, and thus contributing to the onset of late-phase reactions, both by up-regulating adhesion molecules on vascular endothelial cells through TNFα secretion and by releasing various chemotactic mediators (e.g. LTB_4 and PGD_2) and chemokines (e.g. macrophage inflammatory protein 2, IL-8 and CCL2). [64, 89, 90] Although basophils, which also express FcεRI, may contribute to early-phase responses by producing similar mediators, this is less likely under normal circumstances due to a paucity of basophil populations at peripheral tissues. [91] In addition to the localised events mentioned above, early-phase allergic reactions can also be systemic (i.e. anaphylaxis), where mediators from MCs (e.g. histamine) and/or basophils (e.g. platelet-activating factor) are released into circulation via IgE- and IgG-mediated mechanisms, respectively. [87, 92-94]

1.3.3. Functions of MCs during Late-phase Allergic Reactions

In contrast to early-phase reactions, late-phase reactions (**Figure 1.3**) typically develop within 2-6 h of allergen exposure, and largely reflect the actions of mediators from a variety of recruited leukocytes, including firstly neutrophils followed by eosinophils, basophils and T cells. [87, 95] For example, elastase released by newly recruited neutrophils can promote the activation of matrix metalloproteinases (MMPs) and the degradation of Type III collagen [96], eosinophil-derived basic proteins are shown to cause damage to epithelial linings at allergic sites [97], and IL-13 produced by T cells and basophils can contribute to continuing mucus hyper-production and/or bronchoconstriction [91, 98]. In this regard, the main roles of MCs during this stage of the responses include maintaining

Figure 1.3. Late-phase allergic reactions (in the airway)

Although sharing many features in common with early-phase reactions, last-phase allergic reactions typically occur hours after allergen challenge and are thought to reflect the actions of innate (e.g MCs, neutrophils, basophils and eosinophils) and adaptive (e.g. allergen-specific Th2 cells) immune cells that are resident or have been recruited from the circulation, as well as the release of inflammatory mediators by tissue-resident cells (e.g. epithelial cells). Therefore, MCs contribute to a late-phase reaction predominantly by maintaining the influx of immune cells, activating certain innate cell types (e.g. neutrophils, basophils and eosinophils) and regulating the functionality of others (e.g. T cells, B cells and DCs [not shown]). See text for more details. Figure is adapted from Galli *et al*. [64]

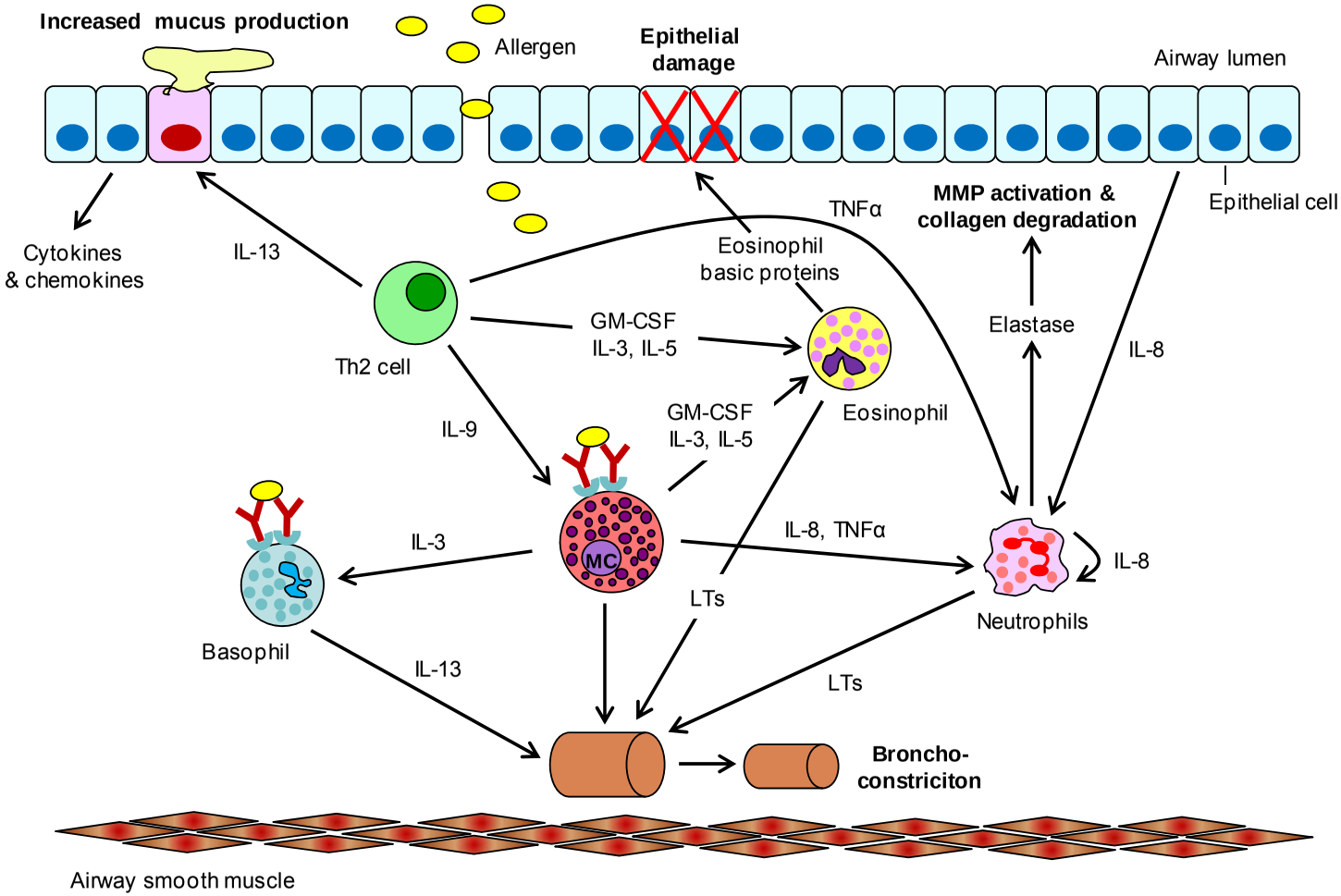
Increased mucus production
Allergen
Epithelial damage
Airway lumen
Epithelial cell
Cytokines & chemokines
IL-13
TNFα
MMP activation & collagen degradation
Eosinophil basic proteins
GM-CSF IL-3, IL-5
Th2 cell
Eosinophil
Elastase
IL-8
IL-9
GM-CSF IL-3, IL-5
IL-3
MC
IL-8, TNFα
IL-8
LTs
Basophil
Neutrophils
IL-13
LTs
Broncho-constriciton
Airway smooth muscle

the influx of these other cell types, activating innate immune cells (e.g. neutrophils by TNFα and eosinophils by IL-5), and affecting many aspects of the functionality of dendritic cells, T cells and B cells (by TNFα, IL-10 and TGF-β). [11, 99] It is, however, important to realise that although MCs are generally regarded as proinflammatory effector cells during allergic reactions, some mediators they secrete, such as IL-10, TGFβ and MMCP-4, do display anti-inflammatory or immunosuppressive properties. [99, 100] Furthermore, certain MC-derived mediators (e.g. histamine, PGDs, LTs, TNFα, IL-4, IL-13 and tryptase) can also affect the biology of various structural cells, including vascular endothelial cells, epithelial cells, fibroblasts, smooth muscle cells and goblet cells. [64, 101]

1.3.4. Functions of MCs during Chronic Allergic Reactions

Chronic allergic reactions (**Figure 1.4**) can develop as a result of repetitive exposure to an allergen. Characteristic of such reactions is the accumulation of a large variety of innate and adaptive immune cells, and the phenotypical as well as functional changes in structural cells (e.g. fibroblasts, myofibroblasts and airway smooth muscle [ASM] cells) at the affected sites. [64] These reactions are often detrimental to the host as they can quickly escalate significant alterations to tissue architecture if left unrestrained. For example, patients with chronic asthma often suffer from substantial thickening of the airway walls and bronchoconstriction, which together cause severe narrowing of the airway lumen. [102, 103] Increased deposition of extracellular matrix proteins (e.g. fibronectins and collagens), hyperplasia of goblet cells, and the resultant additional mucus production are some of the other hallmarks of chronic asthma. Similar tissue remodelling processes are also evident in chronic cases of allergic rhinitis [104] and atopic dermatitis [105], leading to the formation of nasal polyps and fibrotic papules, respectively.

Figure 1.4. Chronic stage of allergic reactions (in the airway)

In chronic allergic reactions, more MCs are recruited to and develop in the tissues. Together with other tissue-resident as well as newly recruited innate (e.g. neutrophils, basophils and eosinophils) and adaptive (e.g. Th2 cells, B cells and DCs) immune cells, they interact with epithelial cells, structural cells (e.g. fibroblasts, myofibroblasts and airway smooth muscles), blood vessels and lymphatic vessels, thus contributing to airway smooth muscle hyperplasia, bronchoconstriction and severe narrowing of airway lumen, goblet-cell metaplasia and many other symptoms of chronic airway allergy. Exacerbated by exposure to pathogens and/or environmental factors, chronic allergy-induced epithelial injury and the consequent repair response can result in the establish of EMTU. This unit helps to sustain a Th2-associated microenvironment, and thereby promoting sensitization to additional allergens or allergen epitopes and regulating the airway remodelling process. See text for more details. Figure is adapted from Galli *et al*. [64]

FGF, fibroblast growth factor; PDGF, platelet-derived growth factor; EGF, epidermal growth factor; VEGF, vascular endothelial growth factor.

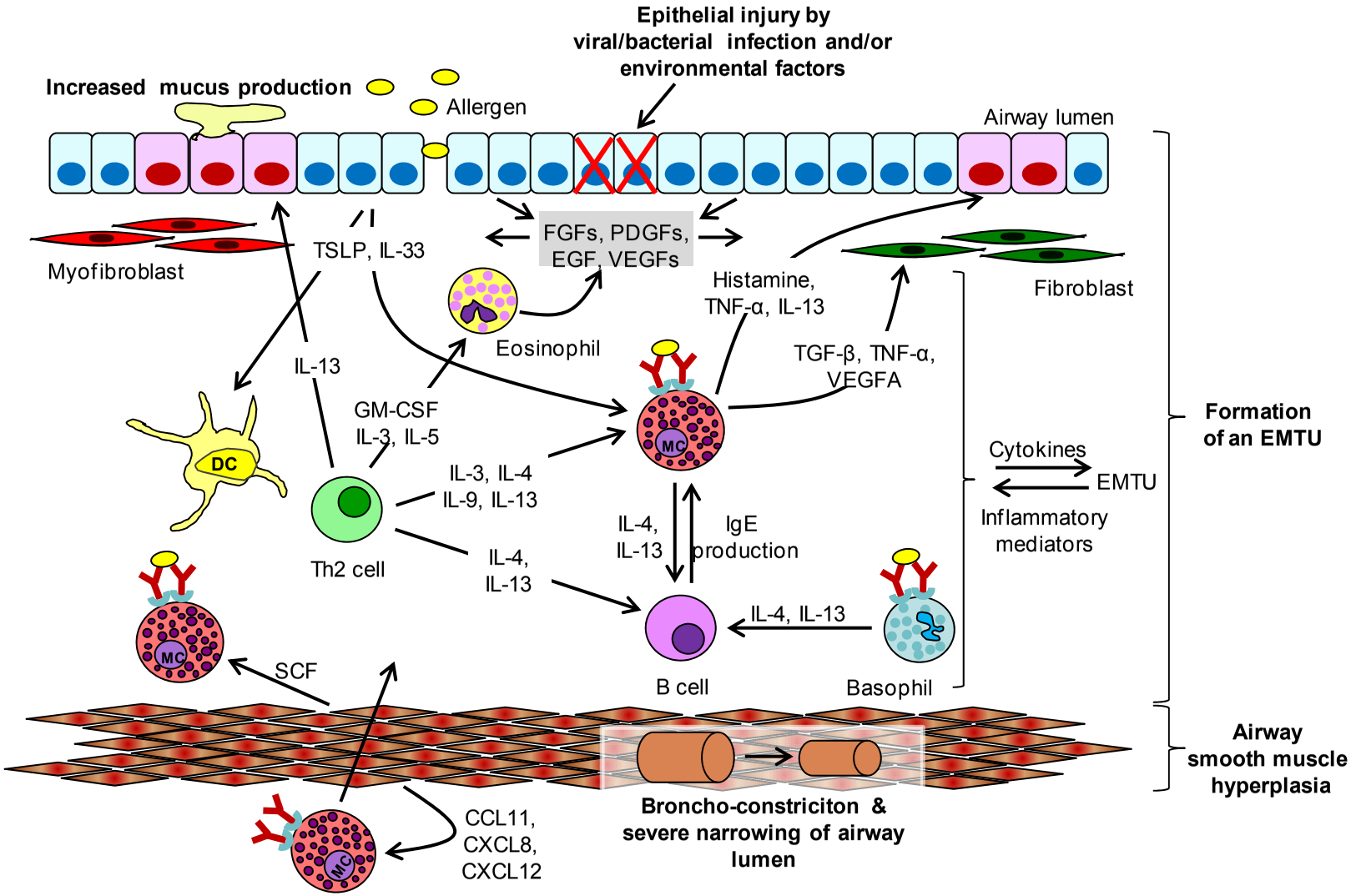
Epithelial injury by
viral/bacterial infection and/or
environmental factors
Increased mucus production
Allergen
Airway lumen
FGFs, PDGFs,
EGF, VEGFs
Myofibroblast
TSLP, IL-33
Histamine,
TNF-α, IL-13
Fibroblast
Eosinophil
TGF-β, TNF-α,
VEGFA
IL-13
GM-CSF
IL-3, IL-5
DC
MC
Cytokines
EMTU
Inflammatory
mediators
Formation
of an EMTU
IL-3, IL-4
IL-9, IL-13
IL-4,
IL-13
IgE
production
Th2 cell
IL-4,
IL-13
IL-4, IL-13
MC
SCF
B cell
Basophil
Airway
smooth muscle
hyperplasia
Broncho-constriciton &
severe narrowing of airway
lumen
MC
CCL11,
CXCL8,
CXCL12

Furthermore, at sites of chronic allergy, damaged epithelial cells and substantial alterations in their barrier functions can result in a higher risk of infections by pathogens or environmental factors. [105-107] Such infections, in the cases of chronic asthma, can in turn exacerbate the signs and symptoms of the disease. [106] Although the precise mechanisms underlying such exacerbation are not yet fully elucidated, an epithelial-mesenchymal trophic unit (EMTU) is thought to be a contributor, as it is established upon repetitive epithelial damage-repair cycles caused by infections and has been shown to sustain a Th2 environment and therefore promote sensitisation to additional allergens. [108] In addition, disruption of the epithelial barrier can also activate keratinocytes and tissue dendritic cells (DCs) to release thymic stromal lymphopoietin (TSLP) and IL-10, respectively, both of which can then enhance Th2 cell differentiation and contribute to the chronic phase of allergic responses. [105]

In the case of chronic asthma, MC hyperplasia is often observed near ASM linings and within the EMTU. At these sites, they further interact with structural cells and thus contribute to many of the hallmarks of the disease, including severe bronchoconstriction, mucus hypersecretion, tissue fibrosis, and the development of "non-specific airway hyperreactivity" to histamine and LTs. [64] An interesting feature associated with chronic stages of the disease is the interaction between MCs and structural cells that becomes reciprocal as the number and functionality of the former are also affected by the latter. For example, ASM cells produce several MC chemotactic factors (e.g. CCL11, CXCL8 and CXCL12) and growth factors (e.g. SCF), resulting in further recruitment and local proliferation of MCs, respectively [101, 109] Epithelial cells within the epithelial-mesenchymal trophic unit also produce TSLP and IL-33, both of which are correlated

with the severity of asthma, likely due to their ability to induce DC-mediated Th2 differentiation and to recruit and activate Th2 cells, respectively. [110-112] The fact that MCs express receptors for both of these cytokines indicates that they can be activated by both to exacerbate the inflammatory response and/or regulate airway remodelling. [111, 112] Moreover, the ability of MCs to be activated by bacterial or viral products (e.g. via TLRs) suggests a role of these cells also during pathogen-mediated exacerbation of allergic symptoms. [101, 113, 114] It should be mentioned that although dispensable for the early- and late-phase responses, basophils play a crucial role in initiating the development of IgE-mediated chronic allergic inflammation of the skin by secreting cytokines and other mediators that in turn act on tissue-resident cells (e.g. fibroblasts) as well as induce recruitment of other leukocytes. [115, 116]

1.3.5. Treatment Strategies for Allergic Reactions and MCs

Although the recent increase in allergy occurrence can be, to some extent, explained by the "hygiene hypothesis", allergy remains a multifactorial disorder, with environmental, genetic, dietary and other lifestyle factors all contributing and possibly interacting as well. [117] It is, therefore, imperative that we continue to widen our understanding of the mechanisms of allergic disorders and, more importantly, continue to develop new treatment strategies.

The two fundamental elements of allergy management are allergen avoidance, both before and after sensitisation, and treatments for individuals with the disorder. [64, 118] Whilst the former strategy is self-explanatory, the application of the latter requires consideration of individual circumstances. For instance, α-adrenoceptor agonists and non-

sedating H1-antihistamines and topical corticosteroids are well-established treatments for allergic rhinitis sufferers; whereas inhaled corticosteroids and β2-adrenoceptor agonists are currently the mainstay of asthma management. [118]

Due to the substantial involvement of MCs in all three phases of IgE-dependent allergic reactions (Section 1.3.1), new allergy treatment strategies that either directly or indirectly alter the functionality of these cells and/or their mediators have been developed. Allergen-specific immunotherapy, via increasing the level of allergen-specific IgA and IgG4 and decreasing that of allergen-specific IgE, can inhibit MC sensitisation and mediator release, as well as reducing MC numbers in affected tissues. [118] Allergen-specific immunotherapy also induces T regulatory (T_{reg}) cells to produce IL-10, which in turn suppress the pro-allergic effects of MCs and their mediators. [119] Similarly, the use of the IgE-specific antibody (Ab) omalizumab leads to reduced levels of free IgE molecules, decreased expression of the high affinity IgE receptor (FcεRI) on MCs, and ultimately reduced secretion of MC-derived mediators. [120-122] Furthermore, a number of allergy treatments that directly target MC activation have also been reported. [123-125]

1.4. Other Biological Functions of MCs

1.4.1. Roles of MCs in Homeostasis

Although MCs are usually studied in pathological scenarios, they also contribute to a number of homeostatic processes. [4] They are important players in all three phases of wound healing: inducing recruitment of other inflammatory cells to the injured site (via corresponding chemotactic factors) during the "acute inflammatory phase", promoting re-

epithelialisation and angiogenesis (via angiogenic factors) during the "proliferative phase", and finally increasing proliferation of epithelial cells and fibroblasts (via vascular endothelial growth factor, platelet-derived growth factor, fibroblast growth factor and nerve growth factor) and thus contributing to tissue scarring and remodelling during the "remodelling phase". [126] MC-derived histamine, TNFα and substance P are also involved in hair follicle recycling [127], whereas the production of osteopontin is shown to participate in bone resorption and calcification [128].

1.4.2. Roles of MCs in Parasitic Infections

IgE-dependent allergic disorders can be viewed as consequences of "misdirected" Th2 responses that have originally evolved as a host-defence mechanism against parasites. In regard to MC biology, the two scenarios do share a number of similarities. For example, during parasitic infections, MCs become heavily sensitized with parasite Ag-specific IgE that are present at high levels. MC numbers and the amount of MC-derived mediators also increase dramatically at the infected sites. [129] However, direct evidence for the involvement of MCs in protective immunity against parasites comes from only a handful of studies to date. [4, 86] For instance, it is demonstrated that both MCs and intact IgE are required for optimal resistance to a secondary infestation of mice skin with larval Ixodid *Haemaphysalis longicornis* ticks, although basophils may also contribute to such protection. [86, 130] In addition, MMCP-1-deficient mice are unable to expel *Trichinella spiralis*, suggesting the anti-helminth properties of this protease, most likely by impairing the epithelial-cell barriers and thus increasing luminal fluid flow and expulsion of the parasites. [131-133] On the other hand, MMCP-1 has little effect on host defense against *Nippostrongylus brasiliensis* which, unlike the intestinal-epithelial-cell-syncytia-residing

T. spiralis, inhabit the intestinal lumen. This seemingly contradicting data raises the possibility that MC-derived mediators may be more efficient at expelling tissue-dwelling nematodes, potentially by increasing vascular permeability and promoting recruitment of other leukocytes. [132, 134] Furthermore, MCs, among many other cell types such as T cells, basophils and eosinophils, are also a major source of IL-4 and IL-13, both of which play key roles in host resistance to helminth infections. [129]

1.4.3. Roles of MCs in Bacterial and Viral Infections

There has been a substantial amount of evidence indicating important sentinel and effector roles of MCs during bacterial infection, which promote clearance of the bacteria, protect the host from detrimental pathology and enhance survival. Mechanistic explanations for these roles include MC activation via TLR4 and anaphylatoxins, phagocytosis of bacteria, enhancement of the recruitment and/or function of granulocytes, and the proteolytic degradation of endogenous mediators that would otherwise accumulate to toxic levels, such as endothelin-1 and neurotensin. [135, 136] There are, however, a few instances where MCs are shown to increase mortality caused by bacterial infection, via the production of TNFα or dipeptidyl peptidase-I (which in turn reduces IL-6 levels). [137, 138] Therefore, it seems that depending on the intrinsic properties of MCs as well as genetic predispositions of the host to produce larger or smaller amounts of TNFα [137] and other cytokines, the type and/or severity of the bacterial infection can be influenced by MCs to be either beneficial or harmful.

Similarly, MCs also serve as a double-edged sword during viral infections. On one hand, upon activation via TLRs (e.g. TLR3 in response to viral double-stranded RNA), rodent

and human MCs can release an array of chemokines and cytokines, including interferon (IFN)α and IFNβ, that contribute to host defense against viruses. [48, 113] On the other hand, co-stimulation of rodent and human MCs via FcεRI and certain TLR can trigger MC secretion of various pro-inflammatory mediators, suggesting a possible mechanism through which MCs might contribute to virus- (and bacteria-) mediated exacerbation of allergic asthma and other IgE and MC-associated disorders (Section 1.3.1). [113] Furthermore, some viruses such as human immunodeficiency virus (HIV) in particular, can infect MC progenitors, which maintain their viral contents during maturation at multiple tissues [139, 140], thus making human MCs a reservoir of persistent HIV infection [141, 142]. In these cases, MC exposure to TLR2, -4, or -9 ligands can trigger HIV-1 replication in latently infected cells, and IgE-FcεRI interactions as well as viral Tat protein has been shown to up-regulate HIV-1 co-receptor (e.g. CCR3) expression by MCs, rendering them more susceptible to HIV infection. [141, 143]

1.4.4. Roles of MCs in Cancers

There is currently controversy regarding the roles of MCs in cancers, as evidence supporting both positive and negative contribution of these cells in various tumor models is present. On one hand, MCs have been reported to accumulate in adenomatous polyps and are required for polyp formation, which is the initiating step of colon cancer. [144] In this study, MC-derived TNFα is suggested responsible for the expansion of MC population at the site of tumor formation. In addition, studies on skin carcinogenesis in MC-deficient WBB6F$_1$-*Kit*$^{W/Wv}$ mice indicate the capacity of MCs to facilitate angiogenesis during early stages of tumor progression. [145] Experiments with another MC-deficient mouse strain (C57BL/6-*Kit*$^{W\text{-}sh/W\text{-}sh}$) also provide evidence that MCs are

required for angiogenesis and macroscopic expansion of c-Myc-induced pancreatic β-cell tumors. [146] However, due to the importance of c-kit signalling and the involvement of non-MC leukocyte lineages during angiogenesis [147], the MC-specific roles in the above *Kit* mutant mice remain to be validated (e.g. via WT MC engraftment experiments). On the other hand, there are certain tumor models in which MCs seem to be beneficial to the host. For example, the offspring of C57BL/6-*Kit*$^{W\text{-}sh/W\text{-}sh}$ mice and mice that bear early intestinal tumorigenesis exhibit greater frequency and size of adenomas with less tumor cell apoptosis and eosinophil infiltration, thereby indicating a protective function for MCs in colorectal tumorigenesis. [148] One possible conclusion drawn from these seemingly contradicting studies is that, similar to the plasticity displayed during bacterial and viral infections, the net contribution of MCs in various tumor models may favour either the tumor or the host depending on the genetic variables as well as microenvironmental factors within the precise tumor model employed. [148, 149]

1.4.5. Roles of MCs in Chronic Obstructive Pulmonary Diseases (COPD)

Cigarette smoke-induced COPD is a debilitating disorder of the lung, with systemic effects in the skeletal muscle, heart, as well as the other organs, and is the fourth leading cause of chronic morbidity and death worldwide. [150-152] Previous studies showed accumulated MCs in patients with COPD, [153, 154], where MC-derived tryptase-β (human) levels in sputum are also correlated with the severity of the disease. [155] Interleukin-3-dependent MCs exposed to cigarette smoke-treated culture medium also led to increased expression of MMCP-6, a tryptase known to promote hallmark features of COPD such as inflammation, chemokine secretion, and macrophage and neutrophil chemotaxis. [156, 157] With the aid of a recently developed short-term mouse model of cigarette-induced COPD,

Beckett *et al*. showed, for the first time, indirect and yet detrimental roles for MMCP-6 and human tryptase-β by causing macrophage accumulation, and macrophage-mediated inflammation, tissue remodelling and emphysema, respectively. [158] In a separate study, the same group further revealed the adverse functional roles of another mouse MC-derived tryptase, Prss31/transmembrane tryptase/tryptase-γ; as Prss31-null mice showed attenuated macrophage and neutrophil accumulation and reduced histopathology in their lungs following smoke treatment. [159] These observations were consistent with previous knowledge that individuals deficient in α_1-antitrypsin (A1AT), are more susceptible to COPD development, [160] and that recombinant human Prss31 can be rapidly inactivated by A1AT. [161]

1.4.6. Negative Immunoregulatory Roles of MCs

In this thesis, a number of key effector as well as positive immunoregulatory roles of MCs have been reviewed, in the context of either IgE-mediated or non-IgE-mediated immune responses. Indeed, MCs have been historically regarded as positive contributors in these settings; and it was not until recent years that certain negative immunoregulatory effects of these cells have been identified. [11, 86, 99] For example, UVB-induced histamine production by MCs can help to suppress sensitisation for CHS responses to 2,4,6-trinitrochlorobenzene in mice. [5] Although the exact mechanisms/mediators involved remain to be defined, MCs have been shown to optimise peripheral tolerance to skin allografts [8] and also contribute to the *Anopheles* mosquito bite-induced suppression of the development of Ag-specific T cell responses in a delayed type hypersensitivity setting [6]. In the former regard, however, it is recently shown that IgE-dependent MC degranulation, either within the graft or systemically, can break established peripheral

tolerance or lead to T cell-mediated acute rejection of skin allograft. [162] The authors demonstrate that MC-derived mediators, such as MMCP-1, IL-4, IL-13 and RANTES, cause a rapid migration of both T_{reg} and MCs out of the graft as well as a transient demise in the secretion of suppressive T_{reg} cytokines. [162]

Furthermore, a considerable number of studies have highlighted the importance of MC-derived IL-10, an anti-inflammatory cytokine, in conveying certain immunosuppressive effects, including suppression of the production of pro-inflammatory cytokines and/or chemokines by both immune (e.g. T cells and monocytes) and structural (e.g. keratinocytes) cells, and enhancement of the ability of DCs to reduce T cell proliferation and cytokine production. [86, 99] Recent studies by Grimbaldeston *et al.* [7] and Biggs *et al.* [163] demonstrated that the mechanisms leading to MC production of IL-10 may also vary in different settings, as the IgG_1-FcγR signalling pathway is required for MC-IL-10-mediated suppression of many features of severe CHS responses [7], whereas $VitD_3$- and MC VDR-dependence is evident for IL-10 production by skin MCs and subsequently limited pathology associated with chronic low-dose UVB irradiation [163]. In contrast to the above beneficial roles, MC-derived IL-10 can also be harmful for the host. In particular, dermal MCs have been shown to migrate to the draining LNs upon UV irradiation and contribute to immune suppression [19]; whilst C57BL/6-*Kit*$^{W\text{-}sh/W\text{-}sh}$ mice engrafted with *IL-10*$^{-/-}$ BMCMCs, unlike their WT and WT mBMCMC-engrafted counterparts, failed to demonstrate UV-induced suppression of T follicular helper cell function, germinal centre formation and humoral immune response associated with regional LNs. [164]

1.5. Experimental Tools for MC Research

1.5.1. In Vitro Tools

MC research had been hindered until recently due to the difficulties in obtaining sizable and experimentable *ex vivo* MC cultures from *in vivo* tissues, where these cells are normally present in low numbers. Although rodent peritoneal MCs are relatively abundant, can be easily accessed and enriched to near purity [165], the isolation process is usually labour-intensive and the enzymatic dispersion utilised disrupts normal cell phenotype and cell-to-cell interactions. In addition, due to the facts that there are significant species differences in MC properties and that the human peritoneal cavity has few MCs, extrapolation of results from rodent peritoneal MCs to human MCs must be carefully considered and adjusted based on individual circumstances. [4] For this reason, MCs isolated from human skin, mucosae (e.g. lung and intestine), heart, uterus and kidney have also been studied. [166] Unfortunately, this approach is disadvantaged by the limited source of fresh tissue specimens, low cell yields and cumbersome isolation and purification procedures involved. [167, 168]

To avoid the difficulties in generating tissue-isolated MC cultures, several MC lines have been developed, such as rat RBL-2H3, mouse MC-9 and human HMC-1 and LAD-2. [4, 166] Despite their abundances and ease of culture, they are transformed cells in nature and therefore could display markedly altered functions. The HMC-1 line, for example, was established from peripheral blood of a MC leukemia patient. [169] As a result, these cells are immature, independent of SCF for growth, and lack well-formed granules as well as functional IgE receptors. Subsequent development of the more mature human MC lines,

LAD-1 and -2, from BM aspirates of a patient with MC sarcoma/leukemia, partially overcame these problems as these cell lines do require SCF for their survival and growth, have the ultrastructural features of human MCs with numerous granules, express surface FcεRI, and degranulate readily upon IgE-mediated activation. [170]

Furthermore, since the early 1980s, primary cultures of MCs from their progenitors have been developed for both mice (e.g. mBMCMCs [171, 172], fetal skin-derived MCs [173], fetal liver-derived MCs [174] and spleen-derived MCs [175]) and humans (e.g. BM-derived MCs [176], fetal liver-derived MCs [177], cord blood-derived MCs (hCBMCs) [178] and more recently peripheral blood-derived MCs [179]). Major drawbacks with this approach are the long (usually 5-12 weeks) and expensive (due to the use of cytokine cocktails) culturing process required,. [166] Moreover, although occasionally considered an advantage rather than disadvantage, *in vitro* cultured primary MCs can represent heterogeneous populations depending on their exact culturing conditions. [4] For instance, whereas IL-3 alone drives the development of typical mBMCMCs, which generally appear immature and MMC-like; the combination of IL-3 and SCF can increase the ratio of MCs to basophils during early-stage (up to 11 days) culturing as well as generate a more mature phenotype of MCs. [180, 181] Mouse BMCMCs cultured in the presence of SCF and IL-4 (i.e. no IL-3), on the other hand, give rise to a more CTMC-like population regarding their histochemical properties and response to certain stimuli, including IgE + sAg and substance P. [165]

While it is important to recognise the limitations of each of the *in vitro* MC-research tools mentioned above, they are nevertheless important sources of MCs and each provides a unique platform to study various aspects of MC biology *in vitro*.

1.5.2. In Vivo Tools

To determine whether MCs play a role in the development of a particular human disease, the number of MCs and/or the level of their mediators between normal and pathologic tissues are generally compared and any significant difference would indicate an affirmative answer. Alternatively, the *c-kit* mutant and thus MC-deficient WBB6F$_1$-*Kit*$^{W/W\text{-}v}$ and C57BL/6-*Kit*$^{W\text{-}sh/W\text{-}sh}$ mice have been widely used, together with their WT counterparts, in the field of MC research. Both mouse strains are profoundly deficient in MCs but also carry other significant phenotypic abnormalities. [11, 137, 182] *Kit*^{W} is a point mutation that causes exon skipping and produces truncated c-kit that is not expressed on the cell surface; *Kit*^{Wv} is a point mutation in the tyrosine kinase domain of *c-KIT*; and *Kit*$^{W\text{-}sh}$ is an inversion mutation that affects the transcriptional regulatory element upstream of the *c-kit* transcription start site on mouse chromosome 5. [182, 183] In addition to a profound deficiency in MC and melanocytes populations, adult WBB6F$_1$-*Kit*$^{W/W\text{-}v}$ and C57BL/6-*Kit*$^{W\text{-}sh/W\text{-}sh}$ mice exhibit other abnormalities including, for the former, macrocytic anaemia, sterility, reduced numbers of BM and blood neutrophils, and lack of interstitial cells of Cajal as well as T cell receptor (TCR)γδ cells in the small intestine; and, for the latter, enlarged spleen, mild cardiomegaly, and increased numbers of BM and blood neutrophils. [137, 182, 183] Unlike the WBB6F$_1$-*Kit*$^{W/Wv}$ strain, however, C57BL/6-*Kit*$^{W\text{-}sh/W\text{-}sh}$ mice are not anaemic, have normal populations of TCR$_{\gamma\delta}$ cells in the intestines and did not exhibit a high incidence of idiopathic dermatitis, ulcers, or squamous papillomas of the stomach. [182]

Due to these additional phenotypic abnormalities, differences in biological responses between WBB6F$_1$-*Kit*$^{W/W\text{-}v}$ and C57BL/6-*Kit*$^{W\text{-}sh/W\text{-}sh}$ mice and WT controls may not

necessarily be caused by their MC deficiency. By repairing the MC deficiency through selective systemic (e.g. intravenous [*i.v.*]) or local (e.g. intraperitoneal [*i.p.*] and intradermal [*i.d.*]) engraftment of genetically compatible and *in-vitro*-derived WT or mutant MCs, so-called "MC knock-in" mice that differ from their *c-kit* mutant parental strains solely because of the presence of MCs, or mice that differ from each other solely because of the genotype of the MCs engrafted, have been developed and become invaluable in the field of MC research. [137, 182] It should be noted that many MC-related studies today employed both MC-deficient mouse strains so as to confirm specific MC-dependent function(s) *in vivo* irrespective of their individual genetic background and additional abnormalities.

The role of specific MC-derived mediators, on the other hand, can be examined *in vivo* by using animals in which the mediator-encoding gene has been knocked out. Examples of these animals are mice that lack MMCP-1[132], MMCP4 [28], tryptase β-2/MMCP-6 [157], or mouse MC carboxypeptidase A3 [184], all of which have been used to determine whether the absence of the corresponding protease can affect other aspects of MC phenotype and/or function. However, before definitive conclusions can be drawn, one must take into consideration the extent to which a particular mediator is selectively expressed by MCs, as well as any influence the deletion of the particular mediator has on the expression of other MC-derived products. [86]

The most recent approach to develop new *in vivo* tools for MC research led to the generation of MC-specific "Cre" mice, where Cre recombinase is expressed under the control of the promoter of the gene encoding either MMCP-5 (called Mcpt5 by the authors) [185] or baboon α-chymase [186]. In the former study, crossing the Mcpt5-Cre

transgenic mice with the ROSA26-EYFP Cre excision reporter strain revealed Cre-mediated recombination in MCs from the peritoneal cavity and the skin, with minimum reporter gene expression outside the MC compartment. [185] In the latter case, on the other hand, the Chymase-Cre-ROSA26R mice generated showed Cre-mediated recombination in MCs from the lungs and colon tissue but not from the peritoneal cavity or *in-vitro*-derived BMCMCs. [186] More recently, Dudeck *et al.* generated mouse models of inducible or constitutive MC deficiency based on the *Mcpt5-Cre* mice. [187] For the inducible MC deficiency model, *Mcpt5-Cre* mice are bred to the *iDTR* strain [188], in which Cre-mediated excision of a *loxP*-flanked STOP cassette would render cells sensitive to diphtheria toxin (DT), thereby resulting in only MCs in the *Mcpt5-Cre*$^{+}$*iDTR*$^{+}$ offspring being sensitive to DT-induced cell death. Indeed, a single *i.p.* injection of DT results in an almost complete depletion (98.7%) of peritoneal MC population, whereas local (subcutaneous) DT treatment leads to similar extent (97.5%) of MC depletion from the ears. [187] For the constitutive MC deficiency model, on the other hand, *Mcpt5-Cre* mice are crossed to the *R-DTA* strain [189], so that only MCs in the progenies, which have Cre-mediated deletion of the STOP cassette, would express DTA and thus undergo self-destruction. [187] This is confirmed by experimental data that *Mcpt5-Cre*$^{+}$*R-DTA*$^{+}$ mice exhibited significant reduction in peritoneal and skin MC numbers, resembling DT-treated *Mcpt5-Cre*$^{+}$*iDTR*$^{+}$ mice mentioned above. [187] Furthermore, by crossing *Mcpt5-Cre* mice with the IL-10 mutant *IL-10*$^{FL/FL}$ strain [190], a new mouse line with a selective inactivation of the *IL-10* gene expression in MCs can be obtained. [187] Together, the data presented above prove *Mcpt5-Cre* mice a powerful tool

for studying the localised and/or systemic roles of MCs as well as particular MC-derived mediators in various disease models.

1.6. $VitD_3$ (Cholecalciferol)

One substance that can potentially enhance the anti-inflammatory properties of MCs is $VitD_3$, the "sunshine" vitamin as a significant amount can be synthesised in human skin upon UVB radiation (wavelengths: 280-320 nm). [191-193] The beneficial effects of $VitD_3$ were first discovered over a century ago, where anecdotal evidence suggested that a lower occurrence of rickets correlated with geographical locations that received an abundance of sunshine, such as the equatorial regions. [194] However, it was not until the 1930s that such sunshine-induced protection against rickets in children, as well as osteomalacia in adults, was due to UVB-initiated $VitD_3$ synthesis and its biological activities. [195] Indeed, $VitD_3$ plays protective and immunoregulatory roles against many detrimental outcomes associated with excess UV exposure, including cutaneous inflammation, photoaging, and gene mutations that can lead to the development of malignancies at the affected sites [193, 196-200]. The recent findings that $VitD_3$ can induce MC production of IL-10 both *in vitro* and in mouse skin following chronic low-dose UVB irradiation *in vivo* [163], have brought our attention to the possibility that the enhancement of anti-inflammatory properties of MCs by $VitD_3$ exposure might represent a novel approach for reducing inflammation and tissue damage in other contexts such as during IgE-dependent allergic responses.

1.7. Biosynthesis and Metabolism of $VitD_3$

In addition to its dietary sources, including oily fish and certain dairy products [201], the majority of $VitD_3$ in the body is generated in the epidermis when pre-vitamin D_3, the photochemical product derived from 7-dehydrocholesterol (pro-vitamin D_3) in response to UVB irradiation, undergoes spontaneous thermal isomerisation. [192, 202, 203] The association with $VitD_3$-binding protein (DBP) allows $VitD_3$ to be transported to the liver, where it is hydroxylated at the C25 position by cytochrome P450 proteins (e.g. CYP2DII, CYP2D25, CYP3A4 or CYP2R1) to generate $25OHD_3$ (calcidiol). DBP-bound $25OHD_3$ is subsequently delivered to the kidney, where further hydroxylation at the C1α position is performed by the 25-hydroxyvitamin D-1α-hydroxylase enzyme (CYP27B1), giving rise to the biologically active form $1\alpha,25(OH)_2D_3$ (calcitriol). [192, 193, 203] It should be mentioned that whilst the level and activity of liver cytochrome P450 proteins remain relatively constant, the conversion from $25OHD_3$ to $1\alpha,25(OH)_2D_3$ by CYP27B1 is tightly regulated, by levels of parathyroid hormone, calcium, phosphate, calcitonin, fibroblast growth factor-23, and $1\alpha,25(OH)_2D_3$ itself. [203] Inactivation of $1\alpha,25(OH)_2D_3$ and $25OHD_3$ to $1\alpha,24R,25(OH)_3D_3$ and $24R,25(OH)_2D_3$, respectively, is commonly attributed to the multifunctional 25-hydroxyvitamin D_3-24-hydroxylase (CYP24A1), which can be transcriptionally induced by the action of both $VitD_3$ analogues in a very sensitive manner. [204, 205] In addition, a second catabolic pathway for $1\alpha,25(OH)_2D_3$ that produces the A-ring diastereomer 1α,25(OH)2D-3epi-D_3 also exists, although the chemical reactions involved are less clear. [206]

In addition to liver and kidney cells, numerous other cell populations, including keratinocytes in the epidermis [207], possess the enzymatic machinery to process $VitD_3$ to

active metabolites. In the immune cell compartment, macrophages, DCs, T and B cells all express CYP27B1 upon activation and are consequently capable of autonomously producing $1\alpha,25(OH)_2D_3$ from $25OHD_3$. [208-210]

1.8. Biological Activities of $VitD_3$: UVB Protection and Immunoregulation

There are two types of signalling pathways through which $1\alpha,25(OH)_2D_3$ exerts its biological effects (**Figure 1.5**); one is a genomic pathway, where $1\alpha,25(OH)_2D_3$ binds to the well characterised nucleus-residing VDR and induces transcriptional regulation; the other is a non-genomic pathway, which utilises certain plasma membrane-associated receptor(s) (VDR_{mem}; yet to be fully characterised) and triggers rapid downstream cellular responses. [202, 203, 211-213]

1.8.1. The Genomic Pathway (Figure 1.5a)

Most known biological functions of $1\alpha,25(OH)_2D_3$ are mediated through VDRs which, upon ligand binding, undergo conformational changes and subsequent heterodimerization with the retinoid X receptor (RXR). [214] The $1\alpha,25(OH)_2D_3$-VDR-RXR complex binds specifically to vitamin D response elements (VDREs) in the promoter regions of target genes, many of which play a role in $VitD_3$-mediated UVB protection and/or immunoregulation. [193, 198, 215] Ligand-bound VDR also mediates coregulator switching for chromatin remodelling and histone modifications in the promoters of target genes by inducing dissociation of corepressor complexes and recruitment of coactivator complexes, thereby stimulating the transcription of a distinct set of genes. [216]

Figure 1.5. Mechanisms for $VitD_3$-mediated Biological Effects (UVB protection).

(a) Genomic $VitD_3$ pathways are triggered by the binding of $1\alpha,25(OH)_2D_3$ or conformationally flexible analogs to VDR, which ultimately lead to regulation of gene expression via interaction with VDRE in the promoter region of corresponding genes. Through these pathways, $VitD_3$ has been shown to reduce accumulation of mutations, oxidative damage as well as cutaneous inflammation caused by UVB irradiation. (b) Non-genomic $VitD_3$ pathways utilise an unidentified plasma membrane receptor (VDR_{mem}), which can bind to 6-s-*cis* locked $VitD_3$ analogs in addition to conventional VDR ligands. by stimulating important cellular signalling components, these pathways can lead to reduced CPD formation and gene mutation, and enhanced DNA repair and cell survival. Non-genomic activities of $VitD_3$ can also activate PKC and the Ras-MAPK signalling cascade, which may engage in cross-talk with the genomic pathways to stabilise VDR and to modulate gene expression, respectively. See text for more details.

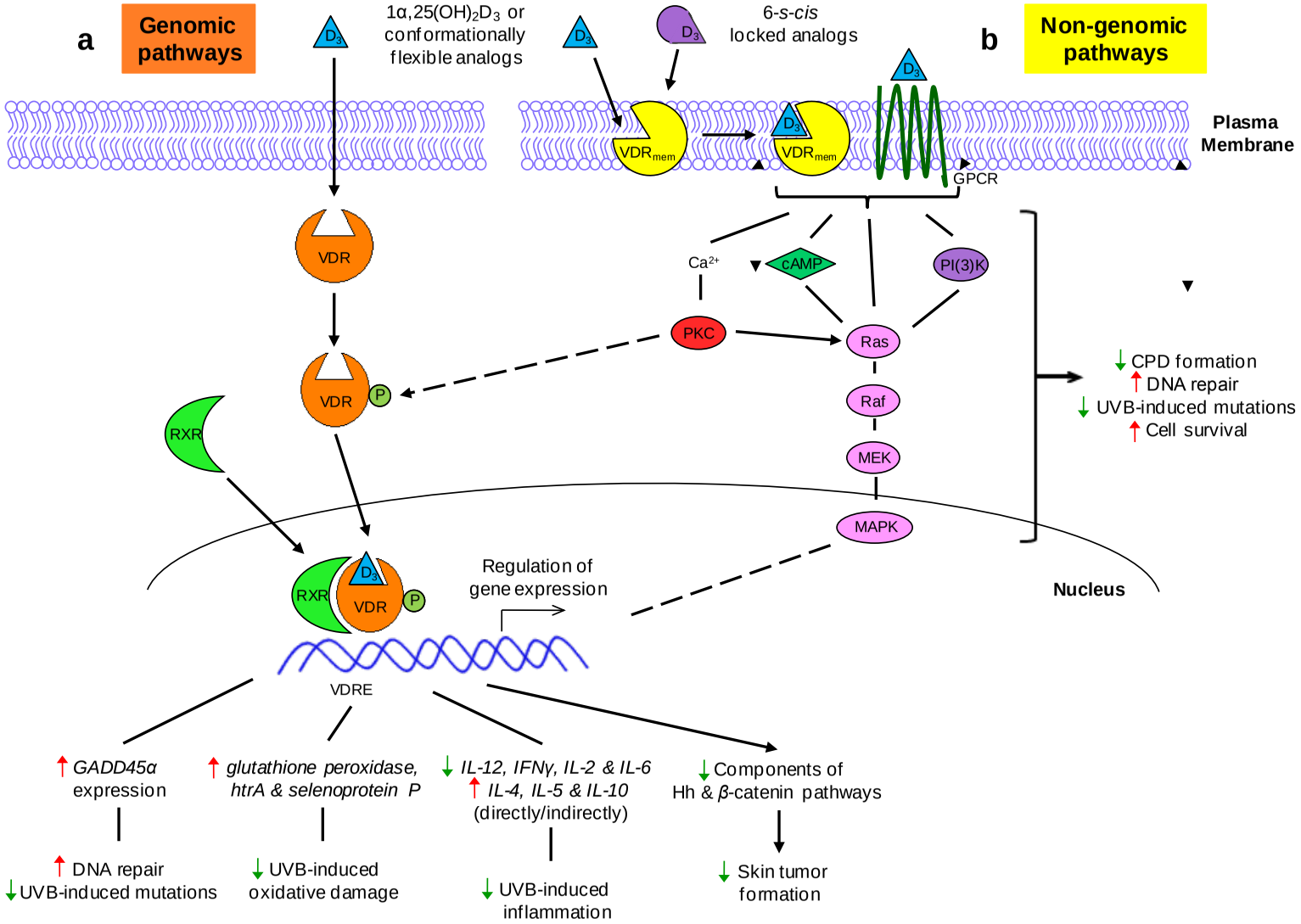
a
Genomic pathways
D3
1α,25(OH)2D3 or conformationally flexible analogs
D3
D3
6-s-cis locked analogs
b
Non-genomic pathways
Plasma Membrane
VDRmem
D3
VDRmem
D3
GPCR
VDR
Ca2+
cAMP
PI(3)K
PKC
Ras
VDR
P
Raf
RXR
MEK
MAPK
↓CPD formation
↑DNA repair
↓UVB-induced mutations
↑Cell survival
Nucleus
Regulation of gene expression
RXR
D3
VDR
P
VDRE
↑GADD45α expression
↑glutathione peroxidase, htrA & selenoprotein P
↓IL-12, IFNγ, IL-2 & IL-6
↑IL-4, IL-5 & IL-10
(directly/indirectly)
↓Components of Hh & β-catenin pathways
↑DNA repair
↓UVB-induced mutations
↓UVB-induced oxidative damage
↓UVB-induced inflammation
↓Skin tumor formation

Among the many genes involved in $VitD_3$-mediated UVB protection is the growth-arrest and DNA-damage gene, *GADD45α*, which encodes a protein important for normal DNA repair and maintenance of global genomic stability. [198]Therefore, by inducing *GADD45α* expression as observed in mouse squamous cell carcinoma cells, $1\alpha,25(OH)_2D_3$ can protect the genome against UVB-induced accumulation of mutations. [197] In addition, a number of genes that possess antioxidant properties, such as *glutathione peroxidase, htrA* and *selenoprotein P,* are also direct transcriptional targets of $1\alpha,25(OH)_2D_3$ and thus can confer $1\alpha,25(OH)_2D_3$ the capacity to reduce cumulative oxidative damage upon UVB irradiation. [198] Furthermore, the ability to transcriptionally finetune the expression balance between cyclin-dependent kinase inhibitors, p21 and p27, in a murine squamous cell carcinoma model allows $1\alpha,25(OH)_2D_3$ to suppress cell proliferation *in vitro* and promote cell differentiation and/or apoptosis *in vivo*. [217] As recently reviewed, critical components of the Hedgehog and *β*-catenin signalling pathways possess VDREs in the promoter region of their corresponding gene. Therefore, by direct transcriptional control of these genes and subsequent down-regulation of signalling events in both pathways, $1\alpha,25(OH)_2D_3$ can suppress the development of skin tumors. [218]

The fact that many immune cells constitutively or inducibly express VDRs enables $1\alpha,25(OH)_2D_3$ to interact with various nuclear transcription factors in these cells and to direct transcriptional regulation of various cytokine-encoding genes, thereby granting the genomic pathways a significant role in $VitD_3$-induced immunoregulation. [219] For instance, by blocking NF-κB activation and impeding its binding to the *p40* gene, $1\alpha,25(OH)_2D_3$ can reduce the secretion of IL-12, a major cytokine that drives the pro-inflammatory course of Th1 responses, from activated macrophages and DCs. [196, 220] By

decreasing the production of IL-23 and IL-6 from activated DCs, both of which are important for Th17 development, $1\alpha,25(OH)_2D_3$ can also dampen the pro-inflammatory Th17 state. [221, 222] Similarly, production of the typical Th1 cytokine IFNγ is inhibited in T cells upon $1\alpha,25(OH)_2D_3$ treatment, due to interaction of the $1\alpha,25(OH)_2D_3$-VDR-RXR complex with a negative VDRE-like binding sequence in the promoter region of the gene. [223] On the other hand, the production of Th2 cytokines such as IL-4, IL-5 and IL-10 is increased because of up-regulated expression of the Th2 specific transcription factors, GATA-3 and c-Maf [224], and/or direct interaction with VDRE in the promoter region of the corresponding gene such as *IL-10* [225]. Findings from *in vivo* mouse studies suggest that the number as well as immunosuppressive activity of $CD4^+CD25^+$ T_{reg} cells can be elevated upon $1\alpha,25(OH)_2D_3$ treatment, leading to further increase in IL-10 levels and an anti-inflammatory response. [222, 226]

Complementing its the ability to dampen certain inflammatory responses by inducing a Th1/Th17-to-Th2 shift, $1\alpha,25(OH)_2D_3$ also has anti-proliferative functions in activated T cells via down-regulation of IL-2 production. [227] In this case, $1\alpha,25(OH)_2D_3$-VDR-RXR complex binds to the NF-AT binding site within *IL-2* promoter and subsequently hinders the formation of NF-AT/AP-1 protein complex. Previous studies in prostatic epithelial cells show that $1\alpha,25(OH)_2D_3$ can also reduce IL-6 production. However, instead of a direct transcriptional regulation of the *IL-6* gene, $1\alpha,25(OH)_2D_3$ targets the VDRE within the promoter of *mitogen-activated protein kinase phosphatase 5* (*MKP5*) gene, leading to increased MKP5 expression, increased inactivation of the MAPK, p38, and ultimately reduced IL-6 production. [228] Furthermore, there are a number of other immunosuppressive properties of $1\alpha,25(OH)_2D_3$, the molecular mechanisms of which

still remain to be fully elucidated but are nevertheless VDR-dependent. Examples are the inhibition of DC maturation and costimulatory molecule expression [222] and enhanced IL-10 production by cutaneous MCs in a chronic UVB irradiation setting as previously mentioned [163].

1.8.2. The Non-genomic Pathway (Figure 1.5b)

While much attention has focussed on the genomic pathway of $VitD_3$ action, there is emerging evidence that $1\alpha,25(OH)_2D_3$ can also generate biological responses via rapid (seconds to minutes), non-genomic pathways. These pathways utilise currently unidentified VDR_{mem} [202, 215], although recent data indicate the conventional VDR being a likely candidate [229, 230], to trigger the activities of important cellular signalling components such as PKC, cyclic AMP (cAMP), intracellular Ca^+ and MAPKs [211]. Because $1\alpha,25(OH)_2D_3$ is capable of facile rotation about its 6, 7 single carbon bond, it can generate a continuum of potential shapes extending from the 6-s-*cis* (6C) to the 6-s-*trans* (6T) conformation. [231] Unlike the genomic pathway, which requires conformationally flexible ligands such as $1\alpha,25(OH)_2D_3$ itself, the non-genomic pathway can utilise 6C-locked analogs as efficiently as the original ligand. [211, 231] This has led to the development of pathway-specific $VitD_3$ agonists and antagonists, which have become valuable tools for determining the nature of $1\alpha,25(OH)_2D_3$-elicited biological effects. For example, with the help of the rapid acting agonists, $1\alpha,25(OH)_2lumisterol_3$ and $1\alpha,25(OH)_2$-7-dehydrocholesterol, and the rapid response antagonist $1\beta,25(OH)_2D_3$, it can be observed that $1\alpha,25(OH)_2D_3$ treatment protects human keratinocytes against UVB-induced CPD formation via a non-genomic pathway, both *in vitro* and *in vivo*, thus promoting DNA repair and cell survival. [232, 233]

Although the non-genomic $VitD_3$ pathways do not depend on transcription, they may indirectly affect transcription through cross-talk with the genomic pathways [215]. It is well known that the Ras-MAPK cascade is one of several that are targeted by rapid $VitD_3$ response. In particular, $1\alpha,25(OH)_2D_3$ can activate Ras-Raf/MEK/ ERK signalling in a PI(3)K-dependent manner in keratinocytes, resulting in increased AP-1 transcriptional activities and ultimately the differentiation of these cells; a UVB-protective outcome. [234] Apart from PI(3)K, Ras-Raf/MEK/MAPK pathway can also be initiated via activation of PKC or cAMP or even directly upon binding of $1\alpha,25(OH)_2D_3$ to VDR_{mem} and/or the G-protein coupled receptors. [215] It is therefore significant that activation of ERK can increase transcriptional activity of VDR and that activation of PCK can stabilize VDR through phosphorylation, as this suggests co-operation between the non-genomic and the genomic pathways to trans-activate VDR and elicit UVB-protective as well as immunoregulatory effects of $1\alpha,25(OH)_2D_3$. [215]

1.9. $VitD_3$ and MCs

1.9.1. $VitD_3$-mediated Immunoregulation of MCs

The recent discovery that MCs, like many other immune cells, express VDR [163] and are therefore $1\alpha,25(OH)_2D_3$ responsive creates another regulatory axis for $VitD_3$, where it elicits its effects by regulating the functionality of MCs. Indeed, in an IgE-dependent allergic asthma model, where MCs are known to play important roles in exacerbating the associated pathology, subcutaneous co-administration of $1\alpha,25(OH)_2D_3$ with allergen is capable of reducing the airway hyperresponsiveness, potentially due to an enhanced IL-10 level in the asthmatic lung tissues. [235] Although T_{reg} cells are claimed to be

responsible for the secretion of IL-10 at the time, the subsequent discovery of MCs being an alternative source of this cytokine [7] suggests that the immunosuppressive roles of $1\alpha,25(OH)_2D_3$ observed could also be due to its stimulatory effects on MC production of IL-10. Direct evidence for this notion is provided by the recent study demonstrating the ability of $1\alpha,25(OH)_2D_3$ to induce VDR-dependent IL-10 production by mBMCMCs *in vitro* as well as by cutaneous MCs upon UVB irradiation *in vivo*. [163]

In addition to stimulating IL-10 production, $1\alpha,25(OH)_2D_3$ can also repress the pro-inflammatory properties of MCs, such as reducing calcium ionophore A23187-induced degranulation (histamine release) of mouse peritoneal MCs [236] and decreasing the release of various pro-inflammatory mediators (e.g. MMCP-1 and LTC_4) by mBMCMCs [237]. Therefore, $1\alpha,25(OH)_2D_3$ can indeed drive the functionality of MCs towards the anti-inflammatory end of the spectrum, as observed so far in IgE-independent immune settings but not yet fully understood during IgE-dependent responses. For the purpose of the current project, we aim to investigate if $1\alpha,25(OH)_2D_3$-mediated anti-inflammatory properties of MCs are also evident in IgE-dependent immune settings. Furthermore, since many other immune cell types express CYP27B1, we will determine the MC expression status of this enzyme and, if expressed, whether $25OHD_3$ can have the same effects as $1\alpha,25(OH)_2D_3$ on MC bioactivities due to the $25OHD_3$ to $1\alpha,25(OH)_2D_3$ conversion by MC CYP27B1.

1.9.2. Potential Mechanisms for $VitD_3$-mediated Immunoregulation of MCs

There are several mechanisms by which $VitD_3$ can modulate the functions of MCs, via either transcriptional or post-transcriptional regulation of $VitD_3$-responsive genes, especially those encoding MC-derived mediators. One mechanism that utilises

transcriptional regulation involves fine-tuning (e.g. alteration in phosphorylation/activation status), via the rapid non-genomic pathways (section 1.8.2), of the FcεRI signalling pathway components, many of which can engage in cross-talk with the genomic pathways (Section 1.8.1) to modulate gene expression. One pathway that might bear relevance to the current project is the Ras-MAPK pathway, which involves phosphorylation of MAPKs, such as ERK1/2, and enhanced production of pro-inflammatory lipid-derived mediators and cytokines upon IgE+sAg-mediated MC activation. [64, 149, 228, 238-240] Another pathway of interest involves activation of the transcription factor, NF-κB, via either the serine-threonine kinase Akt or PKC, which is required for gene expression of many pro-inflammatory cytokines, especially IL-6 and TNFα, in MCs during IgE-mediated inflammation. [241, 242]

1.10. Rationales for this Study

In light of the new concept that MCs can negatively regulate the duration and magnitude of inflammatory responses in IgE-independent settings (Section 1.4.5), three major questions remain to be addressed: (1) Can MCs also display anti-inflammatory properties during IgE-dependent allergy-type immune responses, where they are so accustomed to being regarded as pro-inflammatory effector and immunoregulatory cells (Section 1.3)? and (2) How can the anti-inflammatory properties of MCs be potentiated in these immune settings? and (3) What cellular mechanisms may be involved in such regulation of MC functionality?

Our recent findings that the biologically active $VitD_3$ can induce IL-10 production by MCs and thus limit the pathology associated with chronic low-dose UVB irradiation

suggest the potential use of this well recognised immunomodulatory agent to drive a positive-to-negative-immunoregulatory functional transition of MCs during IgE + sAg-mediated immune responses. The *in vivo* passive cutaneous anaphylaxis (PCA) model used in this study provides a MC-dependent IgE-mediated allergy platform, which exhibits typical early- and late-phase responses including tissue swelling and leukocyte infiltration, respectively. [89] Thus, by examining the effects of $1\alpha,25(OH)_2D_3$ on various functional read-outs (e.g. production of pro-inflammatory and/or anti-inflammatory mediators) of *in vitro*-derived MCs upon IgE + sAg-mediated activation, and studying the effects of topically applied $1\alpha,25(OH)_2D_3$ on the cutaneous pathology associated with the PCA setting using MC knock-in mice as well as WT and MC deficient controls, the first two questions mentioned above could be addressed. Subsequent mechanistic investigation into the effects of $1\alpha,25(OH)_2D_3$ treatment on the functional status of FcεRI signalling components, as well as the functional comparison between $1\alpha,25(OH)_2D_3$ and its non-genomic pathway-specific agonist, curcumin, could then shed light on the third question. In addition to $1\alpha,25(OH)_2D_3$, the effects of other inactive $VitD_3$ metabolites, in particular $25OHD_3$, will also be studied to determine if MCs possess the same capability as other immune cells to autonomously generate their own $1\alpha,25(OH)_2D_3$.

1.11. Hypothesis

The immunoregulatory agent, $VitD_3$, alters IgE + sAg-mediated MC activation from a pro-inflammatory state to an anti-inflammatory one, both *in vitro* and during IgE-dependent PCA *in vivo*.

1.12. Project Aims

There are three main aims of the current project, each of which will be addressed in more details in subsequent chapters.

Aim 1: To characterise the modulation of IgE + sAg-mediated activation of mBMCMCs by 1α,25(OH)$_2$D$_3$ *in vitro*.

This aim, having been dissected into the following three sub-aims, will address the capacity of 1α,25(OH)$_2$D$_3$ to influence the immunological nature of IgE (IgE anti-dinitrophenyl [DNP] Ab) + sAg (human serum albumin [HSA]-DNP)-dependent mBMCMC activation and, at the same time, explore the potential mechanisms involved.

Aim 1.1 To determine the nature of the effects of 1α,25(OH)$_2$D$_3$ on IgE + sAg-stimulated MCs, mBMCMCs from WT mice will be activated in the presence of various concentrations of 1α,25(OH)$_2$D$_3$ and then (a) the extent of MC degranulation will be assessed by histamine enzyme immunoassay (EIA) and β-hexosaminidase assay; (b) the gene expression for a number of MC-derived pro-inflammatory and anti-inflammatory cytokines will be examined using quantitative real-time PCR (qRT-PCR); and (c) the protein secretion of the same set of cytokines will be measured by enzyme-linked immunosorbent assay (ELISA).

Aim 1.2 To determine the VDR-dependence of any effect of 1α,25(OH)$_2$D$_3$ observed during the above investigations, mBMCMCs will be generated from *VDR*$^{-/-}$ mice and analysed in parallel with their WT counterparts in the above experiments. Although VDR-dependence would generally indicate the genomic pathway for 1α,25(OH)$_2$D$_3$, this notion was questioned by the recent findings that conventional VDR may also serve as

VDR_{mem} during non-genomic responses. [229, 230] To ascertain the nature of the $1\alpha,25(OH)_2D_3$ signalling pathway involved in MC immunoregulation, the commercially available curcumin, an agonist for the non-genomic pathway, will be used instead of $1\alpha,25(OH)_2D_3$ in a number of experiments mentioned above. Any effect of curcumin will be compared with that of $1\alpha,25(OH)_2D_3$.

Aim 2: To examine the involvement of autonomous $1\alpha,25(OH)_2D_3$ synthesis in $VitD_3$-mediated immunoregulation of mBMCMC.

This aim is dissected into two sub-aims as follows, which will address the potential ability of MCs to synthesise $1\alpha,25(OH)_2D_3$ from the inactive precursor $25OHD_3$ and subsequently the effect of $25OHD_3$ on IgE + sAg-activated mBMCMCs.

Aim 2.1 To determine if mBMCMCs are capable of converting $25OHD_3$ to $1\alpha,25(OH)_2D_3$. The expression of CYP27B1 in naive mBMCMCs will firstly be examined by intracellular staining followed by flow cytometry and/or immunofluorescence microscopy. If this enzyme is indeed expressed by the cells, then any potential regulatory mechanism for its expression will be investigated. This involves treating mBMCMCs with either its substrate (i.e. $25OHD_3$) or its product (i.e. $1\alpha,25(OH)_2D_3$), and noting any change in its expression level using qRT-PCR and/or western blotting. In addition, if CYP27B1 expression in MCs is confirmed, the extent of endogenous $1\alpha,25(OH)_2D_3$ synthesis from $25OHD_3$-treated mBMCMCs (in both culture supernatants and cell lysates) will be measured using a 1,25-$(OH)_2D$ radioimmunoassay (RIA) kit. Finally, to examine if VDR is required for CYP27B1 expression, its regulation,

and/or endogenous 1α,25$(OH)_2D_3$ synthesis in MCs, *VDR*$^{-/-}$ mBMCMCs will be analysed in parallel with their WT counterparts in all above experiments.

Aim 2.2 To investigate the effect of 25OHD_3 on IgE + sAg-activated mBMCMCs, as sufficiently high concentrations of 25OHD_3 are able to alter the functions of mouse kidney and skin cells by binding directly to VDR. [243] To achieve this purpose, WT mBMCMCs will be stimulated in the presence of various concentrations of 25OHD_3, in the same way as described for 1α,25$(OH)_2D_3$ in Aim 1.1, and the extent of degranulation and cytokine production will be assessed by β-hexosaminidase assay and ELISA, respectively. If MCs are capable of converting 25OHD_3 to 1α,25$(OH)_2D_3$ (Aim 2.1), an alternative experimental setting will also be used, where MCs are treated with 25OHD_3 for an certain period of time prior to IgE preload so that the cells have sufficiently time to generate their own 1α,25$(OH)_2D_3$. Furthermore, to determine the VDR-dependence for any potential immunoregulatory effect of 25OHD_3 in activated MCs, *VDR*$^{-/-}$ mBMCMCs will be used in addition to WT cells in all above experiments.

Aim 3: To investigate the effects of topically applied $VitD_3$ on the cutaneous pathology associated with IgE-mediated PCA *in vivo*

To address this aim, a localised PCA reaction, which provides an almost entirely MC-dependent Type I immediate hypersensitivity setting [89], will be triggered in the ear of WT C57BL/6 mice, together with topical application of either 1α,25$(OH)_2D_3$, 25OHD_3 or just the vehicle. In the case of 25OHD_3 application, alternative experimental settings regarding the duration of 25OHD_3 treatment may be used depending on the outcome of *in vitro* studies described in Aim 2.2. To determine the requirement of VDR for any potential immunoregulatory effects of $VitD_3$ analogues on PCA-associated pathology,

VDR$^{-/-}$ mice will be used in parallel with their WT counterparts. The rationale for this is: if VDR is required then these mice will not be subjected to $VitD_3$-mediated regulation as seen in WT animals. To further verify that $VitD_3$ requires MC-specific VDR expression to elicit its effects, MC knock-in mice (engrafted with WT or *VDR*$^{-/-}$ mBMCMCs) as well as the MC-deficient c-kit mutant mice will also be used together with WT controls. The rationale in this case is: if the effects of $VitD_3$ are indeed dependent on MC VDR expression, then whilst MC-deficient mice will not exhibit a PCA response (due to the lack of MCs), WT MC knock-in mice will mirror the response of WT controls upon all treatments (due to the presence of MCs with functional VDR in the ears) and, *VDR*$^{-/-}$ MC knock-in mice will fail to respond to any $VitD_3$-mediated regulation (due to the absence of VDR expression in MCs in the ears). In all PCA-related experiments, one or more of the following assessments will be performed, in order to gain information on as many aspects of the responses:

(1) Tissue swelling: Ear thickness will be measured at multiple intervals from 30 min – 6 h after the onset of the allergic response.

(2) Local and systemic production of MC-derived mediators: Ear lysate and serum samples will be prepared from treated mice and used to detect the same set of MC-derived cytokines as for *in vitro* assessments (i.e. TNFα, IL-6 and IL-10). Total RNA will also be extracted from ear lysates and subjected to qRT-PCR analysis for the expression of corresponding genes.

(3) Histological detection and enumeration of MCs: Paraffin sections will be prepared from treated mouse ears and stained with toluidine blue, a MC-specific

metachramatic dye. The density, granularity and tissue-distribution of MCs will be demonstrated and determined by light microscopy. This is particularly important in "MC knock-in" mice, which will be compared to their WT and MC-deficient counterparts to ensure successful engraftment of MCs.

Aim 4: To investigate if the immunoregulatory effects of 1α,25(OH)$_2$D$_3$ and/or 25OHD$_3$ on IgE + sAg-activated mBMCMCs *in vitro* can be translated to hCBMCs

To determine whether the regulatory effects of 1α,25(OH)$_2$D$_3$ are also applicable to human MCs, hCBMCs will be generated and activated (in this case by human (h)IgE preload followed by α-hIgE Ab stimulation) in the presence of either 1α,25(OH)$_2$D$_3$ or vehicle. The production of various cytokines will be subsequently measured by ELISA. To assess the ability of hCBMCs to generate endogenous 1α,25(OH)$_2$D$_3$, the gene as well as protein expression of CYP27B1 in hCBMCs will firstly be examined. If its expression is confirmed, then culture supernatants and lysates will be collected from 25OHD$_3$- or vehicle-treated hCBMCs, and the amount of 1α,25(OH)$_2$D$_3$ present in all samples will be analysed by the 1,25-(OH)$_2$D RIA kit.

1.13. Expected Outcomes and Significance

It is becoming increasingly clear that depending on individual immunological circumstances, MCs can either enhance or suppress an innate or adaptive immune response. This raises the necessity to re-visit some MC-related research areas that have been intensely investigated in the past but nevertheless focused primarily on the pro-inflammatory roles of MCs. Allergic conditions that are mediated by IgE and its cognate

allergen is one of these areas, which will therefore be the ultimate focus of the current project. Given already shown attributes of $VitD_3$ with other myeloid-derived cell populations, it is anticipated that MC functions might also be modulated by this immunoregulatory agent. Multiple mechanisms are expected to be responsible for $VitD_3$-mediated immunosuppression via MCs, a number of which will be revealed at the completion of the study. Furthermore, the ability of MCs to synthesise $1\alpha,25(OH)_2D_3$ from inactive precursors, and thus their ability to respond to treatment with these precursors, will also be investigated for the first time. Together, the outcomes of this project will broaden our knowledge on the complexity of MC function in IgE-dependent allergic disorders and, more importantly, it will evaluate the therapeutic potential of $VitD_3$ for the prevention and treatment of these disorders via its immunoregulatory effects on MCs.

CHAPTER 2

MATERIALS & GENERAL METHODS

2.1. Commercial Reagents

2.1.1. Common Tissue Culture Reagents

Dulbecco's modified eagle medium high glucose (DMEM): Gibco

Iscove's modified Dulbecco's medium (IMDM): Gibco

Penicillin (10,000 U/mL)/Streptomycin (10,000 μg/mL) (Pen/Strep): Gibco

2-mercaptoethanol; 1,000× (2-ME): Gibco

Fetal bovine serum (FCS): Gibco

Horse serum (HS): Gibco

Albumin solution from bovine serum; 35% (BSA): Sigma

Dulbecco's phosphate buffered saline; 10× (PBS): Gibco

MEM non-essential amino acid solution; 100× (NEAA): Sigma

Saponin (from Quillaja Bark): Sigma

Anticoagulant citrate dextrose solution (ACD):

Histopaque-1077: Sigma

Dextran: Pharmacosmos

Human Fc receptor blocking Ab: Miltenyi Biotec

Magnetic $CD34^+$ beads: Miltenyi Biotec

Dimethyl sulphoxide (DMSO): BDH

Albumin, dinitrophenol (DNP-HSA): Sigma

Water for irrigation: Baxter

Charcoal: Sigma

Trypan blue: BDH

2.1.2. Vitamin D_3 Analogues

1α,25-Dihydroxyvitamin D_3; ≥ 99% (stock solution [1 mM] and dilutions prepared in 100% ETOH; stored at -80 °C): Sigma

25-Hydroxycholecalciferol; 98% (stock solution [1 mM] and dilutions prepared in 100% ETOH; stored at -80 °C): Sigma

Curcumin; ≥ 94% curcuminoid content (stock solution [1 mM] and dilutions prepared in 100% ETOH; stored at -80 °C): Sigma

4,4`-Diisothiocyanatostilbene-2,2`-disulfonic acid disodium salt hydrate; ≥ 80% (DIDS; stock solution [100 mM] and dilutions prepared in DMSO; stored at 4 °C): Sigma

2.1.3. Cytokines and Recombinant Proteins

Recombinant mouse IL-3 (rmIL-3): ProSpec-Tany

Recombinant human SCF (rhSCF): Shenandoah Biotechnology

Recombinant human IL-6 (rhIL-6): Shenandoah Biotechnology

Recombinant human IL-4 (rhL-4): ProSpec-Tany

2.1.4. Hybridomas

WEHI-3 Hybridoma: Stanford University, USA

SPE-7 Hybridoma: Weizmann Institute of Science, Israel

2.1.5. Antibodies for Tissue Culture

Monoclonal α-DNP (mouse IgE; clone SPE-7): Sigma

Monoclonal α-DNP (mouse IgE; clone H1 ε26): Stanford University, USA

Human myeloma IgE: Merck

Goat α-human IgE: eBioscience

2.1.6. Reagents for SPE-7 Purification

1-Fluoro-2,4-dinitrobenzene (FDNB): Sigma

Dioxane: BDH

HiTrap NHS-activated HP column: GE Healthcare

2,4-dinitrophenol; 97% (DNP): Sigma

Propionic Acid: BDH

Coomassie brilliant blue R-250: Thermo Scientific

VIVASPIN 20 tube: Sartorius Stedim Biotech

2.1.7. β-Hexosaminidase Release Assay Reagents

Phorbol-12 myristate-13 acetate (PMA): Sigma

Calcium ionophore A23187: Sigma

P-Nitrophenyl-N-acetyl-Beta-D-glucosaminide (p-NAG): Sigma

2.1.8. ELISA/EIA Kits and Reagents

BD OptEIA™ mouse IL-3 ELISA Set (≥ 7.81 pg/mL): BD Biosciences

BD OptEIA™ mouse IL-6 ELISA Set (≥ 15.63 pg/mL): BD Biosciences

BD OptEIA™ mouse IL-10 ELISA Set (≥ 31.25 pg/mL): BD Biosciences

BD OptEIA™ mouse TNFα ELISA Set (≥ 15.63 pg/mL): BD Biosciences

Human TNFα ELISA kit: eBioscience

Human IL-10 ELISA kit: eBioscience

EIA histamine kit: Immunotech (Beckman Coulter)

Radioimmunoassay kit (1,25-$(OH)_2$D RIA kit; ≥ 5 pM): Immunodiagnostic Systems Ltd

3,3',5,5'-tetramethyl-benzidine liquid substrate: Sigma

Tween-20: Sigma

2.1.9. Flow Cytometry Reagents

FITC-conjugated α-mouse FcεRIα (American Hamster IgG): eBioscience

Alexa Fluor 647-conjugated α-mouse FcεRIα (American Hamster IgG): eBioscience

PE-conjugated α-mouse CD117 (c-kit; rat IgG2b): eBioscience

Purified α-mouse CD16/32 (blocks Fc binding): eBioscience

FITC-conjugated α-mouse IgE (rat IgG1): BD Biosciences

FITC-conjugated American Hamster IgG isotype control: eBioscience

PE-conjugated rat IgG2b isotype control: eBioscience

FITC-conjugated rat IgG1 isotype control: eBioscience

Polyclonal α-CYP27B1 (rabbit IgG): Santa Cruz Biotechnology

Purified rabbit IgG isotype control: Dako

PE-conjugated α-rabbit IgG: Southern Biotech

Human Tryptase (Mouse): Millipore

1B5 mouse IgG1 isotype control: School of Molecular and Biomedical Science, University of Adelaide

PE-conjugated α-mouse IgG: Southern Biotech

NucView^{TM} 488 Caspase-3 assay kit for live cells: Biotium

Fixation & Permeabilization Kit: eBioscience

2.1.10. Histochemistry & Immunohistochemistry Reagents

Polyclonal α-CYP27B1 (rabbit IgG): Santa Cruz Biotechnology

Rabbit polyclonal IgG (isotype control): Abcam

Alexa 594-conjugated goat α-rabbit: Molecular Probes

Human Tryptase (Mouse): Millipore

1B5 mouse IgG1 isotype control: School of Molecular and Biomedical Science, University of Adelaide

Alexa 594-conjugated goat α-mouse IgG: Molecular Probes

Accustain Geimsa and May-Grűnwald stains: Sigma

Toluidine blue O: Sigma

DePex mounting medium: BDH

Fixation & Permeabilization Kit: eBioscience

DAPI (4',6-Diamidine-2'-phenylindole dihydrochloride): Roche

Fluorescence Mounting Medium: DAKO

2.1.11. SDS-PAGE & Western Blotting Reagents

Polyclonal α-CYP27B1 (rabbit IgG): Santa Cruz Biotechnology

Rabbit α-CYP24A1: Chemicon

α-β-actin: Chemicon

Horse radish peroxidase (HRP)-conjugated α-mouse: Pierce

HRP-conjugated α-rabbit: Pierce

Bio-Rad D_c protein assay: Bio-Rad

BSA standard: New England Biolabs

Benchmark^{TM} pre-stained protein markers: Invitrogen

Nitrocellulose membrane: Advantec

Blocking reagent: Roche

Amersham ECL Plus Western Blotting Detection System: GE Health

Stripping solution: Alpha Diagnostic International

2.1.12. Primers (all used at 5 µg/mL): Geneworks

Common forward (i.e. $VDR^{+/+}$/$VDR^{-/-}$): 5` - TTCTTCAGTGGCCAGCTCTT - 3`

C57/BL6 - $VDR^{+/+}$ reverse: 5` - CTCCATCCCCATGTGTCTTT - 3`

C57/BL6 - $VDR^{-/-}$ reverse: 5` - CTAAAGCGCATGCTCCAGAC - 3`

Mouse β-actin forward (F): 5` - TGGAATCCTGTGGCATCCATGAAAC - 3`

Mouse β-actin reverse (R): 5` - TAAAACGCAGCTCAGTAACAGTCCG - 3

Mouse IL-10 F: 5` - GCCTTATCGGAAATGATCCA - 3`

Mouse IL-10 R: 5` - TTCTCACCCAGGGAATTCAA - 3`

Mouse TNFα F: 5` - GATTATGGCTCAGGGTCCAA - 3`

Mouse TNFα R: 5` - GAGACAGAGGCAACCTGACC - 3`

Mouse IL-6 F: 5` - CAAAGCCAGAGTCCTTCAGA - 3`

Mouse IL-6 R: 5` - GATGGTCTTGGTCCTTAGCC - 3`

Mouse histidine decarboxylase (HDC) F: 5` - AGGAGCAATCCAAGGGAGAT - 3`

Mouse HDC R: 5` - GGTATCCAGGCTGCACATTT - 3`

Mouse CYP27B1 F: 5` - GCTGAAGTCCCTCCTGACAC - 3`

Mouse CYP27B1 R: 5` - GTCTGGAAACTGTGTGGGGT - 3`

Human β-actin F: 5` - AGCACAGAGCCTCGCCT - 3`

Human β-actin R: 5` - CACGATGGAGGGGAAGAC - 3`

Human CYP27B1 F: 5` - TGTTTGCATTTGCTCAGAGG - 3`

Human CYP27B1 R: 5` - CGCCAATAGCAACTCTGTCA - 3`

2.1.13. Molecular Biology Reagents

Proteinase K: Merck

GoTaq green master mix: Promega

pUC19/*HpaII* DNA molecular weight marker: GeneWorks

GelRed™ Nucleic Acid Gel Stain; 10,000×: Biotium

TRIzol reagent: Invitrogen

QuantiTech reverse transcription kit: Qiagen

QuantiTech Sybr green polymerase chain reaction (PCR) master mix: Qiagen

2.1.14. In Vivo Experiment Reagents

Hank's MEM (HMEM): Sigma

Piperazine-*N,N'* bis(2-ethane sulfonic acid; Pipes): Sigma

1,2-propanediol (propalene glycol); 99%: Sigma

0.9% (w/v) sodium chloride: AstraZeneca

T-PER tissue protein extraction reagent: Thermo Scientific

Complete mini EDTA-free (protease inhibitor cocktail tablets): Roche

2.2. Solutions and Buffers

2.2.1. Tissue Culture Media and Solutions

Flushing medium

Reagent	Concentration	Amount
Pen/Strep	2%	10 mL
2-ME	0.1%	0.5 mL
DMEM		To 500 mL

Complete DMEM medium (cDMEM)

Reagent	Concentration	Amount
FCS	10%	50 mL
Pen/Strep	1%	5 mL
2-ME	0.1%	0.5 mL
DMEM		To 500 mL

Complete DMEM medium with csFCS (cDMEM-csFCS)

Reagent	Concentration	Amount
csFCS	10%	50 mL
Pen/Strep	1%	5 mL
2-ME	0.1%	0.5 mL
DMEM		To 500 mL

Complete BMCMC medium – early-stage culturing (cBMCMC-early)

Reagent	Concentration	Amount
WEHI-3-conditioned medium	20%	100 mL
FCS	10%	50 mL
Pen/Strep	2%	10 mL
2-ME	0.1%	0.5 mL
rmIL-3 (10 µg/mL)	Adjust to 3 ng/mL final	Varies depending on the concentration of mIL-3 in the WEHI-conditioned medium used
DMEM		To 500 mL

Complete BMCMC medium – late-stage culturing (cBMCMC-late)

Reagent	Concentration	Amount
WEHI-3-conditioned medium	20%	100 mL
FCS	10%	50 mL
Pen/Strep	2%	10 mL
2-ME	0.1%	0.5 mL
rmIL-3 (10 µg/mL)	Adjust to 4 ng/mL final	Varies depending on the concentration of mIL-3 in the WEHI-conditioned medium used
DMEM		To 500 mL

Sucrose-$MgCl_2$-Hepes solution

Reagent	Concentration	Amount
Sucrose	250 mM	34.23 g
$MgCl_2 \cdot 6H_2O$	1.5 mM	0.122 g
Hepes	10 mM	0.954 g
H_2O		To 400 mL
pH adjusted to 7.4		

Dextran-coated charcoal

Reagent	Concentration	Amount
Activated charcoal powder	0.25%	1 g
Dextran T-70	0.0025%	0.01 g
Sucrose-$MgCl_2$-Hepes solution		400 mL
The above were mixed together and incubated at 4°C overnight with constant agitation		

Charcoal-stripped FCS (csFCS; heat-inactivated)

Reagent	Concentration	Amount
Dextran-coated charcoal		400 mL
FCS		400 mL
Spin the Dextran-coated charcoal (500 g; 10 min) solution to pellet the charcoal. Discard the supernatant, and resuspend the pellet with equal volume of FCS. Incubate the charcoal-FCS solution at 55°C for 45 min, invert the container to mix, and incubate for a further 45 min.		

Complete BMCMC medium with csFCS and 3 ng/mL rmIL-3 (cDMEM-csFCS-3)

Reagent	Concentration	Amount
csFCS	10%	50 mL
Pen/Strep	1%	5 mL
2-ME	0.1%	0.5 mL
rmIL-3 (10 µg/mL)	3 ng/mL	150 µL
DMEM		To 500 mL

Complete BMCMC medium with csFCS and 4 ng/mL rmIL-3 (cDMEM-csFCS-4)

Reagent	Concentration	Amount
csFCS	10%	50 mL
Pen/Strep	1%	5 mL
2-ME	0.1%	0.5 mL
rmIL-3	4 ng/mL	200 µL
DMEM		To 500 mL

SPE-7 culturing medium

Reagent	Concentration	Amount
HS	10%	50 mL
Pen/Strep	1%	5 mL
2-ME	0.1%	0.5 mL

DMEM		To 500 mL

hCBMC medium

Reagent	Concentration	Amount
FCS	10%	50 mL
Pen/Strep	2%	10 mL
2-ME	0.1%	0.5 mL
rhSCF	100 ng/mL	
rhIL-6	50 ng/mL	
NEAA	1×	
IMDM		To 500 mL

hCBMC medium with csFCS (hCBMC-csFCS)

Reagent	Concentration	Amount
csFCS	10%	50 mL
Pen/Strep	2%	10 mL
2-ME	0.1%	0.5 mL
rhSCF	100 ng/mL	
rhIL-6	50 ng/mL	
NEAA	1×	
IMDM		To 500 mL

Dextran solution

Reagent	Concentration	Amount
Dextran	5%	5 g
dH_2O		To 100 mL

PBS

Reagent	Concentration	Amount
PBS (10×)	1 ×	100 mL
dH_2O		To 1 L

$CD34^+$ purification buffer

Reagent	Concentration	Amount
BSA	0.5%	7.14 mL
ACD	0.6%	

PBS		To 500 mL

mBMCMC starvation medium

Reagent	Concentration	Amount
Pen/Strep	1%	5 mL
2-ME	0.1%	0.5 mL
BSA (35%)	0.1%	1.43 mL
DMEM		To 500 mL

hCBMC starvation medium

Reagent	Concentration	Amount
Pen/Strep	1%	5 mL
2-ME	0.1%	0.5 mL
BSA (35%)	0.1%	1.43 mL
IMDM		To 500 mL

Hybridoma freezing solution

Reagent	Concentration	Amount
DMSO	10%	2 mL
FCS/HS	90%	18 mL

2.2.2. Buffers and Solutions for SPE-7 Purification

Conjugation solution

Reagent	Concentration	Amount
Sodium bicarbonate	0.05 M	1.05 g
H_2O		To 250 mL

Coupling buffer

Reagent	Concentration	Amount
Sodium bicarbonate	0.2 M	16.802 g
Sodium chloride	0.5 M	29.22 g
H_2O		To 1 L
pH adjusted to 8.3		

1 M Propionic Acid

Reagent	Concentration	Amount
Propionic acid (99.5%)	1 M	37 mL
H_2O		To 500 mL

Buffer A

Reagent	Concentration	Amount
Ethanolamine (99%)	0.5 M	30 mL
Sodium chloride	0.5 M	29.22 g
H_2O		To 1 L
pH adjusted to 8.3		

Buffer B

Reagent	Concentration	Amount
Sodium acetate	M	8.203 g
Sodium chloride	0.5 M	29.22 g
H_2O		To 1 L
pH adjusted to 4.0		

Storage solution

Reagent	Concentration	Amount
Disodium hydrogen phosphate	0.05 M	7.098 g
Sodium azide (10%)	0.1%	10 mL
H_2O		To 1 L
pH adjusted to 7.0		

Equilibration solution

Reagent	Concentration	Amount
Sodium dihydrogen phosphate	M	13.8 g
Sodium chloride	0.15 M	8.766 g
H_2O		To 1 L
pH adjusted to 7.0		

0.1 M DNP

Reagent	Concentration	Amount

DNP	0.1 M	5.75 g
Tris		Enough to dissolve DNP and adjust pH
H_2O		To 250 mL
pH adjusted to 7.7 with Tris		

Methanol (MeOH)-acetic acid-H_2O (5:4:1 ratio)

Reagent	Concentration	Amount
MeOH	50% (v/v)	500 mL
Glacial acetic acid	40% (v/v)	400 mL
H_2O	10% (v/v)	100 mL

Coomassie blue solution

Reagent	Concentration	Amount
Coomassie brilliant blue R-250	0.2% (w/v)	1 g
MeOH-acetic acid-H_2O		500 mL

2.2.3. Buffers and Solutions for β-Hexosaminidase Release Assay

HEPES buffer

Reagent	Concentration	Amount
HEPES	1 M	23.83 g
H_2O		To 100 mL
pH adjusted to 7.4		

Tyrodes buffer

Reagent	Concentration	Amount
HEPES buffer (1 M)	10 mM	10 mL
Sodium chloride	129 mM	7.54 g
Potassium chloride	5 mM	0.37 g
Calcium chloride	1.4 mM	0.206 g
Magnesium chloride	1 mM	0.203 g
D-glucose	8.4 mM	1.008 g
BSA	0.1%	1 g
H_2O		To 1 L
Filter sterilised		

0.5% Triton-X

Reagent	Concentration	Amount
Triton-X	0.5%	0.5 mL
Tyrodes buffer		To 100 mL

Substrate buffer

Reagent	Concentration	Amount
Disodium hydrogen phosphate (0.2 M)	155 mM	70 mL
Citric acid (0.4 M)	88 mM	20 mL
pH adjusted to 4.5		

p-NAG solution

Reagent	Concentration	Amount
p-NAG	4 mM	150 mg
Substrate buffer		45 mL
H_2O		67.5 mL
Heating is applied until p-NAG is completely dissolved. The final solution is filter sterilised.		

0.2 M glycine

Reagent	Concentration	Amount
Glycine	0.2 M	15.0 g
H_2O		To 1 L
pH adjusted to 10.7		

2.2.4. ELISA Buffers and Solutions

Blocking buffer

Reagent	Concentration	Amount
FCS	10%	100 mL
PBS		To 1 L
Filter sterilised		

PBS-Tween (ELISA wash)

Reagent	Concentration	Amount
Tween-20	0.05%	0.5 mL
PBS		To 1 L

Stop solution

Reagent	Concentration	Amount
Sulphuric acid (98%)	2 N (i.e. 1 M)	100.08 mL
H_2O		To 1 L

2.2.5. Flow Cytometry Buffers and Solutions

FACS buffer

Reagent	Concentration	Amount
FCS	2%	20 mL
PBS		To 1 L
Filter sterilised		

FACS fixation solution (FACS-fix)

Reagent	Concentration	Amount
Formaldehyde	0.1%	1 mL
Glucose	2%	20 g
Sodium azide (10%)	0.02%	2 mL
PBS		To 1 L

2.2.6. Histology/Immunohistology Solutions

10% neutral buffered formalin

Reagent	Concentration	Amount
Formaldehyde	10%	100 mL
PBS		To 1 L

1% aqueous toluidine blue

Reagent	Concentration	Amount
Toluidine blue	1%	1 g

H_2O		100 mL

0.1% acidic toluidine blue

Reagent	Concentration	Amount
1% aqueous toluidine blue	0.1% toluidine blue final	20 mL
1N hydrochloric acid		To 200 mL
pH adjusted to 1.0		

1% acidic toluidine blue

Reagent	Concentration	Amount
Toluidine blue	1%	1 g
1N hydrochloric acid		100 mL
pH adjusted to 0.1		

0.05% toluidine blue solution

Reagent	Concentration	Amount
Toluidine blue	0.05%	0.05 g
1.8% Sodium chloride solution		50 mL
80% (v/v) ETOH		22 mL
H_2O		28 mL

Saturated saponin solution

Reagent	Concentration	Amount
Saponin		Enough to reach saturation (orange appearance)
50% ethanol		100 mL

Kimura staining solution

Reagent	Concentration	Amount
0.05% toluidine blue solution		50 mL
Saturated saponin solution		2.27 mL
0.06 M Sodium dihydrogen phosphate		22.7 mL
Filter sterilised		

2.2.7. Buffers and Solutions for SDS-PAGE & Western Blotting

NP40 lysis buffer

Reagent	Concentration	Amount
Tris	10 mM	1.21 g
Sodium chloride	137 mM	8.01 g
Glycerol	10%	100 mL
NP40	1%	10 mL
H_2O		To 1 L
pH adjusted to 7.4		

Complete NP40 lysis buffer

Reagent	Concentration	Amount
NP40 lysis buffer		10 mL
1 M β glycerol phosphate	10 mM	100 µL
0.1 M PMSF	1 mM	100 µL
0.5 M Sodium fluoride	5 mM	100 µL
1 M Sodium vanadate	10 mM	100 µL
Aprotinin	0.3% (v/v)	30 µL
1 mg/mL Leupeptin	1 µg/mL	10 µL

5× sample loading buffer

Reagent	Concentration	Amount
0.5 M Tris-HCl (pH = 6.8)	62.5 mM	1 mL
Glycerol	10%	0.8 mL
10% SDS	2%	1.6 mL
Bromophenol blue	0.5%	0.04 g
2-ME	5%	0.4 mL
H_2O		4 mL

Lower gel buffer

Reagent	Concentration	Amount
Tris	1.5 M	181.65 g
10% SDS	0.4%	40 mL
H_2O		To 1 L
pH adjusted to 8.8		

Upper gel buffer

Reagent	Concentration	Amount
Tris	0.5 M	60.55 g
10% SDS	0.4%	40 mL
H_2O		To 1 L
pH adjusted to 6.8		

30% Acrylamide

Reagent	Concentration	Amount
Acrylamide	30%	146 g
N'N'-bis-acrylamide	0.8%	4 g
H_2O		To 500 mL
Filter sterilised		

10% ammonium persulphate (APS)

Reagent	Concentration	Amount
APS	10%	1 g
H_2O		To 10 mL

10% SDS-PAGE gel

Reagent	Concentration	Amount
Lower gel buffer		5.2 mL
30% Acrylamide		6.9 mL
10% APS		80 µL
TEMED		40 µL
H_2O		8.7 mL

Stacking gel

Reagent	Concentration	Amount
Upper gel buffer		5 mL
30% Acrylamide		2.8 mL
10% APS		200 µL
TEMED		20 µL
H_2O		12 mL

10× SDS-PAGE running buffer

Reagent	Concentration	Amount

Tris	0.25 M	30.28 g
Glycine	2 M	144 g
10% SDS	1%	100 mL
H_2O		To 1 L
pH adjusted to 8.3		

Transfer buffer

Reagent	Concentration	Amount
Tris	25 mM	12.12 g
Glycine	0.2 M	60.0 g
MeOH	15%	600 mL
H_2O		To 4 L
pH adjusted to 7.4		

Maleic acid buffer

Reagent	Concentration	Amount
Maleic acid	100 mM	11.6 g
Sodium chloride	150 mM	8.766 g
H_2O		To 1 L
pH adjusted to 7.5		

10% blocking solution

Reagent	Concentration	Amount
Blocking reagent	10%	50 g
Maleic acid buffer		To 500 mL
Heating is applied until blocking reagent is completely dissolved. The final solution is dispensed into 200 mL Schott bottles (100 mL/bottle) and autoclaved.		

10× TNT

Reagent	Concentration	Amount
Tris	0.5 M	60.57 g
Sodium chloride	1.54 M	90.0 g
Tween-20	1%	10 mL
H_2O		To 1 L
pH adjusted to 7.4		

1% blocking buffer

Reagent	Concentration	Amount
10% blocking solution	1% final	5 mL
1× TNT		To 50 mL

0.1% blocking buffer

Reagent	Concentration	Amount
10% blocking solution	0.1% final	500 µL
10% sodium azide	0.01% final	50 µL
1× TNT		To 50 mL

2.2.8. Molecular Biology Buffers and Solutions

1 M Tris-HCl

Reagent	Concentration	Amount
Tris	1 M	60.57 g
H_2O		To 500 mL
pH adjusted to 8.0 by adding concentrated HCl		

Tail lysis buffer

Reagent	Concentration	Amount
1 M Tris-HCl	100 mM final	100 mL
0.5 M EDTA	5 mM final	10 mL
10% SDS	0.2% final	20 mL
2 M Sodium chloride	200 mM final	100 mL
H_2O		To 1 L
Proteinase K (10 mg/mL stock solution) is added fresh each time (1/100 dilution) to reach a final concentration of 100 µg/mL.		

TE (Tris-EDTA) buffer

Reagent	Concentration	Amount
1 M Tris-HCl (pH 7.5)	10 mM final	10 mL
0.5 M EDTA (pH 8.0)	1 mM final	2 mL
H_2O		To 1 L

Diethylpyrocarbonate (DEPC)-H2O (RANase-free)

Reagent	Concentration	Amount
DEPC	0.01%	100 µL
H_2O		To 1 L
This solution is prepared in autoclaved glass bottles. After the addition of DEPC, solution is allowed to stand at room temperature (RT) overnight and then autoclaved.		

50× TAE

Reagent	Concentration	Amount
Tris	1.6 M	193.8 g
Sodium acetate	800 mM	65.6 g
EDTA	40.27 mM	14.9 g
H_2O		To 100 mL
pH adjusted to 7.4		

2% agarose gel

Reagent	Concentration	Amount
Agarose	2%	4 g
1× TAE		To 200 mL
Mix and heat in microwave until agarose has completely dissolved.		

GelRed™ nucleic acid gel stain

Reagent	Concentration	Amount
GelRed™ (10,000× stock)	3×	30 µL
0.1 M sodium chloride		To 100 mL

2.2.9. Buffers and Solutions for In Vivo Experiments

HMEM-Pipes

Reagent	Concentration	Amount
Pipes	47 mg/L	235 mg
Sodium hydroxide	105 mg/L	52.5 mg
HMEM		To 500 mL
Filter sterilised		

Ethanol-propylene glycol-H_2O (ETOH-PG-H_2O/Vehicle)

Reagent	Concentration	Amount
Ethanol	50% (v/v)	5 mL
Propylene glycol	25% (v/v)	2.5 mL
H_2O	25% (v/v)	2.5 mL

DNP in NaCl

Reagent	Concentration	Amount
DNP (20 mg/mL aqueous stock)	2 mg/mL	100 µL
0.9% NaCl		900 µL

Tper EDTA-free lysis buffer

Reagent	Concentration	Amount
Complete mini EDTA-free		1 tablet
T-PER reagent		10 mL

Chloroform- MeOH extraction solution

Reagent	Concentration	Amount
Chloroform	33.3% (v/v)	3 mL
MeOH	66.7% (v/v)	6 mL

2.3. Purification of Mouse α-DNP IgE (SPE-7 clone)

2.3.1. Conjugation of DNP and BSA

BSA solution (1 g dissolved in 40 mL of conjugation solution) and FDNB solution (0.1 mL of FDNB stock added to 10 mL of Dioxane) were mixed together and incubated for 2 h at RT, shielded from light. The resultant mixture was subsequently dialysed against reverse osmosis (RO) water (freshened four times) for 48 h at 4 °C. A small aliquot of the dialysed product was taken for examination of the conjugation ratio of DNP and BSA using the formula on the following page:

Ratio (n) = (M.W. × A)/(c × ε × l)

- M.W. = molecular weight of BSA = 66,000 Da
- A = average absorbance at 360 nm (for DNP) obtained using a NanoDrop 1000 spectrophotometer (Thermal Scientific)
- c = concentration of BSA ≈ 1 g/ 55 mL (i.e. volume of the dialysed product) or 18.2 mg/mL
- ε = extinction coefficient of DNP at 360 nm = 17,400 $M^{-1}cm^{-1}$
- l = length of light path used (NanoDrop) = 0.1 cm

Once the ratio was determined to be within the normal range (2 to 9), the dialysed DNP-BSA solution was lyophilized (shielded from light in 50 mL falcon tubes at 10 mL/tube) overnight using the lyophilizing machine, and stored at 4 °C in a dark and dry place.

2.3.2. Coupling of DNP-BSA to HiTrap NHS-activated HP column

The HiTrap NHS-activated HP column was loaded, at 5 mL/min using a pump, with 30 mL of 1 mM HCl followed by 30 mL of coupling buffer. A 10 mg/mL DNP-BSA solution, prepared by diluting 0.2 g of lyophilized power with coupling buffer, was subsequently loaded onto and allowed to re-circulate the column for 90 min at RT, shielded from light. The column was then washed with 10 mL of coupling buffer, stripped off excess DNP with 10 mL of 1 M propionic acid, and rinsed with additional coupling buffer until the run-through became clear.

2.3.3. De-activation of Excess Active Groups

The following solutions were pumped through, at 5 mL/min, the coupled HiTrap column in that order:

- 30 mL of buffer A
- 30 mL of buffer B
- 30 mL of buffer A

(At this stage, the bottom of the column was capped before 30-min incubation at RT, shielded from light.)

- 30 mL of buffer B
- 30 mL of buffer A
- 30 mL of buffer B
- 15 mL of storage buffer.

After sealing the top and bottom with Parafilm, the column was stored at 4 °C (shielded from light) until further use.

2.3.4. Purification of SPE-7 from Hybridoma Culture Supernatant

After washing the DNP-BSA-coupled column with 10 mL of PBS, approximately 700 mL of SPE-7 hybridoma culture supernatant harvested (Section 2.5.4) was pumped through (5 mL/min) and allowed to re-circulate the column for 5 h (i.e. enough time for all supernatant to go through twice). The column was then washed with 25 mL of 1% NP40 in PBS followed by 100 mL of PBS (both at 5 mL/min), prior to elution with 50

mL of 0.1 M DNP solution. A total of ten fractions were collected and analysed by standard SDS-PAGE and Coomassie blue staining. All SPE-7-rich fractions identified were pooled and concentrated using a VIVASPIN 20 tube. The remaining solution (~ 5 mL) was dialysed again 1× PBS until a pale yellow colour was obtained. Finally, the purified SPE-7 was quantified using the SMART system with a Superdex 200PC 3.2/30 column (Amersham Biosciences), aliquoted and stored at -80 °C.

2.4. Mice

Female C57BL/6J (WT) mice and *VDR*-targeted VDR-deficient B6.129S4-*Vdr*^{tm1Mbd}/J mice that had been backcrossed to C57BL/6 mice for greater than 8 generations (*VDR*$^{-/-}$) mice [244] were obtained from The Jackson Laboratories (Bar Harbor, Maine, USA) and bred in house at the Centre for Cancer Biology (Adelaide, Australia). Genetically MC-deficient B6-*Kit*$^{W\text{-}sh/+}$ mice were used as breeding pairs to produce MC-deficient *Kit*$^{W\text{-}sh/W\text{-}sh}$ mice and their normal WT littermates. Adult *Kit*$^{W\text{-}sh/W\text{-}sh}$ mice have a profound deficiency of MCs, including less than 1.0% the wild-type number of MCs in the dermis [182, 245]. Another WT mouse strain, namely (WB/ReJ-*Kit*$^{W/+}$ × C57BL/6J-*Kit*$^{Wv/+}$)F1-*Kit*$^{+/+}$ (WBB6F1-*Kit*$^{+/+}$), was also obtained from The Jackson Laboratory, bred in house, and used in a number of experiments as indicated. Please note that WBB6F1-*Kit*$^{W/W\text{-}v}$ mice were not used in this project. All *in vivo* experiments were performed with age- and sex-matched mice of at least 8 weeks of age. Experiments were performed in compliance with the ethical guidelines of the National Health and Medical Research Council of Australia.

2.5. General Methods

2.5.1. Culturing of mBMCMCs

Bone marrow extracted from femur and tibia bones of mice was cultured in cBMCMC-early medium for the first three weeks (during which period cells were inspected and medium changed 2-3 times a week), and in cBMCMC-late for the remaining of the culturing (during which period cells were inspected and expanded once or twice a week). Cells obtained at the end of 5-6 weeks were examined by flow cytometry (FcεRI and c-kit double staining) as well as May-Grűnwald Geimsa staining (Section 2.5.7.2). Typical culture at this stage would consist of over 95% MCs, identified as $FcεRI^{+}c\text{-}kit^{+}$ and carrying large numbers of intracellular granules. All experiments conducted used 5- to 10-week-old cells.

2.5.2. Culturing of hCBMCs

To a 50 mL falcon tube, 5 mL of ACD was added, followed by 25 mL fresh human umbilical cord blood (Molecular Immunology Laboratory, Women and Children Hospital, Adelaide), 10 mL of dextran solution and 10 mL of PBS. Once the red blood cells have coagulated (approximately 20 min later), the top layer of cells were transferred to another tube containing 12 mL of histopaque-1077 and centrifuged at 650 g for 25 min without break. The resultant interface containing $CD34^{+}$ progenitor cells was carefully collected and washed first with PBS and subsequently with $CD34^{+}$ purification buffer. The cells obtained were incubated with human Fc receptor blocking Ab and magnetic $CD34^{+}$ beads at 4 °C for 30 min. Finally, the labelled $CD34^{+}$ cells were isolated using a magnetic separation column (Miltenyi Biotec), washed in $CD34^{+}$ purification buffer and cultured in

hCBMC medium for the following 10-12 weeks (during which period cells were inspected and medium changed once or twice a week).

2.5.3. Culturing of WEHI-3 hybridoma

A frozen aliquot (kept in liquid nitrogen for long-term storage) was thawed and allowed to recover and expand in cDMEM medium during the initial 1-2 weeks, by the end of which over 99% of cells would be viable. To harvest WEHI-3-conditioned medium, cells were seeded at 10^5 cells/mL and incubated at 37 °C/5% CO_2 for four days. Typical cell concentration at this stage would be approximately 10^6 cells/mL. Supernatant was harvested following two centrifugation steps (first step: 250 g for 10 min at 4 °C; second stop: 350 g for 20 min at 4 °C), an aliquot was taken for analysis by IL-3 ELISA, and the remaining was stored at -20 °C. To generate more frozen WEHI-3 stocks, cells at sub-confluency concentration (where cells would exhibit optimal growth rates) were collected and resuspended in cold hybridoma freezing solution containing FCS, which was added drop-wise onto the cell pellet, to a concentration of 10^7 cells/mL. The resultant cell suspension (1 mL/aliquot in cryovials) was stored at -80 °C in "Mr. Frosty" 1 °C freezing container (Nalgene) for the initial 24 hr, and subsequently transferred into liquid nitrogen.

2.5.4. Culturing of SPE-7 hybridoma

A frozen aliquot (kept in liquid nitrogen for long-term storage) was thawed and allowed to recover and expand in SPE-7 culturing medium during the initial 1-2 weeks, by the end of which over 99% of cells would be viable. To harvest SPE-7-conditioned medium for SPE-7 purification (Section 2.3.4), cells were seeded, incubated, and supernatant harvested in the same manner as for WEHI-3 hybridoma (Section 2.5.3.). The generation

of SPE-7 frozen stocks was also the same as for WEHI-3, except that freezing solution containing HS was used in this case.

2.5.2. Flow Cytometry

2.5.2.1. Surface Ag Labelling

Cells (1-2 × 10^6 cells/sample) were washed with cold FACS buffer and blocked with the appropriate Fc receptor blocking Ab for 15 min on ice. In the case of mBMCMCs, cells were immediately labelled with primary Abs; whereas in the case of hCBMCs, the blocking Ab was washed off first. All primary Ab (all directly conjugated) labelling steps were carried out on ice, shielded from light, for 30 min. Labelled cells were subsequently washed twice with FACS buffer, resuspended in 500 µl of FACS buffer each, and analysed on the same day using a Beckman Coulter Cytomics FC 500 Flow Cytometer equipped with CXP software (version 2.2). When analysis on the same day was not feasible, cells were resuspended in FACS-fix instead and stored at 4 °C in the dark until analysis.

2.5.2.2. Intracellular Ag Labelling

Cells (1-2 × 10^6 cells/sample) were washed with cold FACS buffer and fixed with the 1C fixation buffer (a component of the Fixation & Permeabilization Kit) for 20 min at RT. Cells were then washed with and resuspended in 1 × permeabilization buffer (diluted with H_2O from 10 × Permeabilization Buffer, which is the other component of the Fixation & Permeabilization Kit), and incubated with primary Ab(s) for 30 min on ice. When unconjugated primary Abs were used, cells were washed with 1 × permeabilization buffer following the first incubation and subsequently labelled with corresponding

fluorochrome-conjugated secondary Ab(s) for a further 30 min on ice. In all cases, labelled cells were finally washed with 1 × permeabilization buffer, resuspended in FACS buffer and analysed on a Beckman Coulter Cytomics FC 500 Flow Cytometer equipped with CXP software.

2.5.2.3. Caspase-3 Labelling

Caspase-3 labelling was carried out using the NucView^{TM} 488 Caspase-3 assay kit as instructed by the manufacturer. Briefly, cells were washed with and resuspended in PBS to a concentration of 0.5-1 × 10^6 cells/mL. 200 µL of the resultant cell suspension was transferred to a FACS tube, where 2 µL of Caspase-3 substrate stock solution was subsequently added. After 30-min incubation at RT, 300 µL of PBS was added to the sample, which was then ready for analysis using the Beckman Coulter Cytomics FC 500 Flow Cytometer equipped with CXP software (FL1 channel).

2.5.3. In Vitro Procedures

2.5.3.1. β-hexosaminidase Release Assay

Mouse BMCMCs (10^6 cells/mL) were preloaded with α-DNP IgE (2 µg/mL) in cBMCMC-early medium. After 16-h incubation at 37 °C/5% CO_2, cells were washed with and resuspended in Tyrodes buffer, plated at a concentration of 6.25 × 10^6 cells/mL in 96-well V-bottom plates (Greiner Bio-one), and stimulated for 1 h with DNP-HSA (10 ng/mL) or, as a positive control, PMA (50 ng/mL) / A23187 (10 µM). In experiments investigating the effects of $VitD_3$ analogues on MC degranulation, $VitD_3$/ETOH control was applied to cell culture either 8 h (in the case of $25OHD_3$) or immediately (in the case of $1\alpha,25(OH)_2D_3$) before IgE preload and, in all cases, immediately before DNP or

PMA/A23187 treatment. At the end of 1-h stimulation, culture supernatants and cell lysates were collected following centrifugation at 250 g for 5 min, and subsequent lysis of cell pellets using 0.5% Triton-X. All samples were then incubated with p-NAG solution for 1 h at 37 °C. β-hexosaminidase activity was detected by addition of 0.2 M glycine and absorbance at 405 nm was measured on an ELISA plate reader. Percentage of degranulation was calculated by dividing the β-hexosaminidase activity in the culture supernatant by the total β-hexosaminidase activity detected (supernatant plus lysate).

2.5.3.2. Histamine Release Assay

Mouse BMCMCs were preloaded with α-DNP IgE (SPE-7 clone) and stimulated with DNP-HSA as described in Section 2.5.3.1, except that stimulation was performed in mBMCMC starvation medium at 10^6 cells/mL for 30 min. Culture supernatants and cell lysates were collected following centrifugation at 250 g for 5 min, and subsequent lysis of cell pellets using 0.5% Triton-X in H_2O. The amount of histamine in all samples (1/20 dilution analysed for supernatants and 1/100 dilution for cell lysates) was measured using the EIA histamine kit as instructed by the manufacturer. Briefly, 12.5 µL of acylation buffer was mixed with 25 µL of sample dilutions, calibrators or controls in clean eppendorf tubes. 25 µL of acylation reagent was then added to each tube, immediately followed by vortexing. To the pre-coated plate, 50 µL of acylated samples/calibrators/controls was added per well, followed by 200 µL of histamine-alkaline phosphatase conjugate. After 2-h incubation at 4 °C with constant agitation, wells were washed and further incubated, in the dark with 200 µL of substrate per well, for 30 min at RT under constant agitation. Reaction was ended by the addition of 50 µL of stop solution per well, and absorbance at 405 nm was measured on an ELISA plate

reader. Percentage of histamine release for each sample was calculated by dividing the amount of histamine in the culture supernatant by its total amount (supernatant plus lysate).

2.5.3.3. IgE + sAg Stimulation of mBMCMCs

For ELISA and RNA extraction (quantitative real-time PCR; qRT-PCR), mBMCMCs were preloaded with α-DNP IgE as described in Section 2.5.3.1, following which cells were washed with and resuspended in mBMCMC starvation medium at 10^6 cells/mL. Subsequent stimulation was carried out with 2 ng/mL of DNP-HSA for either 6 h (in the case of cytokine measurement by ELISA; Section 2.5.3.5) or 3 h (in the case of total RNA extraction and qRT-PCR; Sections 2.5.4.2 to 2.5.4.4). For some experiments, $VitD_3$ analogues and their corresponding vehicle solutions were applied as described in later sections.

For cell lysate preparation and western blotting, mBMCMCs (0.5×10^6 cells/mL) were cultured in cDMEM-csFCS-4 medium for three days, at the end of which cells were counted and replated at 10^6 cells/mL in cDMEM-csFCS-3 medium with either ETOH or $1\alpha,25(OH)_2D_3$ (10^{-8} M; 0.1% v/v ETOH) added. After 16-h incubation, cells were washed with and resuspended in cDMEM-csFCS medium at 10^6 cells/mL. ETOH and $1\alpha,25(OH)_2D_3$ was added to the corresponding culture, followed sequentially by 4-h incubation, the addition of SPE-7 at 2 μg/mL, and 4-h further incubation. Cells were then washed with and resuspended in mBMCMC starvation medium at 10^6 cells/mL. ETOH and $1\alpha,25(OH)_2D_3$, followed immediately by 20 ng/mL of DNP-HSA, was added to the designated treatment groups. At either 2 min or 15 min post-stimulation, cells were

washed with cold PBS twice before proceeding to total cell lysate preparation (Section 2.5.5.1).

2.5.3.4. IgE-mediated stimulation of hCBMCs

Human CBMCs (10^6 cells/mL) were cultured, for two days, with 10 ng/mL of rhIL-4 and either ETOH, $25OHD_3$, or $1\alpha,25(OH)_2D_3$ in hCBMC medium. Human myeloma IgE was then added at 2.5 μg/mL, followed by 16-h further incubation. Preloaded cells were washed with and resuspended in hCBMC starvation medium at 10^6 cells/mL, and stimulated with 1 μg/mL of goat α-human IgE in the presence of ETOH or the corresponding $VitD_3$ analogue. Culture supernatants were collected at 6 h post-stimulation for cytokine measurement by ELISA.

2.5.3.5. Cytokine Measurement by ELISA

Freshly harvested culture supernatants from stimulated mBMCMCs and hCBMCs were used in all ELISA analysis according to manufacturers' instructions. In the case of mouse IL-6 ELISA, appropriate dilution of samples ranging from 1/2 to 1/5 was analysed; whereas in all other cases, neat supernatants were used. Briefly, 96-well ELISA plates (Costar) were incubated with capturing Ab diluted in corresponding coating buffer overnight at 4 °C. Coated wells were washed three times with PBS-Tween before 1-h blocking with appropriate ELISA blocking buffer (provided for eBioscience kits and home-made blocking solution for BD Biosciences kits) at RT. This was followed by three washes, 2-h incubation with samples and standards at RT, and three more washes. For BD Biosciences ELISA kits, all wells were then incubated with working detection solution (containing both detection Ab and the enzyme streptavidin- HRP) for 1 h at RT;

whereas for eBioscience kits, wells were incubated with detection Ab for 1 h at RT, followed by three washes and 30-min further incubation with HRP. In all cases, after a final three-wash step, 3,3',5,5'-tetramethyl-benzidine liquid substrate was added to all wells and reaction (RT; shielded from light) was stopped using stop solution when the top standards displayed maximum colour intensity (usually blue precipitates would be observed at the bottom of the wells). The optical density readings were obtained at 450 nm using an ELISA plate reader.

2.5.3.6. $VitD_3$ Treatment (without stimulation)

Mouse BMCMCs and hCBMCs (0.5×10^6 cells/mL) were cultured in cDMEM-csFCS-4 medium and hCBMC-csFCS medium, respectively, for three days, at the end of which cells were replated at 10^6 or 2×10^6 cells/mL in cDMEM-csFCS-3 medium. $VitD_3$ analogues were applied to the culture at required concentrations, and cells were incubated for the required lengths of time as indicated in later chapters.

2.5.3.7. Measurement of $1\alpha,25(OH)_2D_3$

Mouse BMCMCs were treated, at 2×10^6 cells/mL, with $25OHD_3$ (Section 2.5.3.6.) for 6 h before culture supernatants and cell lysates (prepared with NP40 lysis buffer) were collected, snap-frozen in liquid nitrogen, and stored, shielded from light, at -80 °C until analysis. Levels of $1\alpha,25(OH)_2D_3$ in all samples were measured using a radioimmunoassay kit according to the manufacturer's instructions.

2.5.4. Molecular Biology

2.5.4.1. Genotyping of WT and *VDR*$^{-/-}$ Mice

The tip of tails from WT and *VDR*$^{-/-}$ mice were digested overnight (55 °C; with constant agitation) in tail lysis buffer with freshly added proteinase K. Tissue lysates were centrifuged (13,000 g; 10 min; 4 °C) and the liquid layer was transferred to a clean tube containing 500 µL isopropanol. DNA precipitate was formed upon gentle inversion of the tube and subsequently collected by centrifugation (maximum speed [17,000 g]; 5 min; 4 °C), washed with 1 mL of 70% (v/v) ETOH each, and collected again by centrifugation (7,500 g; 5 min; 4 °C). The DNA pellets obtained were briefly dried (on 37 °C heating block) and re-dissolved (65 °C; 30 min) in 300 µL of TE buffer each. Samples were stored at 4 °C (short-term) or -20 °C (long-term) until PCR analysis.

GoTaq Green master PCR cocktail was prepared by mixing GoTaq Green master mix (12.5 µL/sample), nuclease-free H_2O (6.5 µL/sample), and each of the primer pair (both at 2.5 µL/sample). The primer pair used for WT genotype consisted of C57/BL6 - *VDR*$^{+/+}$ and the common primer, whereas that used for *VDR*$^{-/-}$ genotype consisted of C57/BL6 - *VDR*$^{-/-}$ and the common primer (Section 2.1.12). Mouse β-actin primer pair was also used for each sample as loading controls. In 0.2 mL PCR tubes (Ultraflux), 24 µL of each PCR cocktail was mixed with 1 µL of each DNP sample, which was then subjected to thermal cycles (carried out in Veriti® 96-Well Thermal Cycler; Applied Biosystems) as described on the following page:

Holding 1 (denaturing step):	95°C, 3 min
Cycling (35 cycles; amplification step):	94°C, 30 sec 61°C, 1 min 72°C, 1 min
Holding 2 (re-annealing step):	72°C, 2 min
Holding 3 (temporary storage):	4°C, forever

The resultant PCR products were loaded onto a 2% agarose gel (5 µL/lane) and subjected to gel electrophoresis at 80 volts for approximately 30 min. DNA bands were visualised, following 30-min staining in GelRed^{TM} nucleic acid gel stain, under UV light (UVitech) using the UV photo software.

2.5.4.2. RNA Extraction

Unless otherwise stated, 5×10^6 cells of each treatment group were used for RNA extraction to achieve desirable amount and quality of the final product. After collection by centrifugation (250 g, 5 min, 4 °C), cells were lysed with TRIzol reagent (1 mL/sample) by pipetting (Gilson P1000 pipette with filtered tip) up and down at least 10 times and passing through a 26 G needle twice. Samples at this stage were either stored at -80 °C (preferred) or used for immediate RNA extraction. In the former case, samples were thawed and allowed to reach equilibrium at RT for 5 min before proceeding to the next step. In all cases, 200 µL of chloroform was added to each TRIzol preparation and the tube was shaken vigorously for 15 sec, followed by 3-min incubation at RT. Samples were then centrifuged at 12,000 g for 15 min (4 °C) to achieve phase separation into the lower phenol-chloroform layer and the upper aqueous layer, which contained the RNA

and was subsequently transferred to a clean tube. RNA precipitate was obtained upon addition of 500 µL of isopropanol to each tube and centrifugation at 12,000 g for 10 min (4 °C), washed with 1 mL of 75% (v/v) ETOH each, and briefly air-dried on a 37 °C heating block. Finally, each air-dried RNA pellet was re-dissolved in 20 µL of RNase-free H_2O (65 °C, 10 min) and quantified using a NanoDrop 1000 spectrophotometer (Thermal Scientific).

2.5.4.3. Complementary DNA (cDNA) Synthesis

QuantiTech reverse transcription kit was used to generate cDNA from all RNA samples, according to the manufacturer's instructions. Briefly, 1 µg of RNA (adjusted to 12 µL with added RNase-free H_2O) was incubated with 2 µL of the genomic (g)DNA Wipeout Buffer for 2 min at 42 °C. The resultant reaction (14 µL) was subsequently mixed with a master stock containing 1 µL of Reverse Transcriptase, 1 µL of reverse transcription Primer Mix, and 4 µL of reverse transcription Buffer (5×); and incubated for 30 min at 42 °C followed by 3 min at 95 °C. All incubation steps mentioned above were performed using the Veriti® 96-Well Thermal Cycler. The cDNA samples obtained (20 µL each) were stored at 4 °C (short-term) or -20 °C (long-term) until analysis.

2.5.4.4. qRT-PCR

This was performed in triplicate with cDNA samples generated from cell cultures (Section 2.5.4.3) used at an appropriate dilution ranging from 1/3 to 1/10. Each final reaction (10 µL) consisted of 2 µL of cDNA dilution, 5 µL of QuantiTech Sybr green master mix, 1 µL RNase-free H_2O, and 1 µL of each of the designated primer pair (5 µg/mL working diluted used). β-actin primer pair was used at all cases to generate

loading controls. Reactions containing additional RNase-free H_2O instead of cDNA dilution were also included for each primer pair used as "no template" controls. All RT-PCR was carried out in the Rotor-Gene 6000 Real-time Rotary Analyzer (Corbett) using conditions as follows:

Holding 1:	95°C, 15 min
Cycling (45 cycles):	95°C, 20 sec
	52°C, 30 sec
	72°C, 30 sec (acquisition step)
Holding 2:	72°C, 60 sec
Melting:	72°C, 90 sec
	72°C to 99°C at 5 sec/°C

The relative quantity of the PCR product was obtained using the "Comparative Quantitation" option of the Rotor-Gene 6000 Series Software (version 1.7).

2.5.5. SDS-PAGE and Western Blot Analysis

2.5.5.1. Preparation of Total Cell Lysates

Cell cultures (2-3 × 10^6 cells/sample) were washed twice with cold PBS, and supernatant was removed as thoroughly as possible. Each cell pellet was subsequently lysed in 100 μL of complete NP40 lysis buffer, incubated on ice for 30 min, and centrifuged (17,000 g, 15 min, 4 °C) to remove insoluble cell debris. The resultant total cell lysates were quantitated using the Bio-Rad D_c protein assay according to the manufacturer's instructions, and stored at -20 °C until analysis.

2.5.5.2. SDS-PAGE

Total cell lysate samples (Section 2.5.5.1) were thawed, mixed with 5× sample loading buffer (i.e. in a 4:1 ratio), and boiled for 5 min before being subjected to SDS-PAGE (10% running gel; 20-50 μg of protein/lane) at 25 mAmps/gel for 60-90 min. Benchmark™ pre-stained protein markers were loaded in parallel as a reference for different protein sizes.

2.5.5.3. Protein Transfer and Western Blot Analysis

Following SDS-PAGE (Section 2.5.5.2), proteins were transferred onto a nitrocellulose membrane at 250 mAmps for 90 min. The membrane was blocked with 1% blocking buffer for 1 h at RT, and subsequently blotted with designated primary Abs (diluted in 0.1% blocking buffer) overnight at 4 °C, followed by the corresponding HRP-conjugated secondary Ab(s) for 1 h at RT. Three 15-min washes with 1× TNT were carried out after each blotting step. Finally, signals were developed using enhanced chemiluminescence (ECL) with the Amersham ECL Plus Western Blotting Detection System, detected by LAS-4000 Luminescence Analyser, and analysed using the Multi Gauge software (version 3.1). In cases where membranes were re-probed with another primary Ab, they were briefly washed with 1× TNT and stripped with the stripping solution according to the manufacturer's instructions, prior to re-probing in the same manner as described above.

2.5.6. In Vivo and Related Procedures

2.5.6.1. Engraftment of mBMCMCs

After confirmation of over 95% purity (Section 2.5.1), 4- to 6-week-old mBMCMCs (resuspended in DMEM at 4×10^7 cells/mL) were transferred by intra-dermal injection (*i.d.*, 2 injections into each ear with 1×10^6 cells in 25 µl DMEM per injection) into both ears of 4- to 6-week-old $Kit^{W\text{-}sh/W\text{-}sh}$ mice. PCA experiments were carried out 5-8 weeks after *i.d.* transfer of mBMCMCs.

2.5.6.2. PCA with Topical Application of $1\alpha,25(OH)_2D_3$ or $25OHD_3$

For PCA with $1\alpha,25(OH)_2D_3$ application, the right and left ears of mice were injected *i.d.* with 20 µl of SPE-7 (5 µg/mL; diluted in HMEM-Pipes) and 20 µL of HMEM-Pipes, respectively. Immediately following injection, both ears were topically painted (20 µL/ear, 10 µL on the outer surface and 10 µL on the inner surface) with either 3 µM of $1\alpha,25(OH)_2D_3$ diluted in ETOH-PG-H_2O (vehicle) or ETOH-PG-H_2O alone. For PCA with $25OHD_3$ application, ears of mice were topically painted with 3 µM of $25OHD_3$ or ETOH-PG-H_2O alone 8 h prior to SPE-7/HMEM-Pipes injection. Sixteen hours later in both cases, mice were injected *i.v.* (retro-orbitally) with 100 µL of DNP-HSA (2 mg/mL) diluted in sterile 0.9% saline. Ear swelling was quantified by measurements of ear thickness using a Peacock dial thickness gauge (model G-1A) prior to (baseline) and 0.5, 1, 2, 3, or 6 h after DNP-HSA administration. At various time points post-DNP-HSA, mice were sacrificed by CO_2 inhalation and samples of ear were taken for histology (Section 2.5.6.3), cytokine and/or $VitD_3$ measurements (Section 2.5.6.4), or RNA

extraction and qRT-PCR (Section 2.5.6.5). Serum samples were also prepared for cytokine and/or $VitD_3$ measurements (Section 2.5.6.6).

2.5.6.3. Ear Tissue Histology and Numeration of Tissue MCs

Samples of ear pinna (1 mm-wide strips through the centre) were fixed in 10% buffered formalin, embedded in paraffin (with care to ensure a cross-section orientation), and 4 μm sections were cut. Ear sections were dewaxed by being immersed sequentially in Xylene (twice; 5 min each), 100% ETOH (twice; 3 min each), 70% ETOH (3 min), 50% ETOH (3 min), and H_2O (until staining); and stained with 0.1% acidic toluidine blue (Section 2.5.7.4) for detection of MCs (cytoplasmic granules appear purple). Ear pinna MCs were counted in 5-8 consecutive fixed fields of 870 μm width under 200× magnification, and MC numbers were expressed per horizontal ear cartilage field length (mm), using computer-generated image analysis (NIH Image J software, version 1.43×).

2.5.6.4. Ear Tissue Lysate Preparation and Analysis

For cytokine measurement in ear tissues, the remaining halves of each ear, following the removal of sections for histology (Section 2.5.6.3), were finely cut up on an ice cold surface. Tissue samples were each sonicated in 250 μL of Tper EDTA-free lysis buffer containing protease inhibitors, and frozen immediately at –80 ºC until analysis as follows. After thawing at RT, samples were centrifuged twice at 17,000 g (10 min each, 4 ºC) and the supernatants were collected. TNFα, IL-6 and IL-10 protein concentrations in the supernatants were measured by ELISA (eBioscience), according to the manufacturer's instructions (lower limit of detection was 15.6 pg/mL, 7.8 pg/mL, and 31.3 pg/mL, respectively). Data obtained from each group were expressed as pg cytokine/mg protein,

where total protein concentrations in the supernatants were measured by a Bio-Rad Dc protein assay, according to the manufacturer's instructions.

2.5.6.5. Total RNA Extraction from Ear Tissues

Mouse ears were finely chopped on an ice cold surface and each sonicated in 500 µL of TRIzol reagent. Lysates were centrifuged at 17,000 g for 10 min at 4 °C to collect supernatants, to each of which a further 500 µL of TRIzol reagent was then added. After the addition of 200 µL of chloroform to each sample, RNA was prepared as described in Section 2.5.4.2.

2.5.6.6. Serum Preparation and Analysis

For cytokine measurement in serum samples, newly sacrificed mice were bled from the heart, and blood samples were incubated at RT for approximately 30 min before centrifugation twice at 13,000 g (5 min each, 4 °C) to collect serum. Serum samples were stored at -80 °C until analysis as follows. After thawing at RT, TNFα, IL-6 and IL-10 protein concentrations in the sera were measured and analysed as described previously for the ear lysates (Section 2.5.6.4).

2.5.7. Histochemistry and Immunohistochemistry

2.5.7.1. Cytospin Slide Preparation

Various MC cultures (100 µL each) were spun onto Polysine^{TM} slides (Menzel-Gläser) at 100 g for 5 min (Shandon Cytospin 3) and allowed to air-dry prior to subsequent staining.

2.5.7.2. May-Grűnwald Giemsa Staining

Air-dried cytospin slides (Section 2.5.7.1) were stained with the Accustain Giemsa and May-Grűnwald stains according to manufacturer's instructions. Briefly, slides were firstly immersed in May-Grűnwald stain for 5 min and de-stained in PBS for 90 sec. The slides were then counter-stained with Giemsa stain dilution (1/20 with H_2O) for 20 min, rinsed with water and air-dried. Coverslips were mounted onto samples using DePex mounting medium before microscopic observation.

2.5.7.3. Kimura Staining of hCBMCs

Human CBMC culture was mixed with Kimura staining solution in a 2:1 ratio, and incubated for 5 min at RT prior to observation of MCs (with stained granules) using a haemocytometer.

2.5.7.4. Toluidine Blue Staining

For toluidine blue staining of hCBMCs, cytospin preparation (Section 2.5.7.1) of cell culture was stained with 1% acidic toluidine blue solution for 15 min, rinsed with H_2O, air-dried and finally mounted in DePex mounting medium.

For toluidine blue staining of ear tissue MCs, dewaxed ear sections (Section 2.5.6.3) were stained with 0.1% acidic toluidine blue solution for exactly 1 min, thorough rinsed with H_2O, air-dried and finally mounted in DePex mounting medium.

2.5.7.5. Immunohistochemistry

Freshly prepared cytospin slides were fixed with the 1C fixation buffer (a component of the Fixation & Permeabilization Kit) for 20 min at RT. Slides were then rinsed three

times with 1 × permeabilization buffer (diluted with H_2O from 10 × Permeabilization Buffer, which is the other component of the Fixation & Permeabilization Kit) before overnight staining with the designated primary Ab and its corresponding isotype control in a humid box at 4 °C. After three 3-min washes with 1 × permeabilization buffer, slides were stained with the corresponding secondary Ab at RT, shielded from light, for 1 h. Following three additional washes, slides were stained with 1 µg/mL working dilution (with MeOH) of DAPI stained at RT for 2 min, rinsed with 1 × permeabilization buffer, and finally mounted with Fluorescence Mounting Medium. After drying in the dark at 4 °C for at least 4 h, slides were observed and images taken using the Nikon Spectral Imaging Confocal Microscope DIGITAL ECLIPSE C1si equipped with EZ-C1 software (version 3.20).

2.5.8. Centrifugation

Tissue culture centrifugation was performed using either a Heraeus Megafuge (1.0R) or an Eppendorf Centrifuge (5810R), whereas centrifugation of all eppendorf tubes and PCR tubes was performed using a Heraeus FRESCO 17 Centrifuge.

2.5.9. Statistical Analyses

All data shown in Chapters 3, 4, and 6 were tested for statistical significance using the unpaired, two-tailed, Student's *t*-test (GraphPad Software, version 5.04) between each pair of different treatments. For Chapter 5, analysis of variance (ANOVA) for repeated measures was used to assess differences in ear swelling among mouse groups in all PCA experiments, and other experiments that involved repeated measurements on the same animal over a period of time. All other data were tested for statistical significance using

the unpaired, two-tailed, Student's *t*-test between each two treatment groups. In all cases, *P* values less than 0.05 were considered statistically significant, and data are presented as either "mean + SEM", "mean + SD" or "median" as indicated.

CHAPTER 3

$1\alpha,25(OH)_2D_3$ POTENTIATES THE NEGATIVE IMMUNOREGULATORY PROPERTIES OF MAST CELLS DURING IgE+sAg-MEDIATED ACTIVATION *IN VITRO*

3.1. Introduction

Our recent findings provided evidence that 1α,25$(OH)_2D_3$ can enhance the anti-inflammatory properties of dermal MCs during chronic low-dose UVB irradiation. [163] Although much attention has been focused on the effects of $VitD_3$ insufficiency in various settings of autoimmunity [246-248], allergy [249, 250] and the development of certain cancers [251], there is comparatively very little known about the modulatory properties of $VitD_3$ on IgE-mediated MC activation. Excessive activation of MCs in response to IgE and its cognate Ag is a hallmark feature of chronic allergic disease and immediate anaphylaxis. Therefore, it is important to establish the effects of 1α,25$(OH)_2D_3$ on MC degranulation and *de novo* cytokine production during these processes. The anti-inflammatory cytokine IL-10, although rarely mentioned in the context of IgE + sAg-mediated MC activation, is also worth examining in response to 1α,25$(OH)_2D_3$ treatment. The human *IL-10* gene contains a VDRE in its promoter region, thus making its encoded cytokine a direct target of 1α,25$(OH)_2D_3$-mediated production. [225, 252] Furthermore, we recently showed that 1α,25$(OH)_2D_3$ can induce IL-10 production by mBMCMCs *in vitro* as well as by cutaneous MCs following UVB irradiation *in vivo*. [163]

The majority of the biological functions of 1α,25$(OH)_2D_3$ are exerted via the genomic pathway (Section 1.8.1), which utilises VDRs. [253] Therefore, it is important to determine the VDR-dependence and thus the pathway specificity for any potential effect of 1α,25$(OH)_2D_3$ on IgE + sAg-activated MCs. However, due to the recent suggestion that VDRs are also capable of certain interactions in a non-genomic $VitD_3$-dependent manner (Section 1.8.2) [229, 230], additional investigation that utilises certain pathway-specific $VitD_3$ agonists and/or antagonists is required to ascertain the involvement of either one or

both pathways. The determination of $VitD_3$ pathway specificity can also facilitate the search for potential mechanisms responsible for $VitD_3$-mediated immunoregulation of MCs in various immune settings.

The particular non-genomic pathway-specific $1\alpha,25(OH)_2D_3$ agonist utilised in the current study is curcumin (diferuloylmethane). Curcumin is a naturally occurring yellow pigment isolated from the rhizomes of the plant *Curcuma Longa* Lin found in South and Southeast Asia. [254] Its medicinal value has been well documented, highlighting specifically its antioxidant, anti-tumor, and anti-inflammatory properties and its current application in pre-clinical trials for cancer and/or inflammation treatment. [255-259] For example, curcumin can inhibit tumor initiation *in vivo* [255] as well as the proliferation and survival of tumor cells *in vitro* [260]. It can also down-regulate the production of inflammatory cytokines by human monocytes, alveolar macrophages, and T cells. [257, 261] Recent evidence demonstrates that curcumin is able to bind to an alternative ligand binding pocket in VDR with a low micromolar affinity, and thus function as a non-genomic agonist of $1\alpha,25(OH)_2D_3$. [230] Therefore, it will be illuminating to examine the effects of curcumin on IgE + sAg-activated MCs and how they compare to those of $1\alpha,25(OH)_2D_3$.

For this chapter of work, we firstly examined the effects of $1\alpha,25(OH)_2D_3$ on IgE + sAg-mediated MC degranulation, as indicated by histamine and β-hexosaminidase release, as well as the *de novo* synthesis of various cytokines, including TNFα, IL-6 and IL-10. By employing *VDR*$^{-/-}$ as well as WT mBMCMCs in the above assessments, the VDR-dependence for any effect of $1\alpha,25(OH)_2D_3$ would be determined. Furthermore, with the

aid of the non-genomic-pathway-restricted $VitD_3$ agonist, curcumin, we investigated the pathway specificity for the effects of $1\alpha,25(OH)_2D_3$.

3.2. Results

3.2.1. WT and VDR$^{-/-}$ mBMCMCs exhibit similar phenotypical and functional characteristics

The C57BL/6-*VDR*$^{-/-}$ mice used for the current project were generated as a mouse model of VitD-dependent rickets type II by targeted ablation of the second zinc finger of the VDR DNA-binding domain [244], and have since become a valuable tool for exploring new biological functions of $1\alpha,25(OH)_2D_3$ under physiological and/or pathological conditions as well as determining the pathway specificity (i.e. genomic versus non-genomic) for these functions. Nevertheless, before using C57BL/6-*VDR*$^{-/-}$ mBMCMCs as well as their WT counterparts to determine the VDR dependence of any potential effects of various $VitD_3$ analogues, we considered it essential to establish if the two types of MCs exhibit similar intrinsic phenotypical and/or functional properties. As shown in **Figure 3.1**, *VDR*$^{-/-}$ mice differ from their WT counterparts in various physical aspects, such as growth retardation (**Figure 3.1a**), the extensive presence of grey (instead of black) hairs throughout the body (**Figure 3.1a**), dilation of hair follicles and signs of alopecia in the facial area (**Figure 3.1b**), the shorter hind limbs with abnormal morphology (**Figure 3.1c**) and the increased fragility of the bones due to hypercalcemia. Despite the above differences between the two mouse strains, WT and *VDR*$^{-/-}$ mBMCMCs displayed very similar phenotypical properties (**Figure 3.2**). For instance, May-Grűnwald Giemsa staining of 5-week-old cells revealed similar granularity between WT and *VDR*$^{-/-}$

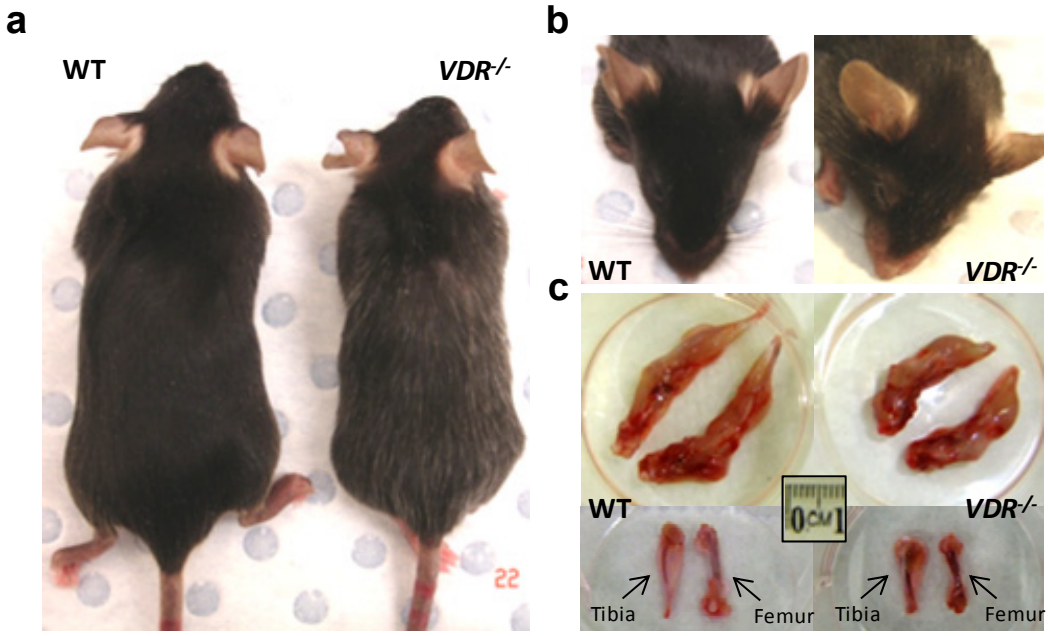

Figure 3.1 Phenotypical comparisons of WT and *VDR*$^{-/-}$ mice.
Body (a) and head (b) images of WT and *VDR*$^{-/-}$ mice. (c) Images of hind limbs (top panel) and separated tibia and femur bones (bottom panel) of WT and *VDR*$^{-/-}$ mice.

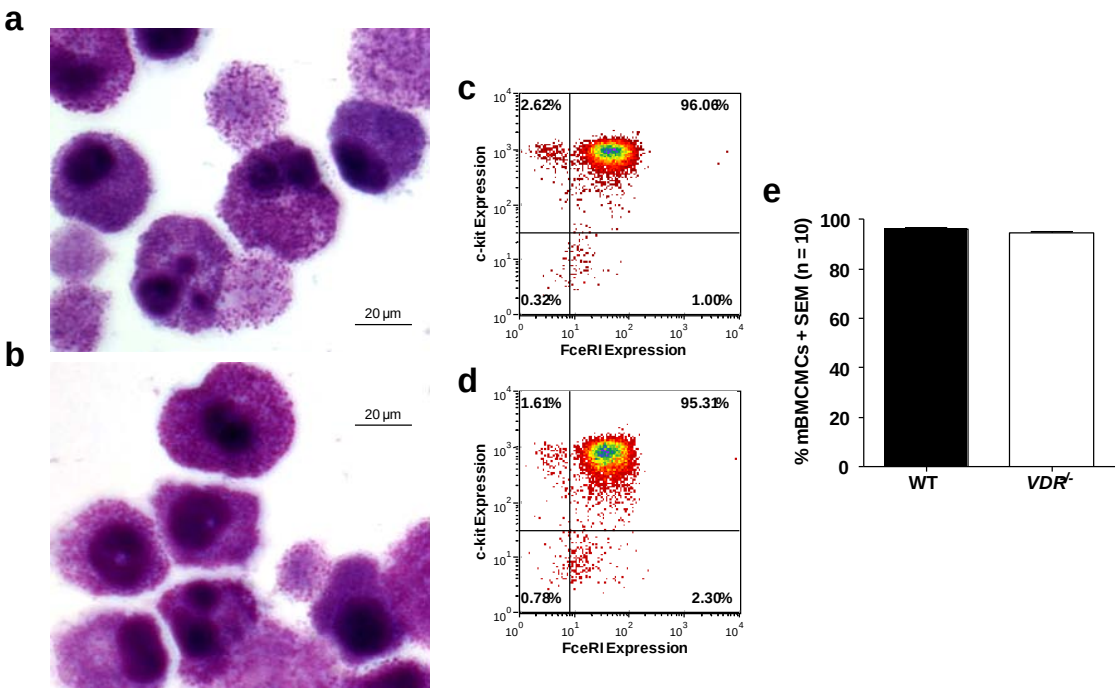

Figure 3.2 Phenotypical comparisons of WT and *VDR*$^{-/-}$ mBMCMCs.
(a and b) May-Grűnwald Giemsa staining of 5-week-old WT (a) and *VDR*$^{-/-}$ (b) mBMCMCs. (c and d) 5-week-old WT (c) and *VDR*$^{-/-}$ (d) mBMCMCs were stained with FITC-FcεRI and PE-c-kit mAbs and analysed by flow cytometry. (e) Purity of 5-week-old WT and *VDR*$^{-/-}$ mBMCMCs as obtained from flow cytometric analysis (indicated by the FcεRI^{+}c-kit^{+} population). Data are representative of ten independent cultures used in this project.

populations (**Figures 3.2 a and b**), surface labelling (by flow cytometry) of FcεRI and c-kit molecules on these cells also showed similar levels of expression for both (**Figures 3.2 c and d**), and there was no disparity in the calculated purity of WT versus *VDR*$^{-/-}$ mBMCMCs at the end of 5-week culturing (**Figure 3.2e**), indicating similar rates of development between the two types of cells.

From various functional aspects, WT and *VDR*$^{-/-}$ mBMCMCs exhibited similar rates of sensitization with α-DNP IgE (SPE-7 clone [**Figure 3.3a]** and HIN-ε26 clone **[Figure 3.4a]**). Upon IgE + DNP-HSA-mediated stimulation, they also demonstrated very similar extents of degranulation as evidenced by both β-hexosaminidase (**Figures 3.3b and 3.4b**) and histamine (**Figure 3.3c**) release, as well as similar production levels of pro-inflammatory cytokines, TNFα and IL-6 (**Figures 3.3 d and e; 3.4 c and d**), and the anti-inflammatory cytokine, IL-10 (**Figure 3.3f**). More importantly, these similarities were observed when two different clones of highly cytokinergic α-DNP IgE molecules, SPE-7 (**Figures 3.3**) and H1 DNP-ε-26 (**Figure 3.4**) [(262)], were used.

3.2.2. 1α,25(OH)$_2$D$_3$ does not affect the efficiency of IgE preload, the expression of surface molecules, and survival of mBMCMCs

Before investigating the effects of 1α,25(OH)$_2$D$_3$ on the pro-inflammatory properties of MCs during IgE + sAg-mediated activation, we first determined if this immunomodulatory agent affects MC development and differentiation, which may have intrinsic impact on their response to IgE-mediated activation. Using a flow cytometry approach, it was confirmed that 1α,25(OH)$_2$D$_3$ had no effect (as compared to the ETOH [0.03% final]-treated controls) on the IgE preload efficiency of both WT and *VDR*$^{-/-}$

Figure 3.3 Functional comparisons of WT and *VDR*$^{-/-}$ mBMCMCs following IgE (SPE-7 clone) + sAg-mediated activation.

Five-week-old WT and *VDR*$^{-/-}$ mBMCMCs were preloaded with 2 μg/mL of α-DNP IgE (SPE-7 clone) for 16 h. (a) Pre-loaded cells were subsequently stained with FITC-mIgE, Alexa 647-FcεRI, and PE-c-kit mAbs, and analysed by flow cytometry to assess the efficiency of the IgE preload. Non-pre-loaded cells (NT) were included as negative controls. Note that only the FcεRI^{+}c-kit^{+} cell population only is displayed. (b) Preloaded cells were stimulated with various concentrations of DNP-HSA for 1 h, and the extent of β-hexosaminidase degranulation was measured using β-hexosaminidase release assay. Unstimulated cells (NT) and cells that were treated with PMA/A23187 were used as negative and positive controls, respectively. (c) Preloaded cells were stimulated with 10 ng/mL of DNP-HSA for 30 min, and the extent of histamine release was measured using histamine release assay. Naive cells and cells that were preloaded only were used as negative controls. (d – f) Preloaded cells were stimulated with 20 ng/mL of DNP-HSA for 6 h, and the secretion of TNF (d), IL-6 (e), and IL-10 (f) into culture supernatant was detected using ELISA. Naive cells and cells that were preloaded only were used as negative controls. Data (b-f, mean ± SEM) are representative of at least three independent experiments.

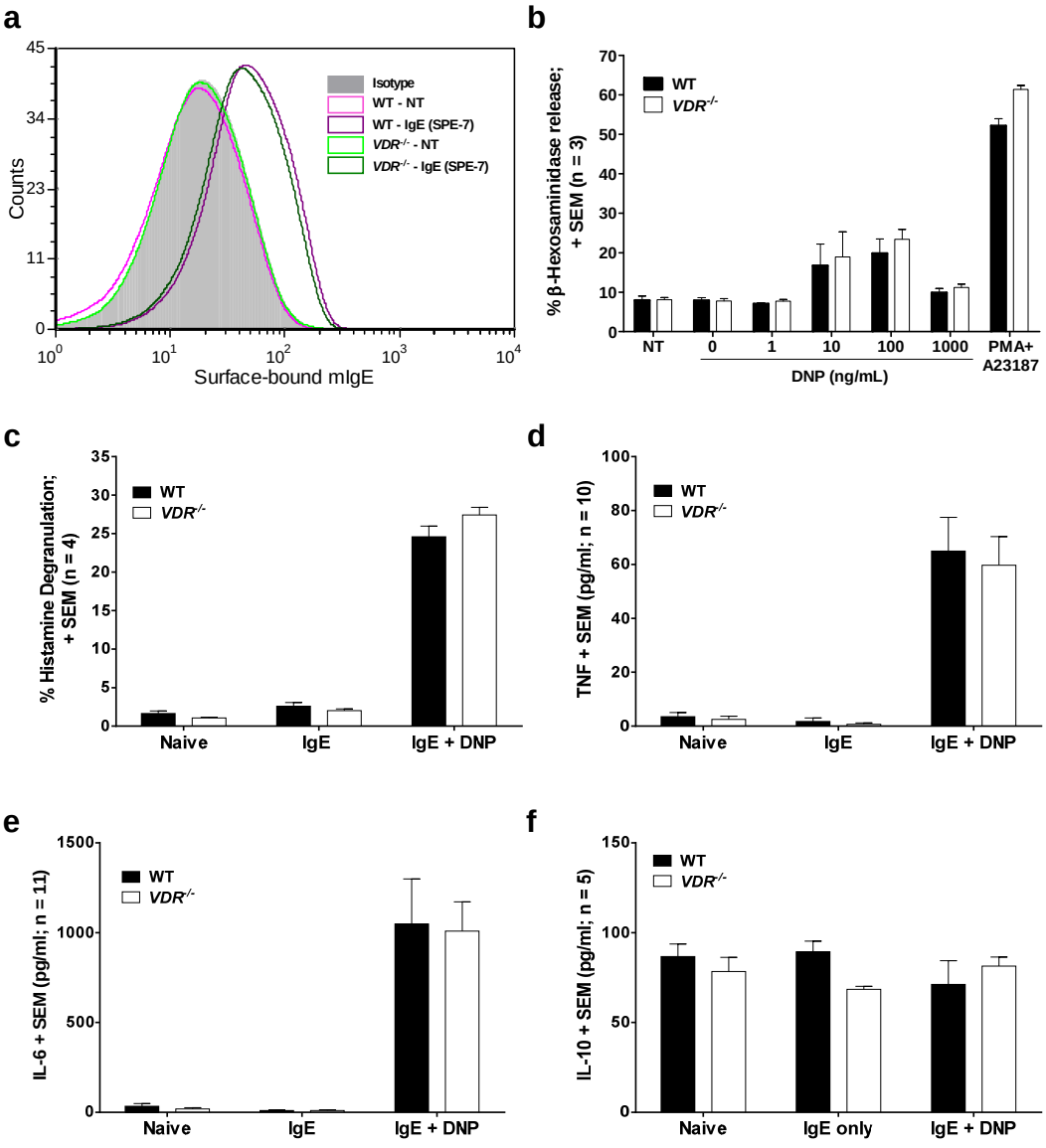
a
Counts
Surface-bound mIgE
Isotype
WT - NT
WT - IgE (SPE-7)
VDR-/- - NT
VDR-/- - IgE (SPE-7)
b
% β-Hexosaminidase release; + SEM (n = 3)
WT
VDR-/-
NT
0
1
10
100
1000
PMA+ A23187
DNP (ng/mL)
c
% Histamine Degranulation; + SEM (n = 4)
WT
VDR-/-
Naive
IgE
IgE + DNP
d
TNF + SEM (pg/ml; n = 10)
WT
VDR-/-
Naive
IgE
IgE + DNP
e
IL-6 + SEM (pg/ml; n = 11)
WT
VDR-/-
Naive
IgE
IgE + DNP
f
IL-10 + SEM (pg/ml; n = 5)
WT
VDR-/-
Naive
IgE only
IgE + DNP

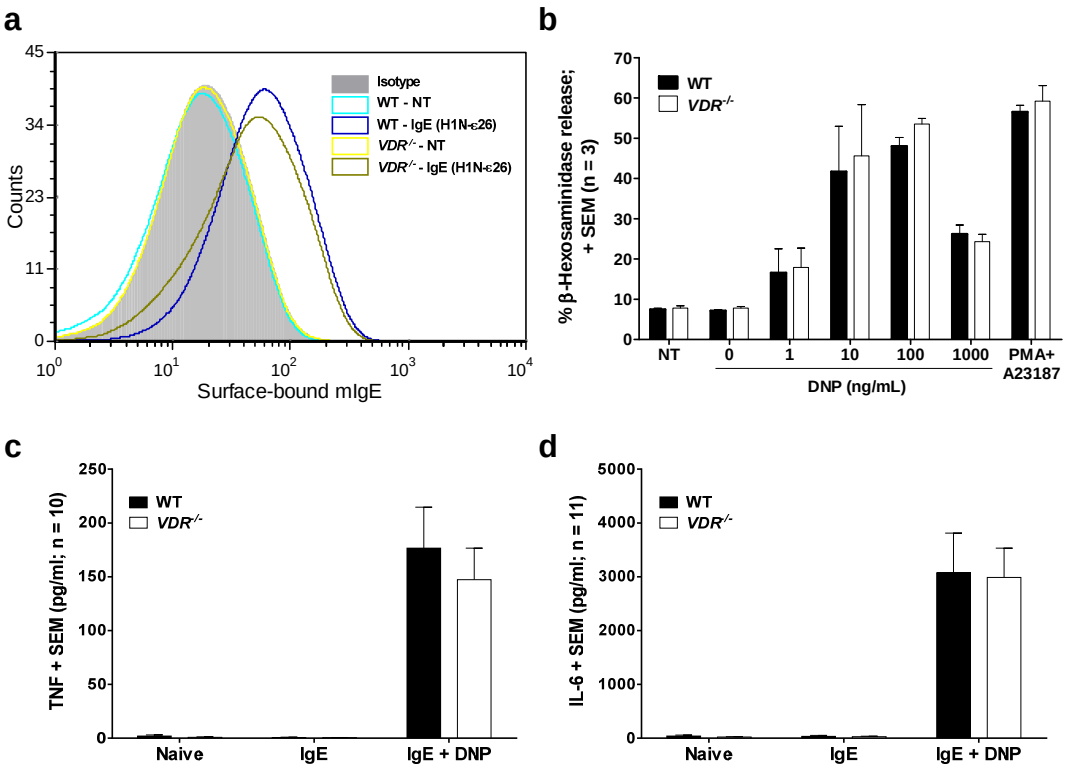

Figure 3.4 Functional comparisons of WT and *VDR*$^{-/-}$ mBMCMCs following IgE (H1N-ε26 clone) + sAg-mediated activation.

Five-week-old WT and *VDR*$^{-/-}$ mBMCMCs were preloaded with 2 µg/mL of α-DNP IgE (H1N-ε26 clone) for 16 h. (a) Pre-loaded cells were subsequently stained with FITC-mIgE, Alexa 647-FcεRI, and PE-c-kit mAbs, and analysed by flow cytometry to assess the efficiency of the IgE sensitization. Non-pre-loaded cells (NT) were included as negative controls. Note that only the FcεRI^{+}c-kit^{+} cell population is displayed. (b) Preloaded cells were stimulated with various concentrations of DNP-HSA for 1 h, and the extent of β-hexosaminidase degranulation was measured using β-hexosaminidase release assay. Unstimulated cells (NT) and cells that were treated with PMA/A23187 were used as negative and positive controls, respectively. (d and e) Preloaded cells were stimulated with 20 ng/mL of DNP-HSA for 6 h, and the secretion of TNF (d) and IL-6 (e) into culture supernatant was detected using ELISA. Naive cells and cells that were preloaded only were used as negative controls. Data are representative of at least three independent experiments.

mBMCMCs following 16-h incubation with SPE-7 (**Figures 3.5 a and b**). Six hours after DNP stimulation, the expression of key surface markers, including FcεRI and c-kit, was also comparable between 1α,25$(OH)_2D_3$ and ETOH co-treatment (**Figures 3.5 c-f**). Although both types of co-treatment slightly down-regulated FcεRI as well as c-kit expression as compared to naïve controls, this was likely due to Ag-triggered receptor internalisation [263, 264], a reduced health status of the cells following IL-3 and FCS deprivation during stimulation [265], and/or simply the addition of ETOH (0.03% final). Cell survival is another process that can directly affect other aspects of MC functionality, and it can be enhanced by highly cytokinergic IgE molecules alone. [262, 266] It was, therefore, significant that the survival rate, as indicated by caspase-3 labelling, of both WT and *VDR*$^{-/-}$ mBMCMCs showed no disparities between the 1α,25$(OH)_2D_3$- and ETOH-treated groups (**Figures 3.5 g and h**). However, the slightly higher caspase-3 expression in all stimulated cell groups when compared to the naive cells is likely also due to the presence of ETOH (0.03% final), as ETOH has been shown to induce apoptosis in HMC-1 cell lines (0.25 %) and mBMCMCs (2 %). [267]

3.2.3. 1α,25$(OH)_2D_3$ reduces IgE + sAg-mediated mBMCMC degranulation in a VDR-dependent manner

Mast cell degranulation and thus the mediators released play major roles in IgE-dependent allergic reactions, especially during the early-phase responses (Section 1.3.2). [64] Therefore, it is important to investigate the immunological effects of 1α,25$(OH)_2D_3$ on IgE + sAg-mediated MC degranulation. To achieve this, WT and *VDR*$^{-/-}$ mBMCMCs were preloaded with SPE-7 in the presence of indicated concentrations of 1α,25$(OH)_2D_3$ or ETOH (0.03 %), and subsequently stimulated with DNP together with 1α,25$(OH)_2D_3$

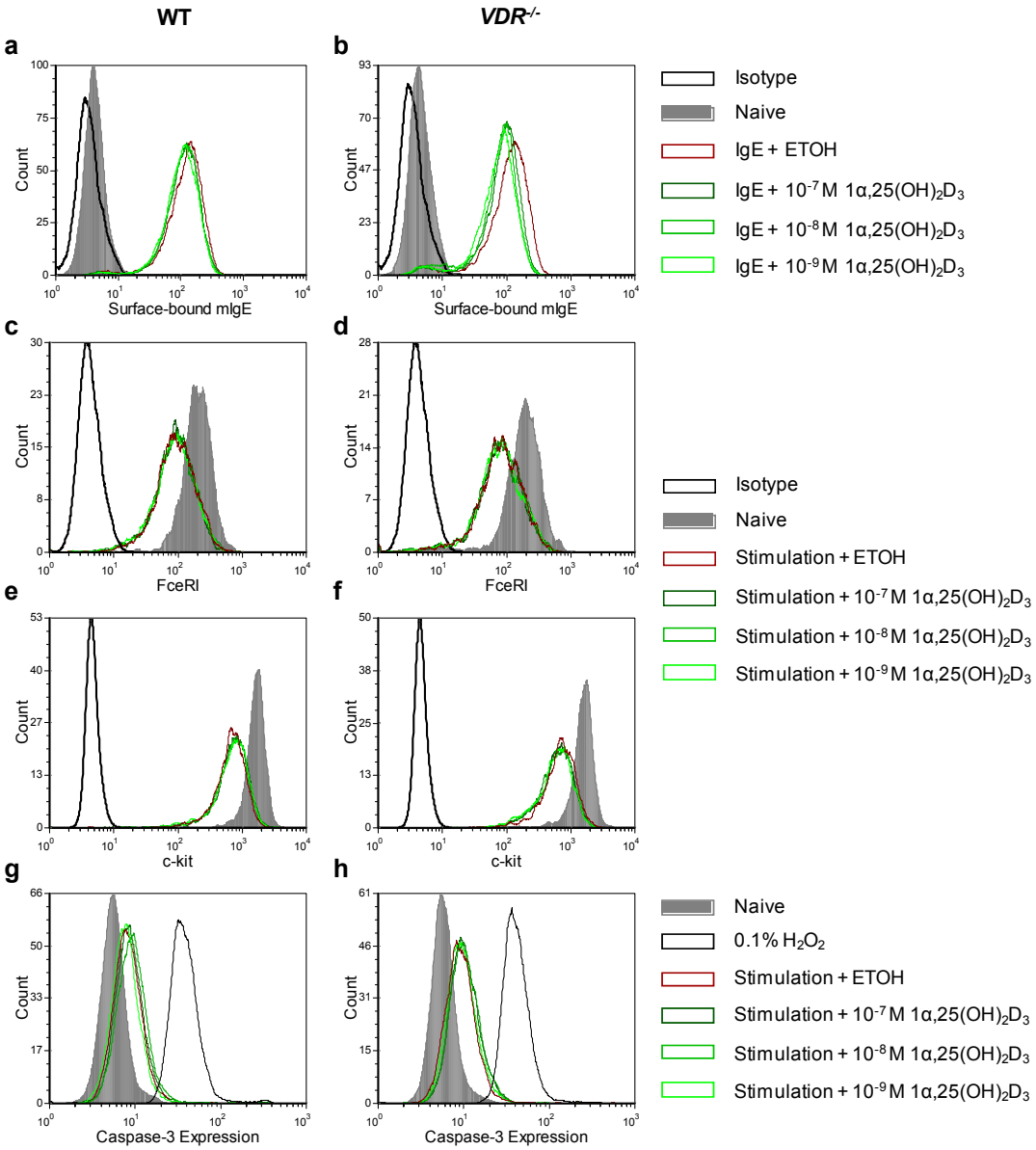

Figure 3.5 1α,25(OH)$_2$D$_3$ has no effect on the efficiency of IgE preload, the expression of surface molecules, and the survival of either WT or *VDR*$^{-/-}$ mBMCMCs
WT (a, c, e, g) and *VDR*$^{-/-}$ (b, d, f, h) mBMCMCs were preloaded with 2 µg/mL of α-DNP IgE Ab (SPE-7 clone), in the presence of different doses of 1α,25(OH)$_2$D$_3$ or ETOH (0.03% final) as a negative control, for 16 h. (a and b) Surface bound IgE was detected on IgE-preloaded cells using flow cytometry to assess the efficiency of IgE preload in cells treated with 1α,25(OH)$_2$D$_3$. Naive cells were used as negative controls. (c – h) IgE-sensitized mBMCMCs were subsequently stimulated with 20 ng/mL of DNP-HSA, upon corresponding 1α,25(OH)$_2$D$_3$ or ETOH treatment, for 6 h. Surface expression of FcεRI (c and d) and c-kit (e and f) on stimulated cells was examined by flow cytometry. Naive cells were used as positive controls. (g and h) Cell survival was also examined by flow cytometry following caspase-3 labelling. Naive cells and cells that were treated with 0.1% H_2O_2 alone for 24 h were included as negative and positive controls for caspase-3 activation, respectively. Data are representative of three independent experiments using different batches of cells.

or ETOH administration. The extent of histamine release, as assessed at 30 min post-stimulation, was significantly reduced in the presence of 1α,25$(OH)_2D_3$ treatment at the two higher concentrations tested (i.e. 10^{-7} and 10^{-8} M), as compared to the ETOH-treated controls; and such effect was only observed in WT, but not *VDR*$^{-/-}$ MCs (**Figure 3.6a**). It was to be noted that the addition of ETOH alone reduced the extent of IgE-induced histamine release, as compared to the IgE+sAg-stimulated MCs in the absence of ETOH, which was consistent with the findings that the ethanolic extract of adley testa can reduce A23187-mediated degranulation in RBL-2H3 cells [(268)] and that ETOH concentrations greater than 0.1 % can reduce IgE-mediated β-hexosaminidase release from rat serosal MCs [(269)]. The suppressive effect of 1α,25$(OH)_2D_3$ on MC degranulation was confirmed by the β-hexosaminidase assay, where WT (**Figure 3.6b**) but not *VDR*$^{-/-}$ (**Figure 3.6c**) mBMCMCs exhibited reduced β-hexosaminidase release when treated with either concentration of 1α,25$(OH)_2D_3$ (i.e. 10^{-7} or 10^{-8} M). More importantly, such effect of 1α,25$(OH)_2D_3$ on β-hexosaminidase release seemed to be exclusive to IgE + sAg-mediated degranulation, as the levels of spontaneous degranulation (as represented by non-stimulated, i.e. "no DNP", cells) and PMA/A23187-mediated degranulation remained constant for both types of cells (**Figures 3.6 b and c**). It is also worth noting that 1α,25$(OH)_2D_3$ was most efficient at down-regulating MC degranulation at the highest physiological concentration applied (i.e. 10^{-7} M).

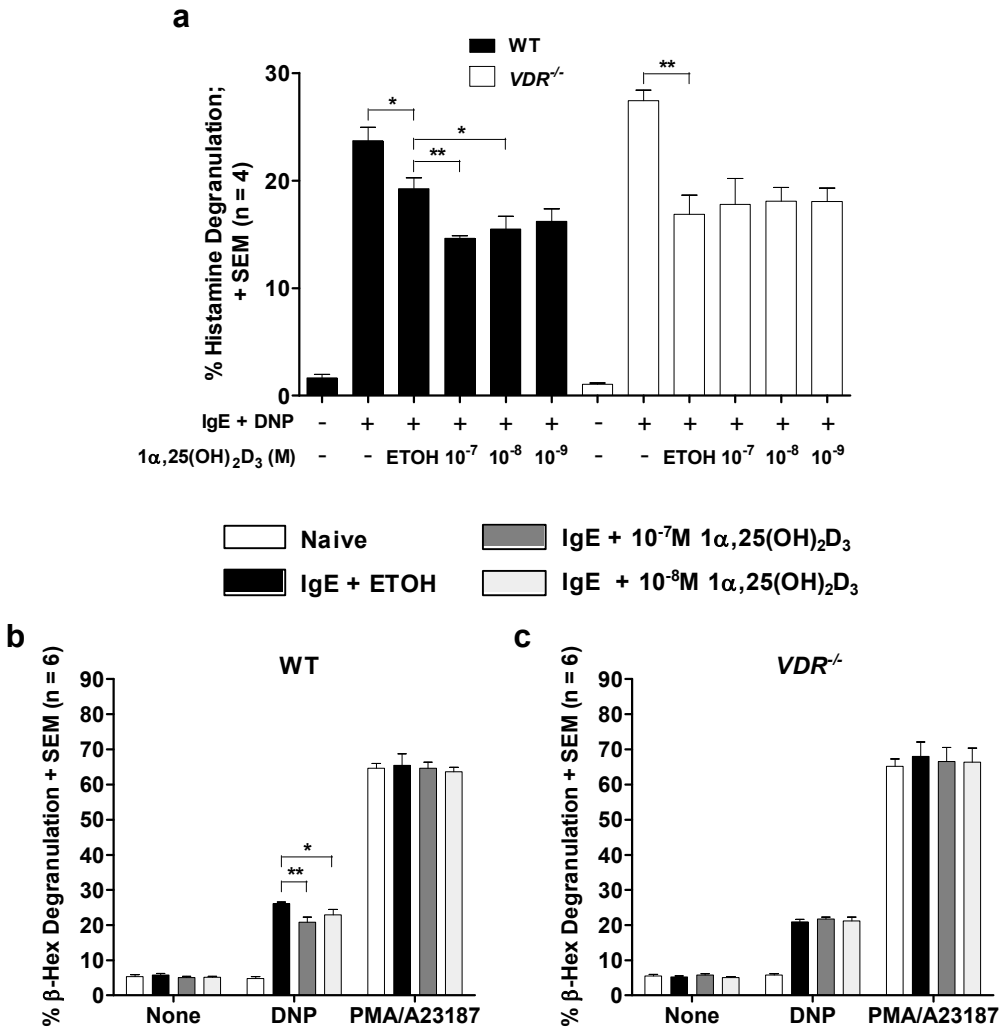

Figure 3.6 1α,25(OH)$_2$D$_3$ partially reduces IgE + sAg-mediated degranulation of WT but not *VDR*$^{-/-}$ mBMCMCs.

WT (a and b) and *VDR*$^{-/-}$ (a and c) mBMCMCs were preloaded with 2 μg/mL of IgE (SPE-7 clone) for 16 h, in the presence of indicated concentrations of 1α,25(OH)$_2$D$_3$. Cells that were preloaded alone and/or in the presence of ETOH (0.03% final) were included as controls. (a) Preloaded cells were subsequently stimulated, upon corresponding 1α,25(OH)$_2$D$_3$ or ETOH treatment, with 10 ng/mL of DNP-HSA for 30 min, and the percentage of histamine release was assessed using histamine EIA assay. Naive cells were included as negative controls. (b and c) Preloaded cells were stimulated, upon corresponding 1α,25(OH)$_2$D$_3$ or ETOH treatment, with 10 ng/mL of DNP-HSA for 1 h, and the extent of β-hexosaminidase degranulation was measured by β-hexosaminidase assay. Naive cells and cells that were treated with PMA/A23187 were used as negative and positive controls, respectively. Data are representative of at least three independent experiments. * $p < 0.05$, ** $p < 0.01$

3.2.4. 1α,25(OH)$_2$D$_3$ VDR-dependently down-regulates the de-novo synthesis and secretion of pro-inflammatory cytokines but up-regulates that of the anti-inflammatory IL-10, from IgE + sAg-activated mBMCMCs

One of the hallmarks of IgE + sAg-mediated MC activation is the production of pro-inflammatory cytokines such as TNFα and IL-6, both of which are contributors of IgE-mediated allergic reactions [64, 270-274], and contain VDRE in the promoter region of their encoding gene [275, 276]. Although not considered a typical product of IgE + sAg-activated MCs, the anti-inflammatory cytokine IL-10 can nevertheless be synthesised and secreted upon 1α,25(OH)$_2$D$_3$ treatment [163]. It was therefore essential, for the purpose of the project, to determine if 1α,25(OH)$_2$D$_3$ can affect the cytokine production profile of IgE + sAg-activated mBMCMCs. To address this aim, WT and *VDR*$^{-/-}$ mBMCMCs were sensitized with IgE anti-DNP Ab (2 μg/mL), and stimulated in the presence of 1α,25(OH)$_2$D$_3$ or ETOH as described previously (Section 2.5.3.3). The production of TNFα, IL-6, and IL-10was examined at either 3 h (for gene expression) or 6 h (for protein secretion) post-stimulation. For WT mBMCMCs, the overall mRNA and protein levels of both TNFα and IL-6 were significantly reduced in response to 1α,25(OH)$_2$D$_3$ treatment (10^{-7} M) as compared to the ETOH (0.03% final) control (**Figures 3.7 a, c, e, g**). The levels of IL-10, on the other hand, were significantly increased by the same concentration of 1α,25(OH)$_2$D$_3$ (**Figures 3.8 a and c**). Notably, for *VDR*$^{-/-}$ mBMCMCs, 1α,25(OH)$_2$D$_3$ had no effect on the production of any of the cytokines examined, whether at the level of mRNA expression or that of protein secretion (**Figures 3.7 b, d, f, h; 3.8 b and d**). Furthermore, 1α,25(OH)$_2$D$_3$ alone did not induce the *de novo* synthesis of TNFα or IL-6 in either WT or *VDR*$^{-/-}$ mBMCMCs (**Figure 3.7 a-d**). It did, however, induce that of IL-

Figure 3.7. 1α,25(OH)$_2$D$_3$ dose-dependently reduces IgE + sAg-mediated production of pro-inflammatory cytokines by WT but not *VDR*$^{-/-}$ mBMCMCs.
WT (a, c, e, g) and *VDR*$^{-/-}$ (b, d, f, h) mBMCMCs were preloaded with 2 μg/mL of IgE (SPE-7 clone) for 16 h, in the presence of various concentrations of 1α,25(OH)$_2$D$_3$ or ETOH as a negative control. (a - d) Cells were subsequently stimulated, upon the same 1α,25(OH)$_2$D$_3$ or ETOH treatment, with 20 ng/mL of DNP-HSA for 3 h, and the level of TNF-encoding (a and b) and IL-6-encoding (c and d) mRNA relative to that of β-actin control was assessed using qRT-PCR. Naive cells, cells that were preloaded only, and cells that were treated with the indicated concentration of 1α,25(OH)$_2$D$_3$ were included as controls. (e - h) Pre-loaded cells were stimulated, upon the same 1α,25(OH)$_2$D$_3$ or ETOH treatment, with 20 ng/mL of DNP-HSA for 6 h, and the secretion of TNF (e and f) and IL-6 (g and h) was measured by ELISA. Non-stimulated cells were used as negative controls. Data are representative of three independent experiments. * $p < 0.05$, ** $p < 0.01$, *** $p < 0.001$

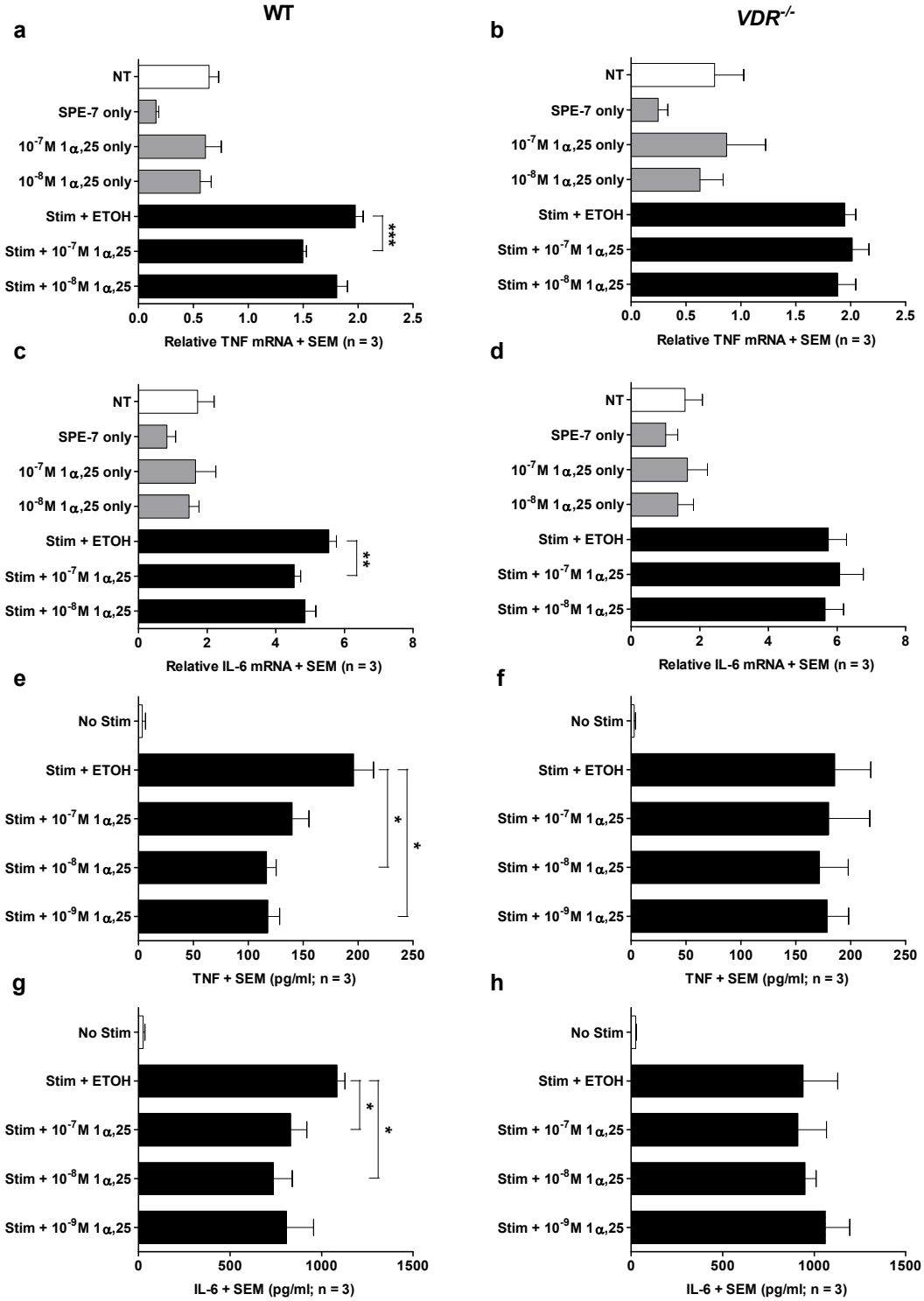
WT
VDR-/-
a
b
NT
SPE-7 only
10-7M 1α,25 only
10-8M 1α,25 only
Stim + ETOH
Stim + 10-7M 1α,25
Stim + 10-8M 1α,25
***
0.0 0.5 1.0 1.5 2.0 2.5
Relative TNF mRNA + SEM (n = 3)
c
d
**
0 2 4 6 8
Relative IL-6 mRNA + SEM (n = 3)
e
f
No Stim
Stim + 10-9M 1α,25
*
*
0 50 100 150 200 250
TNF + SEM (pg/ml; n = 3)
g
h
0 500 1000 1500
IL-6 + SEM (pg/ml; n = 3)

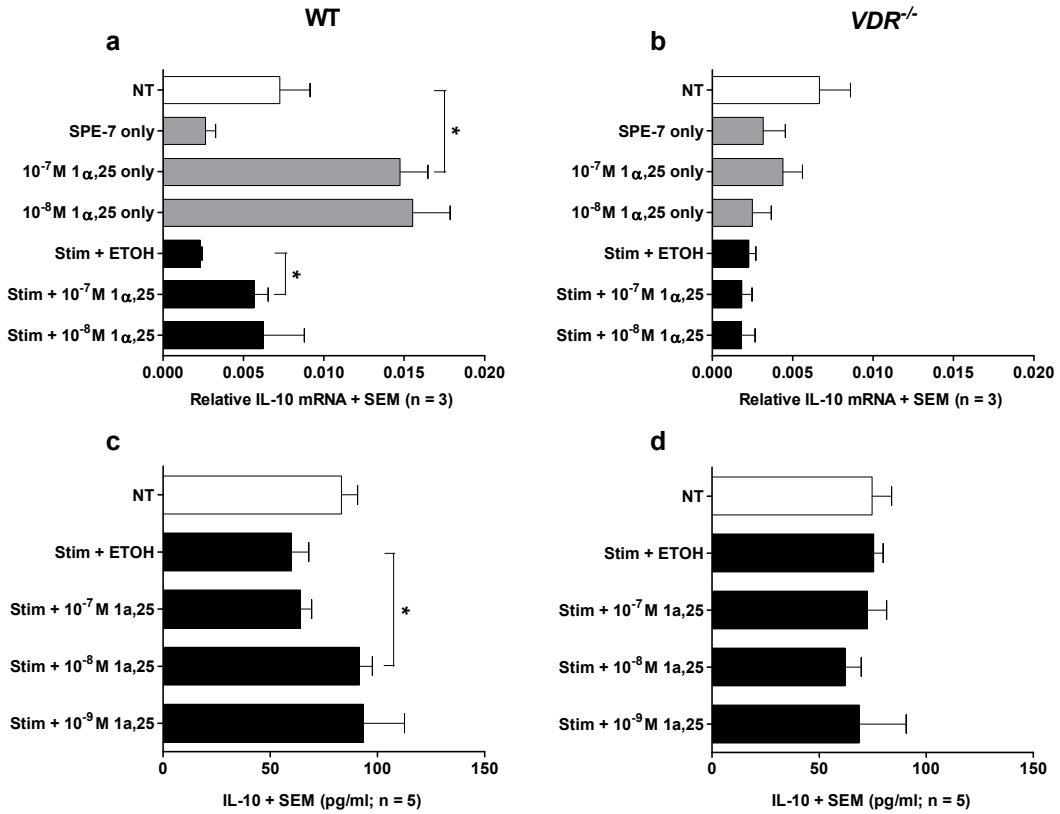

Figure 3.8. 1α,25(OH)$_2$D$_3$ dose-dependently enhances IgE + sAg-mediated production of the anti-inflammatory cytokine, IL-10, by WT but not *VDR*$^{-/-}$ mBMCMCs.

WT (a and c) and *VDR*$^{-/-}$ (b and d) mBMCMCs were preloaded with 2 μg/mL of IgE (SPE-7 clone) for 16 h, in the presence of various concentrations of 1α,25(OH)$_2$D$_3$ or ETOH as a negative control. (a and b) Cells were subsequently stimulated, upon the same 1α,25(OH)$_2$D$_3$ or ETOH treatment, with 20 ng/mL of DNP-HSA for 3 h, and the level of IL-10-encoding mRNA relative to that of β-actin control was assessed using qRT-PCR. Naive cells, cells that were preloaded only, and cells that were treated with the indicated concentration of 1α,25(OH)$_2$D$_3$ were included as controls. (c and d) Pre-loaded cells were subsequently stimulated, upon corresponding 1α,25(OH)$_2$D$_3$ or ETOH treatment, with 20 ng/mL of DNP-HSA for 6 h, and the secretion of IL-10 was measured by ELISA. Naive cells were used as controls. Data are representative 3 – 5 independent experiments. * $p < 0.05$

10 in WT but not *VDR*$^{-/-}$ cells (**Figure 3.8 a and b)**, which is consistent with our previous findings. [163]

It should be pointed out that the concentration of 1α,25$(OH)_2D_3$ required to down-regulate early-stage events following IgE + sAg-mediated MC activation, such as degranulation (0.5 – 1 h post-stimulation) and mRNA expression of various cytokines (i.e. 10^{-7} M), was higher than that required to suppress later-stage events such as cytokine secretion (i.e. 10^{-8} or 10^{-9} M). One possible explanation for these observations is that the expression of CYP24A1, with a VDRE in the promoter region of its corresponding gene, could be up-regulated by higher concentrations of 1α,25$(OH)_2D_3$ and thus contribute to inactivation of this metabolite. [205] Although CYP24A1 protein level did not seem to change after 3-h 1α,25$(OH)_2D_3$ treatment in either WT or *VDR*$^{-/-}$ mBMCMCs (**Figure 3.9)**, other time points as well as *CYP24A1* gene expression need to be examined before a definitive conclusion can be drawn.

3.2.5. Curcumin reduces IgE + sAg-mediated cytokine production by mBMCMCs in a VDR- and non-genomic VitD$_3$ pathway-dependent manner

It has been established so far that VDR is required for the observed effects of 1α,25$(OH)_2D_3$ to regulate MC degranulation and cytokine production upon IgE + sAg-mediated activation, which may suggest the involvement of the genomic $VitD_3$ pathway. Recent studies, however, reported that VDR could also play an important role in the non-genomic $VitD_3$ pathway. [229, 230] Therefore, to determine which $VitD_3$ pathway is (or if both pathways are) responsible for the observed regulatory properties of 1α,25$(OH)_2D_3$, curcumin, a commercially available, non-genomic pathway-restricted agonist of

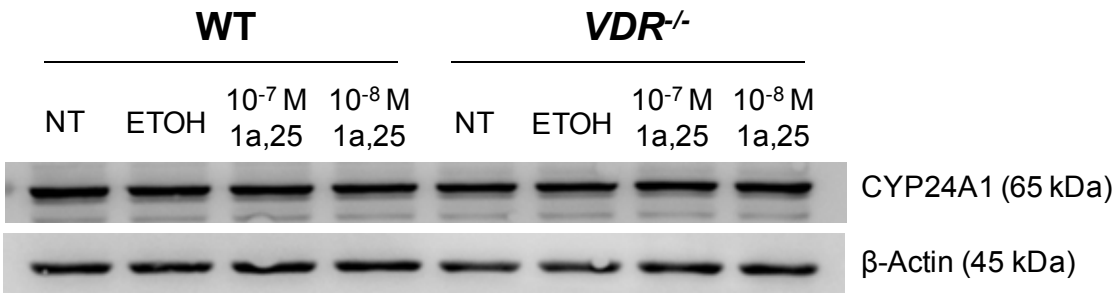

Figure 3.9. 1α,25(OH)$_2$D$_3$ has no effect on CYP24A1 expression in either WT or *VDR*$^{-/-}$ mBMCMCs.

WT and *VDR*$^{-/-}$ mBMCMCs were cultured first in cDMEM-csFCS-4 medium (0.5×10^6 cells/mL) for 4 days, and then in cDMEM-csFCS-3 medium (10^6 cells/mL) supplemented with alternative concentrations of 1α,25(OH)$_2$D$_3$. Naive cells (NT) and cells that were treated with ETOH were included as controls. Total cell lysates were prepared at 3 h post-treatment, and subjected to SDS-PAGE followed by western blot analysis. CYP24A1 expression, as well as that of β-actin loading controls, is shown. Data is from one experiment and represents three individual batches of cells of either genotype.

$1\alpha,25(OH)_2D_3$, was used instead of $1\alpha,25(OH)_2D_3$ to assess its effect on IgE + sAg-mediated cytokine production from mBMCMCs. Unlike $1\alpha,25(OH)_2D_3$, curcumin failed to alter the mRNA expression, 3h post-stimulation, of TNF, IL-6 and IL-10 in either WT or *VDR*$^{-/-}$ mBMCMCs (**Figure 3.10**), which could be explained by its non-genomic function. Surprisingly, although mRNA expression was unaltered at the 3h time point tested, curcumin treatment resulted in a significant reduction of cytokine protein production in the supernatant of WT but not *VDR*$^{-/-}$ mBMCMCs at 6 h post-stimulation (**Figure 3.11**). Recent evidence suggests that curcumin can elicit anticancer properties by post-transcriptional regulation via certain microRNAs in cancer cells [259, 277] (discussed in more detail in the next section). Similar mechanism(s) might allow curcumin to regulate cytokine release without altering their gene expression. Furthermore, the difference between curcumin and $1\alpha,25(OH)_2D_3$ in regulating IL-10 production from MCs was highlighted as curcumin treatment decreased, rather than enhanced, IL-10 secretion from IgE + sAg-stimulated WT mBMCMCs (**Figure 3.11c**, compared to **Figure 3.8c**). At the same time, it also failed to increase the IL-10-encoding mRNA in naive WT mBMCMCs (**Figure 3.10e**, compare to **Figure 3.7a**).

3.3. Discussion

Regarded as crucial pro-inflammatory effector cells during IgE-dependent allergic reactions, MCs play important roles during all three temporal phases of these reactions (Section 1.3.1). [64] In particular, histamine that is released during MC degranulation can lead to vasodilation, increased vascular permeability and bronchoconstriction during early-phase allergic reactions, as well as contribute importantly to non-allergen-specific

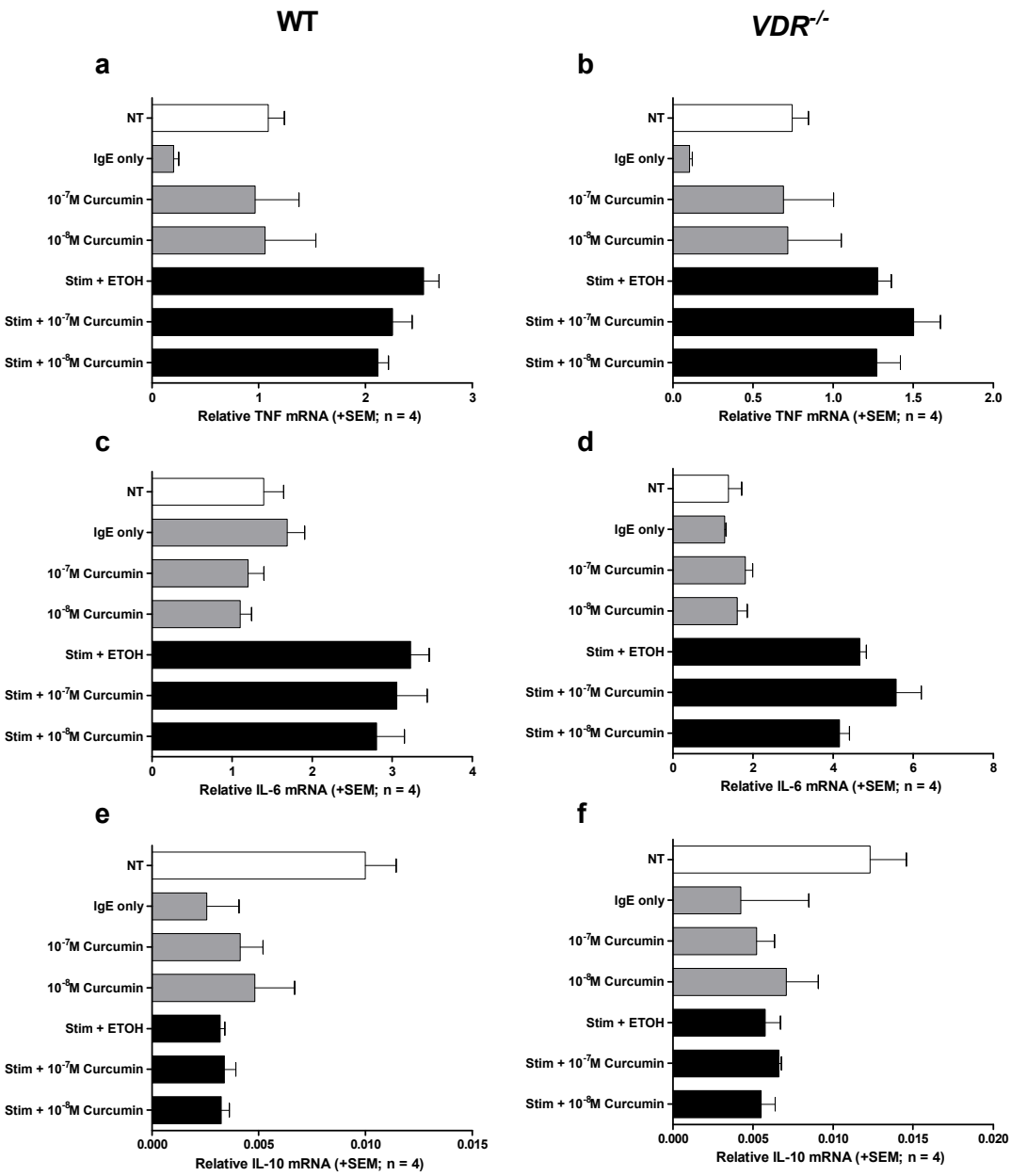

Figure 3.10. Curcumin has no effect on IgE + sAg-mediated mRNA expression for various cytokines by either WT or *VDR*$^{-/-}$ mBMCMCs.

WT (a, c and e) and *VDR*$^{-/-}$ (b, d and f) mBMCMCs were preloaded with 2 µg/mL of IgE (SPE-7 clone) for 16 h, in the presence of indicated concentrations of curcumin or ETOH (0.03% final) as a control. Cells were subsequently stimulated, upon corresponding curcumin or ETOH treatment, with 20 ng/mL of DNP-HSA for 3 h, and the level of TNF- (a and b), IL-6- (c and d), and IL-10-encoding (e and f) mRNA relative to that of β-actin control was measured using qRT-PCR. Naive cells (NT), cells that were preloaded only, and cells that were treated with the indicated concentration of curcumin were included as controls. Data are representative of four independent experiments.

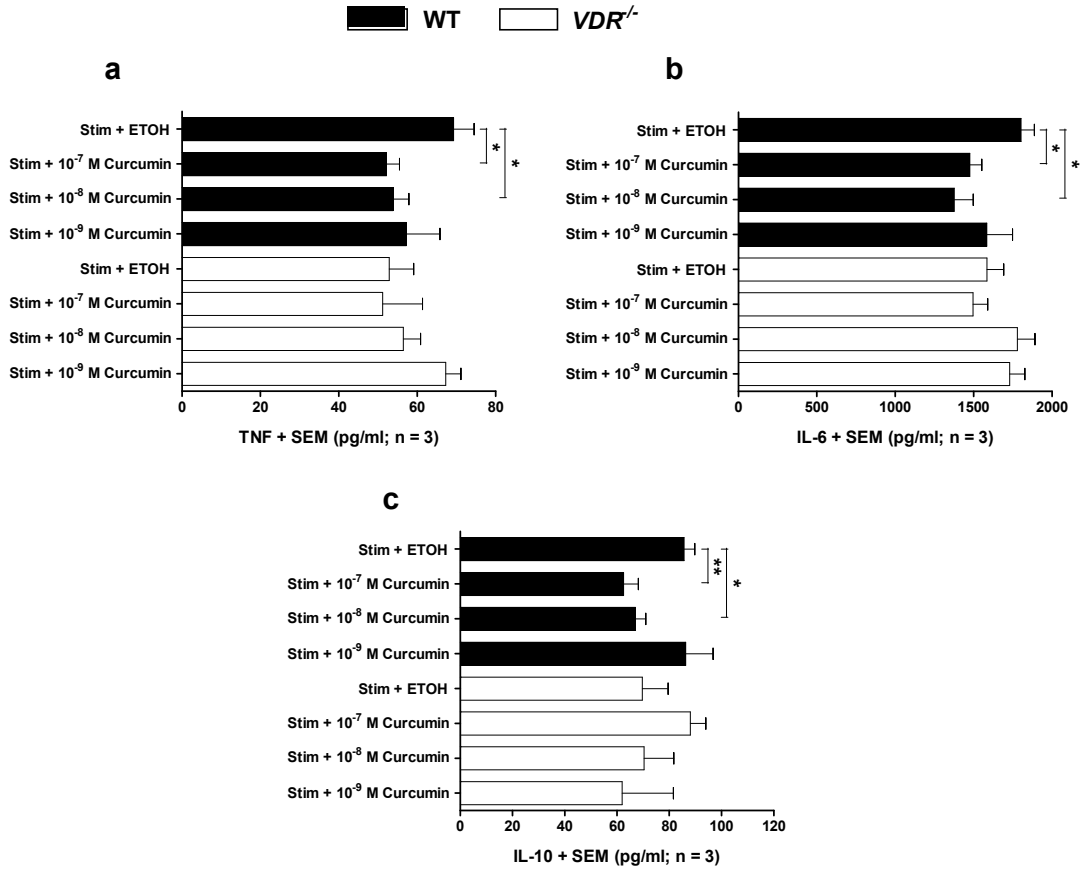

Figure 3.11. Curcumin dose-dependently reduces IgE + sAg-mediated secretion of TNF, IL-6 and IL-10 by WT but not *VDR*$^{-/-}$ mBMCMCs.

WT and *VDR*$^{-/-}$ mBMCMCs were preloaded with 2 μg/mL of IgE (SPE-7 clone) for 16 h, in the presence of indicated concentrations of curcumin or ETOH (0.03% final) as a control. Cells were subsequently stimulated, upon corresponding curcumin or ETOH treatment, with 20 ng/mL of DNP-HSA for 6 h, and the secretion of TNF (a), IL-6 (b), and IL-10 (c) was measured by ELISA. Data are representative of three independent experiments. * $p < 0.05$, ** $p < 0.01$

airway hyperreactivity at the chronic stage of the disease. [278, 279] Pro-inflammatory cytokines secreted by MCs during late-phase reactions, such as those investigated in this project (i.e. TNFα and IL-6), can also promote recruitment and/or activation of a large variety of immune cells (e.g. neutrophils, DCs, T cells and B cells), as well as affecting the biology of various structural cells (e.g. vascular endothelial cells, fibroblasts, smooth muscle cells and goblet cells) [11, 64, 99, 101, 270, 273]. Therefore, by suppressing IgE + sAg-mediated mBMCMC degranulation and their production of pro-inflammatory cytokines (**Figures 3.6 and 3.7**), it is plausible that $1\alpha,25(OH)_2D_3$ could ease the symptoms at various stages of an allergic response, either directly or indirectly via the resultant reduction in MC-mediated leukocyte recruitment and/or activation. In addition to the latter aspect, $1\alpha,25(OH)_2D_3$ can exhibit immunosuppressive effects on several types of leukocytes, including DCs (e.g. reducing the production of Th1 cytokine IL-12) [220] and T cells (e.g. stimulating the development of Th2 and T_{reg} cells) [225, 226], that may be subject to such MC-mediated recruitment, thus further providing protection against exacerbation of allergic disease.

Moreover, it should be pointed out that the effect of $1\alpha,25(OH)_2D_3$ on MC degranulation that we observed in this study contrasts with other reports in the literature. For example, whilst our data demonstrated a suppressive effect of $1\alpha,25(OH)_2D_3$ on IgE + sAg-mediated but not PMA/A23187(a calcium ionophore)-mediated MC degranulation, one previous study showed similar effect on A23187-mediated but not IgE + sAg-mediated MC degranulation [236]; and yet another study reported that $1\alpha,25(OH)_2D_3$ enhances both types of MC degranulation as measured by β-hexosaminidase release assay [280]. Such apparent discrepancy among these findings can be explained by the differences in

experimental procedures, especially the type of MCs used, and the nature as well as length of $1\alpha,25(OH)_2D_3$ treatment. In the study by Toyota *et al.* [236], the MCs used were *ex vivo* from mouse peritoneal cavity. The same study also applied 24-hour $1\alpha,25(OH)_2D_3$ treatment after IgE preload and before sAg/A23187 stimulation, instead of including $1\alpha,25(OH)_2D_3$ during the entire preload-stimulation process. In contrast, although the second study mentioned above used mBMCMCs as well as RBL cell line, it treated all cells with 10^{-7} M of $1\alpha,25(OH)_2D_3$ for 24 or 48 h prior to IgE preload and subsequent stimulation. [280] Since *CYP24A1* expression is up-regulated in mouse ears treated with 4×10^{-9} M of MC903, a low-calcemic analogue of $1\alpha,25(OH)_2D_3$, for 24 hours [281], 10^{-7} M of $1\alpha,25(OH)_2D_3$ is likely to induce CYP24A1 expression and consequently be degraded and lose effectiveness over the 24 or 48 h experimental period.

In addition to its suppressive effect on MC degranulation and production of pro-inflammatory cytokines, the ability of $1\alpha,25(OH)_2D_3$ to induce IL-10 production in IgE + sAg-activated mBMCMCs (**Figure 3.8**) is also of significance, as this well-known anti-inflammatory cytokine contributes substantially to the ability of MCs to reduce inflammation associated with allergic contact hypersensitivity responses to 2,4-dinitrofluorobenzene, urushiol and oxazolone. [7, 282] IL-10 is also required to maintain Foxp3 expression as well as suppressive functionality of T_{reg} cells which, in animal models of allergy and asthma, can produce another anti-inflammatory cytokine, TGF-β, as well as additional IL-10 and thus curtail disease progression. [283-285] Furthermore, it was recently reported that IL-10 can down-regulate FcεRI expression *in vitro*, using mBMCMCs and human skin-derived MCs; as well as *in vivo*, employing *ex vivo* mouse peritoneal MCs [286, 287] Therefore, when $1\alpha,25(OH)_2D_3$ is present during IgE-mediated

allergic reactions, IL-10 produced from MCs (in addition to various other cell types) could potentially function in a autocrine and/or paracrine fashion, dampening their FcεRI expression and downstream activation events.

Although our result showed no difference in CYP24A1 protein levels following 3-h 1α,25$(OH)_2D_3$ treatment as compared to the native and ETOH-treated controls (**Figure 3.9**), we cannot yet exclude the possibility that high concentrations (e.g. 10^{-7} M) of 1α,25$(OH)_2D_3$ do induce CYP24A1 gene and/or protein expression in mBMCMCs at later time points. According to Li *et al.* [281], the low-calcemic analogue of 1α,25$(OH)_2D_3$, MC903, up-regulated *CYP24A1* expression in keratinocytes of mouse ears following at least 24-h treatment. Therefore, longer 1α,25$(OH)_2D_3$-treatment durations, as well as *CYP24A1* gene expression at the end of all durations, must be examined before a definitely conclusion can be drawn as to whether CYP24A1 up-regulation can be induced by high concentrations of 1α,25$(OH)_2D_3$ in mBMCMCs. Furthermore, we showed here, for the first time, that naive WT and *VDR*$^{-/-}$ mBMCMCs express CYP24A1 protein, which is itself a significant finding as it indicates the natural ability of mBMCMCs to adjust intracellular 1α,25$(OH)_2D_3$ concentration. Future studies, however, are required to investigate the physiological significance of this finding.

We and others have reviewed the alternative pathways through which 1α,25$(OH)_2D_3$ elicits its biological effects [193, 215], including the genomic pathway which utilises the classical nuclear VDR and ultimately leads to transcriptional regulation of targe genes, and the non-genomic pathway which utilises a currently unidentified VDR_{mem} and/or VDR. To determine which pathway is responsible for any potential effect of 1α,25$(OH)_2D_3$ on IgE + sAg-activated MCs, WT and *VDR*$^{-/-}$ mBMCMCs were compared

to each other to verify the VDR dependency in each experiment. The rationale for this approach is that if VDR dependency can be established, then the genomic $VitD_3$ pathway would most likely be involved. Indeed, our data showed that VDR was required for the suppressive effect of $1\alpha,25(OH)_2D_3$ on gene expression and secretion of TNFα and IL-6, and its enhancive effect on that of IL-10 (**Figures 3.7 and 3.8**). However, it was also required for the inhibitory effect of $1\alpha,25(OH)_2D_3$ on MC degranulation (**Figure 3.6**), which is an immediate post-stimulation response. Furthermore, experiments using curcumin confirmed that the suppressive effect of this rapid-acting $1\alpha,25(OH)_2D_3$ agonist on IgE + sAg-mediated cytokine (TNF, IL-6 and IL-10) production from mBMCMCs was VDR dependent, but did not involve change in corresponding gene expression (**Figures 3.10 and 3.11**). Therefore, our findings suggest a role of the classical VDR in mediating rapid non-genomic $1\alpha,25(OH)_2D_3$ responses. This notion coincides with a previous claim that the VDR_{mem} found in caveolae-enriched plasma membranes in organs of various species are in fact classical VDR in nature. [288] A more recent study further characterised two overlapping ligand binding pockets in VDR which, together with differential ligand stability and site occupancy, can selectively regulate $VitD_3$-mediated genomic and/or non-genomic cellular responses. [230] From this point of view, the current study essentially provided, for the first time, functional evidence for the involvement of MC VDR during $1\alpha,25(OH)_2D_3$-mediated non-genomic responses in IgE-dependent allergy settings.

The ability of curcumin to regulate cytokine production without affecting corresponding gene expression may appear contradictory. However, as mentioned briefly before, curcumin can post-transcriptionally modify gene expression in cancer cells by regulating

various microRNA (miR) levels. MicroRNAs represent a class of small (19- to 22-nucleotide), often phylogenetically conserved, non-coding RNAs that serve as post-transcriptional repressors of gene expression by either destabilizing target transcripts or inhibiting protein translation. [289-293] Such miR-dependent gene regulation was recently demonstrated to be a reversible process, thus allowing miRs to fine-tune gene expression under different physiological/pathological circumstances[294][286][283][282]. [294] Previous studies have shown that curcumin up-regulates miR-22, with SP1 transcription factor and estrogen receptor as gene targets, in human BxPC-3 pancreatic cancer cells [277]; as well as up-regulates the tumor suppressive miR, miR-203, in bladder cancer [259]. Therefore, it is possible that curcumin can regulate TNF/IL-6/IL-10-targeting miRs and thus affect the translation rather than transcription of corresponding genes.

Moreover, by comparing the effects of $1\alpha,25(OH)_2D_3$ and curcumin, it can be concluded that the suppressive effect of $1\alpha,25(OH)_2D_3$ on TNFα and IL-6 production from activated MCs requires both the non-genomic $VitD_3$ pathway, which contributes to the reduction in overall cytokine secretion (as indicated by the action of curcumin, possibly via the regulation of certain miRs), and the genomic pathway, which alone is responsible for the down-regulation in gene expression of these cytokines. Cross-talk between the two pathways may also exist in this case, but requires further investigation. The ability of $1\alpha,25(OH)_2D_3$ to increase IL-10 production, on the other hand, seems to rely solely on the genomic $VitD_3$ pathway as otherwise the non-genomic pathway as utilised by curcumin would have decreased IL-10 secretion. Therefore, a differential $VitD_3$ pathway-dependency exists for $1\alpha,25(OH)_2D_3$ to regulate different aspects of MC functionality in allergic settings.

The use of *VDR*$^{-/-}$ mice and cells derived from them presents potential problems, as *VDR*$^{-/-}$ animals do differ from their WT counterparts in a number of phenotypical characteristics (**Figure 3.1**) [(295)], and *VDR*$^{-/-}$ mBMCMCs obtained from a different strain of *VDR*$^{-/-}$ mice showed accelerated maturation as well as higher responsiveness to IgE + sAg-mediated cytokine production (e.g IL-6 and IL-13) [(237)]. Our data comparing WT and *VDR*$^{-/-}$ MCs, however, showed little if any difference in their development, morphological properties, and functional characteristics following IgE + sAg-mediated activation (**Figures 3.2, 3.3 and 3.4**), which highlights the differences between alternative strains of mice carrying similar genetic defect, and perhaps also the necessity to confirm our findings using other stains of mice. Nevertheless, due to the absence of intrinsic dissimilarity between activated WT and *VDR*$^{-/-}$ MCs in this study, the differences observed in the effect of 1α,25(OH)$_2$D$_3$ and curcumin on the two types of cells would be solely due to the action of the particular VitD$_3$ analogue.

In conclusion, we demonstrated in this chapter that 1α,25(OH)$_2$D$_3$ can VDR-dependently suppress IgE + sAg-mediated degranulation as well as the production of pro-inflammatory cytokines from mBMCMCs, but at the same time enhance the production of IL-10. Whilst the effect of 1α,25(OH)$_2$D$_3$ on pro-inflammatory cytokine production requires both the non-genomic and genomic pathways; its effect on IL-10 production relies solely on the latter pathway. In the addition, although future investigation is required to determine the effects of high concentrations of 1α,25(OH)$_2$D$_3$ on CYP24A1 expression in mBMCMCs, we did show that mBMCMCs exhibit intrinsic CYP24A1 expression in a VDR-independent manner, the physiological significance of which is yet to be examined.

CHAPTER 4

MAST CELLS CAN CONVERT 25OHD$_3$ TO 1α,25(OH)$_2$D$_3$ AND THUS ENABLE 25OHD$_3$ TO IMMUNOSUPPRESS IgE + sAg-ACTIVATED MAST CELLS *IN VITRO*

4.1. Introduction

The precursor metabolite of $1\alpha,25(OH)_2D_3$, $25OHD_3$, is the major circulating form of $VitD_3$ with a serum concentration of approximately 100 nM in mice [296], and ranging from 25 nM to 200 nM in humans [297]. $25OHD_3$ is generally converted in the kidney by CYP27B1 to generate the biologically active form, $1\alpha,25(OH)_2D_3$ (Section 1.7). [203, 297] In addition to renal cells, other cell types including epidermal keratinocytes [298], epithelial cells [299], and osteoblasts [300] also express CYP27B1 and, therefore, can generate their own $1\alpha,25(OH)_2D_3$ from its inactive precursor *in vitro* and/or *in vivo*. Although such extra-renal synthesis of $1\alpha,25(OH)_2D_3$ contributes little to UVB-mediated protection against conditions such as childhood rickets and osteomalacia (softening of the bones due to defective bone mineralization) in adults, it can still locally provide protective homeostatic functions to regulate excess immune responses. [193] In addition to hepatocytes, other cell types such as keratinocytes also express CYP27A1, and therefore can carry out cutaneous synthesis of $25OHD_3$ upon UVB irradiation and its subsequent conversion to $1\alpha,25(OH)_2D_3$. [301, 302] Dermal fibroblasts, on the other hand, express CYP27A1 but not CYP27B1 and thus function as an additional source of $25OHD_3$ for keratinocytes and, possibly, also for the serum. [303] As mentioned previously, serum provides only minimum levels of $1\alpha,25(OH)_2D_3$. [304, 305] Therefore, it is essential for keratinocytes to generate their own $1\alpha,25(OH)_2D_3$ from cutaneous and, perhaps also circulating, $25OHD_3$, which can then elicit autocrine and/or paracrine effects to regulate the growth, differentiation, apoptosis and other biological processes of these cells. [203] In this regard, it should be pointed out that the effect of keratinocyte-derived $1\alpha,25(OH)_2D_3$ is generally limited to the skin and not resulting in systemic outcomes, as the level

1α,25$(OH)_2D_3$ produced is tightly regulated by CYP24A1 expression in these cells, where substantially high levels of 1α,25$(OH)_2D_3$ up-regulates CYP24A1 expression, which in turn inactivates excess 1α,25$(OH)_2D_3$. [196]

Various immune cells, such as DCs [209], macrophages [306], T cells [209] and B cells [210] also express CYP27B1, but only when they are activated during an immune response. Unlike renal cells and keratinocytes, whose CYP27B1 expression and activity is tightly regulated by parathyroid hormone (PTH) and low levels of calcium and phosphate, immune cells do not respond to these signals but rather up-regulate CYP27B1 in response to certain cytokine(s). [196, 253] In addition, the expression and activity of CYP24A1 in macrophages and DCs is either absent or blocked, removing the feedback control as seen in keratinocytes, by the 1α,25$(OH)_2D_3$ produced. [209, 307, 308] Together, these findings could explain why diseases associated with immune activation, such as sarcoidosis, tuberculosis, peritonitis and inflammatory arthritis, can lead to hypercalcemia and hypercalciuria as a result of elevated levels of circulating 1α,25$(OH)_2D_3$. [196] Furthermore, with the exception of DCs to date, immune cells that have been examined do not express CYP27A1 and, therefore, require 25OHD_3 produced by other cell types and/or from serum to generate their own 1α,25$(OH)_2D_3$. [209] Nevertheless, the ability of immune cells to synthesize 1α,25$(OH)_2D_3$ confers this hormone a wide range of regulatory effects on innate and adaptive immunity. [193, 196]

Despite the ever-increasing number of effector as well as immunoregulatory roles of MCs, and the established negative regulatory effects of 1α,25$(OH)_2D_3$ on MC functionality, the expression and activity of CYP27B1 has not been examined in these cells. Employing WT and *VDR*$^{-/-}$ mBMCMCs, we first examined the expression of this hydroxylase in

MCs and any potential VDR-dependence for such expression. We then investigated the effect of $25OHD_3$ treatment on CYP27B1 expression and subsequently $1\alpha,25(OH)_2D_3$ production by both types of mBMCMCs. If endogenous $1\alpha,25(OH)_2D_3$ production can be achieved by mBMCMCs, then the immunoregulatory ability of $25OHD_3$ on IgE + sAg-activated MCs will be accessed.

4.2. Results

4.2.1. Mouse BMCMCs constitutively express CYP27B1 in their cytosol

As mentioned previously, CYP27B1 is expressed by many immune cell types, including macrophages, dendritic cells, T cells and B cells, upon activation. [196] To date, however, its expression in MCs has not been reported. By labelling naive mBMCMCs intracellularly with an α-CYP27B1 Ab, we revealed, for the first time, that MCs do indeed express this hydroxylase and that such expression is constitutively expressed in the cytosol (i.e. does not require activation of the cells) (**Figures 4.1 a – e**). Importantly, CYP27B1 expression in MCs is not VDR-dependent, as *VDR*$^{-/-}$ mBMCMCs (**Figures 4.1 a and e**) showed an identical level of expression as their WT counterparts (**Figures 4.1 a and d**). These findings were further confirmed by western analysis of lysates from naive mBMCMCs (**Figure 4.1f**).

4.2.2. $25OHD_3$ up-regulates CYP27B1 expression in mBMCMCs in a VDR-dependent manner

It has been shown previously that CYP27B1 expression can be up-regulated by $25OHD_3$ treatment in rat osteoblasts. [309] To investigate if $25OHD_3$ has similar effect on CYP27B1 expression in MCs, WT and *VDR*$^{-/-}$ cells were first cultured in medium containing csFCS

Figure 4.1. Intracellular expression of CYP27B1 in naive mBMCMCs
Five- to 6-week-old WT (a, b, d) and *VDR*$^{-/-}$ (a, c, e) mBMCMCs (10^6 cells each) were labelled intracellularly with α-CYP27B1 Ab, and examined by either flow cytometry (a) or immunofluorescence staining (d and e). An isotype control (a, b, c) was included in both approaches, and the DAPI nucleus stain was used in the latter. Scale bars (b – e) represent 10 μm. (f) Lysates were prepared from WT or *VDR*$^{-/-}$ mBMCMCs (3×10^6 cells each), various amount of which (as indicated) was analysed by western blotting for CYP27B1 expression. Kidney extract from a normal C57BL/6 mouse was used as a positive control. Data are representative of three independent batches of cells of either genotype.

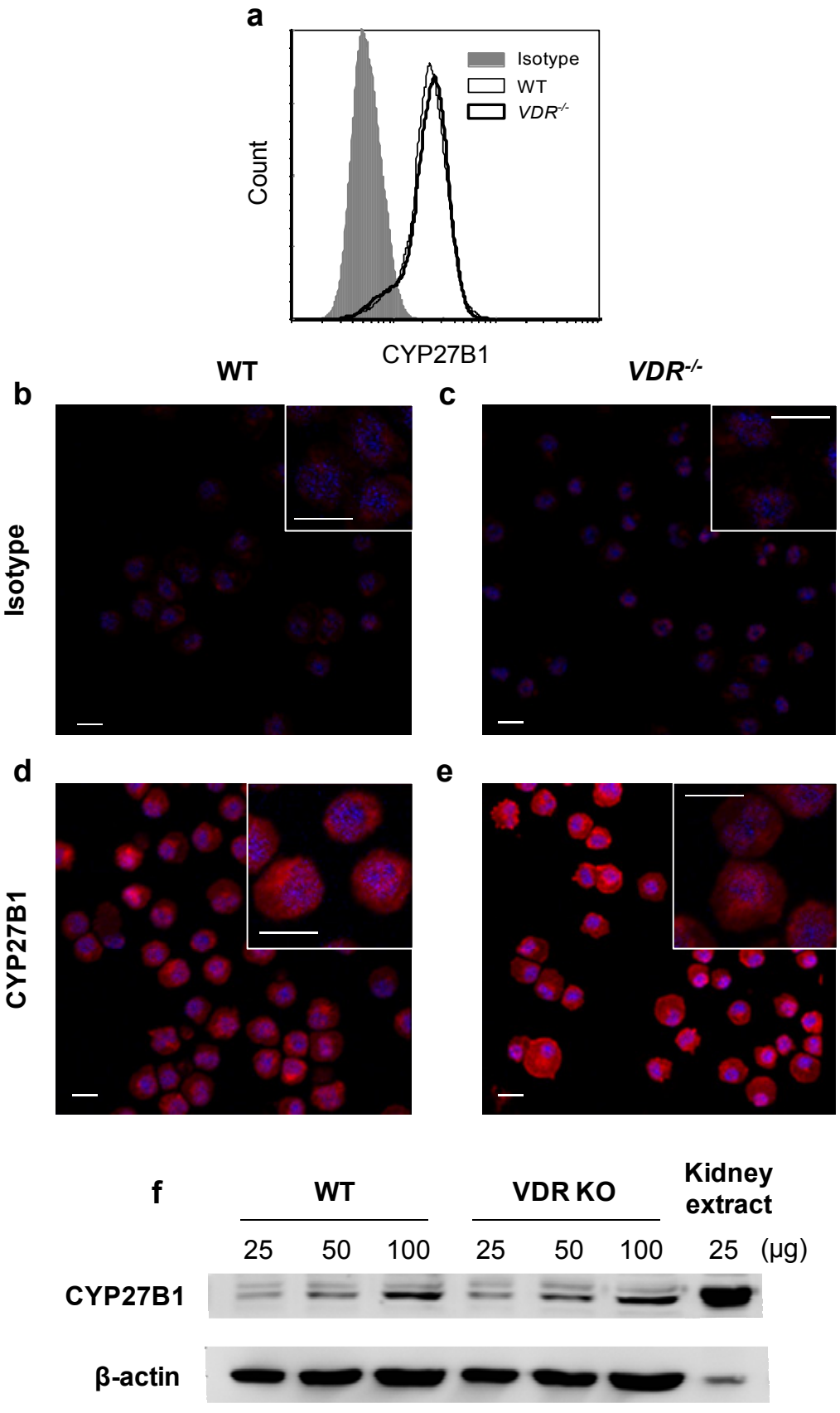
a
Isotype
WT
VDR-/-
Count
CYP27B1
WT
VDR-/-
b
c
Isotype
d
e
CYP27B1
f
WT
VDR KO
Kidney extract
25
50
100
25
50
100
25
(μg)
CYP27B1
β-actin

instead of normal FCS to minimise exogenous $VitD_3$ levels. At the end of 72 h incubation, the purity of the MC populations, based on expression of key surface markers (i.e. FcεRI and c-kit), was maintained (**Figure 4.2a**) prior to treatment with $25OHD_3$ (10^{-7} M) or ETOH (0.03%, which was applied to all subsequent ETOH treatment) and subsequent examination of CYP27B1 mRNA (at 3 h post-treatment) and protein (at 8 h post-treatment) levels, respectively. Our results showed that whilst WT mBMCMCs exhibited up-regulated gene (**Figure 4.2b**) as well as protein (**Figures 4.2 c and d**) expression of CYP27B1, *VDR*$^{-/-}$ cells failed to show any difference in expression on both levels. Therefore, our figures suggest that MC CYP27B1 expression can be enhanced by its $25OHD_3$ substrate in a VDR-dependent manner. Although not having reached statistical significance, a trend towards a difference between CYP27B1 protein expression in ETOH-treated WT and *VDR*$^{-/-}$ mBMCMCs was noted. Further investigation is thus required to explain such observation. Interestingly, in both WT and *VDR*$^{-/-}$ cell types, ETOH-treated group showed a moderate reduction in CYP27B1expression as compared to the naive control, which could due merely to the presence of ETOH (mentioned in the previous chapter).

4.2.3. $25OHD_3$ dose-dependently induces endogenous synthesis of $1\alpha,25(OH)_2D_3$ by mBMCMCs

Because CYP27B1 is the enzyme responsible for converting $25OHD_3$ to $1\alpha,25(OH)_2D_3$ in a number of other cell types [196, 310], the logical experiment performed next investigated if it plays the same role in MCs. After 72-h incubation in medium containing csFCS, WT and *VDR*$^{-/-}$ mBMCMCs were treated with various concentrations of $25OHD_3$ or ETOH for 6 h, and the level of $1\alpha,25(OH)_2D_3$ in culture supernatant as well as cell lysate was

Figure 4.2. 25OHD$_3$ enhances CYP27B1 expression in mBMCMCs on both mRNA and protein levels

Five- to 6-week-old WT and *VDR*$^{-/-}$ mBMCMCs were cultured, at 5×10^5 cells/mL, in cDMEM-csFCS-4 medium for 72 h, when the expression profile of key surface markers was confirmed by flow cytometry (a). All cells were subsequently replated in cDMEM-csFCS-3 medium at 10^6 cells/mL, and treated with either 10^{-7} M of 25OHD$_3$ or ETOH (0.03%). The level of *CYP27B1* gene expression was measured at 3 h post-treatment by qRT-PCR (b), whereas the CYP27B1 protein expression was examined by western blotting at 8 h post-treatment (c and d). Lysates prepared from naive cells and normal mouse kidney extract were analysed by western blotting as controls. Data are representative of three or four independent experiments. * $p < 0.05$

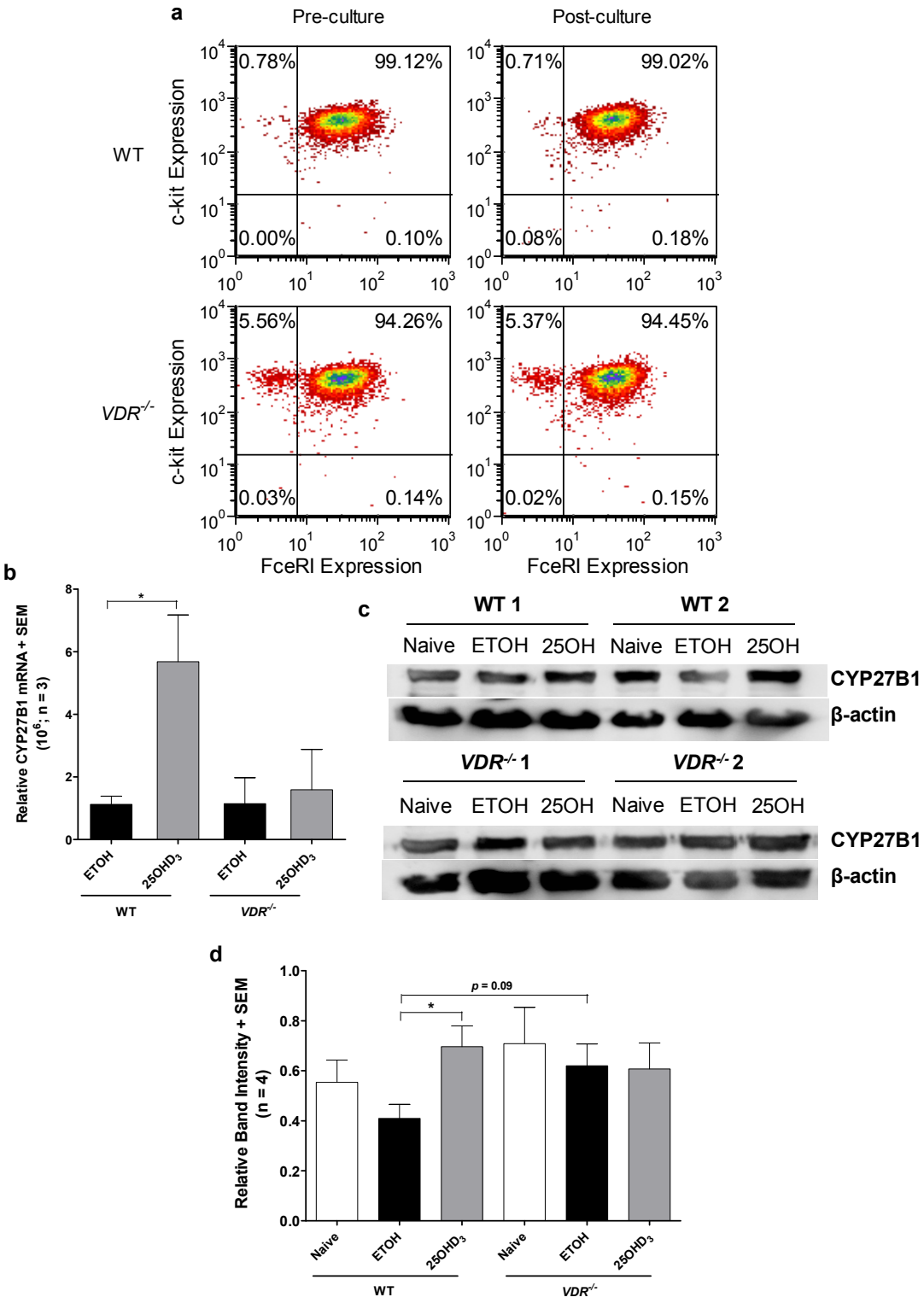
a
Pre-culture
Post-culture
WT
VDR-/-
c-kit Expression
FceRI Expression
0.78%
99.12%
0.00%
0.10%
0.71%
99.02%
0.08%
0.18%
5.56%
94.26%
0.03%
0.14%
5.37%
94.45%
0.02%
0.15%
b
Relative CYP27B1 mRNA + SEM (10^6; n = 3)
ETOH
25OHD3
WT
VDR-/-
c
WT 1
WT 2
Naive
ETOH
25OH
CYP27B1
β-actin
VDR-/- 1
VDR-/- 2
d
Relative Band Intensity + SEM (n = 4)
p = 0.09
Naive

subsequently measured. As illustrated in **Figure 4.3a**, treatment with the higher doses of $25OHD_3$ (i.e. 10^{-6} and 10^{-7} M) led to higher secretion of $1\alpha,25(OH)_2D_3$ from WT mBMCMCs as compared to the ETOH-treated control group. Although $1\alpha,25(OH)_2D_3$ level in cell lysates seemed to increase only with the highest dose (**Figure 4.3b**), both 10^{-6} M and 10^{-7} M of $25OHD_3$ succeeded in elevating the total level of the active product in WT cells (**Figure 4.3c**). More importantly, the highest $25OHD_3$ concentration (i.e. 10^{-6} M) was also able to induce $1\alpha,25(OH)_2D_3$ production and secretion in *VDR*$^{-/-}$ mBMCMCs (**Figure 4.3**). Furthermore, in contrast to previous findings with human keratinocytes [311], most of the endogenously synthesised $1\alpha,25(OH)_2D_3$ by MCs appeared to be secreted instead of accumulating inside the cells.

4.2.4. 25OHD$_3$ treatment reduces IgE + sAg-mediated degranulation and pro-inflammatory cytokine production of mBMCMCs in a dose- and VDR-dependent manner

In chapter 3, evidence was provided demonstrating that $1\alpha,25(OH)_2D_3$ can elicit immunosuppressive effects on IgE + sAg-activated MCs. Since $25OHD_3$ can also induce endogenous $1\alpha,25(OH)_2D_3$ synthesis in MCs, we examined if $25OHD_3$ can affect IgE-mediated mBMCMCs activation. Our initial attempt involved preloading and stimulating WT and *VDR*$^{-/-}$ cells in the presence of indicated concentrations of $25OHD_3$ or ETOH, which was done in the same way as with $1\alpha,25(OH)_2D_3$ treatment (i.e. $25OHD_3$/ETOH was added immediately prior to IgE preload and DNP-HSA stimulation). As revealed by **Figures 4.4 a and c**, only the highest concentration of $25OHD_3$ tested (i.e. 10^{-6} M) was able to decrease the production of proinflammatory cytokines from activated WT MCs. None of the concentrations, however, managed to affect TNFα or IL-6 production by

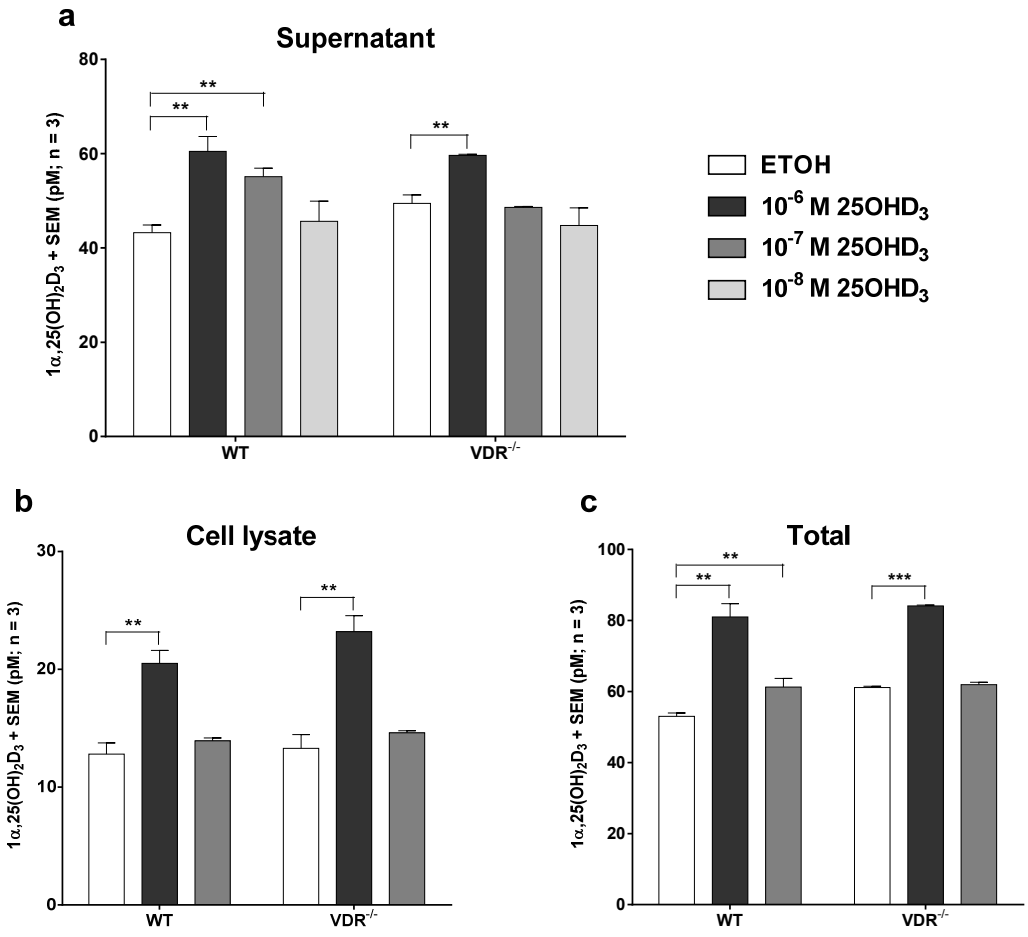

Figure 4.3. Dose-dependent $1\alpha,25(OH)_2D_3$ production by $25OHD_3$-treated mBMCMCs

Five- to 6-week-old WT and *VDR*$^{-/-}$ mBMCMCs were cultured, at 5×10^5 cells/mL, in cDMEM-csFCS-4 medium for 72 h, subsequently replated at 2×10^6 cells/mL in cDMEM-csFCS-3 medium, and treated with indicated concentrations of $25OHD_3$ or ETOH. Culture supernatant (a) as well as cell lysate (b) samples were collected at 6 h post-treatment, and the $1\alpha,25(OH)_2D_3$ level in all samples was measured using the 1,25-$(OH)_2D$ RIA kit. The total $1\alpha,25(OH)_2D_3$ level (c) was calculated by adding together its concentration in the supernatant and that in the corresponding cell lysate. Data are representative of three independent batches of cells examined in two independent experiments, where only supernatant (not cell lysate, and therefore not used to calculate the total value) from cells treated with 10^{-8} M of $25OHD_3$ was analysed. * $p < 0.05$, ** $p < 0.01$

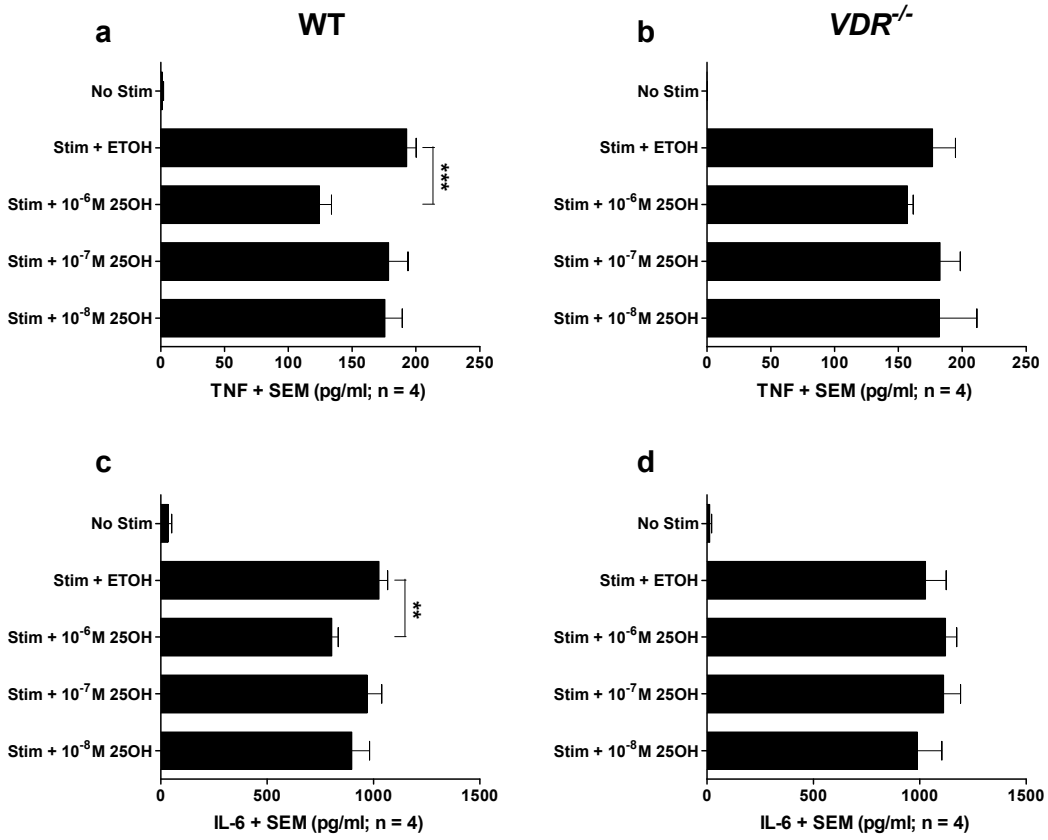

Figure 4.4. Short-term high-dose $25OHD_3$ treatment reduces IgE + sAg-mediated production of pro-inflammatory cytokines by WT and *VDR*$^{-/-}$ mBMCMCs

WT (a and c) and *VDR*$^{-/-}$ (b and d) mBMCMCs were preloaded with 2 µg/mL of IgE (SPE-7 clone) for 16 h, in the presence of indicated concentrations of $25OHD_3$ or ETOH (0.03% final). Cells were subsequently stimulated, upon corresponding $25OHD_3$ or ETOH treatment, with 20 ng/mL of DNP-HSA for 6 h, and the level of TNF (a and b) and IL-6 (c and d) in culture supernatant was measured by ELISA. Non-stimulated cells were used as negative controls. Data are representative of four independent experiments.

VDR$^{-/-}$ cells (**Figures 4.4 b and d**). These data suggest that 25OHD$_3$ might require a longer incubation period with the MCs to be converted to 1α,25(OH)$_2$D$_3$. An alternative possibility is that only at sufficiently high concentrations could 25OHD$_3$ readily regulate the functionality of activated MCs, potentially by binding directly to VDR as demonstrated in mouse kidney and skin cells. [243]

To examine the aforementioned possibility that, given sufficient incubation time with the cells, lower concentrations of 25OHD$_3$ may still elicit immunosuppressive effects on activated MCs upon its conversion to the active form, 1α,25(OH)$_2$D$_3$, we treated WT and *VDR*$^{-/-}$ cells with 25OHD$_3$ or ETOH 8 h prior to IgE preload followed by usual DNP stimulation with 25OHD$_3$/ETOH co-treatment. In this case, the level of both TNFα and IL-6 secreted following MC activation was indeed reduced by 25OHD$_3$ treatment, especially at the highest concentration (i.e. 10^{-7} M); and again such observation was made in WT but not *VDR*$^{-/-}$ cells (**Figures 4.5 a – d**). Similarly, long-term 25OHD$_3$ treatment also appeared capable of reducing IgE + sAg-mediated, but not spontaneous or PMA/A23187-mediated, degranulation in WT but not *VDR*$^{-/-}$ cells (**Figures 4.5 e and f**). Furthermore, the above immunosuppressive effect of long-term 25OHD$_3$ exposure was not due to alteration of the IgE preload efficacy, assessed by the expression of key surface molecules (e.g. FcεRI and c-kit), or the viability of the cells (**Figure 4.6**).

4.3. Discussion

To date, there is a paucity of information in the literature on MC responses to VitD$_3$ metabolites. Here, for the first time, we demonstrate that mBMCMCs express CYP27B1 (**Figure 4.1**), and the resultant ability of these cells to synthesise endogenous

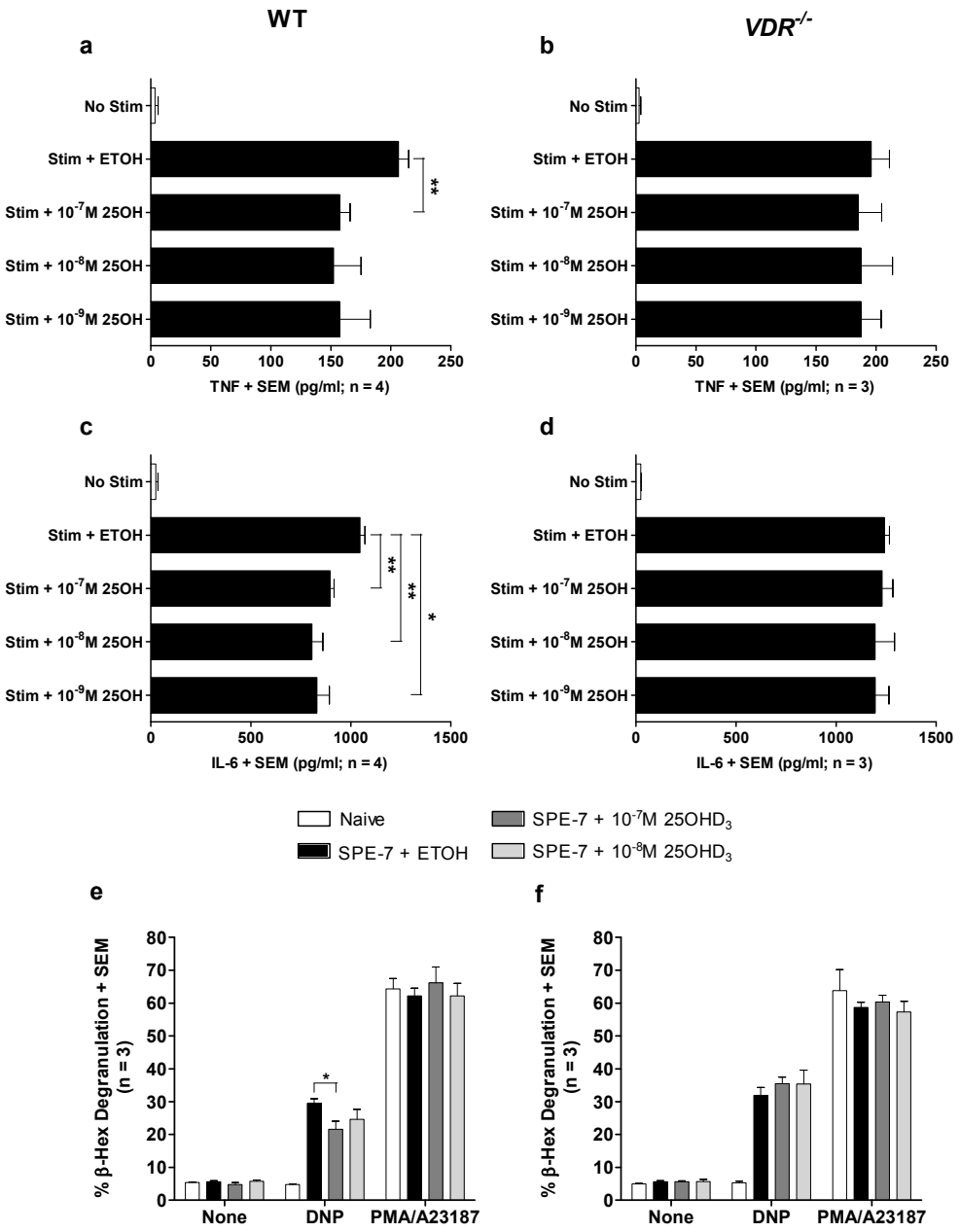

Figure 4.5. Long-term $25OHD_3$ treatment dose-dependently reduces IgE + sAg-mediated pro-inflammatory cytokine production and degranulation of WT but not *VDR*$^{-/-}$ mBMCMCs.

WT (a, c, e) and *VDR*$^{-/-}$ (b, d, f) mBMCMCs were treated with indicated concentrations of $25OHD_3$ or ETOH for 8 h, at the end of which cells were preloaded with 2 µg/mL of IgE (SPE-7 clone) for a further 16 h. Subsequently stimulation was carried out, upon corresponding $25OHD_3$ or ETOH treatment, with 20 ng/mL of DNP-HSA for 6 h, and the level of TNF (a and b) IL-6 (c and d) was determined by ELISA. To examine the effect of $25OHD_3$ on MC degranulation, preloaded cells were stimulated with 10ng/mL DNP for 1 h, and the extent of β-hexosaminidase degranulation was measured by β-hexosaminidase assay. Naive cells and cells that were treated with PMA/A23187 were used as negative and positive controls, respectively. Data are representative of at least three independent experiments. * $p < 0.05$, ** $p < 0.01$

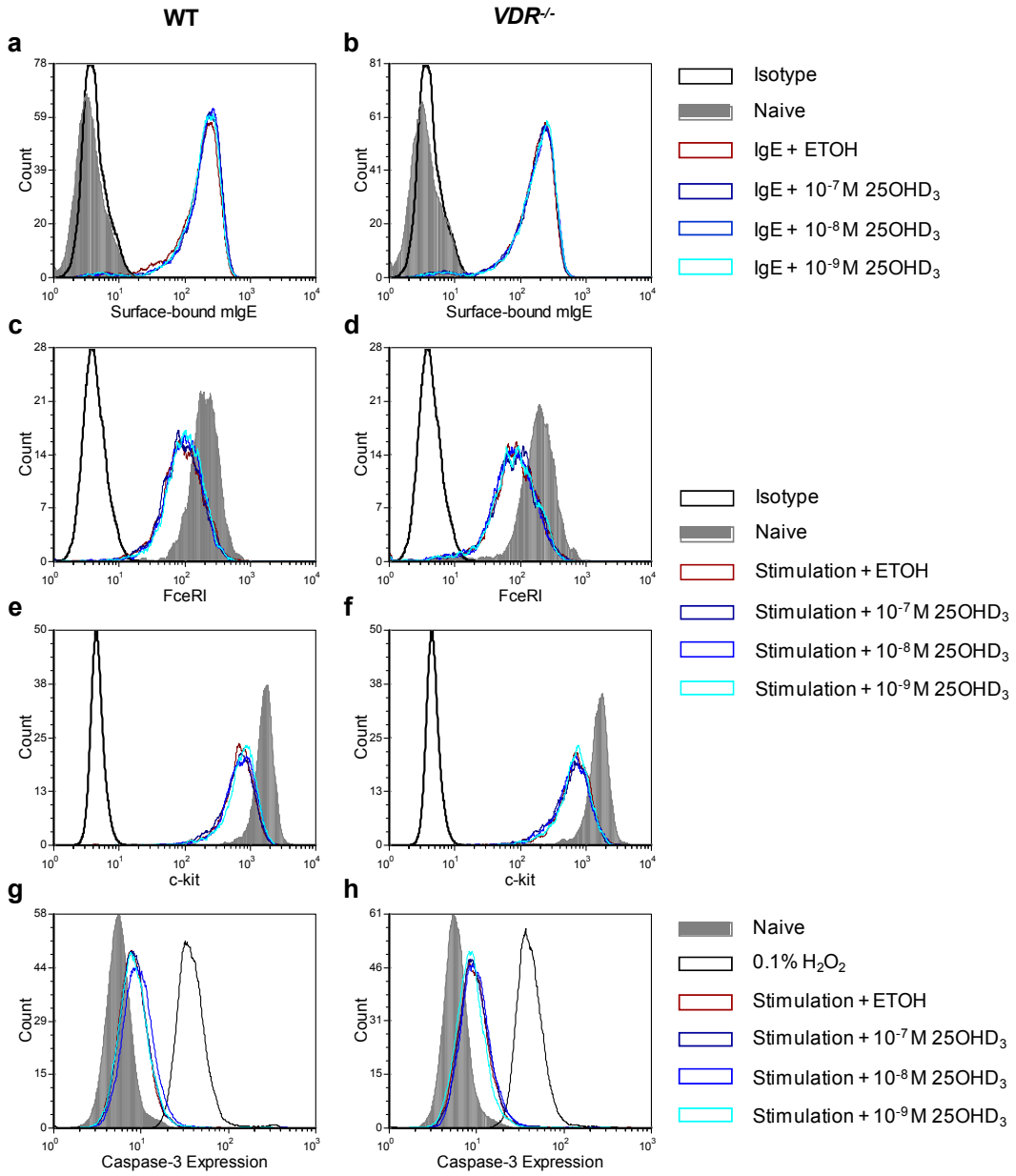

Figure 4.6 25OHD$_3$ has no effect on the efficiency of IgE preload, the expression of surface molecules, and the survival of either WT or *VDR*$^{-/-}$ mBMCMCs

WT (a, c, e, g) and *VDR*$^{-/-}$ (b, d, f, h) mBMCMCs were treated with indicated concentrations of 25OHD$_3$ or ETOH for 8 h prior to preload with 2 µg/mL of α-DNP IgE (SPE-7 clone) for a further 16 h. (a and b) Surface bound IgE was detected on preloaded cells using flow cytometry to assess the efficiency of IgE preload. Naive cells were used as negative controls. (c - h) Preloaded cells were subsequently stimulated with 20 ng/mL of DNP-HSA, upon 25OHD$_3$ or ETOH treatment, for 6 h. Surface expression of FcεRI (c and d) and c-kit (e and f) on stimulated cells was examined by flow cytometry. Naive cells were used as positive controls. (g and h) Cell survival was also examined by flow cytometry following caspase-3 labelling. Naive cells and cells that were treated with 0.1% H_2O_2 alone for 24 h were included as negative and positive controls for caspase-3 activation, respectively. Data are representative of three independent batches of cells.

$1\alpha,25(OH)_2D_3$ from $25OHD_3$ (**Figure 4.3**). The fact that mBMCMCs, unlike other immune cells, constitutively express this hydroxylase enzyme is significant in a number of aspects. Firstly, it allows MCs, which are abundant in the skin in close proximity to blood vessels, to readily utilise $25OHD_3$ in the serum and/or synthesised within the tissues by structural cells such as keratinocytes under normal physiological conditions. Given that excessive MC activation can exacerbate IgE-mediated allergic responses, their ability to synthesise $1\alpha,25(OH)_2D_3$ in the naive state could potentially generate an immunosuppressive local environment well before the onset of any allergic responses. It is tantalising to speculate that one possible contributing factor to the recent allergy epidemic in Western countries is the increase in $VitD_3$ insufficiency among the populations. [312]

Furthermore, the basal level of CYP27B1 expression seemed sufficient to allow high concentrations (e.g. 10^{-6} M) of $25OHD_3$ to induce $1\alpha,25(OH)_2D_3$ production, even in *VDR*$^{-/-}$ mBMCMCs (**Figure 4.3**). Since the endogenously produced $1\alpha,25(OH)_2D_3$ was mostly secreted (**Figure 4.3**), it could increase the local concentration of this hormone in an autocrine and/or paracrine fashion to functional levels as determined in the previous chapter, and hence provide an additional mechanism for immune cells to negatively regulate their activation. In addition to the specific anti-allergy property as implied by our results, serum and/or tissue $25OHD_3$ allows $1\alpha,25(OH)_2D_3$ production and, in turn, IL-10 production from naive MCs, thus conferring these cells a more general anti-inflammatory role in physiological as well as pathological circumstances.

Whilst renal CYP27B1 expression is mainly regulated by mediators of calcium and bone homeostasis, such as parathyroid hormone and $1\alpha,25(OH)_2D_3$ itself, immune cells often

adjust their CYP27B1 level differently [310]. Macrophage- and DC-derived CYP27B1, for example, is under the control of inflammatory signals such as interferon-γ, and the p38 MAP Kinase/NF-κB-dependent maturation, respectively; and neither is subject to the negative feedback mechanism by $1\alpha,25(OH)_2D_3$ [219, 313]. As mentioned above, CYP27B1 expression in mBMCMCs is up-regulatable by the $25OHD_3$ substrate in a VDR-dependent manner (**Figures 4.2**). Such a regulatory mechanism could be significant, as it allows MCs to monitor the level of $25OHD_3$ available in their local environment and to only up-regulate CYP27B1 expression when required and the optimal range is reached. It is possible, therefore, that to synthesize maximum amounts of the active $1\alpha,25(OH)_2D_3$ product, MCs need to elevate their CYP27B1 expression from the basal level, which in turn depends on the availability of $25OHD_3$ substrate. Indeed, this notion was supported by our data that $1\alpha,25(OH)_2D_3$ was produced by WT mBMCMCs from $25OHD_3$ in a dose-dependent manner (**Figure 4.3**). It is important to mention that the VDR-dependence for such positive regulation of CYP27B1 expression by $25OHD_3$ may only be significant/relevant when the substrate concentration is within physiological range (10^{-7} M), as pharmacological concentrations of $25OHD_3$ (e.g. 10^{-6} M) were able to induce $1\alpha,25(OH)_2D_3$ production even in *VDR*$^{-/-}$ MCs. However, any change in CYP27B1 expression in *VDR*$^{-/-}$ MCs when treated with 10^{-6} M of $25OHD_3$ needs to be examined before a definitive conclusion in this regard can be drawn.

Our data also demonstrates that the response of mBMCMCs to $25OHD_3$ treatment depends on the dose of this metabolite as well as the length of time that the MCs had been pre-incubated with it. In this aspect, there is evidence to suggest that $25OHD_3$ can itself act as a VDR ligand, but only when its concentration is sufficiently high (i.e. $\geq$ 400

nM). [243] This could explain the observations from our short-term $25OHD_3$ treatment experiment, where only 10^{-6} M, but not lower concentrations of this analogue, was able to reduce the production of pro-inflammatory cytokines from activated WT MCs (**Figure 4.4**). Such a notion can be further supported by the fact that *VDR*$^{-/-}$ cells failed to respond accordingly to this high $25OHD_3$ concentration. Therefore, it appears that high levels of $25OHD_3$ can induce immediate immunosuppressive effects on IgE + sAg-activated MCs, most likely via direct interaction with VDR, in a manner similar to responses elicited by $1\alpha,25(OH)_2D_3$. The relatively low concentrations of $25OHD_3$ used, on the other hand, did cause similar immunosuppressive effects on activated MCs when coupled with the long-exposure setting (**Figure 4.5**), which allowed sufficient time for the conversion from $25OHD_3$ to the active $1\alpha,25(OH)_2D_3$ form. Taken together all these findings, it is possible that when the concentration of $25OHD_3$ available is optimal (i.e. sufficiently high), it can affect the functionality of activated MCs both promptly by direct binding to VDR and subsequently due to the induction of $1\alpha,25(OH)_2D_3$ production; whereas when the concentration is suboptimal, $25OHD_3$ can elicit similar regulatory effects, but in this case only via endogenously synthesised $1\alpha,25(OH)_2D_3$. In other words, the existence of these alternative pathways to explore the immunoregulatory functions of $25OHD_3$ allows MCs to utilise $25OHD_3$ within a large concentration range. This ability is particularly important, as serum $25OHD_3$ levels generally show large fluctuations and depend partly upon the nutritional status and UVB exposure of the individual. [243]

Another significant finding from this series of experiments is the VDR-dependence for the up-regulation of CYP27B1 expression by $25OHD_3$ and for the immunosuppressive effects of $25OHD_3$ on activated mBMCMCs, which was consistent with the previous

report that $25OHD_3$ takes the same position (although at lower affinity) within the ligand binding pocket of VDR as $1\alpha,25(OH)_2D_3$, thus resulting in the same conformational change of the receptor. [243]

In conclusion, we demonstrated in this chapter, for the first time, the constitutive expression of CYP27B1 in mBMCMCs and the VDR-dependent up-regulation of this enzyme by $25OHD_3$ in its physiological concentration (i.e. 10^{-7} M). The functionality of this enzyme was confirmed by inducing endogenous $1\alpha,25(OH)_2D_3$ synthesis from $25OHD_3$ in *VDR*$^{-/-}$ as well as WT mBMCMCs in a dose-dependent manner. By potentially binding to VDR directly and/or being converted to $1\alpha,25(OH)_2D_3$ (in which case longer treatment time would be required), $25OHD_3$ can elicit immunosuppressive effects on IgE + sAg-activated MCs at a wide range of concentrations. Furthermore, functional VDRs were shown to be essential for the regulation of MC CYP27B1 expression by $25OHD_3$, and for the immunosuppressive effects of this $VitD_3$ analogue on activated MCs using alternative settings. In particular, although *VDR*$^{-/-}$ mBMCMCs are able to synthesise $1\alpha,25(OH)_2D_3$ from $25OHD_3$, they fail to respond to $25OHD_3$ during IgE + sAg-mediated activation due to the lack of VDR.

CHAPTER 5

TOPICALLY APPLIED $1\alpha,25(OH)_2D_3$ AND $25OHD_3$ CAN REDUCE THE CUTANEOUS PATHOLOGY ASSOCIATED WITH IgE-MEDIATED PASSIVE CUTANEOUS ANAPHYLAXIS IN A MAST CELL VITAMIN D RECEPTOR-DEPENDENT MANNER *IN VIVO*

5.1. Introduction

Because of the encouraging *in vitro* findings so far, it is important to translate these findings to corresponding *in vivo* settings. It is widely accepted that MCs play important effector as well as immunoregulatory roles during all three phases of IgE-dependent allergic responses (Section 1.3.1). With particular relevance to the current project, which primarily examines the early- to late-phase reactions following IgE + sAg-mediated MC activation, MCs readily release pre-formed mediators such as histamine and TNFα via degranulation, which can contribute directly to immediate type I hypersensitivity reactions and/or initiate late-phase reactions by recruiting other leukocytes. [64] The PCA model used in this study provides a MC-dependent IgE-mediated immediate hypersensitivity platform, which exhibits typical early- and late-phase responses including tissue swelling and leukocyte infiltration, respectively. [89] In this model, MC-derived TNFα contributes to the observed neutrophil recruitment. Although IL-6 and IL-10 levels are not conventionally examined in relation to IgE-mediated allergy, both cytokines can be produced by MCs, and the former has been shown to contribute to the pathogenesis of certain chronic allergic conditions [273] whereas the latter has general anti-inflammatory effects. Therefore, it is important to investigate whether these cytokines derived from MCs also play a role in the particular PCA model that we employed here.

It is well-recognised that UVB-based phototherapy can be used to treat a multitude of dermatologic disorders, such as atopic dermatitis, psoriasis, and cutaneous T cell lymphoma, and its benefits are to some extent mediated by triggering $VitD_3$ synthesis in the skin. [314] In patients with psoriasis, for instance, previous studies have indicated insufficient basal levels of $VitD_3$ and its metabolites in the circulation as compared to

healthy controls. Therefore, the increase in serum $25OHD_3$, $24,25(OH)_2D_3$ and $1\alpha,25(OH)_2D_3$ levels in these patients following broadband UVB treatment may, at least partially, explain the efficacy of this therapeutic approach. [315] In addition, topically applied $1\alpha,25(OH)_2D_3$ (and its various analogues e.g. calcipotriol and calcipotriene) has also been proven an effective treatment for inflammatory diseases of the skin such as psoriasis and vitiligo, as well as CHS responses in a number of mouse and human experiments. [302, 316-319] A recent study by Gorman *et al.* [317] further demonstrated an additive effect of topical $1\alpha,25(OH)_2D_3$ application upon UVB irradiation on suppressing CHS responses to 2,4-dinitrofluorobenzene in mice as compared to irradiation-only controls. Bearing particular relevance to the current study, $1\alpha,25(OH)_2D_3$ administration may also assist in limiting allergic diseases such as asthma, as subcutaneous immunotherapies incorporating this hormone can reduce respiratory inflammation during allergic airway disease. [235] To date, likely mechanisms responsible for such $1\alpha,25(OH)_2D_3$-mediated immunosuppression include direct effects on keratinocyte proliferation and differentiation in psoriatic lesions, regulation of the trafficking as well as functionality of effector cells (e.g. DCs and T cells) in the diseased skin and skin-draining LNs, and enhancement of the suppressive capacity of regulatory cells such as T_{reg} cells. [226, 316, 317, 320] Despite the involvement of MCs during the pathogenesis of cutaneous disorders including psoriasis [321] and atopic dermatitis [322], the effects of topically applied $VitD_3$ analogues on these cells have not been investigated, especially in the context of anaphylaxis. Previous chapters of this study highlighted that both $1\alpha,25(OH)_2D_3$ and $25OHD_3$ could elicit immunosuppressive effects on IgE + sAg-

activated MCs *in vitro*. We now wanted to determine if these observed *in vitro* effects can be translated to an *in vivo* IgE-mediated PCA model.

Due to the extensive influence of $VitD_3$ on a large variety of immune as well as structural cells, any effect of topically applied $VitD_3$ on PCA-associated cutaneous pathology may not necessarily be mediated by MCs in the skin. To test if MCs are the target of $VitD_3$-induced suppression of PCA responses, we used WT mice, MC-deficient $Kit^{W\text{-}sh/W\text{-}sh}$ mice [182] and $Kit^{W\text{-}sh/W\text{-}sh}$ mice that had been engrafted selectively in to the ears with WT mBMCMCs and therefore differ from the original mutants solely because of the presence of MCs (Section 1.5.2). Furthermore, it was established *in vitro* that VDR is required for both $1\alpha,25(OH)_2D_3$ and $25OHD_3$ (the precursor, inactive metabolite) to elicit immunosuppressive effects on activated MCs. To examine the MC VDR-dependence for the effects of topical $VitD_3$ on PCA, $Kit^{W\text{-}sh/W\text{-}sh}$ mice engrafted with $VDR^{-/-}$ mBMCMCs were also used, which differ from the WT mBMCMC-engrafted counterparts solely due to the lack of functional VDR in the donor MCs. Using all four groups of mice, we intended to investigate firstly the effect of topically applied $1\alpha,25(OH)_2D_3$ and $25OHD_3$ on PCA-associated cutaneous pathology and its dependency on MC VDR expression and, subsequently, the mechanisms (e.g. alteration in MC number, granularity and mediator profile) involved.

5.2. Results

5.2.1. Topical 1α,25(OH)2D3 application alone does not affect ear thickness of WT mice

A recent report by Li *et al.* [281] demonstrated that in WT CD1 mice treated with 1α,25$(OH)_2D_3$ or its low-calcemic analogue MC903 (calcipotriol) topically to the ears (both dissolved in ETOH, and applied at 4 nM for up to 16 consecutive days) exhibited atopic dermatitis-like features such as ear swelling and skin lesions, a process driven by the induction of keratinocyte-derived TSLP. To examine whether such a pro-inflammatory effect of 1α,25$(OH)_2D_3$ also applies to WT C57BL/6 mice, mouse ears were topically treated with either four daily doses of 3 μM (a concentration that has been routinely used [226, 323]) of 1α,25$(OH)_2D_3$ dilution or fifteen doses of 0.03 μM (a concentration that was indicated to be immunosuppressive by *in vitro* experiments illustrated in Chapter 3) dilution. Daily ear thickness measurement showed that these concentrations of 1α,25$(OH)_2D_3$ did not alter ear thickness compared to vehicle-treated controls (**Figure 5.1**).

5.2.2. Topical 1α,25$(OH)_2D_3$ application at the site of inflammation can suppress PCA-associated ear swelling

To determine the optimal dose of topical 1α,25$(OH)_2D_3$ that can suppress IgE-mediated PCA-associated ear swelling, three different concentrations were tested in WT C57BL/6 mice, out of which the highest and the most frequently used concentration (3 μM) seemed the most effective (**Figure 5.2a**). It should be noted that the two lower concentrations also led to a reduction in overall ear swelling response as compared to vehicle treatment, even though the differences did not reach statistical significance. Nevertheless, it was

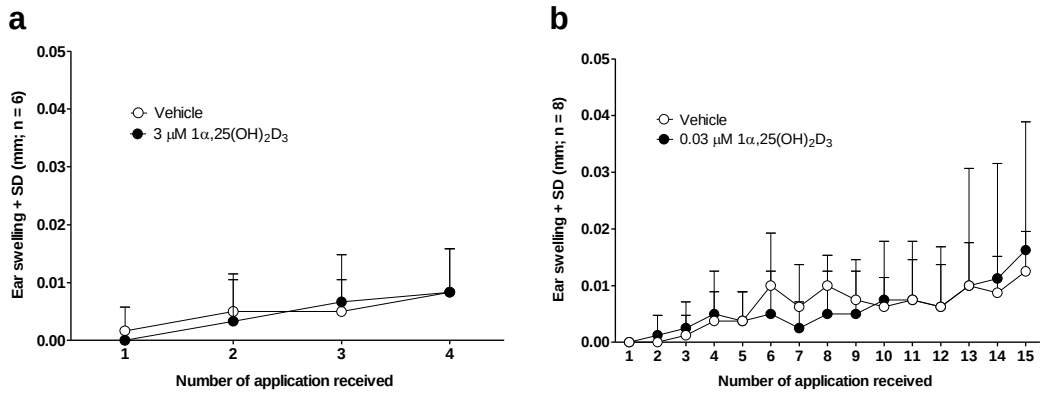

Figure 5.1. Topically applied 1α,25(OH)$_2$D$_3$ alone has no effect on ear thickness of WT mice

Ears of WT C57BL/6 mice were topically applied with either (a) 3 μM of 1α,25(OH)$_2$D$_3$ (20 μL/ear) for four consecutive days or (b) 0.03 μM of 1α,25(OH)$_2$D$_3$ for 15 consecutive days. In both cases, vehicle (ETOH-PG-H$_2$O at 2:1:1 ratio)-treated mice were used as controls, and the change in ear thickness from baseline was measured and recorded every 24 h. Data are representative of one experiment using six or eight (as indicated) mice per treatment.

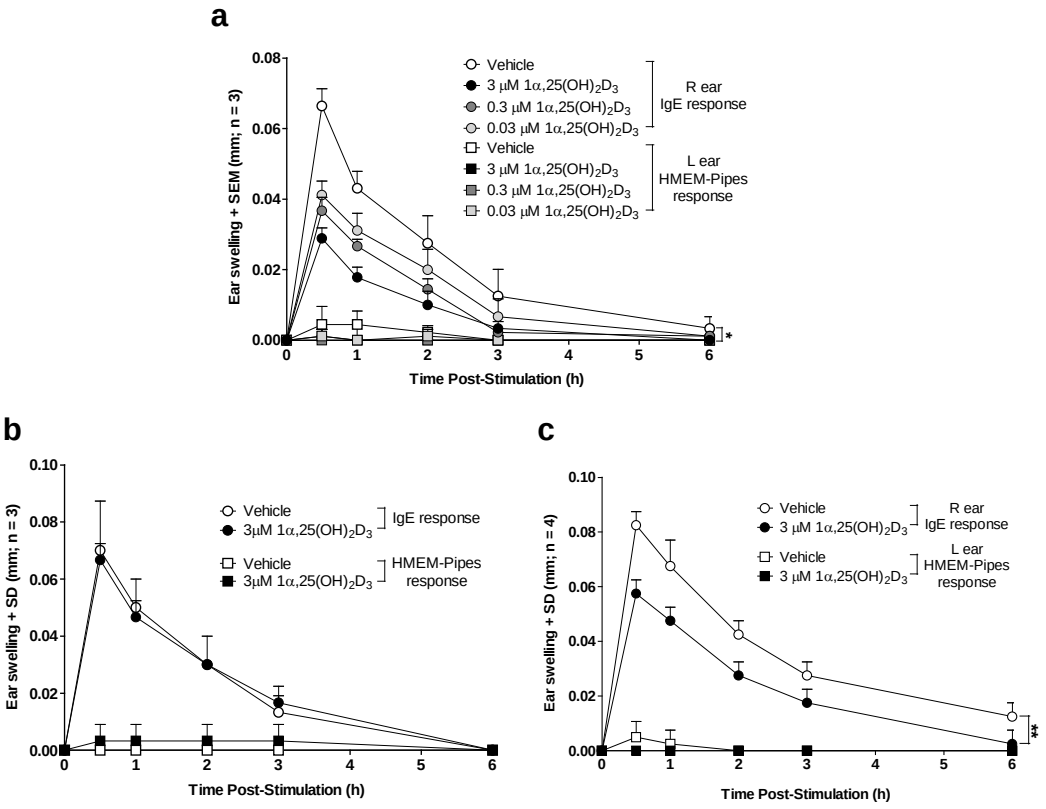

Figure 5.2. Optimisation of the 1α,25(OH)$_2$D$_3$ application strategy to study its effect on PCA-associated cutaneous pathology

Wild-type C57BL/6 (a and b) and WBB6F1 (c) mice were used in this series of experiments. (a and c) Mice were injected *i.d.* with 100 ng (20 µL of 5 µg/mL dilution) of α-DNP IgE (SPE-7 clone) in the right ear and equal volume of HMEM-Pipes in the left ear. Immediately following injection, both ears received topical application (20 µL/ear) of either 1α,25(OH)$_2$D$_3$ dilution at the indicated concentration or vehicle alone. (b) Mice were injected *i.d.* with either 100 ng of SPE-7 or equal volume of HMEM-Pipes in the right ear only. Immediately following injection, the left ear of the mice were topically painted with either 3 µM of 1α,25(OH)$_2$D$_3$ or vehicle alone. In all cases, mice were injected retro-orbitally with 200 µg of DNP-HSA (100 µL of 2 mg/mL dilution) 16 h later, and at indicated time point post-injection, the amount of ear swelling was recorded. Data in (a) are representative of three independent experiments, each using three to four mice per treatment. Data in (b and c) are representative of one experiment using the indicated number of mice per treatment. * $p < 0.05$, ** $p < 0.01$

decided that 3 μM of 1α,25$(OH)_2D_3$ would be used in all subsequent experiments. As expected, in all treatment groups only the IgE-preloaded ears (i.e. right ears) exhibited typical PCA-mediated swelling in response to *i.v.* administration of the specific antigen, DNP-HSA, which subsided by 6 h post-stimulation. By contrast, HMEM-Pipes-preloaded ears (i.e. left ears) maintained their original thickness (i.e. no swelling) throughout the observation period. To examine whether 1α,25$(OH)_2D_3$ needs to be applied to the same ear where PCA was induced, mice received an *i.d.* injection of IgE α-DNP and 1α,25$(OH)_2D_3$/vehicle treatment on different ears. As shown in **Figure 5.2b**, a systemic effect of 1α,25$(OH)_2D_3$ was not observed as topical 1α,25$(OH)_2D_3$ application to the contralateral ear that was not injected with IgE mAb could not suppress PCA-associated ear swelling in the ear that did receive IgE. Therefore, the observed PCA suppression by 1α,25$(OH)_2D_3$ is a localised event. To determine if these findings are restricted to the C57BL/6 background, we also tested WT WBB6F1 mice. Similar to the effects observed in C57BL/6 mice, topical 1α,25$(OH)_2D_3$ application (3 μM) could effectively reduce the PCA-associated ear swelling (**Figure 5.2c**).

5.2.3. Topical 1α,25$(OH)_2D_3$ application reduced the extent of MC degranulation and the expression of various MC-derived mediators associated with PCA in vivo

This series of experiments aimed at investigating potential mechanisms responsible for the observed suppressive effects of topical 1α,25$(OH)_2D_3$ on IgE-mediated PCA-induced ear swelling. Because 1α,25$(OH)_2D_3$ has been reported to directly affect the number of keratinocytes [320], Langerhans cells [324] and T_{reg} cells [316] in various inflammatory settings *in vivo*, its effect on cutaneous MC number in the ears following PCA was examined. Unlike other cell types mentioned, the number of MCs in IgE-preloaded or

medium-preloaded ears were not significantly altered following 1α,25$(OH)_2D_3$ treatment (**Figure 5.3a**). Notably, PCA reaction alone did not seem to affect MC numbers in the ears 6 h after the induction of the response, as there was no difference between IgE- and medium-preloaded ears in this regard. In contrast to total dermal MC number, the extent of MC degranulation (assessed by observing the integrity of MC granules under light microscopy as outlined by Singh *et al.* [325]) did increase dramatically due to PCA reaction, and this was observed in both 1α,25$(OH)_2D_3$-treated (mean: 9.2% versus 34.8%) and vehicle-treated (mean: 10.6% versus 52.3%) mice (**Figure 5.3b**). More importantly, PCA-affected ears, but not non-PCA-affected ears, demonstrated a significant reduction (mean: 34.8% versus 52.3%) in MC degranulation upon 1α,25$(OH)_2D_3$ treatment as compared to vehicle alone. This was illustrated in **Figures 5.3 c – f**, where intact (red arrow) as well as degranulated (green arrow) MCs were pointed out in differently-treated ears.

On the other hand, assessment on the expression of mRNA encoding various MC-derived immunological mediators revealed that mRNA expression for HDC, the enzyme that converts histidine to histamine [326], was unchanged within 30 min (**Figures 5.4 a)** but moderately reduced by 3 h (**Figures 5.4 b**) after the onset of PCA upon 1α,25$(OH)_2D_3$ treatment (grey bars). The non-PCA affected ears, on the other hand, displayed an increase in *HDC* expression upon 1α,25$(OH)_2D_3$ application (white bars). Furthermore, at 3 h post-DNP administration, vehicle-treated mice exhibited a one-fold increase in *HDC* expression in IgE-preloaded ears as compared to medium-preloaded control ears, whereas 1α,25$(OH)_2D_3$-treated mice showed no such difference between IgE and HMEM-Pipes preloaded ears. Please note that the expression of mRNA encoding pro-inflammatory

Figure 5.3. Topically applied 1α,25(OH)$_2$D$_3$ has no effect on dermal MC number but reduces the extent of MC degranulation following PCA response

Wild-type C57BL/6 mice were injected *i.d.* with 100 ng of α-DNP IgE (SPE-7 clone) in the right ear and equal volume of HMEM-Pipes in the left. Immediately following injection, both ears received topical application (20 µL/ear) of either 3 µM of 1α,25(OH)$_2$D$_3$ or vehicle. Sixteen hours later, all mice were injected *i.v.* retro-orbitally with 200 µg of DNP-HSA. (a) The number of dermal MCs in both ear pinnae at 6 h post-injection expressed as number of MCs per mm horizontal dermal length. (b) The percentage of MC degranulation in both ears of each mouse. (c – f) Histological illustration, following toluidine blue staining, of ears that had undergone different treatments. C*, cartilage. Red arrowheads indicate intact MCs, whereas green arrowheads indicate degranulated MCs. Bars: 100 µm. Data in (a) are from three independent experiments performed, each using three to four mice per treatment group. Data in (b) are from two independent experiments performed, each using three to four mice per treatment group. Data in (c – f) are representative of one of the two independent experiments summarised in (b), which showed similar results. *** $p < 0.001$

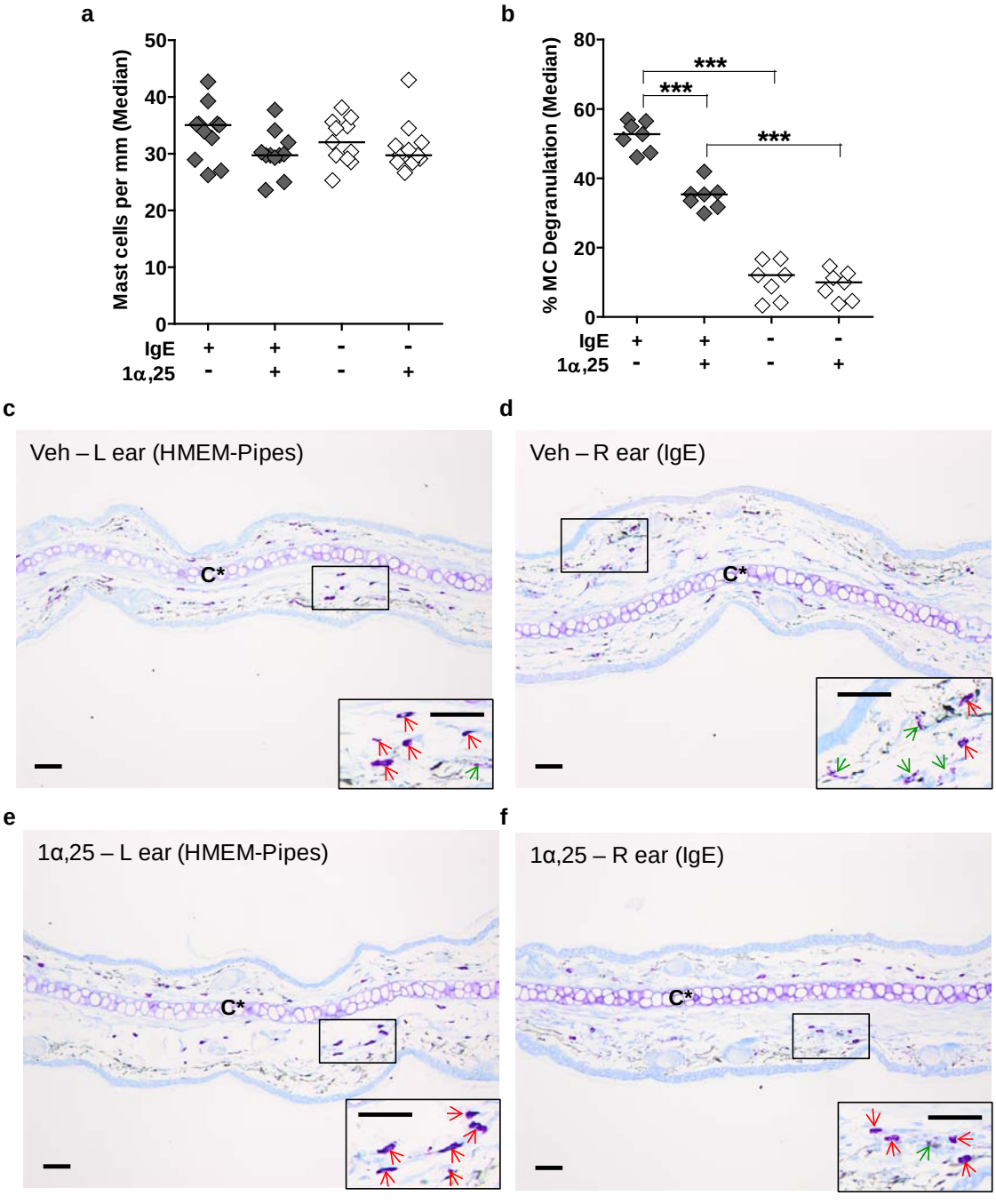
a
Mast cells per mm (Median)
50
40
30
20
10
0
IgE + + - -
1α,25 - + - +
b
% MC Degranulation (Median)
80
60
40
20
0
***
***
***
IgE + + - -
1α,25 - + - +
c
Veh – L ear (HMEM-Pipes)
C*
d
Veh – R ear (IgE)
C*
e
1α,25 – L ear (HMEM-Pipes)
C*
f
1α,25 – R ear (IgE)
C*

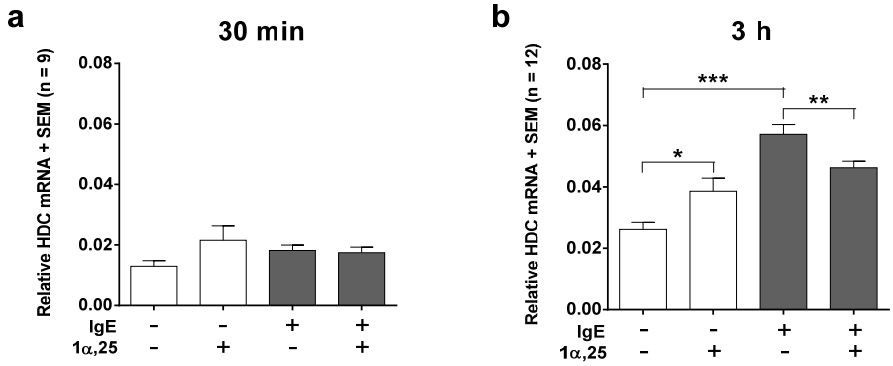

Figure 5.4. Topically applied 1α,25(OH)$_2$D$_3$ reduces HDC-encoding mRNA expression following PCA response

Wild-type C57BL/6 were injected *i.d.* with 100 ng of SPE-7 in the right ear and equal volume of HMEM-Pipes vehicle in the left, followed immediately by topical application of either 3 μM of 1α,25(OH)$_2$D$_3$ or vehicle on both ears. Sixteen hours later, all mice were injected retro-orbitally with 200 μg of DNP-HSA, and at either 30 min (a) or 3 h (b) post-injection, total RNA was extracted from both ear pinnea of each mouse and subjected to qRT-PCR analysis for the relative expression (to that of β-actin) of HDC-encoding mRNA. Data are from three independent experiments, each using three mice per treatment. qRT-PCR was performed in triplicates for each RNA sample. * $p \leq 0.05$, ** $p < 0.01$, *** $p < 0.001$

cytokines TNFα and IL-6, as well as the anti-inflammatory cytokine IL-10, was also measured (data not shown) but yielded variable results.

5.2.4. VDR expression is required for the suppressive effect of 1α,25(OH)$_2$D$_3$ on PCA-associated cutaneous pathology

In chapter 3, we demonstrated that the suppressive activity of 1α,25(OH)$_2$D$_3$ on IgE-mediated MC activation *in vitro* requires MC expression of VDRs. To investigate its relevance in the PCA model, we examined firstly the effect of topical 1α,25(OH)$_2$D$_3$ on PCA-associated ear swelling in *VDR*$^{-/-}$ mice in parallel with WT controls. Similar to the previous result (**Figure 5.2a**), WT mice in this series of experiments exhibited significantly reduced ear swelling in response to 1α,25(OH)$_2$D$_3$ topical treatment during PCA (**Figure 5.5a**). Mice that lack functional VDRs, on the other hand, failed to respond to topical 1α,25(OH)$_2$D$_3$ treatment. However, it is worth noting that although vehicle-treated *VDR*$^{-/-}$ mice have normal MC numbers in their ears (**Figure 5.5b**), they showed significantly reduced PCA-mediated ear swelling than their WT counterparts; the reason for which requires further investigation. As observed before, the total number of dermal MCs did not alter following PCA induction in either WT or *VDR*$^{-/-}$ mice (**Figure 5.5b**), and although *VDR*$^{-/-}$ mice appeared to exhibit more MCs in their medium-preloaded ears upon 1α,25(OH)$_2$D$_3$ application, this needs to be confirmed by future repeats of the experiment. Regarding the extent of MC degranulation, WT but not *VDR*$^{-/-}$ mice showed a 1α,25(OH)$_2$D$_3$-mediated reduction (mean: 58.2% versus 51.0%) in their PCA-affected ears (**Figures 5.5c**). The extent of such reduction was only moderate, possibly due to fact that the analysis was done 3 h post-DNP injection, which was after the peak of the ear swelling response. Therefore, analysis at 30 min post-DNP injection was required to

Figure 5.5. VDR is required for optimal suppression of PCA-mediated responses by topical 1α,25(OH)$_2$D$_3$

Eight- to 12-week-old sex-matched WT and *VDR*$^{-/-}$ C57BL/6 mice were injected *i.d.* with 100 ng of SPE-7 clone in the right ear and equal volume of HMEM-Pipes in the left, followed immediately by topical application of either 3 μM of 1α,25(OH)$_2$D$_3$ or vehicle on both ears. Sixteen hours later, all mice received retro-orbital injection of 200 μg of DNP-HSA, and at indicated time points post-injection, the extent of ear swelling was recorded (a). At 3 h post-injection, the number (b) and percentage degranulation (c) of dermal MCs in both ears of each mouse were measured. (d) Total RNA was also extracted, at the same time point, from both ear pinnea of each mouse and subjected to qRT-PCR analysis for the relative expression (to that of β-actin) of HDC-encoding mRNA. Data in (a) are representative of three independent experiments, each with three mice per treatment. Data in (b and c) are from one of the three experiments summarised in (a). Data in (d) are from three independent experiments, each using three mice per treatment, and qRT-PCR was performed in triplicates for each RNA sample. * $p < 0.05$, ** $p < 0.01$, *** $p < 0.001$

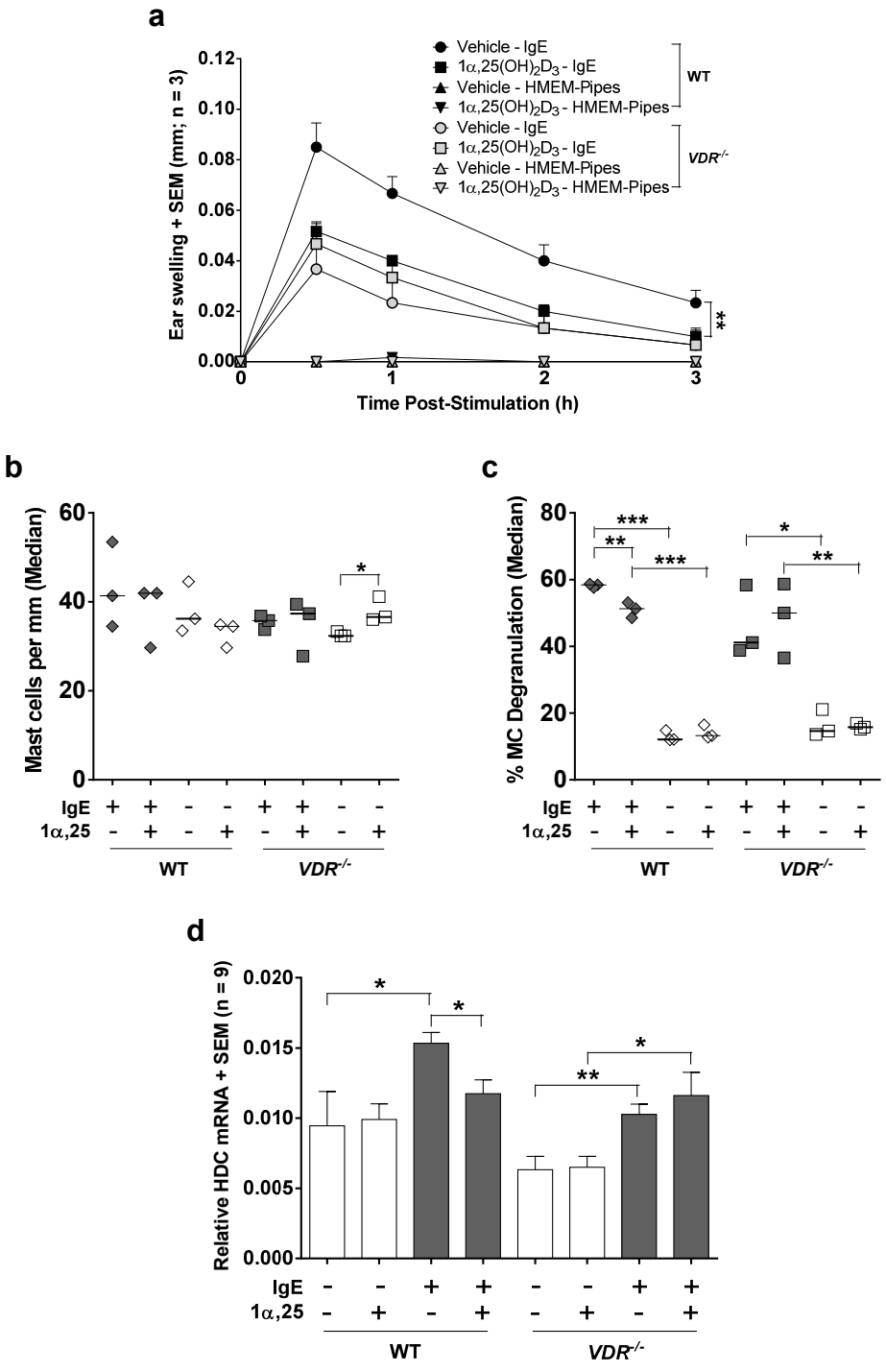
a
Vehicle - IgE
1α,25(OH)2D3 - IgE
Vehicle - HMEM-Pipes
1α,25(OH)2D3 - HMEM-Pipes
WT
VDR-/-
Ear swelling + SEM (mm; n = 3)
Time Post-Stimulation (h)
b
Mast cells per mm (Median)
IgE
1α,25
WT
VDR-/-
c
% MC Degranulation (Median)
d
Relative HDC mRNA + SEM (n = 9)

confirm this observation. Although PCA reaction seemed to induce MC degranulation in both types of mice regardless of 1α,25$(OH)_2D_3$ or vehicle treatment, the extent of increase was lower in vehicle-treated *VDR*$^{-/-}$ mice, which was consistent with the lower level of ear swelling in these mice as compared to WT controls (**Figure 5.5a**).

Analysis of the expression of HDC-encoding mRNAs at 3 h post-PCA induction, on the other hand, showed similar variations between the two treatment groups for WT mice (**Figures 5.5 d**) as previously shown (**Figures 5.4 b**), where 1α,25$(OH)_2D_3$ reduced *HDC* expression upon PCA induction. Such reduction, however, was not observed in IgE-preloaded ears in *VDR*$^{-/-}$ mice (**Figures 5.5 d**). It is worth noting that *HDC* expression in vehicle-treated and PCA-affected ears in *VDR*$^{-/-}$ mice was lower than that in WT controls, which may be another explanation for the reduced ear swelling in these mice upon vehicle treatment and should be investigated further by including naive (i.e. non-treated) *VDR*$^{-/-}$ mice in future experiments. Nevertheless, it seemed so far that the suppressive effect of 1α,25$(OH)_2D_3$ on PCA-associated ear swelling, the extent of MC degranulation, and gene expression for MC-derived HDC did require functional VDRs in the animals.

5.2.5. The PCA-suppressing effect of topical 1α,25$(OH)_2D_3$ treatment requires specifically VDR expression by cutaneous MCs

To further establish if the VDRs specifically expressed by MCs are essential for topical 1α,25$(OH)_2D_3$ to suppress PCA, *Kit*$^{W\text{-}sh/W\text{-}sh}$ mice and WT/*VDR*$^{-/-}$ mBMCMC knock-in mice were employed with the previously stated rationale (Section 1.10). As shown in **Figures 5.6 a and c**, WT mice again exhibited 1α,25$(OH)_2D_3$-mediated reduction of overall ear swelling following PCA induction. *Kit*$^{W\text{-}sh/W\text{-}sh}$ mice, due to the absence of MCs in the ears, did not exhibit swelling in either ear (vehicle or 1α,25$(OH)_2D_3$ treatment)

Figure 5.6. Mast cell VDR-dependence for the effect of topically applied $1\alpha,25(OH)_2D_3$ on PCA-associated ear swelling and cutaneous pathology
Wild-type (*Kit*$^{+/+}$) mice (a and c), MC-deficient (*Kit*$^{W\text{-}sh/W\text{-}sh}$) mice (a and d), and MC-deficient mice that had been engrafted *i.d.* with either WT MCs (WT mBMCMCs → *Kit*$^{W\text{-}sh/W\text{-}sh}$; b and e) or *VDR*$^{-/-}$ MCs (*VDR*$^{-/-}$ mBMCMCs → *Kit*$^{W\text{-}sh/W\text{-}sh}$; b and f) were injected *i.d.* with 100 ng of SPE-7 in the right ear and equal volume of HMEM-Pipes in the left, followed immediately by topical application of either 3 μM of $1\alpha,25(OH)_2D_3$ or vehicle on both ears. Sixteen hours later, all mice were injected retro-orbitally with 200 μg of DNP-HSA, and at indicated time point post-injection the amount of ear swelling was recorded (a and b). In one experiment, cross sections of ears were obtained 30 min after DNP administration and subsequently stained with TB (c – f). C*, cartilage. Red arrowheads indicate MCs. Bars: 200 μm (b – e); 1,000 μm (bottom right insets in c – f); 50 μm (top right insets in c and e). Data in (a and b) are from four independent experiments performed, each with three to four mice analysed per group. Images in (c – f) were obtained from one experiment, and are representative of all mice (3 – 4 mice per group) with the corresponding treatment. ** $p < 0.01$

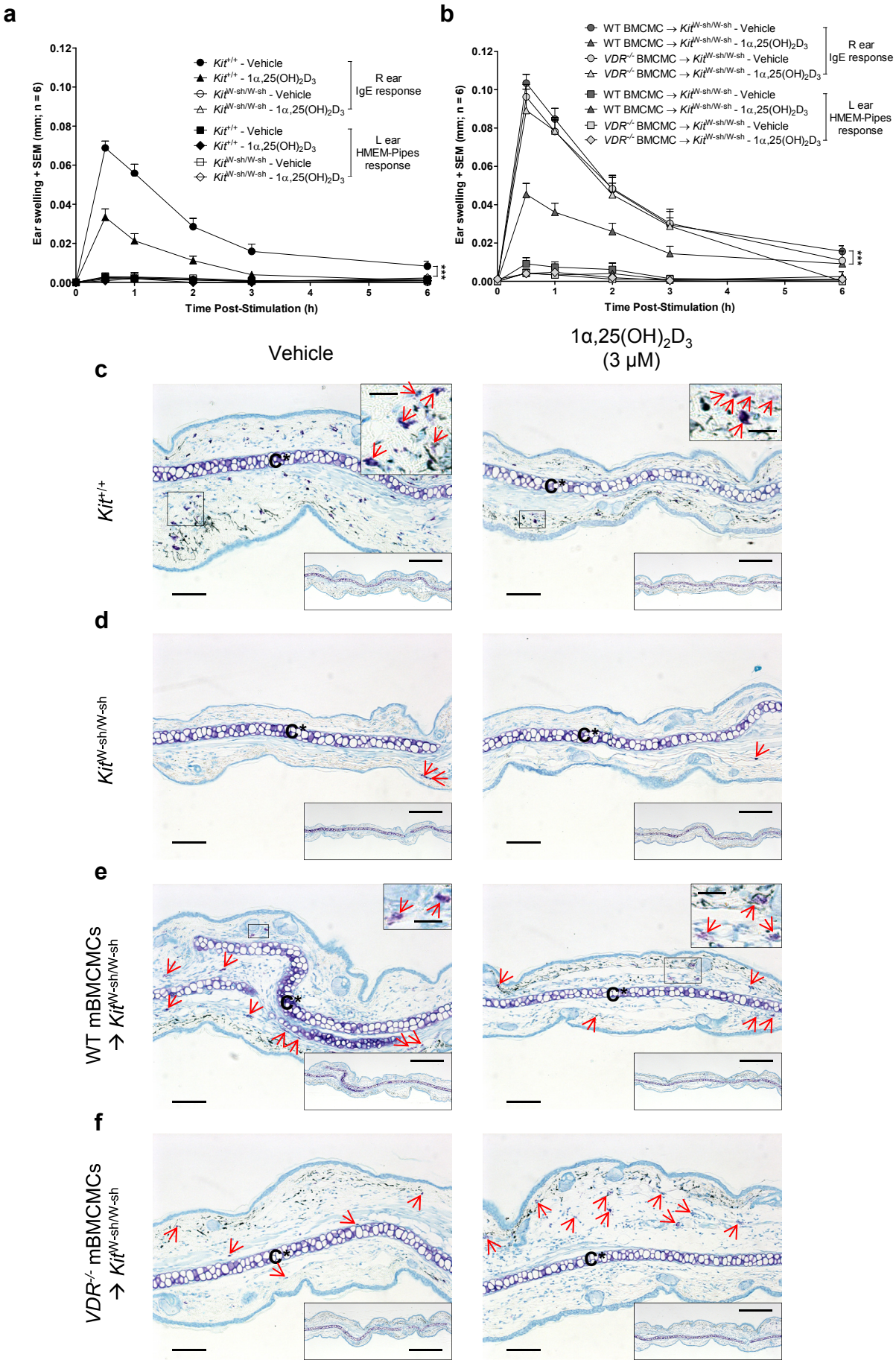
a
b
Ear swelling + SEM (mm; n = 6)
Time Post-Stimulation (h)
Kit+/+ - Vehicle
Kit+/+ - 1α,25(OH)2D3
KitW-sh/W-sh - Vehicle
KitW-sh/W-sh - 1α,25(OH)2D3
R ear IgE response
L ear HMEM-Pipes response
WT BMCMC → KitW-sh/W-sh - Vehicle
WT BMCMC → KitW-sh/W-sh - 1α,25(OH)2D3
VDR-/- BMCMC → KitW-sh/W-sh - Vehicle
VDR-/- BMCMC → KitW-sh/W-sh - 1α,25(OH)2D3
***
Vehicle
1α,25(OH)2D3 (3 μM)
c
d
e
f
Kit+/+
KitW-sh/W-sh
WT mBMCMCs → KitW-sh/W-sh
VDR-/- mBMCMCs → KitW-sh/W-sh
C*

(**Figures 5.6 a and d**). Importantly, repair of MC-deficiency by MC engraftment in the ears of *Kit*$^{W\text{-}sh/W\text{-}sh}$ mice (i.e. WT mBMCMC knock-in mice) not only reinstated their ability to respond to PCA induction but also enabled, like the WT controls, a significant reduction in ear swelling upon 1α,25$(OH)_2D_3$ treatment (**Figures 5.6 b and e**). By contrast, loss of functional MC VDRs in the *VDR*$^{-/-}$ mBMCMC knock-in group of mice, ablated the negative regulatory ability of 1α,25$(OH)_2D_3$ to reduce the IgE-PCA reactions (**Figures 5.6 b and f**), thereby demonstrating the suppressive effect of 1α,25$(OH)_2D_3$ on PCA is MC VDR-dependent.

Confirming our previous finding (**Figure 5.3a**), MC number in both ears of WT mice was unaltered by 1α,25$(OH)_2D_3$ treatment throughout PCA reaction (**Figures 5.7 a and b**). Whilst the WT mBMCMC-engrafted mice showed increased numbers of MC in PCA-affected ears at certain stage of the inflammatory response, the numbers of MC in their *VDR*$^{-/-}$ mBMCMC-engrafted counterparts were decreased (**Figures 5.7 a and b**). However, since similar observations were made in non-PCA-affected ears of these mice, these differences most likely reflected the effectiveness of the initial engraftment in each individual mouse rather than the effect of 1α,25$(OH)_2D_3$. Therefore, future repetitions of the experiment are required before a definitely conclusion can be drawn in this regard. As expected, *Kit*$^{W\text{-}sh/W\text{-}sh}$ mice lacked MCs in both ears that received either 1α,25$(OH)_2D_3$ or vehicle application. The extent of MC degranulation, on the other hand, was reduced in 1α,25$(OH)_2D_3$-treated, PCA-affected ears of WT (mean at 30 min: 39.0% versus 56.9%; mean at 6 h: 34.8% versus 52.3%) and WT mBMCMC knock-in (mean at 30 min: 57.6% versus 70.7%; mean at 6 h: 52.7% versus 73.1%) mice, but was unchanged for *VDR*$^{-/-}$ MC knock-in (mean at 30 min: 68.5% versus 71.5%; mean at 6 h: 66.1% versus 64.2%) mice

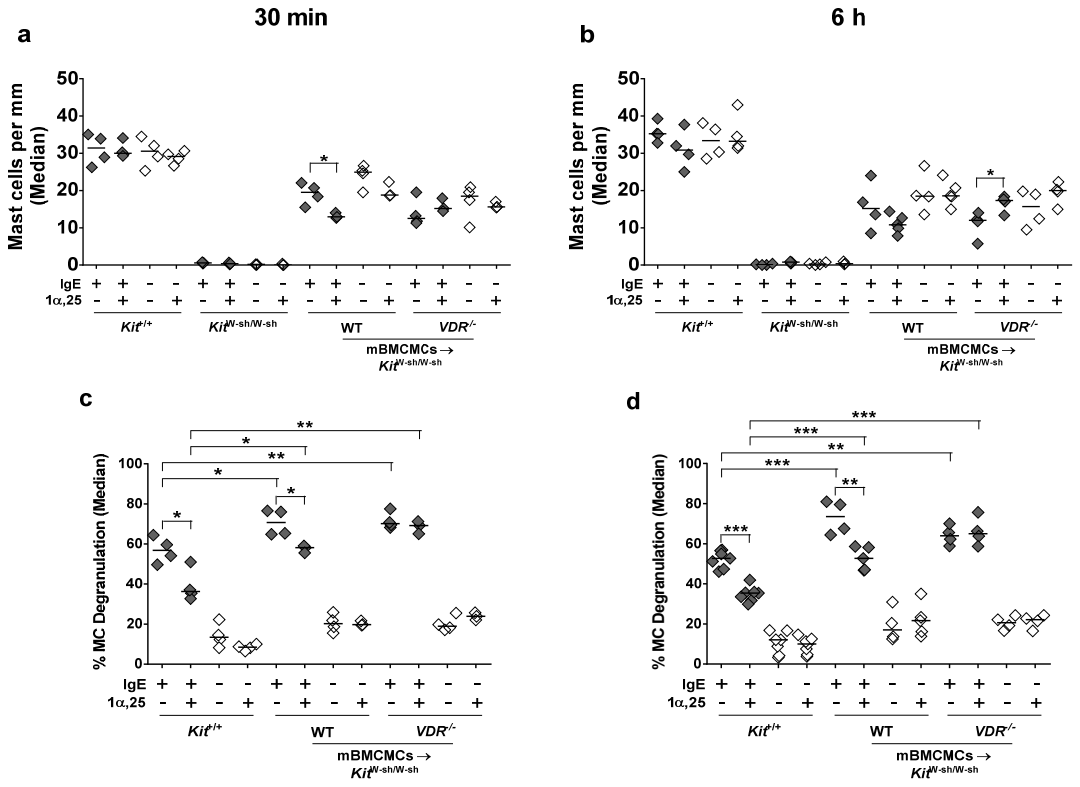

Figure 5.7. Topical 1α,25(OH)$_2$D$_3$ has minimal effect on dermal MC number but reduces moderately the extent of MC degranulation in MC-engrafted *Kit$^{W\text{-}sh/W\text{-}sh}$* mice following PCA response

Wild-type (*Kit$^{+/+}$*) mice, MC-deficient (*Kit$^{W\text{-}sh/W\text{-}sh}$*) mice, and MC-deficient mice that had been engrafted *i.d.* with either WT MCs (WT mBMCMCs → *Kit$^{W\text{-}sh/W\text{-}sh}$*) or *VDR$^{-/-}$* MCs (*VDR$^{-/-}$* mBMCMCs → *Kit$^{W\text{-}sh/W\text{-}sh}$*) were injected *i.d.* with 100 ng of SPE-7 in the right ear and equal volume of HMEM-Pipes in the left, followed immediately by topical application of either 3 μM of 1α,25(OH)$_2$D$_3$ or vehicle on both ears. Sixteen hours later, all mice were injected retro-orbitally with 200 μg of DNP-HSA, and at either 30 min (a and c) or 6 h (b and d) post-injection, the total number of dermal MCs (a and b) as well as the percentage of MC degranulation (c and d) in both ear pinnae were recorded. Data are representative of one of three experiments (each using three to four mice per treatment group) that showed similar ear swelling responses. * $p < 0.05$, ** $p < 0.01$, *** $p < 0.001$

(**Figures 5.7 c and d**). The extent of MC degranulation in non-PCA-affected ears of all mice, however, remained constant upon 1α,25$(OH)_2D_3$ application. It is worth noting that although both types of MC knock-in mice appeared to have considerably lower numbers of MCs in both ears than the WT controls (**Figures 5.7 a and b)**, they both showed higher levels of MC degranulation regardless of vehicle or 1α,25$(OH)_2D_3$ treatment (**Figures 5.7 c and d**). This could be a possible explanation for the observed higher PCA responses in these MC knock-in animals (**Figures 5.6 a and b**).

Analysis on mRNA expression for HDC in all four types of mice indicated similar results for WT animals as previously observed, where it was reduced upon 1α,25$(OH)_2D_3$ treatment (**Figure 5.8**). No significant difference, however, was observed between vehicle- and 1α,25$(OH)_2D_3$-treated ears in the other groups of mice. Moreover, *HDC* seemed to be expressed at similar levels in $Kit^{W\text{-}sh/W\text{-}sh}$ mice and both groups of MC knock-in mice, indicating the engraftment of MCs did not alter *HDC* expression. This in turns suggested that the differences in its expression between WT and $Kit^{W\text{-}sh/W\text{-}sh}$ mice were unlikely to be MC-dependent, either.

Since the gene expression analyses did not yield consistent result, the protein secretion of the proinflammatory cytokines TNF and IL-6, as well as that of the anti-inflammatory IL-10, was measured. According to **Figures 5.9 a, c and e**, topical 1α,25$(OH)_2D_3$ application did not have immediate effect on the secretion of any cytokine examined upon PCA induction in all four groups of mice. Interestingly, $Kit^{W\text{-}sh/W\text{-}sh}$ mice, which did not exhibit PCA-induced ear swelling responses, showed higher "cytokine/total protein" ratios than all three PCA-affected mouse types at this time point. This could be a reflection on the increased overall protein levels in the latter three mouse groups

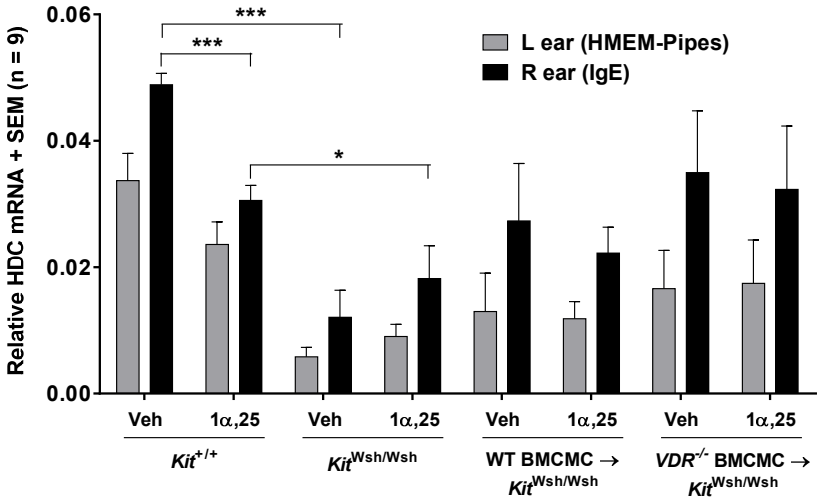

Figure 5.8. MC VDR expression is not required for topically applied 1α,25(OH)$_2$D$_3$ to reduce HDC-encoding mRNA expression following PCA induction

Wild-type (*Kit*$^{+/+}$) mice, MC-deficient (*Kit*$^{W\text{-}sh/W\text{-}sh}$) mice, and MC-deficient mice that had been engrafted *i.d.* with either WT MCs (WT mBMCMCs → *Kit*$^{W\text{-}sh/W\text{-}sh}$) or *VDR*$^{-/-}$ MCs (*VDR*$^{-/-}$ mBMCMCs → *Kit*$^{W\text{-}sh/W\text{-}sh}$) were injected *i.d.* with 100 ng of SPE-7 in the right ear and equal volume of HMEM-Pipes in the left, followed immediately by topical application of either 3 μM of 1α,25(OH)$_2$D$_3$ or vehicle on both ears. Sixteen hours later, all mice were injected retro-orbitally with 200 μg of DNP-HSA, and at 3 h post-injection, total RNA was extracted from both ear pinnea of each mouse and subjected to qRT-PCR analysis for the relative expression (to that of β-actin) of HDC-encoding mRNA. Data are from three independent experiments, each with three mice analysed per treatment. qRT-PCR was performed in triplicates for each RNA sample. * $p < 0.05$, *** $p < 0.001$

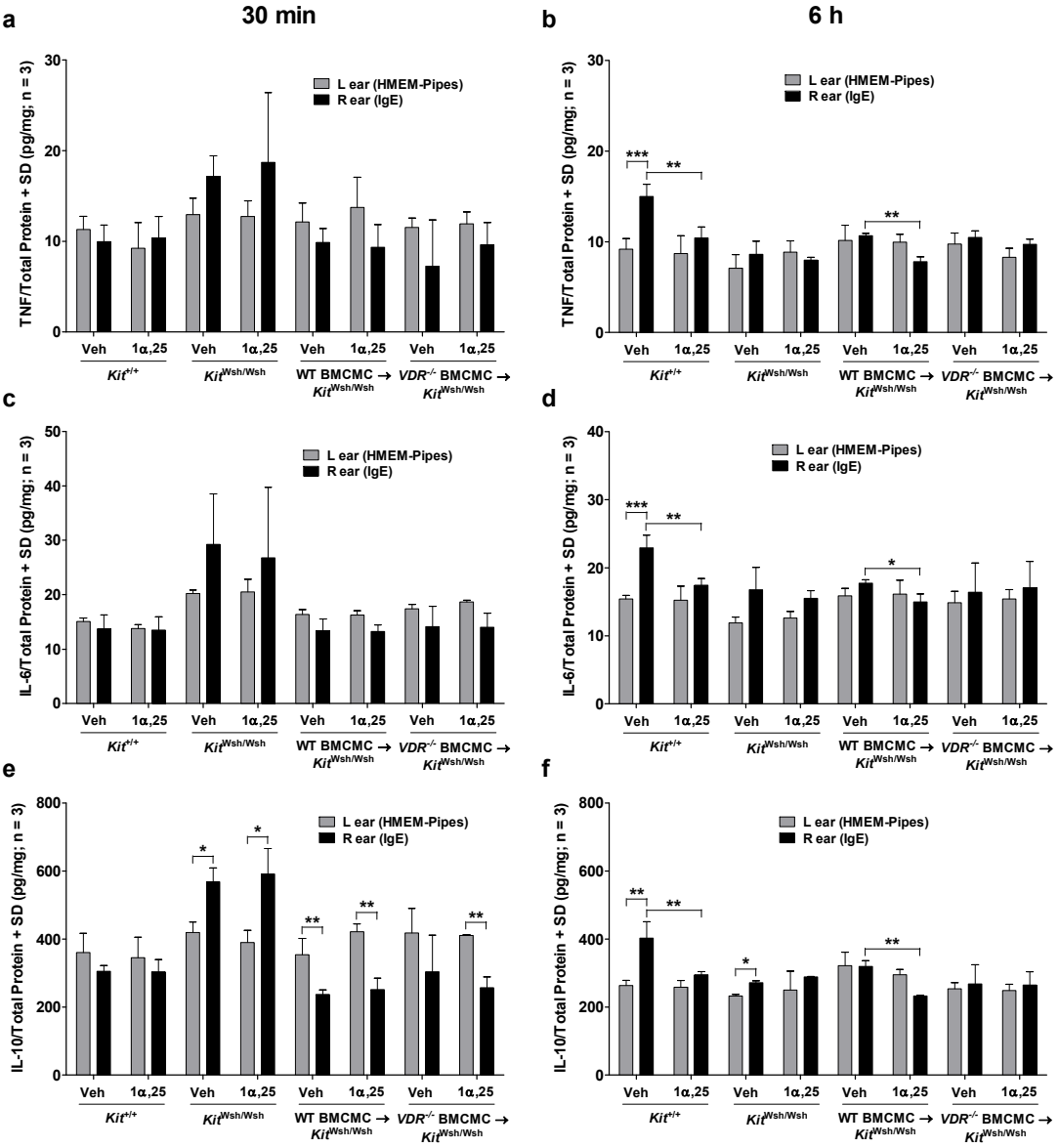

Figure 5.9. MC VDR is required, at least partially, for topically applied 1α,25(OH)$_2$D$_3$ to suppres cytokine secretion in PCA-affected ears

Wild-type (*Kit*$^{+/+}$) mice, MC-deficient (*Kit*$^{W\text{-}sh/W\text{-}sh}$) mice, and MC-deficient mice that had been engrafted *i.d.* with either WT MCs (WT mBMCMCs → *Kit*$^{W\text{-}sh/W\text{-}sh}$) or *VDR*$^{-/-}$ MCs (*VDR*$^{-/-}$ mBMCMCs → *Kit*$^{W\text{-}sh/W\text{-}sh}$) were injected *i.d.* with 100 ng of SPE-7 in the right ear and equal volume of HMEM-Pipes in the left, followed immediately by topical application of either 3 μM of 1α,25(OH)$_2$D$_3$ or vehicle on both ears. Sixteen hours later, all mice were injected retro-orbitally with 200 μg of DNP-HSA. At either 30 min (a, c, e) or 6 h (b, d, f) post-injection, the levels of TNF (a and b), IL-6 (c and d), and IL-10 (e and f) in lysates of both ears were measured. Data were obtained from one experiment using three mice per treatment. * $p < 0.05$, *** $p < 0.001$

immediately following PCA induction, due to the secretion of other types of inflammatory mediators. [81] At 6 h post-DNP induction, on the other hand, vehicle-treated WT mice showed the highest secretion level of all cytokines, which was significantly reduced upon 1α,25$(OH)_2D_3$ treatment (**Figures 5.9 b, d, f**). Importantly, WT but not *VDR*$^{-/-}$ mBMCMC knock-in mice, demonstrated similar 1α,25$(OH)_2D_3$-mediated suppression of cytokine secretion as the WT controls. Therefore, although MCs are unlikely the sole contributor to PCA-associated cytokine production, these cells, through their VDR expression, do appear to play a role in 1α,25$(OH)_2D_3$-mediated overall cytokine reduction. However, due to the relatively moderate (even though statistically significant) reduction in the production of measured cytokines following 1α,25$(OH)_2D_3$ treatment of both groups of knock-in mice, other more immediately-released MC-derived mediators such as histamine and leukotrienes need to be measured in subsequent studies. In addition to ear lysates, serum sample from all animals was also analysed for cytokine levels, so as to determine whether the effect of 1α,25$(OH)_2D_3$ on cytokine secretion was localised or systemic. Since the level of all three cytokines examined in all serum samples was below the detection limit of the ELISA kits (data not shown), it was unlikely that topical 1α,25$(OH)_2D_3$ would cause any systemic change in cytokine production.

5.2.6. Topical 25OHD_3 can suppress PCA-associated ear swelling via similar mechanisms to 1α,25$(OH)_2D_3$

It was demonstrated in Chapter 4 that 25OHD_3, depending on its concentration and the length of treatment, could also elicit immunosuppressive effects on IgE + sAg-activated MCs. It was, therefore, important to investigate the relevance of these findings in the

PCA model *in vivo*. In order to optimise concentration of $25OHD_3$ for further study, a dose response experiment was performed similar to **Figure 5.2a** for $1\alpha,25(OH)_2D_3$ optimisation, where various concentrations of $25OHD_3$ was applied immediately after IgE injection. However, unlike $1\alpha,25(OH)_2D_3$, no reduction in the swelling of IgE-preloaded ears was observed in all $25OHD_3$-treated groups (**Figure 5.10a**). Given that MCs required a longer exposure time to $25OHD_3$ than $1\alpha,25(OH)_2D_3$ before IgE preload to reduce mediator release *in vitro* (**Figures 4.6 and 4.7**), subsequent *in vivo* experiments were designed to provide a longer exposure time (8 h) of the ears to $25OHD_3$ prior to IgE injection and sensitization of the dermal MCs. Allowing more time for $25OHD_3$ to penetrate the ears and be converted to the active metabolite $1\alpha,25(OH)_2D_3$, enabled the highest dose (3 μM) of topical $25OHD_3$ to significantly impair PCA-associated ear swelling compared to vehicle treatment (**Figure 5.10b**). Although the differences did not reach statistical significance, the two lower concentrations of $25OHD_3$ also managed to reduce the swelling of PCA-affected ears to certain extents. As expected, all HMEM-Pipes-preloaded ears in both short and long treatment settings showed only minimum levels of swelling (**Figures 5.10 a and b**). Based on these results, longer treatment with 3 μM of topical $25OHD_3$/vehicle was used in all subsequent experiments. Furthermore, like topical $1\alpha,25(OH)_2D_3$, topical $25OHD_3$ also had to be applied at the site of PCA to suppress ear swelling, as mice that received either $25OHD_3$ or vehicle treatment on the different ear as to IgE preload, exhibited similar levels of swelling with both ears (**Figure 5.10c**). Also similar to topical $1\alpha,25(OH)_2D_3$, $25OHD_3$-mediated suppression of ear swelling was not restricted to the C57BL/6 background, as it gave similar results in WT WBB6F1 mice (**Figure 5.10d**).

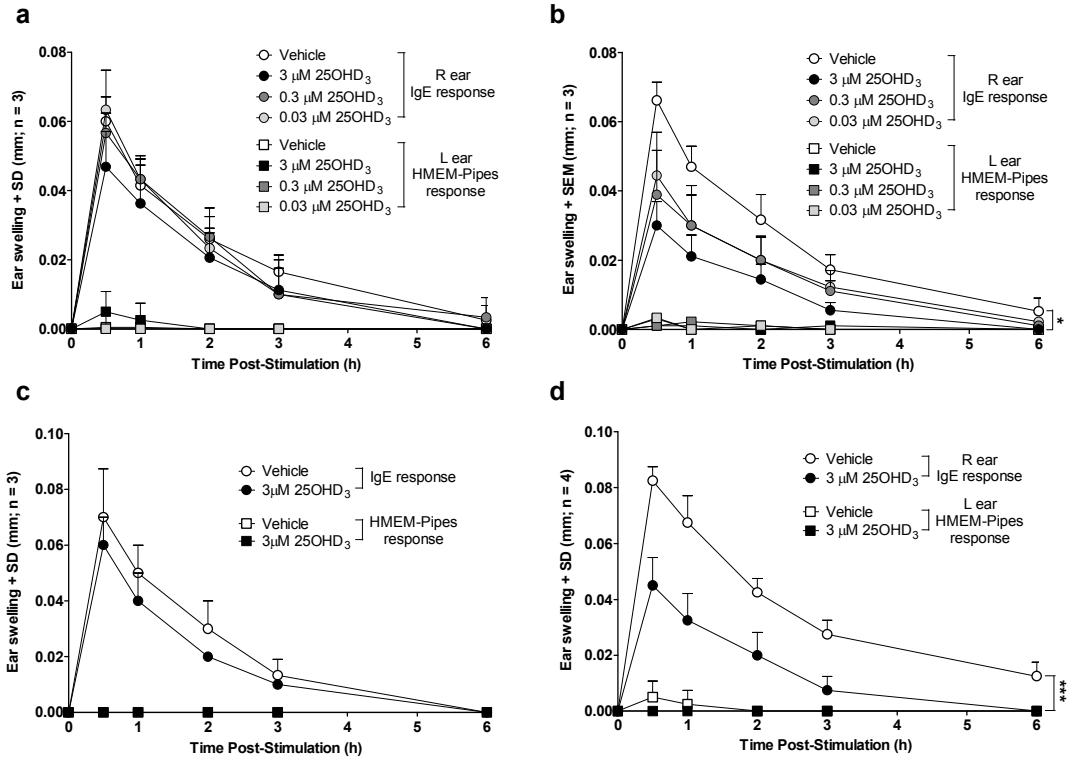

Figure 5.10. Optimisation of the *in vivo* PCA model to study the effect of topically applied 25OHD$_3$

Wild-type C57BL/6 (a – c) and WBB6F1-*Kit*$^{+/+}$ (e) mice were used in this series of experiments. (a) Mice were injected *i.d.* with 100 ng of α-DNP IgE (SPE-7 clone) in the right ear and equal volume of HMEM-Pipes in the left. Immediately following injection, both ears received topical application (20 μL/ear) of either 25OHD$_3$ dilution at the indicated concentration or vehicle alone. (b – d) Mice were topically painted, on both ears, with either 25OHD$_3$ dilution at the indicated concentration or vehicle 8 h prior to *i.d.* injection of 100 ng of SPE-7 in the right ear and equal volume of HMEM-Pipes in the left. In all cases, mice were injected retro-orbitally, 16 h later, with 200 μg of DNP-HSA (100 μL of 2 mg/mL dilution), and the extent of ear swelling was recorded at indicated time point post-injection. Data in (a, c and d) are representative of one experiment with the indicated number of mice per treatment. Data in (b) are representative of three independent experiments, each using three to four mice per treatment. * $p < 0.05$, *** $p < 0.001$

Subsequent experiments were performed to determine whether the potential mechanisms responsible for 1α,25$(OH)_2D_3$-mediated PCA suppression could also apply to topical 25OHD_3. Indeed, topical 25OHD_3 treatment did not alter the number of dermal MCs in either ear of WT mice (**Figure 5.11a**), but instead reduced the extent of MC degranulation in PCA-affected ears (**Figure 5.11b**). Analysis on the gene expression of MC-derived HDC also showed almost identical results as found with topical 1α,25$(OH)_2D_3$ (**Figure 5.4**), where 25OHD_3 application significantly reduced the *HDC* expression (**Figures 5.12**).

5.2.7. The suppressive effect of topical 25OHD$_3$ on PCA-associated cutaneous pathology also requires MC expression of VDR

Due to the similarity between the ability of topical 1α,25$(OH)_2D_3$ and 25OHD_3 to suppress PCA-induced ear swelling in WT mice and potential mechanisms responsible, we decided to determine if MC VDR expression is required for the effects of 25OHD_3. Utilising MC-deficient c-kit mutant mice and WT/*VDR*$^{-/-}$ mBMCMC knock-in mice in addition to WT controls, we demonstrated that topical 25OHD_3 indeed required dermal MCs and functional VDR expression in these cells to reduce swelling of PCA-affected ears, as WT, but not *VDR*$^{-/-}$, BMCMC knock-in mice responded to 25OHD_3 treatment in the same way as WT controls (**Figures 5.13**).

Subsequent investigation showed no change in total MC number in either ear of all groups of mice upon 25OHD_3 application (**Figure 5.14a**). Like 1α,25$(OH)_2D_3$, 25OHD_3-treated and PCA-affected ears showed reduced extent of MC degranulation in WT (mean: 37.4% versus 52.4%) and WT MC knock-in (mean: 53.9% versus 68.2%) mice but not *VDR*$^{-/-}$ MC knock-in (mean: 63.4% versus 60.8%) mice (**Figure 5.14b**). The higher-than-

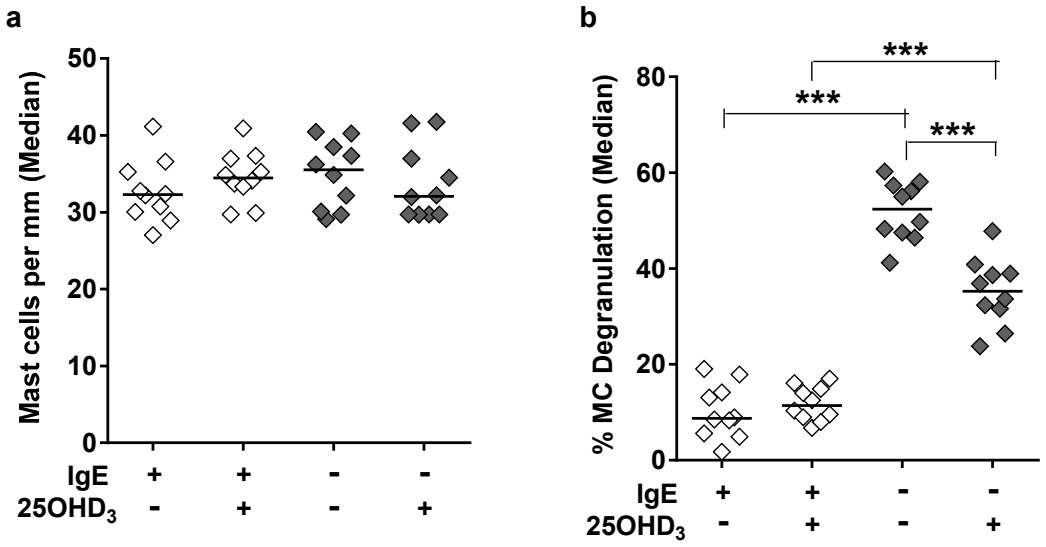

Figure 5.11. Topically applied $25OHD_3$ has little effect on dermal MC number but reduces the extent of MC degranulation following PCA response

Wild-type C57BL/6 mice were topically painted, on both ears, with either 3 μM of $25OHD_3$ or vehicle 8 h prior to *i.d.* injection of 100 ng of α-DNP IgE (SPE-7 clone) in the right ear and equal volume of HMEM-Pipes in the left. Sixteen hours later, all mice received retro-orbital injection of 200 μg of DNP-HSA. (a) The total number of dermal MCs in both ear pinnae at 6 h post-injection were recorded. (b) At the same time point, the percentage of MC degranulation in both ears of each mouse was calculated. Data are from three independent experiments performed, each using three to four mice per treatment group. *** $p < 0.001$

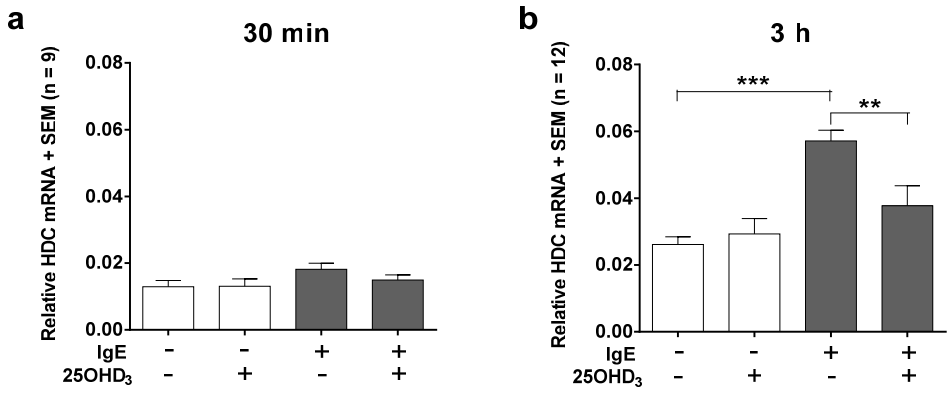

Figure 5.12. Topically applied $25OHD_3$ moderately reduces the expression of HDC-encoding mRNAs following PCA response

Wild-type C57BL/6 mice received, on both ears, topical application of either 3 μM of $25OHD_3$ or vehicle 8 h prior to *i.d.* injection of 100 ng of SPE-7 in the right ear and equal volume of HMEM-Pipes in the left. Sixteen hours later, all mice were injected retro-orbitally with 200 μg of DNP-HSA, and at either 30 min (a) or 3 h (b) post-injection, total RNA was extracted from both ear pinnea of each mouse and subjected to qRT-PCR analysis for the relative expression (to that of β-actin) of mRNA encoding HDC. Data are from three independent experiments, each using three mice per treatment. qRT-PCR was performed in triplicates for each RNA sample. * $p < 0.05$, ** $p < 0.01$, *** $p < 0.001$

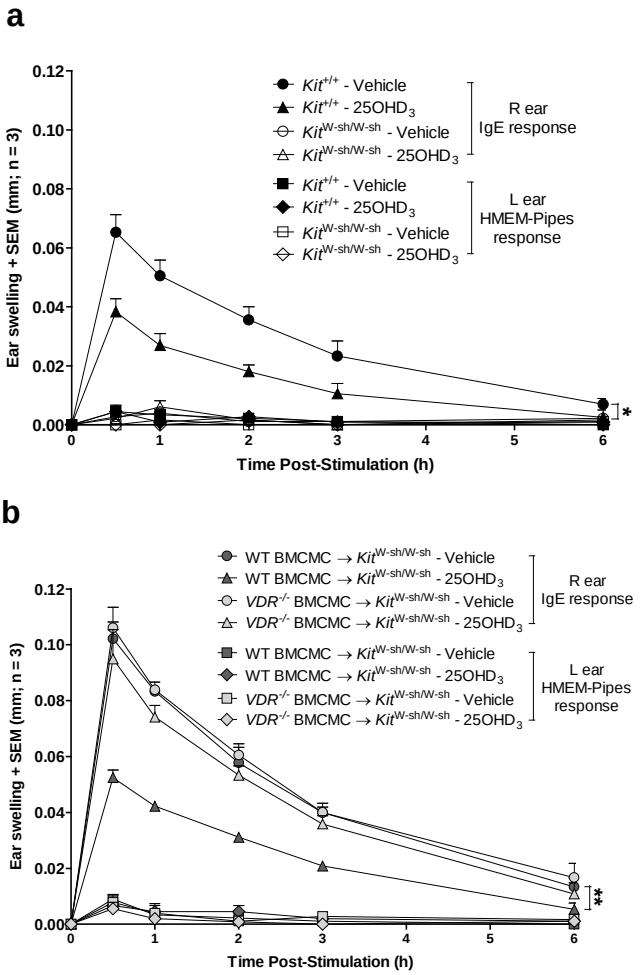

Figure 5.13. MC VDR expression is required for topically applied 25OHD$_3$ to reduce PCA-associated ear swelling

(a) Wild-type (*Kit*$^{+/+}$) mice, MC-deficient (*Kit*$^{W\text{-}sh/W\text{-}sh}$) mice, and (b) MC-deficient mice that had been engrafted *i.d.* with either WT MCs (WT mBMCMCs → *Kit*$^{W\text{-}sh/W\text{-}sh}$) or *VDR*$^{-/-}$ MCs (*VDR*$^{-/-}$ mBMCMCs → *Kit*$^{W\text{-}sh/W\text{-}sh}$) were topically administered, on both ears, with either 3 μM of 25OHD$_3$ or vehicle 8 h prior to *i.d.* injection of 100 ng of SPE-7 in the right ear and equal volume of HMEM-Pipes in the left. Sixteen hours later, all mice were injected retro-orbitally with 200 μg of DNP-HSA, and at indicated time point post-injection the amount of ear swelling was recorded. Data are from three independent experiments performed, each with three to four mice analysed per group. * $p < 0.05$, ** $p < 0.01$

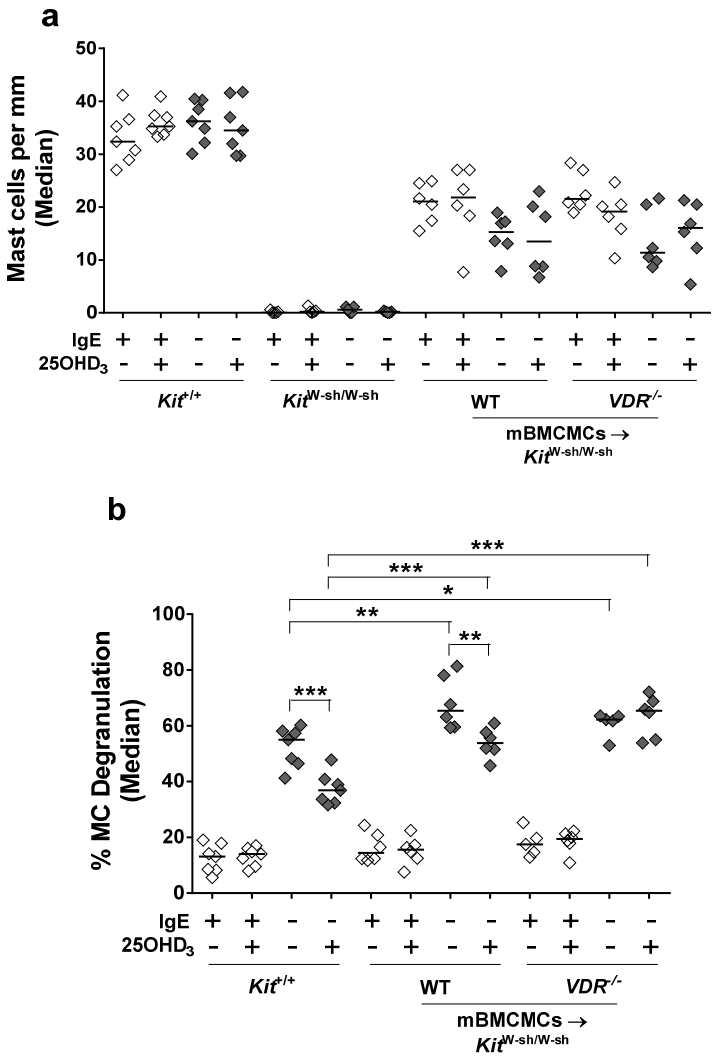

Figure 5.14. MC VDR expression does not convey topically applied 25OHD$_3$ the ability to change dermal MC number but is required for this metabolite to reduce the extent of MC degranulation following PCA induction

Wild-type (*Kit*$^{+/+}$) mice, MC-deficient (*Kit*$^{W\text{-}sh/W\text{-}sh}$) mice, and MC-deficient mice that had been engrafted *i.d.* with either WT MCs (WT mBMCMCs → *Kit*$^{W\text{-}sh/W\text{-}sh}$) or *VDR*$^{-/-}$ MCs (*VDR*$^{-/-}$ mBMCMCs → *Kit*$^{W\text{-}sh/W\text{-}sh}$) were topically painted, on both ears, with either 3 μM of 25OHD$_3$ or vehicle 8 h prior to *i.d.* injection of 100 ng of SPE-7 in the right ear and equal volume of HMEM-Pipes in the left. Sixteen hours later, all mice were injected retro-orbitally with 200 μg of DNP-HSA. (a) The total number of dermal MCs in both ear pinnae was recorded at 6 h post-injection. (b) At the same time point, the percentage of MC degranulation in both ears of each mouse was also calculated. Data are from two independent experiments, each using two to four mice per treatment group. * $p < 0.05$, ** $p < 0.01$, *** $p < 0.001$

WT percentages of degranulated MCs in MC knock-in mice as observed previously (**Figures 5.7 c and d**) were confirmed here, providing consistency with the stronger ear swelling responses in these animals upon PCA induction (**Figure 5.13**). Cytokine secretion analysis at 6 h post-DNP administration showed reduction in the level of proinflammatory cytokines, TNFα and IL-6, in WT and WT MC knock-in mice with $1\alpha,25(OH)_2D_3$ treatment (**Figures 5.15 a and b**). The level of IL-10, however, remained unchanged in all groups of mice (**Figure 5.15c**). Interestingly, the secretion of all three cytokines increased substantially upon $25OHD_3$ treatment in the non-PCA-affected ears of MC deficient mice, the explanation for which required further investigation. Taken together, our *in vivo* data demonstrates that MC VDR expression is required for optimal $25OHD_3$ suppression of PCA responses. However, more experiments are needed to establish with certainty if $25OHD_3$ reduces PCA-induced cytokine production *in vivo*.

5.3. Discussion

By using MC-deficient $Kit^{W/W\text{-}v}$ mice and $Kit^{W\text{-}W\text{-}v}$ mice that had been selectively engrafted with mBMCMCs into ear pinnae, Wershil *et al.* [89] showed that the PCA model employed for the current project is an IgE- as well as MC-dependent immediate hypersensitivity model. Our data confirmed the findings of Wershil *et al.*, where a different MC-deficient mouse strain, $Kit^{W\text{-}sh/W\text{-}sh}$, showed no sign of PCA-mediated ear swelling, whereas local engraftment of WT or $VDR^{-/-}$ mBMCMCs to these mice restored their ability to respond to PCA induction (**Figures 5.6 a and b; 5.13**). In fact, it was noticeable that both types of MC knock-in mice showed considerably stronger PCA response, indicated by the higher levels of ear swelling, than the WT controls. There are

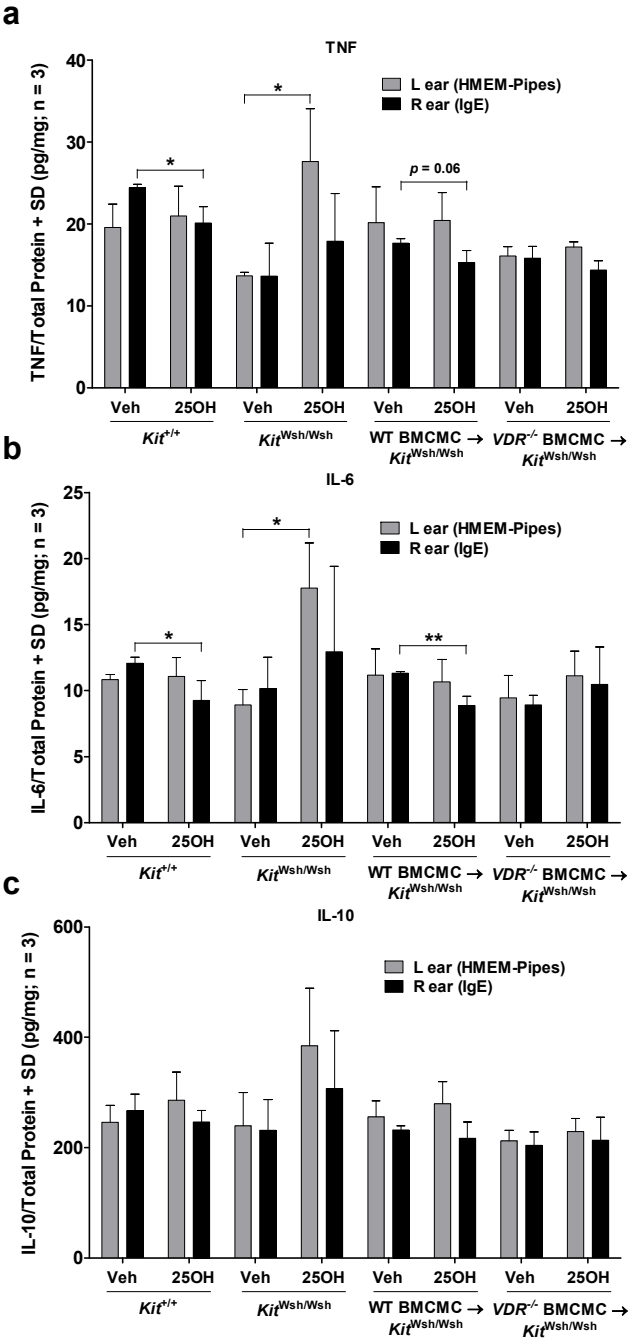

Figure 5.15. MC VDR-dependence for the effect of topical 25OHD$_3$ on cytokine secretion in PCA-affected ears

Wild-type (*Kit*$^{+/+}$) mice, MC-deficient (*Kit*$^{W\text{-}sh/W\text{-}sh}$) mice, and MC-deficient mice that had been engrafted *i.d.* with either WT MCs (WT mBMCMCs → *Kit*$^{W\text{-}sh/W\text{-}sh}$) or *VDR*$^{-/-}$ MCs (*VDR*$^{-/-}$ mBMCMCs → *Kit*$^{W\text{-}sh/W\text{-}sh}$) were topically painted, on both ears, with either 3 μM of 25OHD$_3$ or vehicle 8 h prior to *i.d.* injection of 100 ng of SPE-7 in the right ear and equal volume of HMEM-Pipes in the left. Sixteen hours later, all mice were injected retro-orbitally with 200 μg of DNP-HSA, and at 6 h post-injection the levels of TNF (a), IL-6 (b), and IL-10 (c) in lysates of both ears were measured. Data were obtained from one experiment (one of three experiments that showed similar ear swelling responses) using three mice per treatment. * $p < 0.05$, ** $p < 0.01$

several possible explanations for such observation. Firstly, as mentioned before, the higher extent of MC degranulation (**Figures 5.7 c and d; 5.14b**) and, consequently, the release of more pre-stored MC-derived mediators such as histamine in MC knock-in mice could contribute to more severe vasodilation and higher vascular permeability with oedema. Secondly, although total number of dermal MCs in MC knock-in mice appeared lower than WT controls, this could simply be due to the increased MC degranulation in these animals which would render some (i.e. completely degranulated) MCs unable to be detected by toluidine blue staining. [327] In other words, MC knock-in mice could in fact have more dermal MCs which, in combination with higher degranulation percentage, represent an even larger supply of histamine and other mediators that could exacerbate ear swelling. Furthermore, the more profound PCA response exhibited by MC knock-in mice could also be due to certain unknown non-MC-related intrinsic defects that these animals carry.

Despite the discovered ability of topical $1\alpha,25(OH)_2D_3$ to improve inflammatory conditions such as psoriasis, vitiligo and CHS [302, 316-319], its *in vivo* effects on IgE-mediated allergic responses, especially those that are mediated via MCs, have not been directly examined to date. Using the IgE + sAg-mediated PCA model, our data demonstrates for the first time that topical $1\alpha,25(OH)_2D_3$ can suppress PCA-associated ear swelling, and such effect is observed in WT mice of both C57BL/6 and WBB6F1 backgrounds (**Figures 5.2 a and c**). Utilising MC-deficient and MC knock-in mice, the MC-dependence for such PCA-dampening effect of $1\alpha,25(OH)_2D_3$ was also established (**Figure 5.6**). Subsequent mechanistic investigation revealed several possible explanations for the observed $1\alpha,25(OH)_2D_3$-mediated PCA suppression. Firstly, topical

$1\alpha,25(OH)_2D_3$ treatment resulted in a lower percentage of MC degranulation in PCA-affected ears (**Figure 5.3**), reducing in turn the release of histamine and other pre-stored pro-inflammatory cytokines and ultimately easing the ear swelling response. This notion was supported by the finding that the expression of *HDC* is significantly decreased in PCA-affected ears topically treated with $1\alpha,25(OH)_2D_3$ (**Figures 5.4**). HDC is the enzyme that generates histamine from histidine [(326)], therefore, a reduction in its gene expression could indicate lower-level MC degranulation and a lesser need for additional histamine to be produced during MC regranulation (i.e. re-generation of MC granules) [(328)]. In addition to HDC, topical $1\alpha,25(OH)_2D_3$ also reduced the protein content of pro-inflammatory cytokine, TNFα and IL-6, in mouse ears following PCA induction (**5.9 b and d**), thus helping further improve subsequent ear swelling response by, for instance, limiting the recruitment of other inflammatory cells. [(64)] Indeed, TNFα is a potent chemotactic factor for neutrophils, which counted for over 90% of infiltrating leukocytes, as shown in a similar PCA model previously. [(89)] Unexpectedly, the protein secretion of the anti-inflammatory cytokine, IL-10, in PCA-affected ears also seemed to decrease in response to $1\alpha,25(OH)_2D_3$ treatment (**Figures 5.9 f**), which indicated a decrease in MC-derived mediators, perhaps due to suppressed MC activation in general. Because of the majority of these mediators being pro-inflammatory in nature, a decrease in their levels could result in a net reduction of the overall inflammatory response. Furthermore, it should be pointed out that MCs are not the only sources of the cytokines examined in this chapter. For example, TNFα and IL-6 can be produced and secreted by newly recruited and/or resident neutrophils and DCs, respectively; whereas T_{reg} cells are well-established sources of IL-10. Kerotinocytes can also produce all three types of cytokines. [(329-331)]

Therefore, further investigation is required to examine the effects of topical 1α,25$(OH)_2D_3$ on leukocyte recruitment and the associated change in cytokine profile in PCA-affected ear pinnae, as well as its effects on structural cell types such as keratinocytes and fibroblasts.

In our *in vitro* study (**Chapter 3**), the immunosuppressive effects of 1α,25$(OH)_2D_3$ on IgE + sAg-activated MCs are dependent on the expression of functional VDR, and that VDR may play a role in non-genomic as well as genomic $VitD_3$ pathways. The initial use of *VDR*$^{-/-}$ mice in parallel to WT controls, which was to determine the VDR-dependence for the effects of topical 1α,25$(OH)_2D_3$ on PCR-associated ear swelling *in vivo*, yielded promising results as *VDR*$^{-/-}$ but not WT animals failed to show suppressed ear swelling upon 1α,25$(OH)_2D_3$ application as compared to vehicle (**Figure 5.5a**). The extent of MC degranulation and the gene expression for MC-derived HDC in these mice following PCA induction were also unchanged by topical 1α,25$(OH)_2D_3$ treatment (**Figures 5.5 c and d**). However, the substantially lower-than-WT ear swelling response, percentage MC degranulation, and the gene expression of HDC, in *VDR*$^{-/-}$ mice when topically applied with vehicle alone indicated either a lower baseline PCA response in these animals or a higher susceptibility of these animals to the vehicle contents. Future studies are, therefore, required to explain these observations. Because *VDR*$^{-/-}$ mice have a global deficiency of VDR, to establish the specific contribution of MC VDR, we performed the critical experiments of adoptively transferring MCs that either have (WT) or are deficient in (*VDR*$^{-/-}$) VDR function into MC deficient animals. Importantly, by comparing the PCA reactions of WT and *VDR*$^{-/-}$ mBMCMC knock-in mice with and without topical 1α,25$(OH)_2D_3$ treatment, we also established that VDR expression in dermal MCs is

essential for the 1α,25(OH)$_2$D$_3$-mediated PCA suppression *in vivo* (**Figure 5.6**). Furthermore, MC VDR expression is also required for topical 1α,25(OH)$_2$D$_3$ to reduce the extent of MC degranulation and the production of TNF, IL-6 and IL-10 upon PCA induction *in vivo* (**Figures 5.7 e and f; 5.9 b, d, f**). Since the observed reduction in cytokine production is relatively subtle, other MC-derived mediators such as histamine and leukotrienes will need to be assessed in subsequent studies. Nevertheless, observations made in the current study strengthened the possibility that topical 1α,25(OH)$_2$D$_3$ suppressed PCA-associated ear swelling at least partially via down-regulating the degranulation and overall cytokine secretion of dermal MCs. Intriguingly, the ability of topical 1α,25(OH)$_2$D$_3$ to VDR-dependently reduce the production of IL-10 as well as TNFα and IL-6 is similar to the effects of curcumin on activated mBMCMCs *in vitro* (**Figure 3.11**). This suggests that the non-genomic effects of 1α,25(OH)$_2$D$_3$ played a role in PCA suppression, and that VDRs are also important for these effect *in vivo*. However, further investigation utilising pathway-specific 1α,25(OH)$_2$D$_3$ agonists and/or antagonists, is required before definite conclusions can be drawn.

One of the most novel findings of the current project is the susceptibility of activated MCs to be negatively regulated by not only 1α,25(OH)$_2$D$_3$ but also its inactive precursor, 25OHD$_3$, most likely via the production of endogenous 1α,25(OH)$_2$D$_3$ (**Chapter 4**). The *in vivo* relevance of such finding was confirmed in the current chapter, where topical application of 25OHD$_3$ demonstrated very similar PCA-suppressive effects, via similar potential mechanisms, to 1α,25(OH)$_2$D$_3$ in a MC VDR-dependent manner (**Figures 5.10 – 5.15**). Again, these effects were unlikely to be direct but rather indirect via the production of endogenous 1α,25(OH)$_2$D$_3$ by dermal MCs, which was indicated by the

requirement of topical $25OHD_3$ treatment for an extended period of time prior to IgE preload (**Figure 5.10**). To confirm this theory, *CYP27B1*$^{-/-}$ mice [332] and *CYP27B1*$^{-/-}$ mBMCMC-engrafted *Kit*$^{W\text{-}sh/W\text{-}sh}$ mice can be used to compare with WT and WT MC knock-in responses in the current topical $1\alpha,25(OH)_2D_3$/vehicle-incorporated PCA model. Furthermore, unlike the *in vitro* scenario, cell types other than MCs are also likely to respond to topical $25OHD_3$ *in vivo*. Keratinocytes, in particular, can synthesise $1\alpha,25(OH)_2D_3$ from $25OHD_3$ and therefore represent an alternative and yet perhaps more abundant source of $1\alpha,25(OH)_2D_3$ to regulate dermal MCs and PCA-associated ear swelling subsequently. [203] In this regard, the significance of MC-derived $1\alpha,25(OH)_2D_3$ can be determined by comparing the responses of WT and *CYP27B1*$^{-/-}$ MC knock-in mice towards topical $25OHD_3$ treatment followed by PCA induction. Nevertheless, the ability of MCs to respond to $25OHD_3$ and to potentially generate $1\alpha,25(OH)_2D_3$ autonomously *in vivo* as well as *in vitro*, highlights the potential for serum $25OHD_3$ (which is the major form of circulating $VitD_3$) to dampen MC over-activity throughout the body during allergic and/or other immune settings.

In conclusion, in this chapter we demonstrated that topical $1\alpha,25(OH)_2D_3$ and $25OHD_3$ could suppress PCA-mediated cutaneous pathology in a MC VDR-dependent manner, although in the latter case the effects may not be direct but rather via the production of the active analogue by MCs. Potential mechanisms responsible include a reduction in PCA-induced MC-degranulation and the secretion of MC-derived TNF, IL-6 and IL-10 upon topical application of $VitD_3$ analogues. Although the involvement of other newly recruited as well as resident cell types requires further investigation, our findings so far nonetheless provide another possible explanation for the beneficial effects of UVB

irradiation in a number of allergic and non-allergic diseases of the skin, which is via the modulation of dermal MC activation to elevate serum $25OHD_3$ levels and cutaneous $1\alpha,25(OH)_2D_3$ production.

CHAPTER 6

FROM THE MOUSE TO THE HUMAN – TRANSLATIONAL ASPECTS

6.1. Introduction

As mentioned previously, Vitamin D deficiency has been associated with epidemiologic patterns observed in the asthma epidemic, which is more common with obesity, African American ethnicity, and westernization of countries with higher-risk populations for asthma. In Italian children, low serum levels of $25OHD_3$ are associated with reduced asthma control, as assessed according to the Global Initiative for Asthma guidelines and the Childhood Asthma Control Test. [333] Other reports show a beneficial association between higher maternal VitD intake during pregnancy and protection from childhood asthma and allergic diseases in the offspring. [334-336] As Hansdottir *et al.* [337] demonstrated, primary lung epithelial cells express high baseline levels of CYP27B1 and low levels of CYP24A1, thus allowing these cells to constitutively convert serum $25OHD_3$ to the active $1\alpha,25(OH)_2D_3$. $1\alpha,25(OH)_2D_3$ can, in turn, inhibit the proliferation of normal and asthmatic airway smooth muscle cells by inhibiting their progression to S phase of the cell cycle [338]. By reducing the production of RANTES [339], MMP-9 and a disintegrin and metalloprotease 33 [340] from airway smooth muscle cells, $1\alpha,25(OH)_2D_3$ can also restrain the recruitment of other leukocytes to the asthmatic lungs and ease the symptoms during asthmatic airway remodelling, respectively. Furthermore, $1\alpha,25(OH)_2D_3$ can increase the synthesis of IL-10 by T_{reg} and DCs [222, 226], while concurrently suppressing DC activation by down-regulating expression of costimulatory molecules CD40 and CD80/86 [222]. However, it remains to be investigated if $VitD_3$ can negatively regulate human MC activity during allergic settings.

It has been known for decades that human MCs are key effector cells of allergic inflammation. [64] In particular, they contribute to the early-phase of type I

hypersensitivity reactions by releasing histamine, LTC_4 and other mediators following cross-linking of surface-bound IgE by allergen in sensitized individuals. [341-343] Human MCs are also found, during late-phase allergic responses, to induce the recruitment of neutrophils by secreting IL-8 and TNF [344, 345], induce the recruitment as well as local activation of eosinophils by secreting IL-5 [346], and regulate T cell functions by secreting PGD_2 [347]. Furthermore, research in the past 10 years or so has re-established MCs as cells that not only regulate allergy, but also many other physiological/biological functions, such as blood flow and coagulation, smooth muscle contraction and peristalsis of the intestine, mucosal secretion, wound healing, modulation of innate and adaptive immunity, and peripheral tolerance. [8, 348, 349] Due to the difficulty in obtaining adequate numbers as well as quality of human MC for *in vitro* studies, a large proportion of the available data on MC biology and function is generated using murine primary and/or cultured MCs; an approach that is coupled with the further advantage of the availability of multiple animal models (e.g. transgene, knockout and adoptive transfer models) that allow the study of MC function in complex *in vivo* settings, as well as the ability to access over-expression and/or deletion of MC-derived mediators in MCs generated from gene targeted mice *in vitro*. In this regard, there are many similarities between the roles of MCs in human asthma and murine asthma models, including the ability of murine MCs to trigger early-phase responses by releasing histamine and leukotrienes, and to contribute to late-phase responses by recruiting other leukocytes such as neutrophils, eosinophils and T cells. [350, 351] Therefore, it will be of great clinical importance to investigate if our previous findings in the mouse can be translated into human studies.

In this chapter, therefore, human cord blood-derived MCs were generated and used to firstly determine the effect of 1α,25$(OH)_2D_3$ during IgE + α-IgE-mediated activation and, subsequently, examine CYP27B1 expression and their ability to produce 1α,25$(OH)_2D_3$ endogenously upon 25OHD_3 treatment.

6.2. Results

6.2.1. 1α,25$(OH)_2D_3$ reduces IgE + α-IgE-mediated TNFα but not IL-10 production by hCBMCs

10- to 13-week-old hCBMCs, the identity and purity of which was confirmed by their morphological characteristics (**Figure 6.1a**) and intracellular tryptase expression (**Figures 6.1 b – d**), were used in this series of experiments. After 2-day culturing with rhIL-4 (10 ng/mL) to up-regulate their surface FcεRI expression [352], hCBMCs were preloaded with IgE and stimulated, in this case, with α-IgE in the presence of alternative concentrations of 1α,25$(OH)_2D_3$ or ETOH (0.03% final). The secretion of hTNFα and hIL-10 was measured 6 h post-stimulation by ELISA. Similar to mBMCMCs, hCBMCs produced significantly less TNFα when stimulated in the presence of both concentrations (i.e. 10^{-7} and 10^{-8} M) of 1α,25$(OH)_2D_3$ and the reduction was more profound than that observed with WT mBMCMCs (**Figure 6.2a**, compared to **Figure 3.7e**). On the other hand, 1α,25$(OH)_2D_3$ treatment did not alter levels of IL-10 produced in response to IgE + α-IgE-mediated hCBMC activation (**Figure 6.2b**). It is significant, however, that the lower concentration (10^{-8} M) of 1α,25$(OH)_2D_3$ alone increased the secretion of hIL-10, at least when compared to the higher concentration. This is consistent with our previous

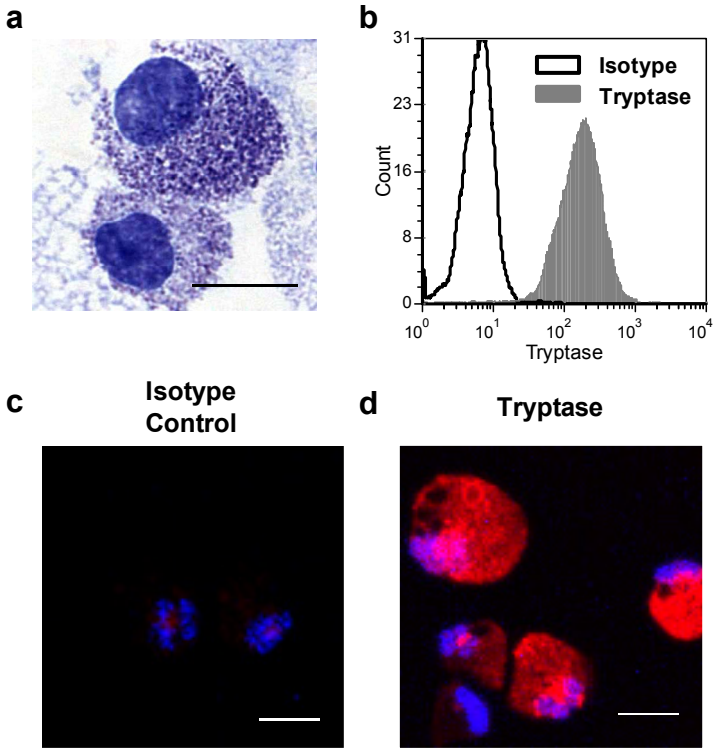

Figure 6.1. Morphological properties of hCBMCs

The identity and purity of 10- to 13-week-old hCBMCs was examined and confirmed by toluidine blue staining (a), and intracellular tryptase staining followed by either flow cytometry (b) or immunofluorescence staining (c and d; DAPI nucleus stain was used to locate cell populations). Scale bars (a, c and d) represent 10 μm. Data are representative of cells from two independent donors.

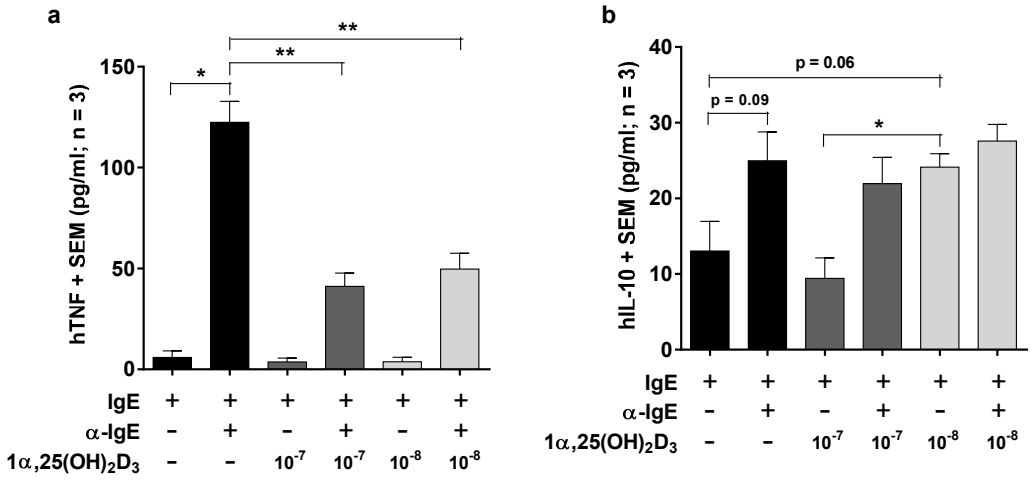

Figure 6.2. 1α,25(OH)$_2$D$_3$ suppresses IgE + α-IgE-mediated hCBMC production of TNF but not IL-10

Ten- to 13-week-old hCBMCs were cultured in the presence of rhIL-4 (10 ng/mL) for two days, prior to 16 h preload with human IgE (2.5 µg/mL) followed by 6 h α-human IgE (1 µg/mL) stimulation. 1α,25(OH)$_2$D$_3$ (10^{-7} or 10^{-8} M) or ETOH (0.3 % final) were included in the culture throughout the experiment. The secretion of hTNF (a) and hIL-10 (b) was measured using ELISA. Data are representative of three independent experiments. * $p < 0.05$, ** $p < 0.01$

findings that 1α,25$(OH)_2D_3$ can dose-dependently increase IL-10 production from WT mBMCMCs *in vitro*. [163]

6.3.2. Human CBMCs constitutively express CYP27B1, which can be up-regulated by 25OHD$_3$ treatment

Due to the novelty of the previous findings regarding CYP27B1 expression in mBMCMCs, it was necessary to investigate whether similar results could be obtained in MCs derived from other species. **Figure 6.3a** shows hCBMCs constitutively express CYP27B1 throughout their cytosol. Similar to WT mBMCMCs, hCBMCs also exhibit up-regulated CYP27B1 protein expression at 8-h after 25OHD_3 addition (**Figures 6.3 b and c**). Therefore, MC expression of the CYP27B1 hydroxylase and its positive regulation by 25OHD_3 is unlikely to be species-restricted.

6.3.3. Human CBMCs produce endogenous 1α,25$(OH)_2D_3$ following 25OHD$_3$ treatment in a dose-dependent manner

Since it was established that hCBMCs express CYP27B1, we decided to examine if this enzyme enables hCBMCs to generate 1α,25$(OH)_2D_3$ endogenously from its precursor. Similar to the experiments using mBMCMCs (**Chapter 4**), hCBMCs were firstly cultured in medium containing csFCS for 72 h, and then treated with 25OHD_3 (10^{-6} or 10^{-7} M) or ETOH for 6 h. The level of 1α,25$(OH)_2D_3$ in culture supernatant as well as cell lysate was subsequently measured using the 1,25-$(OH)_2$D RIA kit. As demonstrated in **Figure 6.4**, treatment with both doses of 25OHD_3 led to endogenous 1α,25$(OH)_2D_3$ production in hCBMCs from two independent donors, and the level of 1α,25$(OH)_2D_3$ production was considerably higher than that in mBMCMCs (**Figure 4.3**). The higher

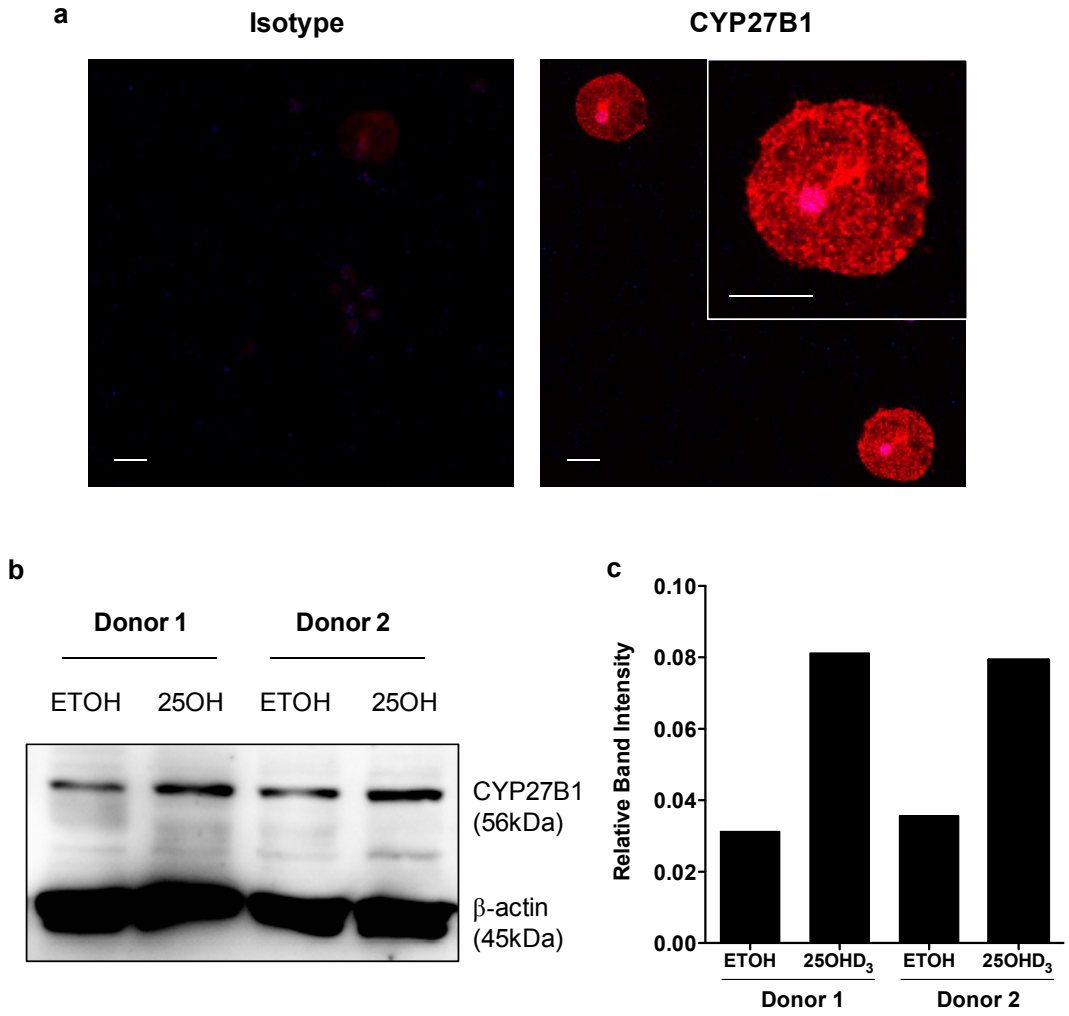

Figure 6.3. CYP27B1 expression in naive and 25OHD$_3$-treated hCBMCs
Cytospins of naive 12-week-old hCBMCs were prepared, which were labelled intracellularly with α-CYP27B1 Ab followed by Alexa594-conjugated secondary Ab, and examined using confocal microscopy (a). Isotype Ab labelling was included as the negative control, and the DAPI nucleus stain was used to locate cell populations. Scale bars represent 10 μm. To examine the effect of 25OHD$_3$ on CYP27B1 expression in hCBMCs, cells were cultured, at 5×10^5 cells/mL, in hCBMC-csFCS medium for 72 h, replated at 10^6 cells/mL, and treated with either 10^{-7} M of 25OHD$_3$ or vehicle (ETOH, 0.03%) for 8 h. Cell lysates were subsequently prepared and the CYP27B1 protein expression was examined by western blotting (b and c). Data are representative of cells from two independent donors.

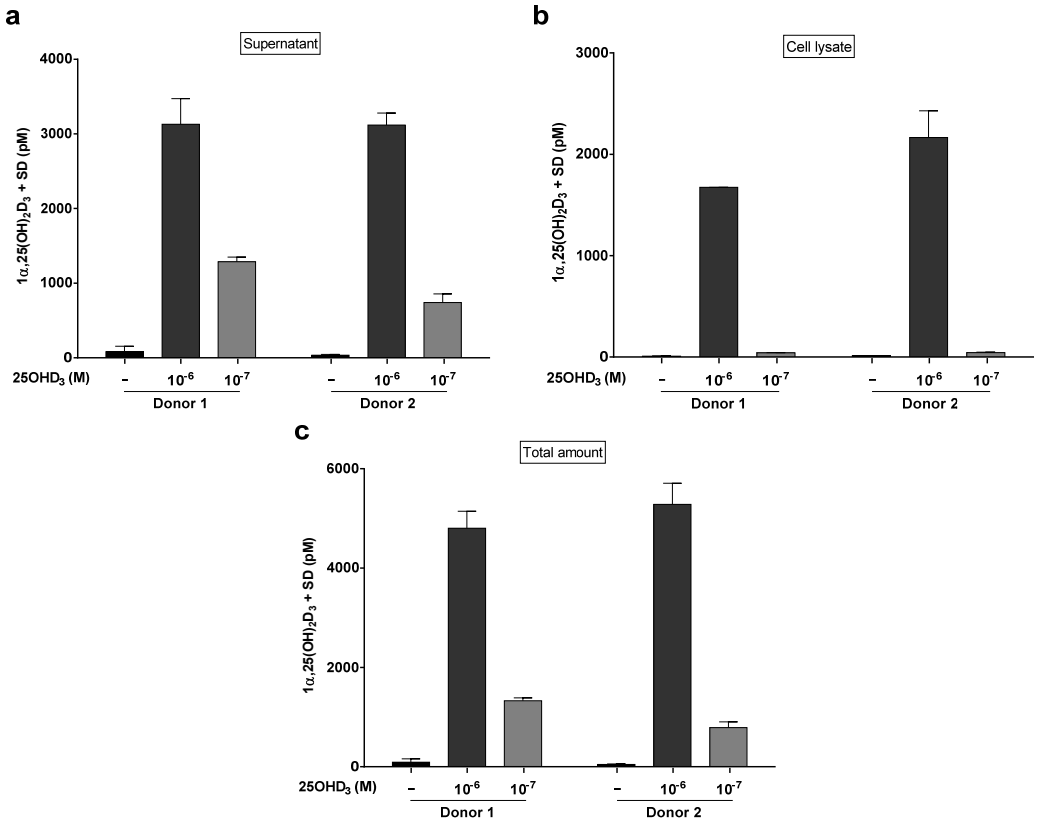

Figure 6.4. Dose-dependent 1α,25(OH)$_2$D$_3$ production by 25OHD$_3$-treated hCBMCs

Nine- to 12-week-old hCBMCs were cultured, at 5 × 10^5 cells/mL, in hCBMC-csFCS medium for 72 h, subsequently replated at 2 × 10^6 cells/mL in the same medium, and treated with indicated concentrations of 25OHD$_3$ or ETOH. Culture supernatant (a) as well as cell lysate (b) samples were collected at 6 h post-treatment, and the 1α,25(OH)$_2$D$_3$ level in all samples was measured using the 1,25-(OH)$_2$D RIA kit. The total 1α,25(OH)$_2$D$_3$ level (c) was calculated by adding together its concentration in the supernatant and that in the corresponding cell lysate. Data show results from cells from two independent donors examined in one experiment.

dose (i.e. 10^{-6} M) of $25OHD_3$, in particular, triggered conversion to $1\alpha,25(OH)_2D_3$ to levels 50 times higher in hCBMCs than in mBMCMCs. Like their mouse counterparts (**Figure 4.3**), however, hCBMCs also seemed to secrete approximately 75% of endogenously generated $1\alpha,25(OH)_2D_3$ (**Figure 6.4a**) and accumulate the rest inside the cells (**Figure 6.4b**).

6.3. Discussion

Despite the similarities between human and murine MCs mentioned at the beginning of this chapter, a number of developmental and functional differences have become obvious during the past few years. For example, whilst mouse MCs can derive from common basophil/MC progenitors and share some functional properties with murine basophils [4, 9]; human MCs appear to develop along a different lineage from human basophils, and they morphologically as well as functionally resemble monocytes and macrophages more closely than basophils [353-355]. In addition, although many findings on FcεRI signal transduction in MCs, such as activation of the RAS-MAPK pathway, have been confirmed in both mouse and human systems, some mechanisms that operate in murine MCs do not apply to their human counterparts. [166] One example is PI3K being required for FcεRI-mediated TNF synthesis by murine but not human intestinal MCs. [356] MCs from different species also display distinct mediator profiles. In contrast to human MCs possessing several tryptases (α-, β-, γ-, and δ-tryptases) but only a single chymase, their murine counterparts synthesise a greater array of chymases (MMCP-1, -2, -4, -5 and -9). [357, 358] Furthermore, many cytokines, such as IL-4, IL-5 and TNF, are produced at different levels in human MC_T's and murine BMCMCs. Therefore, results from studies

using murine MCs are not always transferable to the human situation, and the relevance of findings from murine disease models is not always evident. [359, 360] A good example set by an eosinophil-based study is that whereas anti-IL5 Ab completely blocked the airway hypersensitivity in experimental mouse models of asthma [361], the therapeutic application of humanized anti-IL5 Ab failed to improve the bronchial hypersensitivity of asthmatics [362].

Like mBMCMCs, hCBMCs also represent primary MC cultures that are derived from MCPs and, therefore, are a suitable cell type choice for the aims of the current chapter. As shown in **Figure 6.2a**, 1α,25$(OH)_2D_3$ treatment during IgE + α-IgE-mediated hCBMC activation substantially reduced hTNFα secretion from the cells, in a manner similar to that observed with IgE-activated WT mBMCMCs (**Figure 3.7e**). The percentage of reduction in TNFα secretion, however, was more profound in hCBMCs (≥ 60% for both 10^{-7} and 10^{-8} M of 1α,25$(OH)_2D_3$) than in mBMCMCs (25% for 10^{-7} M and 40% for 10^{-8} M of 1α,25$(OH)_2D_3$), the reason for which requires further investigation but might merely reflect the difference between MCs from different species as discussed above. The production of hIL-10 by activated hCBMCs, on the other hand, was unchanged following 1α,25$(OH)_2D_3$ treatment (**Figure 6.2b**). Although limited literature is available on the production of IL-10 from IgE + sAg-activated human MCs, one paper did report that human lung-derived MCs are capable of producing IL-10 in response to IgE-dependent stimulation, and that such production was highest in the presence of SCF and following at least 10 hrs of stimulation. [363] Therefore, it is possible that the activated hCBMCs in our experiments, in the absence of any growth factor such as SCF, reached their maximum IL-10 producing capacity, which could not be further enhanced by 1α,25$(OH)_2D_3$. It is

also possible that the cells were not stimulated long enough (6 h only) with $1\alpha,25(OH)_2D_3$ for this metabolite to elicit its effects. Future experiments are, therefore, required to examine these possibilities. At any rate, even if $1\alpha,25(OH)_2D_3$ is unable to increase IL-10 production from human MCs during IgE-mediated activation, its capacity to down-regulate pro-inflammatory cytokines such as TNFα would shift the micro-environmental balance from pro-inflammatory to anti-inflammatory during allergic responses with relatively more IL-10 being present. Furthermore, despite the difference in $1\alpha,25(OH)_2D_3$-mediated IL-10 regulation between activated mBMCMCs and hCBMCs, non-activated hCBMCs treated with the lower concentration of $1\alpha,25(OH)_2D_3$ did show increased IL-10 secretion (**Figure 6.2b**), which is consistent with our findings in mBMCMCs both previously [163] and from the current study (**Figure 3.8a**).

Since there are no reports in the literature regarding human MC expression of CYP27B1 or their $1\alpha,25(OH)_2D_3$-producing capacity, it was exciting to discover these findings in hCBMCs during the current body of work (**Figures 6.3 and 6.4**). More importantly, hCBMCs (**Figure 6.4**) appear to produce over 50 times more endogenous $1\alpha,25(OH)_2D_3$ than mBMCMCs (**Figure 4.3**). Studies using human primary renal cultures show $1\alpha,25(OH)_2D_3$ is produced at approximately 2×10^{-10} mol/mg protein/h [364], whereas mouse kidney cell cultures produce $1\alpha,25(OH)_2D_3$ at approximately 5×10^{-10} mol/mg protein/h [365]. The difference between these mouse and human results is relatively small, and as such could merely be a consequence of the different $25OHD_3$ concentrations used (10^{-8} M versus 5×10^{-6} M) and/or the different $1\alpha,25(OH)_2D_3$ measurements (western versus competitive receptor assay) employed. By contrast, we observed significant differences between the amount of $1\alpha,25(OH)_2D_3$ produced by mBMCMC and hCBMC

in the current study. Further research, therefore, is required to confirm and/or explain our observations. Especially considering the recent discovery that *in vitro* human MCP-derived MC cultures have the limitation of not being able to achieve complete MC-maturation [366, 367], more physiologically relevant cellular representative of human MCs (such as primary human MC cultures) need to be examined in subsequent experiments.

In conclusion, we confirmed in this chapter that the overall immunosuppressive effect of $1\alpha,25(OH)_2D_3$ is applicable to IgE + α-IgE-activated hCBMCs, even though it does not alter the amount of hIL-10 produced using the current settings. We also demonstrated, again for the first time, the constitutive expression of CYP27B1 in hCBMCs and the up-regulation of this enzyme following $25OHD_3$ treatment. Subsequent functional investigations confirmed the ability of CYP27B1 in hCBMCs to stimulate substantial $1\alpha,25(OH)_2D_3$ production in a dose-dependent manner. Although further investigation is required to explain certain observations as mentioned above, this chapter nevertheless emphasizes the physiological relevance of our previous findings (especially **chapters 3 and 4**) and thus offers evidence for the application of $VitD_3$ analogues in treating certain potentially IgE-mediated allergic disorders, such as anaphylaxis.

CHAPTER 7

CONCLUDING REMARKS & FUTURE DIRECTIONS

Despite the concurrence of increased $VitD_3$ deficiency and increased incidence of IgE-mediated allergic disorders among the Australian population [368], the potential effects of $1\alpha,25(OH)_2D_3$ on activated MCs in allergic settings to our knowledge has not been investigated extensively to date. Findings of the current project suggest that the increased $VitD_3$ insufficiency among the Australian population, a possible result of the recent "Slip Slop Slap" sun protection campaign by the Australian Cancer Council, can lead to more intrinsically pro-inflammatory MC populations (not only those in the skin but also throughout the body due to the lower circulating $25OHD_3$ levels) and ultimately a higher predisposition to develop IgE-mediated allergies. In particular, we observed that $1\alpha,25(OH)_2D_3$ can down-regulate the pro-inflammatory properties of IgE + sAg-activated MCs both *in vitro* and *in vivo*. Moreover, it was revealed, for the first time, the capacity of MCs to convert $25OHD_3$ to its active metabolite, thus conferring this inactive $VitD_3$ analogue similar immunosuppressive effects on activated MCs. Although these effects of $25OHD_3$ seemed most likely indirect, via endogenous $1\alpha,25(OH)_2D_3$ production by MCs, it is also possible that $25OHD_3$ can elicit direct effects on activated MCs, as demonstrated by the *in vitro* data using the highest concentration of this metabolite (**Figures 4.4 a and c**). To determine the exact nature of the action of $25OHD_3$ in MCs, mBMCMCs from *CYP27B1*$^{-/-}$ mice could be generated and analysed in parallel with WT controls in *in vitro* experiments with $25OHD_3$ treatment. As mentioned in **Chapter 5**, *CYP27B1*$^{-/-}$ mice and *CYP27B1*$^{-/-}$ MC knock-in mice will be equally valuable tools to achieve the same aim in *in vivo* PCA settings.

In addition to CYP27B1, DCs and macrophages also express CYP27A1, the hydroxylase that converts $VitD_3$ to $25OHD_3$, and therefore possess the complete autonomous $VitD_3$

pathway. [196, 369] Since MCs also express CYP27B1, even in their naive state, it will be of great interest to examine the expression of CYP24A1 (as well as CYP2DII, CYP2D25, CYP3A4 and CYP2R1) by these cells; for if the expression is confirmed, then cutaneous MCs can theoretically utilise $VitD_3$ generated in the skin upon UVB irradiation directly to produce endogenous $1\alpha,25(OH)_2D_3$. In similar regards, it will also be illuminating to repeat some of our *in vivo* experiments using an alternative source of $1\alpha,25(OH)_2D_3$. Instead of topical $1\alpha,25(OH)_2D_3$ application, mice could be exposed to repeated low-dose (e.g. 5 exposures to 2 kJ/m^2) UVB irradiation, which we have recently reported can dramatically increase endogenous production of $1\alpha,25(OH)_2D_3$ in the skin [370], and followed by PCA induction. If the resultant ear swelling is reduced upon UVB exposure, then although MCs make little if any contribution to the cutaneous $1\alpha,25(OH)_2D_3$ production as indicated by the similar increase in $1\alpha,25(OH)_2D_3$ levels between WT and MC deficient mice [370], the physiological relevance of our findings will nevertheless be reinforced.

As part of the future investigation to identify potential mechanisms responsible for the immunosuppressive effects of $1\alpha,25(OH)_2D_3$ on activated MCs, FcεRI-initiated signalling pathways (e.g. MAPK pathway) and whether and how they are affected by $1\alpha,25(OH)_2D_3$ could be examined. The ultimate goals in this regard are to map out as many pathways as possible that are regulated by $1\alpha,25(OH)_2D_3$ treatment, and to examine the potential integration of the FcεRI-mediated and VDR/mVDR-mediated signalling networks in MCs. This can be achieved by running cDNA samples from differently treated MC groups through the newly developed RT^2 Profiler™ PCR arrays to identify potential signalling molecule targets, and then validating the result by western blotting.

In addition, 1α,25$(OH)_2D_3$ seemed capable of reducing MC degranulation upon IgE + sAg-mediated activation both *in vitro* (**Figure 3.6**) and *in vivo* (**Figure 5.3**), which is an immediate response triggered by an increase in Ca^{2+} concentration in the cytoplasm. [371, 372] According to the literature, there are two main sources of intracellular Ca^{2+}, one being its storage in the endoplasmic reticulum and the other its additional supply among the extracellular space [371, 372]; and whereas Ca^{2+} is essential for the fusion of MC granules and the plasma membrane and subsequent exocytosis, the initial translocation of MC granules to the plasma membrane is in fact a Ca^{2+}-independent and microtubule-dependent process [373]. Interestingly, using VitD-deficient chicks which had been fed with either 1α,25$(OH)_2D_3$ or vehicle, it was shown that dietary supplement of 1α,25$(OH)_2D_3$ could indeed increase the synthesis of microtubule proteins by chick intestinal epithelial cells, resulting in an accelerated Ca^{2+} absorption from the intestines of the birds. [374] Therefore, it will be important to examine the effects of 1α,25$(OH)_2D_3$ on microtubule formation in MCs upon IgE + sAg-mediated activation, and the speed as well as magnitude of Ca^{2+} entry into the cytoplasm from either of the sources mentioned above.

In addition to the above mechanisms, which are most likely responsible for the non-genomic effects of 1α,25$(OH)_2D_3$, mechanisms that regulate the genomic effects of this hormone also and need to be clarified. To achieve this aim, a DNA microarray can be carried out initially, using total RNA extracted from mBMCMCs that have undergone different treatments, to pinpoint particular genes whose expression is altered with 1α,25$(OH)_2D_3$ treatment followed by activation. The importance of the top candidates can then be individually validated by qRT-PCR and/or western blotting.

Another potential mechanism of 1α,25$(OH)_2D_3$-induced MC regulation involves post-transcriptional control of relevant genes by miRs. It was discovered recently that miR-221-222, with their elevated expression, regulate cell cycle checkpoints and thus proliferation of mBMCMCs in response to acute activation stimuli. [375] Subsequent data using lentivirally transduced MCs showed that this family of miRs also have pleiotropic effects on other essential aspects of MC biology, including survival, homing and migration. [376] For the future direction of the current project, it will be interesting to determine whether IgE + sAg-mediated MC activation is subjected to the post-transcriptional regulation of miRs and, if so, which ones are affected by 1α,25$(OH)_2D_3$ treatment. This can be achieved by firstly performing a miR microarray using total RNA from differently treated MCs, and then confirming the involvement of top candidates by miR qRT-PCR and western analysis on proteins encoded by their known gene targets.

There are indeed a number of mechanisms that could explain the immunosuppressive effects of 1α,25$(OH)_2D_3$ on activated MCs *in vitro*, but these effects alone are unlikely to be solely responsible for the observed 1α,25$(OH)_2D_3$-mediated PCA suppression *in vivo*. Recently, we reported that chronic low-dose UVB irradiation, which increases 1α,25$(OH)_2D_3$ levels in ear pinnae, could limit the number of various leukocytes (e.g. granulocytes, macrophages and T cells) within the tissues in a MC VDR-dependent manner. [163] Given that 1α,25$(OH)_2D_3$ can also alter the functional properties of structural cells (e.g. keratinocytes) as well as leukocytes in various inflammatory settings [226, 316, 317, 320], the effects of topical 1α,25$(OH)_2D_3$ on the recruitment and/or functionality of these cells need to be examined to explore additional explanations for the capacity of this hormone to suppress PCA-associated cutaneous pathology. Other *in vivo* allergy

models, such as the mouse atopic dermatitis models [377] which provide a persistent rather than transient inflammation scenario, should also be utilised to determine whether topical $1\alpha,25(OH)_2D_3$ or dietary supplements of $VitD_3$ metabolites can also influence chronic-phase events (i.e. tissue remodelling) of allergic disorders.

Data obtained from the current project clearly demonstrated VDR-dependence for the immunosuppressive effect of $1\alpha,25(OH)_2D_3$ on IgE + sAg-mediated MC activation both *in vitro* (**Chapter 3**) and *in vivo* (**Chapter 5**). This, however, does not mean that such effect is genomic, as the non-genomic pathway-specific analogue, curcumin, exhibited similar effects to $1\alpha,25(OH)_2D_3$ on the secretion but not gene expression of pro-inflammatory cytokines also in a VDR-dependent manner (**Figures 3.11 and 3.12**). As pointed out previously, these results represent the first set of functional evidence that VDR could function as mVDR and initiate non-genomic signalling pathways. In addition, it was intriguing the fact that curcumin exhibited the opposite effect to $1\alpha,25(OH)_2D_3$ on IL-10 secretion, which suggests that whereas the non-genomic action of $1\alpha,25(OH)_2D_3$ (as represented by curcumin) can decrease IL-10 secretion (along with that of other cytokines), its genomic action counteracts with this effects and results in a net increase in IL-10 production. To substantiate this theory, other $VitD_3$ pathway-specific agonists and antagonists will be used either instead of or in conjunction with $1\alpha,25(OH)_2D_3$, respectively, in *in vitro* experiments. Furthermore, our *in vivo* data demonstrated that the IL-10 level in ear tissues, as well as that of TNFα and IL-6, was moderately reduced upon topical $1\alpha,25(OH)_2D_3$ treatment, which could suggest the action of non-genomic $VitD_3$ pathways and/or post-translational modification by microRNAs. Again, other pathway specific agonists and antagonists, preferentially the ones that are low-calcemic in nature

and therefore will not cause hypercalcemia and related symptoms *in vivo*, should be tested before definite conclusions are drawn in this regard.

Taken together, the current thesis presented novel findings indicating the capacity of MCs to generate endogenous 1α,25$(OH)_2D_3$ and the MC VDR-dependent immunosuppressive effects of 1α,25$(OH)_2D_3$ on IgE-mediated inflammatory responses both *in vitro* and *in vivo*. It also provided a strong basis for future studies exploring other potential mechanisms responsible for the observed effects of 1α,25$(OH)_2D_3$ on activated MCs and confirming these effects using other appropriate *in vitro* and *in vivo* models. Overall, the outcome of this project highlighted the complexity of MC functions in IgE-dependent allergic disorders and, more importantly, the therapeutic potential of $VitD_3$ analogues for the prevention and treatment of these disorders via its immunoregulatory effects on MCs.

References

1. Enerback, L. 1966. Mast cells in rat gastrointestinal mucosa. I. Effects of fixation. *Acta pathologica et microbiologica Scandinavica* 66:289-302.

2. el Sayed, S. O., and M. Dyson. 1993. Histochemical heterogeneity of mast cells in rat dermis. *Biotech Histochem* 68:326-332.

3. Metcalfe, D. D. 2008. Mast cells and mastocytosis. *Blood* 112:946-956.

4. Moon, T. C., C. D. St Laurent, K. E. Morris, C. Marcet, T. Yoshimura, Y. Sekar, and A. D. Befus. 2010. Advances in mast cell biology: new understanding of heterogeneity and function. *Mucosal immunology* 3:111-128.

5. Hart, P. H., M. A. Grimbaldeston, G. J. Swift, A. Jaksic, F. P. Noonan, and J. J. Finlay-Jones. 1998. Dermal mast cells determine susceptibility to ultraviolet B-induced systemic suppression of contact hypersensitivity responses in mice. *J Exp Med* 187:2045-2053.

6. Depinay, N., F. Hacini, W. Beghdadi, R. Peronet, and S. Mecheri. 2006. Mast cell-dependent down-regulation of antigen-specific immune responses by mosquito bites. *J Immunol* 176:4141-4146.

7. Grimbaldeston, M. A., S. Nakae, J. Kalesnikoff, M. Tsai, and S. J. Galli. 2007. Mast cell-derived interleukin 10 limits skin pathology in contact dermatitis and chronic irradiation with ultraviolet B. *Nat Immunol* 8:1095-1104.

8. Lu, L. F., and e. al. 2006. Mast cells are essential intermediaries in regulatory T-cell tolerance. *Nature* 442:997-1002.

9. Gurish, M. F., and J. A. Boyce. 2006. Mast cells: ontogeny, homing, and recruitment of a unique innate effector cell. *J Allergy Clin Immunol* 117:1285-1291.

10. Chen, C. C., M. A. Grimbaldeston, M. Tsai, I. L. Weissman, and S. J. Galli. 2005. Identification of mast cell progenitors in adult mice. *Proc Natl Acad Sci U S A* 102:11408-11413.

11. Galli, S. J., J. Kalesnikoff, M. A. Grimbaldeston, A. M. Piliponsky, C. M. Williams, and M. Tsai. 2005. Mast cells as "tunable" effector and immunoregulatory cells: recent advances. *Annu Rev Immunol* 23:749-786.

12. Gurish, M. F., H. Tao, J. P. Abonia, A. Arya, D. S. Friend, C. M. Parker, and K. F. Austen. 2001. Intestinal mast cell progenitors require CD49dbeta7 (alpha4beta7 integrin) for tissue-specific homing. *J Exp Med* 194:1243-1252.

13. Abonia, J. P., K. F. Austen, B. J. Rollins, S. K. Joshi, R. A. Flavell, W. A. Kuziel, P. A. Koni, and M. F. Gurish. 2005. Constitutive homing of mast cell progenitors to the intestine depends on autologous expression of the chemokine receptor CXCR2. *Blood* 105:4308-4313.

14. Abonia, J. P., J. Hallgren, T. Jones, T. Shi, Y. Xu, P. Koni, R. A. Flavell, J. A. Boyce, K. F. Austen, and M. F. Gurish. 2006. Alpha-4 integrins and VCAM-1, but not MAdCAM-1, are essential for recruitment of mast cell progenitors to the inflamed lung. *Blood* 108:1588-1594.

15. Smith, T. J., and J. H. Weis. 1996. Mucosal T cells and mast cells share common adhesion receptors. *Immunology today* 17:60-63.

16. Ochi, H., W. M. Hirani, Q. Yuan, D. S. Friend, K. F. Austen, and J. A. Boyce. 1999. T helper cell type 2 cytokine-mediated comitogenic responses and CCR3 expression during differentiation of human mast cells in vitro. *J Exp Med* 190:267-280.

17. Wang, H. W., N. Tedla, A. R. Lloyd, D. Wakefield, and P. H. McNeil. 1998. Mast cell activation and migration to lymph nodes during induction of an immune response in mice. *J Clin Invest* 102:1617-1626.

18. Kovach, N. L., N. Lin, T. Yednock, J. M. Harlan, and V. C. Broudy. 1995. Stem cell factor modulates avidity of alpha 4 beta 1 and alpha 5 beta 1 integrins expressed on hematopoietic cell lines. *Blood* 85:159-167.

19. Byrne, S. N., A. Y. Limon-Flores, and S. E. Ullrich. 2008. Mast cell migration from the skin to the draining lymph nodes upon ultraviolet irradiation represents a key step in the induction of immune suppression. *J Immunol* 180:4648-4655.

20. Zweifel, M., K. Breu, K. Matozan, E. Renner, M. Welle, T. Schaffner, and P. A. Clavien. 2005. Restoration of hepatic mast cells and expression of a different mast cell protease phenotype in regenerating rat liver after 70%-hepatectomy. *Immunol Cell Biol* 83:587-595.

21. Fischer, M., M. Juremalm, N. Olsson, C. Backlin, C. Sundstrom, K. Nilsson, G. Enblad, and G. Nilsson. 2003. Expression of CCL5/RANTES by Hodgkin and Reed-Sternberg cells and its possible role in the recruitment of mast cells into lymphomatous tissue. *International journal of cancer* 107:197-201.

22. Juremalm, M., N. Olsson, and G. Nilsson. 2002. Selective CCL5/RANTES-induced mast cell migration through interactions with chemokine receptors CCR1 and CCR4. *Biochem Biophys Res Commun* 297:480-485.

23. Misiak-Tloczek, A., and E. Brzezinska-Blaszczyk. 2009. IL-6, but not IL-4, stimulates chemokinesis and TNF stimulates chemotaxis of tissue mast cells: involvement of both mitogen-activated protein kinases and phosphatidylinositol 3-kinase signalling pathways. *Apmis* 117:558-567.

24. Metcalfe, D. D., D. Baram, and Y. A. Mekori. 1997. Mast cells. *Physiological reviews* 77:1033-1079.

25. Pejler, G., E. Ronnberg, I. Waern, and S. Wernersson. Mast cell proteases: multifaceted regulators of inflammatory disease. *Blood* 115:4981-4990.

26. Irani, A. M., and L. B. Schwartz. 1994. Human mast cell heterogeneity. *Allergy Proc* 15:303-308.

27. Welle, M. 1997. Development, significance, and heterogeneity of mast cells with particular regard to the mast cell-specific proteases chymase and tryptase. *J Leukoc Biol* 61:233-245.

28. Pejler, G., M. Abrink, M. Ringvall, and S. Wernersson. 2007. Mast cell proteases. *Advances in immunology* 95:167-255.

29. Okayama, Y., and T. Kawakami. 2006. Development, migration, and survival of mast cells. *Immunologic research* 34:97-115.

30. Chabot, B., D. A. Stephenson, V. M. Chapman, P. Besmer, and A. Bernstein. 1988. The proto-oncogene c-kit encoding a transmembrane tyrosine kinase receptor maps to the mouse W locus. *Nature* 335:88-89.

31. Copeland, N. G., D. J. Gilbert, B. C. Cho, P. J. Donovan, N. A. Jenkins, D. Cosman, D. Anderson, S. D. Lyman, and D. E. Williams. 1990. Mast cell growth factor maps near the steel locus on mouse chromosome 10 and is deleted in a number of steel alleles. *Cell* 63:175-183.

32. Sawai, N., K. Koike, H. H. Mwamtemi, T. Kinoshita, Y. Kurokawa, K. Sakashita, T. Higuchi, K. Takeuchi, M. Shiohara, T. Kamijo, S. Ito, T. Kato, H. Miyazaki, T. Yamashita, and A. Komiyama. 1999. Thrombopoietin augments stem cell factor-dependent growth of human mast cells from bone marrow multipotential hematopoietic progenitors. *Blood* 93:3703-3712.

33. Galli, S. J. 1990. New insights into "the riddle of the mast cells": microenvironmental regulation of mast cell development and phenotypic heterogeneity. *Lab Invest* 62:5-33.

34. Hamaguchi, Y., Y. Kanakura, J. Fujita, S. Takeda, T. Nakano, S. Tarui, T. Honjo, and Y. Kitamura. 1987. Interleukin 4 as an essential factor for in vitro clonal growth of murine connective tissue-type mast cells. *J Exp Med* 165:268-273.

35. Takagi, M., T. Nakahata, T. Kubo, M. Shiohara, K. Koike, A. Miyajima, K. Arai, S. Nishikawa, K. M. Zsebo, and A. Komiyama. 1992. Stimulation of mouse connective tissue-type mast cells by hemopoietic stem cell factor, a ligand for the c-kit receptor. *J Immunol* 148:3446-3453.

36. Nakahata, T., K. Tsuji, R. Tanaka, K. Muraoka, N. Okumura, N. Sawai, M. Takagi, S. Itoh, C. Ra, and H. Saito. 1995. Synergy of stem cell factor and other cytokines in mast cell development. In *Biological and Molecular Aspects of Mast Cell and Basophil Differentiation and Function*. Y. Kitamura, S. Yamamoto, S. J. Galli, and M. W. Greaves, eds. Raven Press, New York. 13-24.

37. Kinoshita, T., N. Sawai, E. Hidaka, T. Yamashita, and K. Koike. 1999. Interleukin-6 directly modulates stem cell factor-dependent development of human mast cells derived from CD34(+) cord blood cells. *Blood* 94:496-508.

38. Blank, U. 2011. The mechanisms of exocytosis in mast cells. *Advances in experimental medicine and biology* 716:107-122.

39. Galli, S. J., A. M. Dvorak, and H. F. Dvorak. 1984. Basophils and mast cells: morphologic insights into their biology, secretory patterns, and function. *Progress in allergy* 34:1-141.

40. Taylor, A. M., S. J. Galli, and J. W. Coleman. 1995. Stem-cell factor, the kit ligand, induces direct degranulation of rat peritoneal mast cells in vitro and in vivo: dependence of the in vitro effect on period of culture and comparisons of stem-cell factor with other mast cell-activating agents. *Immunology* 86:427-433.

41. Subramanian, N., and M. A. Bray. 1987. Interleukin 1 releases histamine from human basophils and mast cells in vitro. *J Immunol* 138:271-275.

42. Alam, R., D. Kumar, D. Anderson-Walters, and P. A. Forsythe. 1994. Macrophage inflammatory protein-1 alpha and monocyte chemoattractant peptide-1 elicit immediate and late cutaneous reactions and activate murine mast cells in vivo. *J Immunol* 152:1298-1303.

43. Hugli, T. E., and H. J. Muller-Eberhard. 1978. Anaphylatoxins: C3a and C5a. *Advances in immunology* 26:1-53.

44. Theoharides, T. C., J. Donelan, K. Kandere-Grzybowska, and A. Konstantinidou. 2005. The role of mast cells in migraine pathophysiology. *Brain research* 49:65-76.

45. Rychter, J. W., L. Van Nassauw, J. P. Timmermans, L. M. Akkermans, R. H. Westerink, and A. B. Kroese. 2011. CGRP1 receptor activation induces piecemeal release of protease-1 from mouse bone marrow-derived mucosal mast cells. *Neurogastroenterol Motil* 23:e57-68.

46. Redegeld, F. A., and F. P. Nijkamp. 2003. Immunoglobulin free light chains and mast cells: pivotal role in T-cell-mediated immune reactions? *Trends Immunol* 24:181-185.

47. Varadaradjalou, S., F. Feger, N. Thieblemont, N. B. Hamouda, J. M. Pleau, M. Dy, and M. Arock. 2003. Toll-like receptor 2 (TLR2) and TLR4 differentially activate human mast cells. *Eur J Immunol* 33:899-906.

48. Kulka, M., L. Alexopoulou, R. A. Flavell, and D. D. Metcalfe. 2004. Activation of mast cells by double-stranded RNA: evidence for activation through Toll-like receptor 3. *J Allergy Clin Immunol* 114:174-182.

49. Heib, V., M. Becker, T. Warger, G. Rechtsteiner, C. Tertilt, M. Klein, T. Bopp, C. Taube, H. Schild, E. Schmitt, and M. Stassen. 2007. Mast cells are crucial for

early inflammation, migration of Langerhans cells, and CTL responses following topical application of TLR7 ligand in mice. *Blood* 110:946-953.

50. Matsushima, H., N. Yamada, H. Matsue, and S. Shimada. 2004. TLR3-, TLR7-, and TLR9-mediated production of proinflammatory cytokines and chemokines from murine connective tissue type skin-derived mast cells but not from bone marrow-derived mast cells. *J Immunol* 173:531-541.

51. Moller, C. 2004. Regulation of Mast Cell Survial. Acta Universitatis Upsaliensis.

52. Alam, R., J. B. Welter, P. A. Forsythe, M. A. Lett-Brown, and J. A. Grant. 1989. Comparative effect of recombinant IL-1, -2, -3, -4, and -6, IFN-gamma, granulocyte-macrophage-colony-stimulating factor, tumor necrosis factor-alpha, and histamine-releasing factors on the secretion of histamine from basophils. *J Immunol* 142:3431-3435.

53. Kalesnikoff, J., M. Huber, V. Lam, J. E. Damen, J. Zhang, R. P. Siraganian, and G. Krystal. 2001. Monomeric IgE stimulates signaling pathways in mast cells that lead to cytokine production and cell survival. *Immunity* 14:801-811.

54. Kumar, V., and A. Sharma. 2010. Mast cells: emerging sentinel innate immune cells with diverse role in immunity. *Molecular immunology* 48:14-25.

55. Nigrovic, P. A., and D. M. Lee. 2005. Mast cells in inflammatory arthritis. *Arthritis research & therapy* 7:1-11.

56. Lindstedt, K. A., and P. T. Kovanen. 2006. Isolation of mast cell granules. *Current protocols in cell biology / editorial board, Juan S. Bonifacino ... [et al* Chapter 3:Unit 3 16.

57. Gordon, J. R., and S. J. Galli. 1990. Mast cells as a source of both preformed and immunologically inducible TNF-alpha/cachectin. *Nature* 346:274-276.

58. Orinska, Z., M. Maurer, F. Mirghomizadeh, E. Bulanova, M. Metz, N. Nashkevich, F. Schiemann, J. Schulmistrat, V. Budagian, J. Giron-Michel, E. Brandt, R. Paus, and S. Bulfone-Paus. 2007. IL-15 constrains mast cell-dependent antibacterial defenses by suppressing chymase activities. *Nature medicine* 13:927-934.

59. Lukacs, N. W., R. M. Strieter, S. W. Chensue, M. Widmer, and S. L. Kunkel. 1995. TNF-alpha mediates recruitment of neutrophils and eosinophils during airway inflammation. *J Immunol* 154:5411-5417.

60. Kirman, I., B. Vainer, and O. H. Nielsen. 1998. Interleukin-15 and its role in chronic inflammatory diseases. *Inflamm Res* 47:285-289.

61. Gilfillan, A. M., and C. Tkaczyk. 2006. Integrated signalling pathways for mast-cell activation. *Nat Rev Immunol* 6:218-230.

62. Kraft, S., and J. P. Kinet. 2007. New developments in FcepsilonRI regulation, function and inhibition. *Nat Rev Immunol* 7:365-378.

63. Cambier, J. C. 1995. Antigen and Fc receptor signaling. The awesome power of the immunoreceptor tyrosine-based activation motif (ITAM). *J Immunol* 155:3281-3285.

64. Galli, S. J., M. Tsai, and A. M. Piliponsky. 2008. The development of allergic inflammation. *Nature* 454:445-454.

65. Armstrong, S. C. 2006. Analysis of mitogen-activated protein kinase activation. *Methods in molecular biology (Clifton, N.J* 315:151-163.

66. Kopec, A., B. Panaszek, and A. M. Fal. 2006. Intracellular signaling pathways in IgE-dependent mast cell activation. *Archivum immunologiae et therapiae experimentalis* 54:393-401.

67. Jabril-Cuenod, B., C. Zhang, A. M. Scharenberg, R. Paolini, R. Numerof, M. A. Beaven, and J. P. Kinet. 1996. Syk-dependent phosphorylation of Shc. A potential link between FcepsilonRI and the Ras/mitogen-activated protein kinase signaling pathway through SOS and Grb2. *J Biol Chem* 271:16268-16272.

68. Beaven, M. A., and R. A. Baumgartner. 1996. Downstream signals initiated in mast cells by Fc epsilon RI and other receptors. *Curr Opin Immunol* 8:766-772.

69. Hamawy, M. M., S. E. Mergenhagen, and R. P. Siraganian. 1995. Protein tyrosine phosphorylation as a mechanism of signalling in mast cells and basophils. *Cell Signal* 7:535-544.

70. Parravicini, V., M. Gadina, M. Kovarova, S. Odom, C. Gonzalez-Espinosa, Y. Furumoto, S. Saitoh, L. E. Samelson, J. J. O'Shea, and J. Rivera. 2002. Fyn kinase initiates complementary signals required for IgE-dependent mast cell degranulation. *Nat Immunol* 3:741-748.

71. Xie, Z. H., I. Ambudkar, and R. P. Siraganian. 2002. The adapter molecule Gab2 regulates Fc epsilon RI-mediated signal transduction in mast cells. *J Immunol* 168:4682-4691.

72. Iwaki, S., C. Tkaczyk, A. B. Satterthwaite, K. Halcomb, M. A. Beaven, D. D. Metcalfe, and A. M. Gilfillan. 2005. Btk plays a crucial role in the amplification of Fc epsilonRI-mediated mast cell activation by kit. *J Biol Chem* 280:40261-40270.

73. Kitaura, J., K. Asai, M. Maeda-Yamamoto, Y. Kawakami, U. Kikkawa, and T. Kawakami. 2000. Akt-dependent cytokine production in mast cells. *J Exp Med* 192:729-740.

74. Saitoh, S., R. Arudchandran, T. S. Manetz, W. Zhang, C. L. Sommers, P. E. Love, J. Rivera, and L. E. Samelson. 2000. LAT is essential for Fc(epsilon)RI-mediated mast cell activation. *Immunity* 12:525-535.

75. Brdicka, T., M. Imrich, P. Angelisova, N. Brdickova, O. Horvath, J. Spicka, I. Hilgert, P. Luskova, P. Draber, P. Novak, N. Engels, J. Wienands, L. Simeoni, J. Osterreicher, E. Aguado, M. Malissen, B. Schraven, and V. Horejsi. 2002. Non-T cell activation linker (NTAL): a transmembrane adaptor protein involved in immunoreceptor signaling. *J Exp Med* 196:1617-1626.

76. Tkaczyk, C., V. Horejsi, S. Iwaki, P. Draber, L. E. Samelson, A. B. Satterthwaite, D. H. Nahm, D. D. Metcalfe, and A. M. Gilfillan. 2004. NTAL phosphorylation is a pivotal link between the signaling cascades leading to human mast cell degranulation following Kit activation and Fc epsilon RI aggregation. *Blood* 104:207-214.

77. Australian Bureau of Statistics 2004-2005 National Health Survey: Summary of Results ABS 4364.0.

78. Cook, M., J. Douglass, D. Mallon, J. Smith, M. Wong, and R. Mullins. 2007. The economic impact of allergic disease in Australia: not to be sneezed at. Australasian Society of Clinical Immunology and Allergy.

79. Asher, M. I., S. Montefort, B. Bjorksten, C. K. Lai, D. P. Strachan, S. K. Weiland, and H. Williams. 2006. Worldwide time trends in the prevalence of symptoms of asthma, allergic rhinoconjunctivitis, and eczema in childhood: ISAAC Phases One and Three repeat multicountry cross-sectional surveys. *Lancet* 368:733-743.

80. von Pirquet, C. 1906. Allergie. *Munch. Med. Wochenschr.* 53:1457-1458.

81. Kay, A. B. 2001. Allergy and allergic diseases. First of two parts. *The New England journal of medicine* 344:30-37.

82. Geha, R. S., H. H. Jabara, and S. R. Brodeur. 2003. The regulation of immunoglobulin E class-switch recombination. *Nat Rev Immunol* 3:721-732.

83. Larche, M., C. A. Akdis, and R. Valenta. 2006. Immunological mechanisms of allergen-specific immunotherapy. *Nat Rev Immunol* 6:761-771.

84. Gould, H. J., and B. J. Sutton. 2008. IgE in allergy and asthma today. *Nat Rev Immunol* 8:205-217.

85. Gauchat, J. F., S. Henchoz, G. Mazzei, J. P. Aubry, T. Brunner, H. Blasey, P. Life, D. Talabot, L. Flores-Romo, J. Thompson, and et al. 1993. Induction of human IgE synthesis in B cells by mast cells and basophils. *Nature* 365:340-343.

86. Galli, S. J., and M. Tsai. 2010. Mast cells in allergy and infection: versatile effector and regulatory cells in innate and adaptive immunity. *Eur J Immunol* 40:1843-1851.

87. Marone, G., M. Triggiani, and A. de Paulis. 2005. Mast cells and basophils: friends as well as foes in bronchial asthma? *Trends Immunol* 26:25-31.

88. Berin, M. C., and L. Mayer. 2009. Immunophysiology of experimental food allergy. *Mucosal immunology* 2:24-32.

89. Wershil, B. K., Z. S. Wang, J. R. Gordon, and S. J. Galli. 1991. Recruitment of neutrophils during IgE-dependent cutaneous late phase reactions in the mouse is mast cell-dependent. Partial inhibition of the reaction with antiserum against tumor necrosis factor-alpha. *J Clin Invest* 87:446-453.

90. Biedermann, T., M. Kneilling, R. Mailhammer, K. Maier, C. A. Sander, G. Kollias, S. L. Kunkel, L. Hultner, and M. Rocken. 2000. Mast cells control neutrophil recruitment during T cell-mediated delayed-type hypersensitivity reactions through tumor necrosis factor and macrophage inflammatory protein 2. *J Exp Med* 192:1441-1452.

91. Karasuyama, H., K. Mukai, Y. Tsujimura, and K. Obata. 2009. Newly discovered roles for basophils: a neglected minority gains new respect. *Nat Rev Immunol* 9:9-13.

92. Sampson, H. A., A. Munoz-Furlong, S. A. Bock, C. Schmitt, R. Bass, B. A. Chowdhury, W. W. Decker, T. J. Furlong, S. J. Galli, D. B. Golden, R. S. Gruchalla, A. D. Harlor, Jr., D. L. Hepner, M. Howarth, A. P. Kaplan, J. H. Levy, L. M. Lewis, P. L. Lieberman, D. D. Metcalfe, R. Murphy, S. M. Pollart, R. S. Pumphrey, L. J. Rosenwasser, F. E. Simons, J. P. Wood, and C. A. Camargo, Jr. 2005. Symposium on the definition and management of anaphylaxis: summary report. *J Allergy Clin Immunol* 115:584-591.

93. MacGlashan, D., Jr., G. Gauvreau, and J. T. Schroeder. 2002. Basophils in airway disease. *Current allergy and asthma reports* 2:126-132.

94. Tsujimura, Y., K. Obata, K. Mukai, H. Shindou, M. Yoshida, H. Nishikado, Y. Kawano, Y. Minegishi, T. Shimizu, and H. Karasuyama. 2008. Basophils play a pivotal role in immunoglobulin-G-mediated but not immunoglobulin-E-mediated systemic anaphylaxis. *Immunity* 28:581-589.

95. Bonness, S., and T. Bieber. 2007. Molecular basis of atopic dermatitis. *Current opinion in allergy and clinical immunology* 7:382-386.

96. Gadek, J. E., G. A. Fells, D. G. Wright, and R. G. Crystal. 1980. Human neutrophil elastase functions as a type III collagen "collagenase". *Biochem Biophys Res Commun* 95:1815-1822.

97. Robinson, B. W., T. Venaille, R. Blum, and A. H. Mendis. 1992. Eosinophils and major basic protein damage but do not detach human amniotic epithelial cells. *Experimental lung research* 18:583-593.

98. Larche, M., D. S. Robinson, and A. B. Kay. 2003. The role of T lymphocytes in the pathogenesis of asthma. *J Allergy Clin Immunol* 111:450-463; quiz 464.

99. Galli, S. J., M. Grimbaldeston, and M. Tsai. 2008. Immunomodulatory mast cells: negative, as well as positive, regulators of immunity. *Nat Rev Immunol* 8:478-486.

100. Waern, I., S. Jonasson, J. Hjoberg, A. Bucht, M. Abrink, G. Pejler, and S. Wernersson. 2009. Mouse mast cell protease 4 is the major chymase in murine airways and has a protective role in allergic airway inflammation. *J Immunol* 183:6369-6376.

101. Bradding, P., A. F. Walls, and S. T. Holgate. 2006. The role of the mast cell in the pathophysiology of asthma. *J Allergy Clin Immunol* 117:1277-1284.

102. Doherty, T., and D. Broide. 2007. Cytokines and growth factors in airway remodeling in asthma. *Curr Opin Immunol* 19:676-680.

103. Mauad, T., E. H. Bel, and P. J. Sterk. 2007. Asthma therapy and airway remodeling. *J Allergy Clin Immunol* 120:997-1009; quiz 1010-1001.

104. Pawankar, R., M. Nonaka, S. Yamagishi, and T. Yagi. 2004. Pathophysiologic mechanisms of chronic rhinosinusitis. *Immunology and allergy clinics of North America* 24:75-85.

105. Leung, D. Y., M. Boguniewicz, M. D. Howell, I. Nomura, and Q. A. Hamid. 2004. New insights into atopic dermatitis. *J Clin Invest* 113:651-657.

106. Gern, J. E., and W. W. Busse. 2002. Relationship of viral infections to wheezing illnesses and asthma. *Nat Rev Immunol* 2:132-138.

107. Takano, K., T. Kojima, M. Go, M. Murata, S. Ichimiya, T. Himi, and N. Sawada. 2005. HLA-DR- and CD11c-positive dendritic cells penetrate beyond well-developed epithelial tight junctions in human nasal mucosa of allergic rhinitis. *J Histochem Cytochem* 53:611-619.

108. Holgate, S. T. 2007. Epithelium dysfunction in asthma. *J Allergy Clin Immunol* 120:1233-1244; quiz 1245-1236.

109. Brightling, C. E., P. Bradding, I. D. Pavord, and A. J. Wardlaw. 2003. New insights into the role of the mast cell in asthma. *Clin Exp Allergy* 33:550-556.

110. Ziegler, S. F., and Y. J. Liu. 2006. Thymic stromal lymphopoietin in normal and pathogenic T cell development and function. *Nat Immunol* 7:709-714.

111. Ying, S., B. O'Connor, J. Ratoff, Q. Meng, K. Mallett, D. Cousins, D. Robinson, G. Zhang, J. Zhao, T. H. Lee, and C. Corrigan. 2005. Thymic stromal lymphopoietin expression is increased in asthmatic airways and correlates with expression of Th2-attracting chemokines and disease severity. *J Immunol* 174:8183-8190.

112. Prefontaine, D., S. Lajoie-Kadoch, S. Foley, S. Audusseau, R. Olivenstein, A. J. Halayko, C. Lemiere, J. G. Martin, and Q. Hamid. 2009. Increased expression of

IL-33 in severe asthma: evidence of expression by airway smooth muscle cells. *J Immunol* 183:5094-5103.

113. Hofmann, A. M., and S. N. Abraham. 2009. New roles for mast cells in modulating allergic reactions and immunity against pathogens. *Curr Opin Immunol* 21:679-686.

114. Metz, M., and M. Maurer. 2009. Innate immunity and allergy in the skin. *Curr Opin Immunol* 21:687-693.

115. Mukai, K., K. Matsuoka, C. Taya, H. Suzuki, H. Yokozeki, K. Nishioka, K. Hirokawa, M. Etori, M. Yamashita, T. Kubota, Y. Minegishi, H. Yonekawa, and H. Karasuyama. 2005. Basophils play a critical role in the development of IgE-mediated chronic allergic inflammation independently of T cells and mast cells. *Immunity* 23:191-202.

116. Obata, K., K. Mukai, Y. Tsujimura, K. Ishiwata, Y. Kawano, Y. Minegishi, N. Watanabe, and H. Karasuyama. 2007. Basophils are essential initiators of a novel type of chronic allergic inflammation. *Blood* 110:913-920.

117. Yazdanbakhsh, M., P. G. Kremsner, and R. van Ree. 2002. Allergy, parasites, and the hygiene hypothesis. *Science* 296:490-494.

118. Holgate, S. T., and R. Polosa. 2008. Treatment strategies for allergy and asthma. *Nat Rev Immunol* 8:218-230.

119. Wu, K., Y. Bi, K. Sun, and C. Wang. 2007. IL-10-producing type 1 regulatory T cells and allergy. *Cellular & molecular immunology* 4:269-275.

120. Holgate, S. T., R. Djukanovic, T. Casale, and J. Bousquet. 2005. Anti-immunoglobulin E treatment with omalizumab in allergic diseases: an update on anti-inflammatory activity and clinical efficacy. *Clin Exp Allergy* 35:408-416.

121. Bez, C., R. Schubert, M. Kopp, Y. Ersfeld, M. Rosewich, J. Kuehr, W. Kamin, A. V. Berg, U. Wahu, and S. Zielen. 2004. Effect of anti-immunoglobulin E on nasal inflammation in patients with seasonal allergic rhinoconjunctivitis. *Clin Exp Allergy* 34:1079-1085.

122. Plewako, H., M. Arvidsson, K. Petruson, I. Oancea, K. Holmberg, E. Adelroth, H. Gustafsson, T. Sandstrom, and S. Rak. 2002. The effect of omalizumab on nasal allergic inflammation. *J Allergy Clin Immunol* 110:68-71.

123. Leonardi, A. 2005. Emerging drugs for ocular allergy. *Expert opinion on emerging drugs* 10:505-520.

124. Yanni, J. M., S. T. Miller, D. A. Gamache, J. M. Spellman, S. Xu, and N. A. Sharif. 1997. Comparative effects of topical ocular anti-allergy drugs on human conjunctival mast cells. *Ann Allergy Asthma Immunol* 79:541-545.

125. Sharif, N. A., S. X. Xu, S. T. Miller, D. A. Gamache, and J. M. Yanni. 1996. Characterization of the ocular antiallergic and antihistaminic effects of olopatadine (AL-4943A), a novel drug for treating ocular allergic diseases. *The Journal of pharmacology and experimental therapeutics* 278:1252-1261.

126. Noli, C., and A. Miolo. 2001. The mast cell in wound healing. *Veterinary dermatology* 12:303-313.

127. Maurer, M., E. Fischer, B. Handjiski, E. von Stebut, B. Algermissen, A. Bavandi, and R. Paus. 1997. Activated skin mast cells are involved in murine hair follicle regression (catagen). *Lab Invest* 77:319-332.

128. Nagasaka, A., H. Matsue, H. Matsushima, R. Aoki, Y. Nakamura, N. Kambe, S. Kon, T. Uede, and S. Shimada. 2008. Osteopontin is produced by mast cells and affects IgE-mediated degranulation and migration of mast cells. *Eur J Immunol* 38:489-499.

129. Anthony, R. M., L. I. Rutitzky, J. F. Urban, Jr., M. J. Stadecker, and W. C. Gause. 2007. Protective immune mechanisms in helminth infection. *Nat Rev Immunol* 7:975-987.

130. Matsuda, H., N. Watanabe, Y. Kiso, S. Hirota, H. Ushio, Y. Kannan, M. Azuma, H. Koyama, and Y. Kitamura. 1990. Necessity of IgE antibodies and mast cells for manifestation of resistance against larval Haemaphysalis longicornis ticks in mice. *J Immunol* 144:259-262.

131. Newlands, G. F., H. R. Miller, A. MacKellar, and S. J. Galli. 1995. Stem cell factor contributes to intestinal mucosal mast cell hyperplasia in rats infected with Nippostrongylus brasiliensis or Trichinella spiralis, but anti-stem cell factor treatment decreases parasite egg production during N brasiliensis infection. *Blood* 86:1968-1976.

132. Knight, P. A., S. H. Wright, C. E. Lawrence, Y. Y. Paterson, and H. R. Miller. 2000. Delayed expulsion of the nematode Trichinella spiralis in mice lacking the mucosal mast cell-specific granule chymase, mouse mast cell protease-1. *J Exp Med* 192:1849-1856.

133. McDermott, J. R., R. E. Bartram, P. A. Knight, H. R. Miller, D. R. Garrod, and R. K. Grencis. 2003. Mast cells disrupt epithelial barrier function during enteric nematode infection. *Proc Natl Acad Sci U S A* 100:7761-7766.

134. Finkelman, F. D., T. Shea-Donohue, S. C. Morris, L. Gildea, R. Strait, K. B. Madden, L. Schopf, and J. F. Urban, Jr. 2004. Interleukin-4- and interleukin-13-mediated host protection against intestinal nematode parasites. *Immunol Rev* 201:139-155.

135. Maurer, M., J. Wedemeyer, M. Metz, A. M. Piliponsky, K. Weller, D. Chatterjea, D. E. Clouthier, M. M. Yanagisawa, M. Tsai, and S. J. Galli. 2004. Mast cells

promote homeostasis by limiting endothelin-1-induced toxicity. *Nature* 432:512-516.

136. Piliponsky, A. M., C. C. Chen, T. Nishimura, M. Metz, E. J. Rios, P. R. Dobner, E. Wada, K. Wada, S. Zacharias, U. M. Mohanasundaram, J. D. Faix, M. Abrink, G. Pejler, R. G. Pearl, M. Tsai, and S. J. Galli. 2008. Neurotensin increases mortality and mast cells reduce neurotensin levels in a mouse model of sepsis. *Nature medicine* 14:392-398.

137. Piliponsky, A. M., C. C. Chen, M. A. Grimbaldeston, S. M. Burns-Guydish, J. Hardy, J. Kalesnikoff, C. H. Contag, M. Tsai, and S. J. Galli. 2010. Mast cell-derived TNF can exacerbate mortality during severe bacterial infections in C57BL/6-KitW-sh/W-sh mice. *Am J Pathol* 176:926-938.

138. Mallen-St Clair, J., C. T. Pham, S. A. Villalta, G. H. Caughey, and P. J. Wolters. 2004. Mast cell dipeptidyl peptidase I mediates survival from sepsis. *J Clin Invest* 113:628-634.

139. Li, Y., L. Li, R. Wadley, S. W. Reddel, J. C. Qi, C. Archis, A. Collins, E. Clark, M. Cooley, S. Kouts, H. M. Naif, M. Alali, A. Cunningham, G. W. Wong, R. L. Stevens, and S. A. Krilis. 2001. Mast cells/basophils in the peripheral blood of allergic individuals who are HIV-1 susceptible due to their surface expression of CD4 and the chemokine receptors CCR3, CCR5, and CXCR4. *Blood* 97:3484-3490.

140. Bannert, N., M. Farzan, D. S. Friend, H. Ochi, K. S. Price, J. Sodroski, and J. A. Boyce. 2001. Human Mast cell progenitors can be infected by macrophagetropic human immunodeficiency virus type 1 and retain virus with maturation in vitro. *Journal of virology* 75:10808-10814.

141. Sundstrom, J. B., D. M. Little, F. Villinger, J. E. Ellis, and A. A. Ansari. 2004. Signaling through Toll-like receptors triggers HIV-1 replication in latently infected mast cells. *J Immunol* 172:4391-4401.

142. Sundstrom, J. B., J. E. Ellis, G. A. Hair, A. S. Kirshenbaum, D. D. Metcalfe, H. Yi, A. C. Cardona, M. K. Lindsay, and A. A. Ansari. 2007. Human tissue mast cells are an inducible reservoir of persistent HIV infection. *Blood* 109:5293-5300.

143. Marone, G., G. Florio, A. Petraroli, M. Triggiani, and A. de Paulis. 2001. Role of human FcepsilonRI+ cells in HIV-1 infection. *Immunol Rev* 179:128-138.

144. Gounaris, E., S. E. Erdman, C. Restaino, M. F. Gurish, D. S. Friend, F. Gounari, D. M. Lee, G. Zhang, J. N. Glickman, K. Shin, V. P. Rao, T. Poutahidis, R. Weissleder, K. M. McNagny, and K. Khazaie. 2007. Mast cells are an essential hematopoietic component for polyp development. *Proc Natl Acad Sci U S A* 104:19977-19982.

145. Coussens, L. M., W. W. Raymond, G. Bergers, M. Laig-Webster, O. Behrendtsen, Z. Werb, G. H. Caughey, and D. Hanahan. 1999. Inflammatory mast cells up-

regulate angiogenesis during squamous epithelial carcinogenesis. *Genes & development* 13:1382-1397.

146. Soucek, L., E. R. Lawlor, D. Soto, K. Shchors, L. B. Swigart, and G. I. Evan. 2007. Mast cells are required for angiogenesis and macroscopic expansion of Myc-induced pancreatic islet tumors. *Nature medicine* 13:1211-1218.

147. Kopp, H. G., C. A. Ramos, and S. Rafii. 2006. Contribution of endothelial progenitors and proangiogenic hematopoietic cells to vascularization of tumor and ischemic tissue. *Current opinion in hematology* 13:175-181.

148. Sinnamon, M. J., K. J. Carter, L. P. Sims, B. Lafleur, B. Fingleton, and L. M. Matrisian. 2008. A protective role of mast cells in intestinal tumorigenesis. *Carcinogenesis* 29:880-886.

149. Kalesnikoff, J., and S. J. Galli. 2008. New developments in mast cell biology. *Nat Immunol* 9:1215-1223.

150. 2008. Global burden of disease: 2004 update. World Health Organization, Geneva.

151. Rabe, K. F., S. Hurd, A. Anzueto, P. J. Barnes, S. A. Buist, P. Calverley, Y. Fukuchi, C. Jenkins, R. Rodriguez-Roisin, C. van Weel, and J. Zielinski. 2007. Global strategy for the diagnosis, management, and prevention of chronic obstructive pulmonary disease: GOLD executive summary. *American journal of respiratory and critical care medicine* 176:532-555.

152. Vlahos, R., S. Bozinovski, R. C. Gualano, M. Ernst, and G. P. Anderson. 2006. Modelling COPD in mice. *Pulmonary pharmacology & therapeutics* 19:12-17.

153. Andersson, C. K., M. Mori, L. Bjermer, C. G. Lofdahl, and J. S. Erjefalt. 2010. Alterations in lung mast cell populations in patients with chronic obstructive pulmonary disease. *American journal of respiratory and critical care medicine* 181:206-217.

154. Ballarin, A., E. Bazzan, R. H. Zenteno, G. Turato, S. Baraldo, D. Zanovello, E. Mutti, J. C. Hogg, M. Saetta, and M. G. Cosio. 2012. Mast cell infiltration discriminates between histopathological phenotypes of chronic obstructive pulmonary disease. *American journal of respiratory and critical care medicine* 186:233-239.

155. Zhang, X., H. Zheng, W. Ma, F. Wang, X. Zeng, C. Liu, and S. He. 2011. Tryptase enzyme activity is correlated with severity of chronic obstructive pulmonary disease. *The Tohoku journal of experimental medicine* 224:179-187.

156. Mortaz, E., M. E. Givi, C. A. Da Silva, G. Folkerts, and F. A. Redegeld. 2012. A relation between TGF-beta and mast cell tryptase in experimental emphysema models. *Biochim Biophys Acta* 1822:1154-1160.

157. Thakurdas, S. M., E. Melicoff, L. Sansores-Garcia, D. C. Moreira, Y. Petrova, R. L. Stevens, and R. Adachi. 2007. The mast cell-restricted tryptase mMCP-6 has a

critical immunoprotective role in bacterial infections. *J Biol Chem* 282:20809-20815.

158. Beckett, E. L., R. L. Stevens, A. G. Jarnicki, R. Y. Kim, I. Hanish, N. G. Hansbro, A. Deane, S. Keely, J. C. Horvat, M. Yang, B. G. Oliver, N. van Rooijen, M. D. Inman, R. Adachi, R. J. Soberman, S. Hamadi, P. A. Wark, P. S. Foster, and P. M. Hansbro. 2013. A new short-term mouse model of chronic obstructive pulmonary disease identifies a role for mast cell tryptase in pathogenesis. *J Allergy Clin Immunol* 131:752-762.

159. Hansbro, P. M., M. J. Hamilton, M. Fricker, S. L. Gellatly, A. G. Jarnicki, D. Zheng, S. M. Frei, G. W. Wong, S. Hamadi, S. Zhou, P. S. Foster, S. A. Krilis, and R. L. Stevens. 2014. Importance of Mast Cell Prss31/Transmembrane Tryptase/Tryptase-gamma in Lung Function and Experimental Chronic Obstructive Pulmonary Disease and Colitis. *J Biol Chem* 289:18214-18227.

160. Cohen, B. H., W. C. Ball, Jr., S. Brashears, E. L. Diamond, P. Kreiss, D. A. Levy, H. A. Menkes, S. Permutt, and M. S. Tockman. 1977. Risk factors in chronic obstructive pulmonary disease (COPD). *American journal of epidemiology* 105:223-232.

161. Wong, G. W., P. S. Foster, S. Yasuda, J. C. Qi, S. Mahalingam, E. A. Mellor, G. Katsoulotos, L. Li, J. A. Boyce, S. A. Krilis, and R. L. Stevens. 2002. Biochemical and functional characterization of human transmembrane tryptase (TMT)/tryptase gamma. TMT is an exocytosed mast cell protease that induces airway hyperresponsiveness in vivo via an interleukin-13/interleukin-4 receptor alpha/signal transducer and activator of transcription (STAT) 6-dependent pathway. *J Biol Chem* 277:41906-41915.

162. de Vries, V. C., A. Wasiuk, K. A. Bennett, M. J. Benson, R. Elgueta, T. J. Waldschmidt, and R. J. Noelle. 2009. Mast cell degranulation breaks peripheral tolerance. *Am J Transplant* 9:2270-2280.

163. Biggs, L., C. Yu, B. Fedoric, A. F. Lopez, S. J. Galli, and M. A. Grimbaldeston. 2010. Evidence that vitamin D(3) promotes mast cell-dependent reduction of chronic UVB-induced skin pathology in mice. *J Exp Med* 207:455-463.

164. Chacon-Salinas, R., A. Y. Limon-Flores, A. D. Chavez-Blanco, A. Gonzalez-Estrada, and S. E. Ullrich. 2011. Mast cell-derived IL-10 suppresses germinal center formation by affecting T follicular helper cell function. *J Immunol* 186:25-31.

165. Karimi, K., F. A. Redegeld, B. Heijdra, and F. P. Nijkamp. 1999. Stem cell factor and interleukin-4 induce murine bone marrow cells to develop into mast cells with connective tissue type characteristics in vitro. *Experimental hematology* 27:654-662.

166. Bischoff, S. C. 2007. Role of mast cells in allergic and non-allergic immune responses: comparison of human and murine data. *Nat Rev Immunol* 7:93-104.

167. Bischoff, S. C., G. Sellge, S. Schwengberg, A. Lorentz, and M. P. Manns. 1999. Stem cell factor-dependent survival, proliferation and enhanced releasability of purified mature mast cells isolated from human intestinal tissue. *International archives of allergy and immunology* 118:104-107.

168. Sellge, G., and S. C. Bischoff. 2006. Isolation, culture, and characterization of intestinal mast cells. *Methods in molecular biology (Clifton, N.J* 315:123-138.

169. Butterfield, J. H., D. Weiler, G. Dewald, and G. J. Gleich. 1988. Establishment of an immature mast cell line from a patient with mast cell leukemia. *Leukemia research* 12:345-355.

170. Kirshenbaum, A. S., C. Akin, Y. Wu, M. Rottem, J. P. Goff, M. A. Beaven, V. K. Rao, and D. D. Metcalfe. 2003. Characterization of novel stem cell factor responsive human mast cell lines LAD 1 and 2 established from a patient with mast cell sarcoma/leukemia; activation following aggregation of FcepsilonRI or FcgammaRI. *Leukemia research* 27:677-682.

171. Tertian, G., Y. P. Yung, D. Guy-Grand, and M. A. Moore. 1981. Long-term in vitro culture of murine mast cells. I. Description of a growth factor-dependent culture technique. *J Immunol* 127:788-794.

172. Razin, E., J. N. Ihle, D. Seldin, J. M. Mencia-Huerta, H. R. Katz, P. A. LeBlanc, A. Hein, J. P. Caulfield, K. F. Austen, and R. L. Stevens. 1984. Interleukin 3: A differentiation and growth factor for the mouse mast cell that contains chondroitin sulfate E proteoglycan. *J Immunol* 132:1479-1486.

173. Matsue, H., N. Kambe, and S. Shimada. 2009. Murine fetal skin-derived cultured mast cells: a useful tool for discovering functions of skin mast cells. *J Invest Dermatol* 129:1120-1125.

174. Vig, M., W. I. DeHaven, G. S. Bird, J. M. Billingsley, H. Wang, P. E. Rao, A. B. Hutchings, M. H. Jouvin, J. W. Putney, and J. P. Kinet. 2008. Defective mast cell effector functions in mice lacking the CRACM1 pore subunit of store-operated calcium release-activated calcium channels. *Nat Immunol* 9:89-96.

175. Konno, S., M. Adachi, K. Asano, K. Okamoto, and T. Takahashi. 1993. Inhibitory effect of interferon-beta on mouse spleen-derived mast cells. *Mediators of inflammation* 2:243-246.

176. Gilead, L., E. Rahamim, I. Ziv, R. Or, and E. Razin. 1988. Cultured human bone marrow-derived mast cells, their similarities to cultured murine E-mast cells. *Immunology* 63:669-675.

177. Shimizu, Y., A. M. Irani, E. J. Brown, L. K. Ashman, and L. B. Schwartz. 1995. Human mast cells derived from fetal liver cells cultured with stem cell factor express a functional CD51/CD61 (alpha v beta 3) integrin. *Blood* 86:930-939.

178. Theoharides, T. C., D. Kempuraj, M. Tagen, M. Vasiadi, and C. L. Cetrulo. 2006. Human umbilical cord blood-derived mast cells: a unique model for the study of neuro-immuno-endocrine interactions. *Stem cell reviews* 2:143-154.

179. Saito, H., A. Kato, K. Matsumoto, and Y. Okayama. 2006. Culture of human mast cells from peripheral blood progenitors. *Nature protocols* 1:2178-2183.

180. Dvorak, A. M., R. A. Seder, W. E. Paul, E. S. Morgan, and S. J. Galli. 1994. Effects of interleukin-3 with or without the c-kit ligand, stem cell factor, on the survival and cytoplasmic granule formation of mouse basophils and mast cells in vitro. *Am J Pathol* 144:160-170.

181. Rottem, M., J. P. Goff, J. P. Albert, and D. D. Metcalfe. 1993. The effects of stem cell factor on the ultrastructure of Fc epsilon RI+ cells developing in IL-3-dependent murine bone marrow-derived cell cultures. *J Immunol* 151:4950-4963.

182. Grimbaldeston, M. A., C. C. Chen, A. M. Piliponsky, M. Tsai, S. Y. Tam, and S. J. Galli. 2005. Mast cell-deficient W-sash c-kit mutant Kit W-sh/W-sh mice as a model for investigating mast cell biology in vivo. *Am J Pathol* 167:835-848.

183. Nigrovic, P. A., D. H. Gray, T. Jones, J. Hallgren, F. C. Kuo, B. Chaletzky, M. Gurish, D. Mathis, C. Benoist, and D. M. Lee. 2008. Genetic inversion in mast cell-deficient (Wsh) mice interrupts corin and manifests as hematopoietic and cardiac aberrancy. *Am J Pathol* 173:1693-1701.

184. Feyerabend, T. B., H. Hausser, A. Tietz, C. Blum, L. Hellman, A. H. Straus, H. K. Takahashi, E. S. Morgan, A. M. Dvorak, H. J. Fehling, and H. R. Rodewald. 2005. Loss of histochemical identity in mast cells lacking carboxypeptidase A. *Mol Cell Biol* 25:6199-6210.

185. Scholten, J., K. Hartmann, A. Gerbaulet, T. Krieg, W. Muller, G. Testa, and A. Roers. 2008. Mast cell-specific Cre/loxP-mediated recombination in vivo. *Transgenic Res* 17:307-315.

186. Musch, W., A. K. Wege, D. N. Mannel, and T. Hehlgans. 2008. Generation and characterization of alpha-chymase-Cre transgenic mice. *Genesis* 46:163-166.

187. Dudeck, A., J. Dudeck, J. Scholten, A. Petzold, S. Surianarayanan, A. Kohler, K. Peschke, D. Vohringer, C. Waskow, T. Krieg, W. Muller, A. Waisman, K. Hartmann, M. Gunzer, and A. Roers. 2011. Mast cells are key promoters of contact allergy that mediate the adjuvant effects of haptens. *Immunity* 34:973-984.

188. Buch, T., F. L. Heppner, C. Tertilt, T. J. Heinen, M. Kremer, F. T. Wunderlich, S. Jung, and A. Waisman. 2005. A Cre-inducible diphtheria toxin receptor mediates cell lineage ablation after toxin administration. *Nature methods* 2:419-426.

189. Voehringer, D., H. E. Liang, and R. M. Locksley. 2008. Homeostasis and effector function of lymphopenia-induced "memory-like" T cells in constitutively T cell-depleted mice. *J Immunol* 180:4742-4753.

190. Roers, A., L. Siewe, E. Strittmatter, M. Deckert, D. Schluter, W. Stenzel, A. D. Gruber, T. Krieg, K. Rajewsky, and W. Muller. 2004. T cell-specific inactivation of the interleukin 10 gene in mice results in enhanced T cell responses but normal innate responses to lipopolysaccharide or skin irritation. *J Exp Med* 200:1289-1297.

191. Lehmann, B. 2005. The vitamin D3 pathway in human skin and its role for regulation of biological processes. *Photochem Photobiol* 81:1246-1251.

192. Bouillon, R., G. Carmeliet, L. Verlinden, E. van Etten, A. Verstuyf, H. F. Luderer, L. Lieben, C. Mathieu, and M. Demay. 2008. Vitamin D and human health: lessons from vitamin D receptor null mice. *Endocrine reviews* 29:726-776.

193. Yu, C., B. Fedoric, P. H. Anderson, A. F. Lopez, and M. A. Grimbaldeston. 2011. Vitamin D_3 Signalling to Mast Cells: a new regulatory axis. *The International Journal of Biochemistry & Cell Biology* 43:41-46.

194. Mozołowski, W. 1939. Jędrzej Sniadecki (1768-1838) on the Cure of Rickets *Nature* 143:121.

195. Mohr, S. B. 2009. A brief history of vitamin d and cancer prevention. *Annals of epidemiology* 19:79-83.

196. Bikle, D. D. 2009. Vitamin D and immune function: understanding common pathways. *Current osteoporosis reports* 7:58-63.

197. Akutsu, N., R. Lin, Y. Bastien, A. Bestawros, D. J. Enepekides, M. J. Black, and J. H. White. 2001. Regulation of gene Expression by 1alpha,25-dihydroxyvitamin D3 and Its analog EB1089 under growth-inhibitory conditions in squamous carcinoma Cells. *Molecular endocrinology (Baltimore, Md* 15:1127-1139.

198. Lin, R., and J. H. White. 2004. The pleiotropic actions of vitamin D. *Bioessays* 26:21-28.

199. Halliday, G. M. 2005. Inflammation, gene mutation and photoimmunosuppression in response to UVR-induced oxidative damage contributes to photocarcinogenesis. *Mutation research* 571:107-120.

200. Melnikova, V. O., and H. N. Ananthaswamy. 2005. Cellular and molecular events leading to the development of skin cancer. *Mutation research* 571:91-106.

201. Lu, Z., T. C. Chen, A. Zhang, K. S. Persons, N. Kohn, R. Berkowitz, S. Martinello, and M. F. Holick. 2007. An evaluation of the vitamin D3 content in fish: Is the vitamin D content adequate to satisfy the dietary requirement for vitamin D? *The Journal of steroid biochemistry and molecular biology* 103:642-644.

202. Dixon, K. M., and R. S. Mason. 2009. Vitamin d. *Int J Biochem Cell Biol* 41:982-985.

203. Lehmann, B., and M. Meurer. 2010. Vitamin D metabolism. *Dermatologic therapy* 23:2-12.

204. Bar, M., D. Domaschke, A. Meye, B. Lehmann, and M. Meurer. 2007. Wavelength-dependent induction of CYP24A1-mRNA after UVB-triggered calcitriol synthesis in cultured human keratinocytes. *J Invest Dermatol* 127:206-213.

205. Masuda, S., V. Byford, A. Arabian, Y. Sakai, M. B. Demay, R. St-Arnaud, and G. Jones. 2005. Altered pharmacokinetics of 1alpha,25-dihydroxyvitamin D3 and 25-hydroxyvitamin D3 in the blood and tissues of the 25-hydroxyvitamin D-24-hydroxylase (Cyp24a1) null mouse. *Endocrinology* 146:825-834.

206. Masuda, S., M. Kamao, N. J. Schroeder, H. L. Makin, G. Jones, R. Kremer, J. Rhim, and T. Okano. 2000. Characterization of 3-epi-1alpha,25-dihydroxyvitamin D3 involved in 1alpha,25-dihydroxyvitamin D3 metabolic pathway in cultured cell lines. *Biological & pharmaceutical bulletin* 23:133-139.

207. Bikle, D. D., M. K. Nemanic, J. O. Whitney, and P. W. Elias. 1986. Neonatal human foreskin keratinocytes produce 1,25-dihydroxyvitamin D3. *Biochemistry* 25:1545-1548.

208. Overbergh, L., B. Decallonne, D. Valckx, A. Verstuyf, J. Depovere, J. Laureys, O. Rutgeerts, R. Saint-Arnaud, R. Bouillon, and C. Mathieu. 2000. Identification and immune regulation of 25-hydroxyvitamin D-1-alpha-hydroxylase in murine macrophages. *Clin Exp Immunol* 120:139-146.

209. Sigmundsdottir, H., J. Pan, G. F. Debes, C. Alt, A. Habtezion, D. Soler, and E. C. Butcher. 2007. DCs metabolize sunlight-induced vitamin D3 to 'program' T cell attraction to the epidermal chemokine CCL27. *Nat Immunol* 8:285-293.

210. Chen, S., G. P. Sims, X. X. Chen, Y. Y. Gu, S. Chen, and P. E. Lipsky. 2007. Modulatory effects of 1,25-dihydroxyvitamin D3 on human B cell differentiation. *J Immunol* 179:1634-1647.

211. Norman, A. W., H. L. Henry, J. E. Bishop, X. D. Song, C. Bula, and W. H. Okamura. 2001. Different shapes of the steroid hormone 1alpha,25(OH)(2)-vitamin D(3) act as agonists for two different receptors in the vitamin D endocrine system to mediate genomic and rapid responses. *Steroids* 66:147-158.

212. Nemere, I., Y. Yoshimoto, and A. W. Norman. 1984. Calcium transport in perfused duodena from normal chicks: enhancement within fourteen minutes of exposure to 1,25-dihydroxyvitamin D3. *Endocrinology* 115:1476-1483.

213. Nemere, I., M. C. Farach-Carson, B. Rohe, T. M. Sterling, A. W. Norman, B. D. Boyan, and S. E. Safford. 2004. Ribozyme knockdown functionally links a 1,25(OH)2D3 membrane binding protein (1,25D3-MARRS) and phosphate uptake in intestinal cells. *Proc Natl Acad Sci U S A* 101:7392-7397.

214. Carlberg, C., I. Bendik, A. Wyss, E. Meier, L. J. Sturzenbecker, J. F. Grippo, and W. Hunziker. 1993. Two nuclear signalling pathways for vitamin D. *Nature* 361:657-660.

215. Deeb, K. K., D. L. Trump, and C. S. Johnson. 2007. Vitamin D signalling pathways in cancer: potential for anticancer therapeutics. *Nat Rev Cancer* 7:684-700.

216. Kato, S., M. S. Kim, K. Yamaoka, and R. Fujiki. 2007. Mechanisms of transcriptional repression by 1,25(OH)2 vitamin D. *Current opinion in nephrology and hypertension* 16:297-304.

217. Hershberger, P. A., R. A. Modzelewski, Z. R. Shurin, R. M. Rueger, D. L. Trump, and C. S. Johnson. 1999. 1,25-Dihydroxycholecalciferol (1,25-D3) inhibits the growth of squamous cell carcinoma and down-modulates p21(Waf1/Cip1) in vitro and in vivo. *Cancer Res* 59:2644-2649.

218. Palmer, H. G., F. Anjos-Afonso, G. Carmeliet, H. Takeda, and F. M. Watt. 2008. The vitamin D receptor is a Wnt effector that controls hair follicle differentiation and specifies tumor type in adult epidermis. *PLoS One* 3:e1483.

219. van Etten, E., and C. Mathieu. 2005. Immunoregulation by 1,25-dihydroxyvitamin D3: basic concepts. *The Journal of steroid biochemistry and molecular biology* 97:93-101.

220. D'Ambrosio, D., M. Cippitelli, M. G. Cocciolo, D. Mazzeo, P. Di Lucia, R. Lang, F. Sinigaglia, and P. Panina-Bordignon. 1998. Inhibition of IL-12 production by 1,25-dihydroxyvitamin D3. Involvement of NF-kappaB downregulation in transcriptional repression of the p40 gene. *J Clin Invest* 101:252-262.

221. Daniel, C., N. A. Sartory, N. Zahn, H. H. Radeke, and J. M. Stein. 2008. Immune modulatory treatment of trinitrobenzene sulfonic acid colitis with calcitriol is associated with a change of a T helper (Th) 1/Th17 to a Th2 and regulatory T cell profile. *The Journal of pharmacology and experimental therapeutics* 324:23-33.

222. Penna, G., and L. Adorini. 2000. 1 Alpha,25-dihydroxyvitamin D3 inhibits differentiation, maturation, activation, and survival of dendritic cells leading to impaired alloreactive T cell activation. *J Immunol* 164:2405-2411.

223. Cippitelli, M., and A. Santoni. 1998. Vitamin D3: a transcriptional modulator of the interferon-gamma gene. *Eur J Immunol* 28:3017-3030.

224. Boonstra, A., F. J. Barrat, C. Crain, V. L. Heath, H. F. Savelkoul, and A. O'Garra. 2001. 1alpha,25-Dihydroxyvitamin d3 has a direct effect on naive CD4(+) T cells to enhance the development of Th2 cells. *J Immunol* 167:4974-4980.

225. Heine, G., U. Niesner, H. D. Chang, A. Steinmeyer, U. Zugel, T. Zuberbier, A. Radbruch, and M. Worm. 2008. 1,25-dihydroxyvitamin D(3) promotes IL-10 production in human B cells. *Eur J Immunol* 38:2210-2218.

226. Gorman, S., L. A. Kuritzky, M. A. Judge, K. M. Dixon, J. P. McGlade, R. S. Mason, J. J. Finlay-Jones, and P. H. Hart. 2007. Topically applied 1,25-dihydroxyvitamin D3 enhances the suppressive activity of CD4+CD25+ cells in the draining lymph nodes. *J Immunol* 179:6273-6283.

227. Takeuchi, A., G. S. Reddy, T. Kobayashi, T. Okano, J. Park, and S. Sharma. 1998. Nuclear factor of activated T cells (NFAT) as a molecular target for 1alpha,25-dihydroxyvitamin D3-mediated effects. *J Immunol* 160:209-218.

228. Nonn, L., L. Peng, D. Feldman, and D. M. Peehl. 2006. Inhibition of p38 by vitamin D reduces interleukin-6 production in normal prostate cells via mitogen-activated protein kinase phosphatase 5: implications for prostate cancer prevention by vitamin D. *Cancer Res* 66:4516-4524.

229. Mizwicki, M. T., and A. W. Norman. 2009. The vitamin D sterol-vitamin D receptor ensemble model offers unique insights into both genomic and rapid-response signaling. *Science signaling* 2:re4.

230. Mizwicki, M. T., D. Menegaz, S. Yaghmaei, H. L. Henry, and A. W. Norman. 2010. A molecular description of ligand binding to the two overlapping binding pockets of the nuclear vitamin D receptor (VDR): structure-function implications. *The Journal of steroid biochemistry and molecular biology* 121:98-105.

231. Norman, A. W., W. H. Okamura, M. W. Hammond, J. E. Bishop, M. C. Dormanen, R. Bouillon, H. van Baelen, A. L. Ridall, E. Daane, R. Khoury, and M. C. Farach-Carson. 1997. Comparison of 6-s-cis- and 6-s-trans-locked analogs of 1alpha,25-dihydroxyvitamin D3 indicates that the 6-s-cis conformation is preferred for rapid nongenomic biological responses and that neither 6-s-cis- nor 6-s-trans-locked analogs are preferred for genomic biological responses. *Molecular endocrinology (Baltimore, Md* 11:1518-1531.

232. Wong, G., R. Gupta, K. M. Dixon, S. S. Deo, S. M. Choong, G. M. Halliday, J. E. Bishop, S. Ishizuka, A. W. Norman, G. H. Posner, and R. S. Mason. 2004. 1,25-Dihydroxyvitamin D and three low-calcemic analogs decrease UV-induced DNA damage via the rapid response pathway. *The Journal of steroid biochemistry and molecular biology* 89-90:567-570.

233. Dixon, K. M., S. S. Deo, G. Wong, M. Slater, A. W. Norman, J. E. Bishop, G. H. Posner, S. Ishizuka, G. M. Halliday, V. E. Reeve, and R. S. Mason. 2005. Skin cancer prevention: a possible role of 1,25dihydroxyvitamin D3 and its analogs. *The Journal of steroid biochemistry and molecular biology* 97:137-143.

234. Johansen, C., K. Kragballe, J. Henningsen, M. Westergaard, K. Kristiansen, and L. Iversen. 2003. 1alpha,25-dihydroxyvitamin D3 stimulates activator protein 1 DNA-binding activity by a phosphatidylinositol 3-kinase/Ras/MEK/extracellular signal regulated kinase 1/2 and c-Jun N-terminal kinase 1-dependent increase in c-Fos, Fra1, and c-Jun expression in human keratinocytes. *J Invest Dermatol* 120:561-570.

235. Taher, Y. A., B. C. van Esch, G. A. Hofman, P. A. Henricks, and A. J. van Oosterhout. 2008. 1alpha,25-dihydroxyvitamin D3 potentiates the beneficial effects of allergen immunotherapy in a mouse model of allergic asthma: role for IL-10 and TGF-beta. *J Immunol* 180:5211-5221.

236. Toyota, N., H. Sakai, H. Takahashi, Y. Hashimoto, and H. Iizuka. 1996. Inhibitory effect of 1 alpha,25-dihydroxyvitamin D3 on mast cell proliferation and A23187-induced histamine release, also accompanied by a decreased c-kit receptor. *Arch Dermatol Res* 288:709-715.

237. Baroni, E., M. Biffi, F. Benigni, A. Monno, D. Carlucci, G. Carmeliet, R. Bouillon, and D. D'Ambrosio. 2007. VDR-dependent regulation of mast cell maturation mediated by 1,25-dihydroxyvitamin D3. *J Leukoc Biol* 81:250-262.

238. Cuenda, A., and S. Rousseau. 2007. p38 MAP-kinases pathway regulation, function and role in human diseases. *Biochim Biophys Acta* 1773:1358-1375.

239. Brinkman, B. M., J. B. Telliez, A. R. Schievella, L. L. Lin, and A. E. Goldfeld. 1999. Engagement of tumor necrosis factor (TNF) receptor 1 leads to ATF-2- and p38 mitogen-activated protein kinase-dependent TNF-alpha gene expression. *J Biol Chem* 274:30882-30886.

240. Park, J. I., M. G. Lee, K. Cho, B. J. Park, K. S. Chae, D. S. Byun, B. K. Ryu, Y. K. Park, and S. G. Chi. 2003. Transforming growth factor-beta1 activates interleukin-6 expression in prostate cancer cells through the synergistic collaboration of the Smad2, p38-NF-kappaB, JNK, and Ras signaling pathways. *Oncogene* 22:4314-4332.

241. Marquardt, D. L., and L. L. Walker. 2000. Dependence of mast cell IgE-mediated cytokine production on nuclear factor-kappaB activity. *J Allergy Clin Immunol* 105:500-505.

242. Klemm, S., and J. Ruland. 2006. Inflammatory signal transduction from the Fc epsilon RI to NF-kappa B. *Immunobiology* 211:815-820.

243. Lou, Y. R., F. Molnar, M. Perakyla, S. Qiao, A. V. Kalueff, R. St-Arnaud, C. Carlberg, and P. Tuohimaa. 2010. 25-Hydroxyvitamin D(3) is an agonistic vitamin D receptor ligand. *The Journal of steroid biochemistry and molecular biology* 118:162-170.

244. Li, Y. C., A. E. Pirro, M. Amling, G. Delling, R. Baron, R. Bronson, and M. B. Demay. 1997. Targeted ablation of the vitamin D receptor: an animal model of vitamin D-dependent rickets type II with alopecia. *Proc Natl Acad Sci U S A* 94:9831-9835.

245. Wolters, P. J., J. Mallen-St Clair, C. C. Lewis, S. A. Villalta, P. Baluk, D. J. Erle, and G. H. Caughey. 2005. Tissue-selective mast cell reconstitution and differential lung gene expression in mast cell-deficient Kit(W-sh)/Kit(W-sh) sash mice. *Clin Exp Allergy* 35:82-88.

246. Lemire, J. M., and D. C. Archer. 1991. 1,25-dihydroxyvitamin D3 prevents the in vivo induction of murine experimental autoimmune encephalomyelitis. *J Clin Invest* 87:1103-1107.

247. Cantorna, M. T., C. E. Hayes, and H. F. DeLuca. 1996. 1,25-Dihydroxyvitamin D3 reversibly blocks the progression of relapsing encephalomyelitis, a model of multiple sclerosis. *Proc Natl Acad Sci U S A* 93:7861-7864.

248. Cantorna, M. T., C. E. Hayes, and H. F. DeLuca. 1998. 1,25-Dihydroxycholecalciferol inhibits the progression of arthritis in murine models of human arthritis. *The Journal of nutrition* 128:68-72.

249. Alyasin, S., T. Momen, S. Kashef, A. Alipour, and R. Amin. 2011. The relationship between serum 25 hydroxy vitamin d levels and asthma in children. *Allergy, asthma & immunology research* 3:251-255.

250. Weiss, S. T., and A. A. Litonjua. 2007. Maternal diet vs lack of exposure to sunlight as the cause of the epidemic of asthma, allergies and other autoimmune diseases. *Thorax* 62:746-748.

251. Arends, J. 2011. Vitamin d in oncology. *Forschende Komplementarmedizin (2006)* 18:176-184.

252. Matilainen, J. M., A. Rasanen, P. Gynther, and S. Vaisanen. 2010. The genes encoding cytokines IL-2, IL-10 and IL-12B are primary 1alpha,25(OH)2D3 target genes. *The Journal of steroid biochemistry and molecular biology* 121:142-145.

253. Bikle, D. D. 2007. What is new in vitamin D: 2006-2007. *Current opinion in rheumatology* 19:383-388.

254. Chen, C. M., and H. C. Fang. 1997. Chemical analysis of the active principles of Curcuma species. In *Modern Treatise on Chinese Herbal Medicines*. C. Y. Sung, D. W. Chou, C. J. Fung, and H. M. Zhao, eds. Institute of Pharmaceutical Sciences, Medical Academia, Beijing, PRC. 95 - 105.

255. Huang, M. T., Y. R. Lou, J. G. Xie, W. Ma, Y. P. Lu, P. Yen, B. T. Zhu, H. Newmark, and C. T. Ho. 1998. Effect of dietary curcumin and dibenzoylmethane on formation of 7,12-dimethylbenz[a]anthracene-induced mammary tumors and lymphomas/leukemias in Sencar mice. *Carcinogenesis* 19:1697-1700.

256. Bharti, A. C., N. Donato, and B. B. Aggarwal. 2003. Curcumin (diferuloylmethane) inhibits constitutive and IL-6-inducible STAT3 phosphorylation in human multiple myeloma cells. *J Immunol* 171:3863-3871.

257. Abe, Y., S. Hashimoto, and T. Horie. 1999. Curcumin inhibition of inflammatory cytokine production by human peripheral blood monocytes and alveolar macrophages. *Pharmacol Res* 39:41-47.

258. Natarajan, C., and J. J. Bright. 2002. Curcumin inhibits experimental allergic encephalomyelitis by blocking IL-12 signaling through Janus kinase-STAT pathway in T lymphocytes. *J Immunol* 168:6506-6513.

259. Saini, S., S. Arora, S. Majid, V. Shahryari, Y. Chen, G. Deng, S. Yamamura, K. Ueno, and R. Dahiya. 2011. Curcumin Modulates MicroRNA-203-Mediated Regulation of the Src-Akt Axis in Bladder Cancer. *Cancer prevention research (Philadelphia, Pa* 4:1698-1709.

260. Li, L., B. B. Aggarwal, S. Shishodia, J. Abbruzzese, and R. Kurzrock. 2004. Nuclear factor-kappaB and IkappaB kinase are constitutively active in human pancreatic cells, and their down-regulation by curcumin (diferuloylmethane) is associated with the suppression of proliferation and the induction of apoptosis. *Cancer* 101:2351-2362.

261. Fahey, A. J., R. Adrian Robins, and C. S. Constantinescu. 2007. Curcumin modulation of IFN-beta and IL-12 signalling and cytokine induction in human T cells. *Journal of cellular and molecular medicine* 11:1129-1137.

262. Kitaura, J., J. Song, M. Tsai, K. Asai, M. Maeda-Yamamoto, A. Mocsai, Y. Kawakami, F. T. Liu, C. A. Lowell, B. G. Barisas, S. J. Galli, and T. Kawakami. 2003. Evidence that IgE molecules mediate a spectrum of effects on mast cell survival and activation via aggregation of the FcepsilonRI. *Proc Natl Acad Sci U S A* 100:12911-12916.

263. Molfetta, R., F. Belleudi, G. Peruzzi, S. Morrone, L. Leone, I. Dikic, M. Piccoli, L. Frati, M. R. Torrisi, A. Santoni, and R. Paolini. 2005. CIN85 regulates the ligand-dependent endocytosis of the IgE receptor: a new molecular mechanism to dampen mast cell function. *J Immunol* 175:4208-4216.

264. Molfetta, R., F. Gasparrini, G. Peruzzi, L. Vian, M. Piccoli, L. Frati, A. Santoni, and R. Paolini. 2009. Lipid raft-dependent FcepsilonRI ubiquitination regulates receptor endocytosis through the action of ubiquitin binding adaptors. *PLoS One* 4:e5604.

265. Mekori, Y. A., C. K. Oh, and D. D. Metcalfe. 1993. IL-3-dependent murine mast cells undergo apoptosis on removal of IL-3. Prevention of apoptosis by c-kit ligand. *J Immunol* 151:3775-3784.

266. Asai, K., J. Kitaura, Y. Kawakami, N. Yamagata, M. Tsai, D. P. Carbone, F. T. Liu, S. J. Galli, and T. Kawakami. 2001. Regulation of mast cell survival by IgE. *Immunity* 14:791-800.

267. Nurmi, K., T. Methuen, T. Maki, K. A. Lindstedt, P. T. Kovanen, C. Sandler, and K. K. Eklund. 2009. Ethanol induces apoptosis in human mast cells. *Life sciences* 85:678-684.

268. Chen, H. J., C. K. Shih, H. Y. Hsu, and W. Chiang. 2010. Mast cell-dependent allergic responses are inhibited by ethanolic extract of adlay (Coix lachryma-jobi

L. var. ma-yuen Stapf) testa. *Journal of agricultural and food chemistry* 58:2596-2601.

269. Gruchalla, R. S., T. T. Dinh, and D. A. Kennerly. 1990. An indirect pathway of receptor-mediated 1,2-diacylglycerol formation in mast cells. I. IgE receptor-mediated activation of phospholipase D. *J Immunol* 144:2334-2342.

270. Lee, C. E., M. E. Neuland, H. G. Teaford, B. F. Villacis, P. S. Dixon, S. Valtier, C. H. Yeh, D. C. Fournier, and E. N. Charlesworth. 1992. Interleukin-6 is released in the cutaneous response to allergen challenge in atopic individuals. *J Allergy Clin Immunol* 89:1010-1020.

271. Gosset, P., F. Malaquin, Y. Delneste, B. Wallaert, A. Capron, M. Joseph, and A. B. Tonnel. 1993. Interleukin-6 and interleukin-1 alpha production is associated with antigen-induced late nasal response. *J Allergy Clin Immunol* 92:878-890.

272. Delneste, Y., P. Lassalle, P. Jeannin, M. Joseph, A. B. Tonnel, and P. Gosset. 1994. Histamine induces IL-6 production by human endothelial cells. *Clin Exp Immunol* 98:344-349.

273. Neveu, W. A., J. B. Allard, O. Dienz, M. J. Wargo, G. Ciliberto, L. A. Whittaker, and M. Rincon. 2009. IL-6 is required for airway mucus production induced by inhaled fungal allergens. *J Immunol* 183:1732-1738.

274. Neveu, W. A., J. L. Allard, D. M. Raymond, L. M. Bourassa, S. M. Burns, J. Y. Bunn, C. G. Irvin, D. A. Kaminsky, and M. Rincon. 2010. Elevation of IL-6 in the allergic asthmatic airway is independent of inflammation but associates with loss of central airway function. *Respiratory research* 11:28.

275. Hakim, I., and Z. Bar-Shavit. 2003. Modulation of TNF-alpha expression in bone marrow macrophages: involvement of vitamin D response element. *Journal of cellular biochemistry* 88:986-998.

276. Masood, R., S. Nagpal, T. Zheng, J. Cai, A. Tulpule, D. L. Smith, and P. S. Gill. 2000. Kaposi sarcoma is a therapeutic target for vitamin D(3) receptor agonist. *Blood* 96:3188-3194.

277. Sun, M., Z. Estrov, Y. Ji, K. R. Coombes, D. H. Harris, and R. Kurzrock. 2008. Curcumin (diferuloylmethane) alters the expression profiles of microRNAs in human pancreatic cancer cells. *Molecular cancer therapeutics* 7:464-473.

278. Sarin, S., B. Undem, A. Sanico, and A. Togias. 2006. The role of the nervous system in rhinitis. *J Allergy Clin Immunol* 118:999-1016.

279. Wills-Karp, M. 1999. Immunologic basis of antigen-induced airway hyperresponsiveness. *Annu Rev Immunol* 17:255-281.

280. Shalita-Chesner, M., R. Koren, Y. A. Mekori, D. Baram, C. Rotem, U. A. Liberman, and A. Ravid. 1998. 1,25-Dihydroxyvitamin D3 enhances degranulation of mast cells. *Mol Cell Endocrinol* 142:49-55.

281. Li, M., P. Hener, Z. Zhang, S. Kato, D. Metzger, and P. Chambon. 2006. Topical vitamin D3 and low-calcemic analogs induce thymic stromal lymphopoietin in mouse keratinocytes and trigger an atopic dermatitis. *Proc Natl Acad Sci U S A* 103:11736-11741.

282. Norman, M. U., J. Hwang, S. Hulliger, C. S. Bonder, J. Yamanouchi, P. Santamaria, and P. Kubes. 2008. Mast cells regulate the magnitude and the cytokine microenvironment of the contact hypersensitivity response. *Am J Pathol* 172:1638-1649.

283. Murai, M., O. Turovskaya, G. Kim, R. Madan, C. L. Karp, H. Cheroutre, and M. Kronenberg. 2009. Interleukin 10 acts on regulatory T cells to maintain expression of the transcription factor Foxp3 and suppressive function in mice with colitis. *Nat Immunol* 10:1178-1184.

284. Hara, M., C. I. Kingsley, M. Niimi, S. Read, S. E. Turvey, A. R. Bushell, P. J. Morris, F. Powrie, and K. J. Wood. 2001. IL-10 is required for regulatory T cells to mediate tolerance to alloantigens in vivo. *J Immunol* 166:3789-3796.

285. Hawrylowicz, C. M., and A. O'Garra. 2005. Potential role of interleukin-10-secreting regulatory T cells in allergy and asthma. *Nat Rev Immunol* 5:271-283.

286. Kennedy Norton, S., B. Barnstein, J. Brenzovich, D. P. Bailey, M. Kashyap, K. Speiran, J. Ford, D. Conrad, S. Watowich, M. R. Moralle, C. L. Kepley, P. J. Murray, and J. J. Ryan. 2008. IL-10 suppresses mast cell IgE receptor expression and signaling in vitro and in vivo. *J Immunol* 180:2848-2854.

287. Gillespie, S. R., R. R. DeMartino, J. Zhu, H. J. Chong, C. Ramirez, C. P. Shelburne, L. A. Bouton, D. P. Bailey, A. Gharse, P. Mirmonsef, S. Odom, G. Gomez, J. Rivera, K. Fischer-Stenger, and J. J. Ryan. 2004. IL-10 inhibits Fc epsilon RI expression in mouse mast cells. *J Immunol* 172:3181-3188.

288. Huhtakangas, J. A., C. J. Olivera, J. E. Bishop, L. P. Zanello, and A. W. Norman. 2004. The vitamin D receptor is present in caveolae-enriched plasma membranes and binds 1 alpha,25(OH)2-vitamin D3 in vivo and in vitro. *Molecular endocrinology (Baltimore, Md* 18:2660-2671.

289. Lai, E. C. 2003. microRNAs: runts of the genome assert themselves. *Curr Biol* 13:R925-936.

290. Carrington, J. C., and V. Ambros. 2003. Role of microRNAs in plant and animal development. *Science* 301:336-338.

291. Ambros, V. 2004. The functions of animal microRNAs. *Nature* 431:350-355.

292. Bartel, D. P. 2004. MicroRNAs: genomics, biogenesis, mechanism, and function. *Cell* 116:281-297.

293. Shivdasani, R. A. 2006. MicroRNAs: regulators of gene expression and cell differentiation. *Blood* 108:3646-3653.

294. Gantier, M. P., A. J. Sadler, and B. R. Williams. 2007. Fine-tuning of the innate immune response by microRNAs. *Immunol Cell Biol* 85:458-462.

295. 2011. B6.129S4-*Vdr*^{tm1Mbd}/J. The Jackson Laboratory.

296. Rowling, M. J., C. Gliniak, J. Welsh, and J. C. Fleet. 2007. High dietary vitamin D prevents hypocalcemia and osteomalacia in CYP27B1 knockout mice. *The Journal of nutrition* 137:2608-2615.

297. Heaney, R. P., L. A. Armas, J. R. Shary, N. H. Bell, N. Binkley, and B. W. Hollis. 2008. 25-Hydroxylation of vitamin D3: relation to circulating vitamin D3 under various input conditions. *The American journal of clinical nutrition* 87:1738-1742.

298. Bikle, D. D., M. K. Nemanic, E. Gee, and P. Elias. 1986. 1,25-Dihydroxyvitamin D3 production by human keratinocytes. Kinetics and regulation. *J Clin Invest* 78:557-566.

299. Tokar, E. J., and M. M. Webber. 2005. Chemoprevention of prostate cancer by cholecalciferol (vitamin D3): 25-hydroxylase (CYP27A1) in human prostate epithelial cells. *Clinical & experimental metastasis* 22:265-273.

300. Ichikawa, F., K. Sato, M. Nanjo, Y. Nishii, T. Shinki, N. Takahashi, and T. Suda. 1995. Mouse primary osteoblasts express vitamin D3 25-hydroxylase mRNA and convert 1 alpha-hydroxyvitamin D3 into 1 alpha,25-dihydroxyvitamin D3. *Bone* 16:129-135.

301. Lehmann, B., T. Genehr, P. Knuschke, J. Pietzsch, and M. Meurer. 2001. UVB-induced conversion of 7-dehydrocholesterol to 1alpha,25-dihydroxyvitamin D3 in an in vitro human skin equivalent model. *J Invest Dermatol* 117:1179-1185.

302. Lehmann, B., W. Sauter, P. Knuschke, S. Dressler, and M. Meurer. 2003. Demonstration of UVB-induced synthesis of 1 alpha,25-dihydroxyvitamin D3 (calcitriol) in human skin by microdialysis. *Arch Dermatol Res* 295:24-28.

303. Vantieghem, K., P. De Haes, R. Bouillon, and S. Segaert. 2006. Dermal fibroblasts pretreated with a sterol Delta7-reductase inhibitor produce 25-hydroxyvitamin D3 upon UVB irradiation. *Journal of photochemistry and photobiology* 85:72-78.

304. Levine, B. S., F. R. Singer, G. F. Bryce, J. P. Mallon, O. N. Miller, and J. W. Coburn. 1985. Pharmacokinetics and biologic effects of calcitriol in normal humans. *The Journal of laboratory and clinical medicine* 105:239-246.

305. Morimoto, S., T. Onishi, S. Imanaka, H. Yukawa, T. Kozuka, Y. Kitano, K. Yoshikawa, and Y. Kumahara. 1986. Topical administration of 1,25-dihydroxyvitamin D3 for psoriasis: report of five cases. *Calcified tissue international* 38:119-122.

306. Pryke, A. M., C. Duggan, C. P. White, S. Posen, and R. S. Mason. 1990. Tumor necrosis factor-alpha induces vitamin D-1-hydroxylase activity in normal human alveolar macrophages. *J Cell Physiol* 142:652-656.

307. Ren, S., L. Nguyen, S. Wu, C. Encinas, J. S. Adams, and M. Hewison. 2005. Alternative splicing of vitamin D-24-hydroxylase: a novel mechanism for the regulation of extrarenal 1,25-dihydroxyvitamin D synthesis. *J Biol Chem* 280:20604-20611.

308. Vidal, M., C. V. Ramana, and A. S. Dusso. 2002. Stat1-vitamin D receptor interactions antagonize 1,25-dihydroxyvitamin D transcriptional activity and enhance stat1-mediated transcription. *Mol Cell Biol* 22:2777-2787.

309. Tang, W. J., L. F. Wang, X. Y. Xu, Y. Zhou, W. F. Jin, H. F. Wang, and J. Gao. 2010. Autocrine/paracrine action of vitamin D on FGF23 expression in cultured rat osteoblasts. *Calcified tissue international* 86:404-410.

310. Bikle, D. D. 2010. Vitamin D: newly discovered actions require reconsideration of physiologic requirements. *Trends in endocrinology and metabolism: TEM* 21:375-384.

311. Matsumoto, K., Y. Azuma, M. Kiyoki, H. Okumura, K. Hashimoto, and K. Yoshikawa. 1991. Involvement of endogenously produced 1,25-dihydroxyvitamin D-3 in the growth and differentiation of human keratinocytes. *Biochim Biophys Acta* 1092:311-318.

312. Hart, P. H., S. Gorman, and J. J. Finlay-Jones. 2011. Modulation of the immune system by UV radiation: more than just the effects of vitamin D? *Nat Rev Immunol* 11:584-596.

313. Hewison, M., L. Freeman, S. V. Hughes, K. N. Evans, R. Bland, A. G. Eliopoulos, M. D. Kilby, P. A. Moss, and R. Chakraverty. 2003. Differential regulation of vitamin D receptor and its ligand in human monocyte-derived dendritic cells. *J Immunol* 170:5382-5390.

314. Sage, R. J., and H. W. Lim. 2010. UV-based therapy and vitamin D. *Dermatologic therapy* 23:72-81.

315. Staberg, B., A. Oxholm, P. Klemp, and D. Hartwell. 1988. Is the effect of phototherapy in psoriasis partly due to an impact on vitamin D metabolism? *Acta Derm Venereol* 68:436-439.

316. Ghoreishi, M., P. Bach, J. Obst, M. Komba, J. C. Fleet, and J. P. Dutz. 2009. Expansion of antigen-specific regulatory T cells with the topical vitamin d analog calcipotriol. *J Immunol* 182:6071-6078.

317. Gorman, S., M. A. Judge, and P. H. Hart. 2010. Immune-modifying properties of topical vitamin D: Focus on dendritic cells and T cells. *The Journal of steroid biochemistry and molecular biology* 121:247-249.

318. Damian, D. L., Y. J. Kim, K. M. Dixon, G. M. Halliday, A. Javeri, and R. S. Mason. 2010. Topical calcitriol protects from UV-induced genetic damage but suppresses cutaneous immunity in humans. *Experimental dermatology* 19:e23-30.

319. Hanneman, K. K., H. M. Scull, K. D. Cooper, and E. D. Baron. 2006. Effect of topical vitamin D analogue on in vivo contact sensitization. *Archives of dermatology* 142:1332-1334.

320. Sigmon, J. R., B. A. Yentzer, and S. R. Feldman. 2009. Calcitriol ointment: a review of a topical vitamin D analog for psoriasis. *The Journal of dermatological treatment* 20:208-212.

321. Harvima, I. T., G. Nilsson, M. M. Suttle, and A. Naukkarinen. 2008. Is there a role for mast cells in psoriasis? *Arch Dermatol Res* 300:461-478.

322. Kawakami, T., T. Ando, M. Kimura, B. S. Wilson, and Y. Kawakami. 2009. Mast cells in atopic dermatitis. *Curr Opin Immunol* 21:666-678.

323. Gorman, S., M. A. Judge, and P. H. Hart. 2010. Topical 1,25-dihydroxyvitamin D3 subverts the priming ability of draining lymph node dendritic cells. *Immunology* 131:415-425.

324. Guo, Z., H. Okamoto, and S. Imamura. 1992. The effect of 1,25(OH)2-vitamin D3 on Langerhans cells and contact hypersensitivity in mice. *Arch Dermatol Res* 284:368-370.

325. Singh, L. K., X. Pang, N. Alexacos, R. Letourneau, and T. C. Theoharides. 1999. Acute immobilization stress triggers skin mast cell degranulation via corticotropin releasing hormone, neurotensin, and substance P: A link to neurogenic skin disorders. *Brain, behavior, and immunity* 13:225-239.

326. Riley, W. D., and E. E. Snell. 1968. Histidine decarboxylase of Lactobacillus 30a. IV. The presence of covalently bound pyruvate as the prosthetic group. *Biochemistry* 7:3520-3528.

327. Romao, P. R., H. Da Costa Santiago, C. D. Ramos, C. F. De Oliveira, M. C. Monteiro, F. De Queiroz Cunha, and L. Q. Vieira. 2009. Mast cell degranulation contributes to susceptibility to Leishmania major. *Parasite immunology* 31:140-146.

328. Fitz, L. J., A. Brennan, C. R. Wood, S. J. Goldman, and M. T. Kasaian. 2008. Activation-induced cellular accumulation of histamine in immature but not mature murine mast cells. *Cell Mol Life Sci* 65:1585-1595.

329. Dubravec, D. B., D. R. Spriggs, J. A. Mannick, and M. L. Rodrick. 1990. Circulating human peripheral blood granulocytes synthesize and secrete tumor necrosis factor alpha. *Proc Natl Acad Sci U S A* 87:6758-6761.

330. Hope, J. C., M. Cumberbatch, I. Fielding, R. J. Dearman, I. Kimber, and S. J. Hopkins. 1995. Identification of dendritic cells as a major source of interleukin-6

in draining lymph nodes following skin sensitization of mice. *Immunology* 86:441-447.

331. Pestka, S., C. D. Krause, D. Sarkar, M. R. Walter, Y. Shi, and P. B. Fisher. 2004. Interleukin-10 and related cytokines and receptors. *Annu Rev Immunol* 22:929-979.

332. Dardenne, O., J. Prud'homme, A. Arabian, F. H. Glorieux, and R. St-Arnaud. 2001. Targeted inactivation of the 25-hydroxyvitamin D(3)-1(alpha)-hydroxylase gene (CYP27B1) creates an animal model of pseudovitamin D-deficiency rickets. *Endocrinology* 142:3135-3141.

333. Chinellato, I., M. Piazza, M. Sandri, D. Peroni, G. Piacentini, and A. L. Boner. Vitamin D serum levels and markers of asthma control in Italian children. *The Journal of pediatrics* 158:437-441.

334. Camargo, C. A., Jr., S. L. Rifas-Shiman, A. A. Litonjua, J. W. Rich-Edwards, S. T. Weiss, D. R. Gold, K. Kleinman, and M. W. Gillman. 2007. Maternal intake of vitamin D during pregnancy and risk of recurrent wheeze in children at 3 y of age. *The American journal of clinical nutrition* 85:788-795.

335. Devereux, G., A. A. Litonjua, S. W. Turner, L. C. Craig, G. McNeill, S. Martindale, P. J. Helms, A. Seaton, and S. T. Weiss. 2007. Maternal vitamin D intake during pregnancy and early childhood wheezing. *The American journal of clinical nutrition* 85:853-859.

336. Erkkola, M., M. Kaila, B. I. Nwaru, C. Kronberg-Kippila, S. Ahonen, J. Nevalainen, R. Veijola, J. Pekkanen, J. Ilonen, O. Simell, M. Knip, and S. M. Virtanen. 2009. Maternal vitamin D intake during pregnancy is inversely associated with asthma and allergic rhinitis in 5-year-old children. *Clin Exp Allergy* 39:875-882.

337. Hansdottir, S., M. M. Monick, S. L. Hinde, N. Lovan, D. C. Look, and G. W. Hunninghake. 2008. Respiratory epithelial cells convert inactive vitamin D to its active form: potential effects on host defense. *J Immunol* 181:7090-7099.

338. Damera, G., H. W. Fogle, P. Lim, E. A. Goncharova, H. Zhao, A. Banerjee, O. Tliba, V. P. Krymskaya, and R. A. Panettieri, Jr. 2009. Vitamin D inhibits growth of human airway smooth muscle cells through growth factor-induced phosphorylation of retinoblastoma protein and checkpoint kinase 1. *British journal of pharmacology* 158:1429-1441.

339. Banerjee, A., G. Damera, R. Bhandare, S. Gu, Y. Lopez-Boado, R. Panettieri, Jr., and O. Tliba. 2008. Vitamin D and glucocorticoids differentially modulate chemokine expression in human airway smooth muscle cells. *British journal of pharmacology* 155:84-92.

340. Song, Y., H. Qi, and C. Wu. 2007. Effect of 1,25-(OH)2D3 (a vitamin D analogue) on passively sensitized human airway smooth muscle cells. *Respirology (Carlton, Vic* 12:486-494.

341. Cole, Z. A., G. F. Clough, and M. K. Church. 2001. Inhibition by glucocorticoids of the mast cell-dependent weal and flare response in human skin in vivo. *British journal of pharmacology* 132:286-292.

342. Marone, G., M. Triggiani, A. Genovese, and A. De Paulis. 2005. Role of human mast cells and basophils in bronchial asthma. *Advances in immunology* 88:97-160.

343. Wood, J. D. 2004. Enteric neuroimmunophysiology and pathophysiology. *Gastroenterology* 127:635-657.

344. Lorentz, A., S. Schwengberg, G. Sellge, M. P. Manns, and S. C. Bischoff. 2000. Human intestinal mast cells are capable of producing different cytokine profiles: role of IgE receptor cross-linking and IL-4. *J Immunol* 164:43-48.

345. Bischoff, S. C., A. Lorentz, S. Schwengberg, G. Weier, R. Raab, and M. P. Manns. 1999. Mast cells are an important cellular source of tumour necrosis factor alpha in human intestinal tissue. *Gut* 44:643-652.

346. Lorentz, A., S. Schwengberg, C. Mierke, M. P. Manns, and S. C. Bischoff. 1999. Human intestinal mast cells produce IL-5 in vitro upon IgE receptor cross-linking and in vivo in the course of intestinal inflammatory disease. *Eur J Immunol* 29:1496-1503.

347. Dahlen, S. E., and M. Kumlin. 2004. Monitoring mast cell activation by prostaglandin D2 in vivo. *Thorax* 59:453-455.

348. Vliagoftis, H., and A. D. Befus. 2005. Mast cells at mucosal frontiers. *Current molecular medicine* 5:573-589.

349. Galli, S. J., S. Nakae, and M. Tsai. 2005. Mast cells in the development of adaptive immune responses. *Nat Immunol* 6:135-142.

350. Bloemen, K., S. Verstraelen, R. Van Den Heuvel, H. Witters, I. Nelissen, and G. Schoeters. 2007. The allergic cascade: review of the most important molecules in the asthmatic lung. *Immunol Lett* 113:6-18.

351. Reuter, S., M. Stassen, and C. Taube. 2011. Mast cells in allergic asthma and beyond. *Yonsei medical journal* 51:797-807.

352. Toru, H., C. Ra, S. Nonoyama, K. Suzuki, J. Yata, and T. Nakahata. 1996. Induction of the high-affinity IgE receptor (Fc epsilon RI) on human mast cells by IL-4. *International immunology* 8:1367-1373.

353. Kempuraj, D., H. Saito, A. Kaneko, K. Fukagawa, M. Nakayama, H. Toru, M. Tomikawa, H. Tachimoto, M. Ebisawa, A. Akasawa, T. Miyagi, H. Kimura, T. Nakajima, K. Tsuji, and T. Nakahata. 1999. Characterization of mast cell-

committed progenitors present in human umbilical cord blood. *Blood* 93:3338-3346.

354. Kocabas, C. N., A. S. Yavuz, P. E. Lipsky, D. D. Metcalfe, and C. Akin. 2005. Analysis of the lineage relationship between mast cells and basophils using the c-kit D816V mutation as a biologic signature. *J Allergy Clin Immunol* 115:1155-1161.

355. Agis, H., W. Fureder, H. C. Bankl, M. Kundi, W. R. Sperr, M. Willheim, G. Boltz-Nitulescu, J. H. Butterfield, K. Kishi, K. Lechner, and P. Valent. 1996. Comparative immunophenotypic analysis of human mast cells, blood basophils and monocytes. *Immunology* 87:535-543.

356. Lorentz, A., I. Klopp, T. Gebhardt, M. P. Manns, and S. C. Bischoff. 2003. Role of activator protein 1, nuclear factor-kappaB, and nuclear factor of activated T cells in IgE receptor-mediated cytokine expression in mature human mast cells. *J Allergy Clin Immunol* 111:1062-1068.

357. Hallgren, J., and G. Pejler. 2006. Biology of mast cell tryptase. An inflammatory mediator. *The FEBS journal* 273:1871-1895.

358. Miller, H. R., and A. D. Pemberton. 2002. Tissue-specific expression of mast cell granule serine proteinases and their role in inflammation in the lung and gut. *Immunology* 105:375-390.

359. Gelfand, E. W. 2002. Pro: mice are a good model of human airway disease. *American journal of respiratory and critical care medicine* 166:5-6; discussion 7-8.

360. Persson, C. G. 2002. Con: mice are not a good model of human airway disease. *American journal of respiratory and critical care medicine* 166:6-7; discussion 8.

361. Hamelmann, E., A. Oshiba, J. Loader, G. L. Larsen, G. Gleich, J. Lee, and E. W. Gelfand. 1997. Antiinterleukin-5 antibody prevents airway hyperresponsiveness in a murine model of airway sensitization. *American journal of respiratory and critical care medicine* 155:819-825.

362. Leckie, M. J., A. ten Brinke, J. Khan, Z. Diamant, B. J. O'Connor, C. M. Walls, A. K. Mathur, H. C. Cowley, K. F. Chung, R. Djukanovic, T. T. Hansel, S. T. Holgate, P. J. Sterk, and P. J. Barnes. 2000. Effects of an interleukin-5 blocking monoclonal antibody on eosinophils, airway hyper-responsiveness, and the late asthmatic response. *Lancet* 356:2144-2148.

363. Ishizuka, T., Y. Okayama, H. Kobayashi, and M. Mori. 1999. Interleukin-10 is localized to and released by human lung mast cells. *Clin Exp Allergy* 29:1424-1432.

364. Zehnder, D., R. Bland, E. A. Walker, A. R. Bradwell, A. J. Howie, M. Hewison, and P. M. Stewart. 1999. Expression of 25-hydroxyvitamin D3-1alpha-hydroxylase in the human kidney. *J Am Soc Nephrol* 10:2465-2473.

365. Korkor, A. B., R. W. Gray, H. L. Henry, J. G. Kleinman, S. S. Blumenthal, and J. C. Garancis. 1987. Evidence that stimulation of 1,25(OH)2D3 production in primary cultures of mouse kidney cells by cyclic AMP requires new protein synthesis. *J Bone Miner Res* 2:517-524.

366. Dahl, C., H. J. Hoffmann, H. Saito, and P. O. Schiotz. 2004. Human mast cells express receptors for IL-3, IL-5 and GM-CSF; a partial map of receptors on human mast cells cultured in vitro. *Allergy* 59:1087-1096.

367. Schernthaner, G. H., A. W. Hauswirth, M. Baghestanian, H. Agis, M. Ghannadan, C. Worda, M. T. Krauth, D. Printz, G. Fritsch, W. R. Sperr, and P. Valent. 2005. Detection of differentiation- and activation-linked cell surface antigens on cultured mast cell progenitors. *Allergy* 60:1248-1255.

368. 2006. 2004 - 05 National Health Survey: Summary of Results. A. B. o. Statistics, ed, Canberra, Australia.

369. Mora, J. R., M. Iwata, and U. H. von Andrian. 2008. Vitamin effects on the immune system: vitamins A and D take centre stage. *Nat Rev Immunol* 8:685-698.

370. Biggs, L., C. Yu, B. Fedoric, A. F. Lopez, S. J. Galli, and M. A. Grimbaldeston. 2010. Evidence that vitamin D_3 promotes mast cell-dependent reduction of chronic UVB-induced skin pathology in mice. J Exp Med. 455-463.

371. Lee, R. J., and J. M. Oliver. 1995. Roles for Ca2+ stores release and two Ca2+ influx pathways in the Fc epsilon R1-activated Ca2+ responses of RBL-2H3 mast cells. *Molecular biology of the cell* 6:825-839.

372. Parekh, A. B., and R. Penner. 1997. Store depletion and calcium influx. *Physiological reviews* 77:901-930.

373. Nishida, K., S. Yamasaki, Y. Ito, K. Kabu, K. Hattori, T. Tezuka, H. Nishizumi, D. Kitamura, R. Goitsuka, R. S. Geha, T. Yamamoto, T. Yagi, and T. Hirano. 2005. Fc{epsilon}RI-mediated mast cell degranulation requires calcium-independent microtubule-dependent translocation of granules to the plasma membrane. *The Journal of cell biology* 170:115-126.

374. Nemere, I., C. Feld, and A. W. Norman. 1991. 1,25-Dihydroxyvitamin D3-mediated alterations in microtubule proteins isolated from chick intestinal epithelium: analyses by isoelectric focusing. *Journal of cellular biochemistry* 47:369-379.

375. Mayoral, R. J., M. E. Pipkin, M. Pachkov, E. van Nimwegen, A. Rao, and S. Monticelli. 2009. MicroRNA-221-222 regulate the cell cycle in mast cells. *J Immunol* 182:433-445.

376. Deho, L., and S. Monticelli. 2010. Human Mast Cells and Mastocytosis: Harnessing MicroRNA Expression as a New Approach to Therapy? *Arch Immunol Ther Exp* 58:279-286.

377. Jin, H., R. He, M. Oyoshi, and R. S. Geha. 2009. Animal models of atopic dermatitis. *J Invest Dermatol* 129:31-40.